Identification and Investigation of Novel Membrane Proteins in Colon and Pancreatic Cancer for Potential Therapeutic Antibody Targeting

A thesis submitted for the degree of Ph.D.

by

Edel McAuley, B.Sc. (Hons)

September 2017

The research work in this thesis was performed under the supervision of

Dr. Annemarie Larkin

&

Prof. Martin Clynes

National Institute for Cellular Biotechnology

School of Biotechnology

Dublin City University

I hereby certify that this material, which I now submit for assessment on the programme of study leading to the award of PhD is entirely my own work, that I have exercised reasonable care to ensure that the work is original, and does not to the best of my knowledge breach any law of copyright, and has not been taken from the work of others save and to the extent that such work has been cited and acknowledged within the text of my work.

Signed: _____

ID No.: _____

Date: _____

Acknowledgements

First and foremost, I would like to thank Dr. Annemarie Larkin and Prof. Martin Clynes for giving me the opportunity to carry out this PhD. Annemarie, I am sincerely grateful for your guidance and advice throughout the PhD, and particularly for your patience and support during the dreaded writing-up period. Martin, thank you for all your invaluable advice and encouragement over the years, and for making the NICB such a great place to work.

I couldn't have completed this thesis without a lot of help along the way. I'd like to acknowledge Dr. Stephen Madden and Dr. Padraig Doolan for carrying out the bioinformatic microarray analysis that began this thesis. A sincere thank you to Dr. Niall Swan and Ms. Jean Murphy, St. Vincent's University Hospital and to Dr. Susan Kennedy, Royal Victoria Eye and Ear Hospital for access to the clinical tissue specimens used in this study. I'd like to also thank Niall for kindly taking the time to review some of the Immunohistochemical analysis and Annemarie for all her help with scoring of the IHC analysis. A big thank you to Dr. Andrew McCann for teaching me the ropes when I first arrived in the NICB, and for all your help and friendship since then.

Thank you to Dr. Niall Barron for his advice on molecular biology, and to Gemma Moore and Alan Costello for help in carrying out the molecular biology experiments in this thesis, it was greatly appreciated. I'd also like to thank Michael Henry and Orla Coleman for their help with mass spec analysis that didn't quite make its way into the thesis. Thank you to Dr. Sandra Roche and Dr. Fiona O'Neill for kindly sharing specimens from your PDX models of PDAC. Thanks to Dr. Joanne Keenan, Michael Moriarty, and Dr. Helena Joyce for help and friendly advice over the years. Thanks also to the people working behind the scenes in the NICB, Carol, Mairead and Emer in the office, and Gillian for her work in stores and the prep room.

A big thank you to the second floor office gang, Gemma, Mark, Shane, Andrew, Alan, Orla and Kevin for the great company and laughs along the way. Thank you for all the help and cheering up when needed on those days when nothing seems to work out as planned.

Finally, a very special thank you to my family, my parents, Noeleen and James and my sisters, Lisa, Natalie and Ellen, for all their love and support throughout my PhD. Your help and encouragement, especially in the final stages was greatly appreciated!

Table of Contents

Abbreviations:

AA	Amino acid
α-SMA	Alpha-smooth muscle actin
ADCC	Antibody-dependent cell-mediated cytotoxicity
ADEX	Aberrantly differentiated endocrine exocrine
AML	Acute myelogenous leukaemia
APC	Adenomatous polyposis coli
B2M	Beta-2-microglobulin
BACE2	Beta-site APP-cleaving enzyme 2
BM	Basement membrane
BMDC	Bone marrow-derived cell
CAF	Cancer-associated fibroblast
CDC	Complement-dependent cytotoxicity
cDNA	Complementary DNA
CFS	Common fragile site
CIMP	CpG island hypermethylation phenotype
CIN	Chromosomal instability
CM	Conditioned medium
CML	Chronic myelogenous leukaemia
CNS	Central nervous system
Co-IP	Co-Immunoprecipitation
CRC	Colorectal cancer
CRGF	Cripto-1 growth factor
CSF-1	Colony-stimulating factor-1
Ct	Threshold cycle
CT	Computed tomography
CTL	Cytotoxic T-lymphocyte
CTLA-4	Cytotoxic T-lymphocyte-associated antigen 4
ECM	Extracellular matrix
EGF	Epidermal growth factor
EGFR	Epidermal growth factor receptor
EMT	Epithelial-mesenchymal transition
EPHX4	Epoxide hydrolase 4

ER	Estrogen receptor
E.V.	Empty vector
FAK	Focal adhesion kinase
FAMMM	Familial atypical mole-malignant melanoma
FAP	Familial adenomatous polyposis
FC	Fold change
FCS	Foetal calf serum
FFPE	Formalin-fixed, paraffin-embedded
FGF	Fibroblast growth factor
FOXP3	Forkhead box P3
GBM	Glioblastoma multiforme
GEO	Gene Expression Omnibus
GI	Gastrointestinal
GPI	Glycosylphosphatidylinositol
Grb	Growth factor receptor bound protein
GSK3B	Glycogen synthase kinase 3b
HER2	Human epidermal growth factor receptor 2
HGF	Hepatocyte growth factor
HLA	Human leukocyte antigen
HNPCC	Hereditary nonpolyposis colon cancer
IFN-γ	Interferon-γ
IGF	Insulin-like growth factor
Ig	Immunoglobulin
IHC	Immunohistochemistry
IL	Interleukin
IL-1R	Interleukin-1 receptor
IL1RAP	Interleukin 1 receptor accessory protein
IL1RAPL1	Interleukin 1 receptor accessory protein-like 1
IL20RA	Interleukin 20 receptor, subunit Alpha
IMS	Industrial methylated spirits
IP	Immunoprecipitation
IPMN	Intraductal papillary mucinous neoplasm
JNK	c-Jun amino-terminal kinase
KD	Knockdown

LRRC8E	Leucine rich repeat containing 8 family, member E
LVI	Lymphovascular invasion
LY6G6D	Lymphocyte antigen 6 complex, locus G6D
LY6G6F	Lymphocyte antigen 6 complex, locus G6F
mAb	Monoclonal antibody
MAPK	Mitogen-activated protein kinase
MCN	Mucinous cystadenoma
MHC	Major histocompatibility complex
MK	Megakaryocyte
MMAE	Monomethyl auristatin-E
MMP	Matrix metalloproteinase
MRI	Magnetic Resonance Imaging
mRNA	Messenger RNA
miRNA	Micro RNA
MSI	Microsatellite instable
MSS	Microsatellite stable
MT	Mutant
MUC5AC	Mucin 5AC
MW	Molecular weight
NAT	Normal adjacent tissue
NGF	Nerve growth factor
NK	Natural killer
NTC	No template control
NTM	Neurotrimin
OAC	Oesophageal adenocarcinoma
O.E.	Overexpression
OSCC	Oesophageal squamous cell carcinoma
PanIN	Pancreatic intraepithelial neoplasia
PARP	Poly (ADP-ribose) polymerase
PBS	Phosphate buffered saline
PD-1	Programmed cell death protein 1
PDAC	Pancreatic ductal adenocarcinoma
PDGF	Platelet-derived growth factor
PDGFR	Platelet-derived growth factor receptor

PD-L1	Programmed death ligand 1
PGE	Prostaglandin E
PI3K	Phosphatidylinositol 3-kinase
PIP3	Phosphatidylinositol-3,4,5-triphosphate
PNI	Perineural invasion
PR	Progesterone receptor
PSC	Pancreatic stellate cell
PVI	Portal vein involvement
QM	Quasi-mesenchymal
RQ	Relative quantitation
RTK	Receptor tyrosine kinase
RVEEH	Royal Victoria Eye and Ear Hospital
SD	Standard deviation
SFM	Serum-free media
Shh	Sonic hedgehog
shRNA	Short hairpin RNA
siRNA	Small interfering RNA
SVUH	St. Vincent's University Hospital
TAM	Tumour-associated macrophage
TF	Transcription factor
TGF-β	Transforming growth factor-beta
TGFBR2	TGF-β Receptor 2
Th1	T helper 1
TLR	Toll-like receptor
TMA	Tissue microarray
TNF-α	Tumour necrosis factor-α
TNM	Tumour, node, metastasis
Treg	Regulatory T cell
UHP	Ultrapure water
VEGF	Vascular endothelial growth factor
WT	Wildtype
qRT-PCR	Quantitative real-time polymerase chain reaction

List of Tables:

List of Figures:

Abstract

Title: Identification and Investigation of Novel Membrane Proteins in Colon and Pancreatic Cancer for Potential Therapeutic Antibody Targeting.

Author: Edel McAuley

Advanced colorectal cancer (CRC) and pancreatic ductal adenocarcinoma (PDAC) are highly aggressive and heterogeneous diseases which urgently require the development of more effective treatment strategies. Novel membrane proteins overexpressed in CRC and PDAC, could have the potential to represent attractive molecular targets for development of antibody-based targeted therapeutics.

Candidate molecular targets were identified by Bioinformatic, transcriptomic analysis of publicly available colon cancer gene microarray datasets. Lists were generated of genes overexpressed in colon adenoma and adenocarcinoma vs. normal colon with predicted membrane localisation. Seven novel candidate targets (LY6G6F, IL1RAPL1, IL20RA, BACE2, NTM, LRRC8E and EPHX4) were selected for protein validation in normal and colon cancer tissue sections. Two targets, LY6G6F and IL1RAPL1, both previously unexploited in cancer were found to be minimally expressed in normal colon and show strong expression in CRC, warranting further investigation and functional characterisation.

LY6G6F is a type 1 transmembrane protein, first identified as a novel platelet plasma membrane protein, linking to downstream signal transduction pathways upon platelet activation. However, a ligand for LY6G6F remains unknown. LY6G6F was found in this study to be significantly overexpressed in colon adenocarcinoma, PDAC and gastric adenocarcinoma, with minimal expression observed in normal proliferating cells and tissues. IHC analysis of a 57 PDAC patient cohort revealed that 78.9% showed strong LY6G6F immunoreactivity; using Kaplan-Meier survival analysis, a clear trend was observed between high LY6G6F expression and decreased survival in this cohort, however this failed to reach significance (p-value: 0.182). High LY6G6F mRNA expression is significantly associated with decreased survival in gastric cancer using KM plotter survival analysis (logrank-p: $4.3e^{-05}$). Transient protein knockdown of LY6G6F in the colon cancer cell line HCT116 and the PDAC cell line MIA PaCa-2 significantly inhibits proliferation, 2D colony formation, migration and invasion of these cells *in vitro*. These effects were found to be potentially mediated by a decrease in FAK activation and an increase in apoptosis. Thus, taken together these results implicate LY6G6F in the proliferation and survival of these cancers.

IL1RAPL1 is a type 1 transmembrane protein highly expressed in brain neurons, with a reported role in synapse formation. Deletions and mutations in IL1RAPL1 have been associated with X-linked intellectual disability. IL1RAPL1 was found to be significantly overexpressed in all CRC subtypes vs. normal colon and showed limited expression in a range of other normal tissues and highly proliferating cells. Furthermore, IL1RAPL1 expression was associated with oesophageal squamous cell carcinoma (OSCC), with significant overexpression compared to normal oesophagus and also other oesophageal cancer subtypes. The potential functional role of IL1RAPL1 in the colon cancer cell phenotype could not be determined.

LY6G6F and IL1RAPL1 both represent novel candidate proteins overexpressed in these cancer types with restricted expression in normal tissues and should be investigated further as potential molecular targets for antibody-based therapeutic targeting.

Chapter 1. Introduction

1.1. Colorectal Cancer

Colorectal cancer (CRC) has a high incidence rate worldwide. It is the third most commonly diagnosed cancer and ranks 4th in mortality. Approximately one third of CRC patients die from the disease. (Aslam *et al.*, 2010) The development of CRC typically follows several consecutive steps, from a benign adenomatous polyp, which develops into an advanced adenoma with high-grade dysplasia and then progresses to an invasive cancer. The model of progressive step-wise accumulation of genetic events leading to CRC, was first described by Fearon and Vogelstein (1990), with the progression of adenomas to CRC probably occurring over years to decades. Early stage CRC tumours confined within the wall of the colon are curable, but if left untreated they spread to regional lymph nodes and then metastasise to distant sites. (Markowitz and Bertagnolli, 2010) Whilst the primary CRC tumour can take decades to develop, once the tumour invades the colonic wall, dissemination and metastasis to predominantly the liver can rapidly ensue. The second most frequent sites of metastasis are the lungs, with metastatic spread thought to progress sequentially in many patients, from liver to lung, then to bone and brain as late sites of involvement. (Nguyen, Bos and Massagué, 2009; Yaeger *et al.*, 2015)

Metastatic disease is estimated to develop in 50% of CRC patients, and despite significant advances in the treatment of metastatic CRC, which have prolonged median overall survival up to 28 months, 5-year survival rates of just 10% remain disappointingly low. (Dietvorst and Eskens, 2013) Treatment of metastatic CRC includes targeted therapeutics and a range of cytotoxic chemotherapeutics, with fluoropyrimidines, oxaliplatin and irinotecan, representing the main chemotherapy regimens utilised. (Dienstmann *et al.*, 2017) Target specific agents that are used in metastatic CRC treatment, include the monoclonal antibody (mAb) Bevacizumab which targets vascular endothelial growth factor (VEGF), thereby inhibiting angiogenesis and the mAb Cetuximab, which targets epidermal growth factor receptor (EGFR) on tumour cells, thereby blocking ligand-induced EGFR tyrosine kinase activation, initiating cell cycle arrest. (Ciardiello and Tortora, 2008; Dienstmann *et al.*, 2017) However, despite great promise observed in preclinical models, the overall added value of angiogenesis inhibition in the treatment of metastatic CRC is modest at best. The suitability of patients for anti-EGFR therapy is based on the absence of activating KRAS mutations, which confer innate resistance. There is a need for new and more active targeted therapeutics in the treatment of metastatic CRC. (Dietvorst and Eskens, 2013)

It is estimated that 15-30% of CRCs may have a hereditary component and studies of the molecular basis of inherited cases have greatly improved the understanding of the specific factors and mechanisms that contribute to sporadic CRC development. The bulk of hereditary CRC cases are attributable to hereditary nonpolyposis colon cancer (HNPCC), also known as the Lynch syndrome, or to familial adenomatous polyposis (FAP). A relatively limited number of oncogenes and tumour suppressor genes (most prominently the APC, KRAS and p53 genes) are mutated in the majority of CRCs, with a larger collection of genes that are mutated in subsets of CRC beginning to be defined. (Markowitz and Bertagnolli, 2010)

1.1.1. Genetics of Colorectal Cancer

CRC arises from epithelial cells at the base of intestinal crypts, which accumulate activating oncogenic mutations with concomitant loss of tumour suppressor genes, that confer selective growth advantages, leading to the progression from benign adenoma to adenocarcinoma, as shown in **Figure 1.1.** (Fearon and Vogelstein, 1990) Inactivation of the tumour suppressor gene adenomatous polyposis coli (APC) is viewed as an early initiating event in CRC. The APC protein is an inhibitor of β-catenin, sequestering it in the cytoplasm. In the absence of APC, β-catenin binds to nuclear partners to activate the Wnt signalling pathway, enabling rapid cell division and migration. APC mutations were first identified as giving rise to the FAP form of inherited CRC. Individuals with FAP carry a mutation in one APC allele, with the second APC allele typically inactivated through loss of heterozygosity within the first 30 years of life, which can lead to more than 100 adenomatous polyps developing and an almost 100% risk of developing CRC by the age of 40 years for carriers of the mutated gene. (Groden *et al.*, 1991; Nishisho *et al.*, 1991; Kinzler and Vogelstein, 1996) APC plays an even more prominent role in sporadic colorectal tumours, with 70–80% showing somatic mutations and deletions that inactivate both copies of APC. (Markowitz and Bertagnolli, 2010) In the absence of APC mutations, colorectal tumours can also be initiated by mutations in β–catenin itself, that render the protein resistant to the β-catenin degradation complex. Mutations in other components of the Wnt signalling pathway can also lead to its activation. Mutations in glycogen synthase kinase 3b (GSK3B), a regulator of the Wnt signalling pathway, can also lead to β–catenin activation. GSK3B phosphorylates β-catenin, leading to ubiquitin-mediated degradation. (Morin *et al.*, 1997; Shakoori *et al.*, 2005)

The second key genetic step in CRC development involves mutation of the TP53 gene resulting in inactivation of the p53 pathway. (Baker *et al.*, 1989) Both TP53 alleles are typically inactivated, usually combining a missense mutation that inactivates the transcriptional activity of p53 and a chromosomal deletion of the second TP53 allele. (Baker *et al.*, 1990) Wild-type p53 functions as a key transcriptional regulator of genes that mediate cell-cycle arrest and cell-death upon activation by multiple cellular stresses. Therefore, mutations in p53 may facilitate continued growth and the acquisition of invasive properties in the face of stresses that might otherwise limit tumour cell survival, with TP53 inactivation often coinciding with the transition of large adenomas into invasive carcinomas. (Baker *et al.*, 1990; Markowitz and Bertagnolli, 2010)

The third step in the progression to CRC is the mutational inactivation of transforming growth factor-beta (TGF-β) signalling, which is involved in many cellular processes, including the control of cell growth, cell proliferation, cell differentiation and apoptosis. (Markowitz *et al.*, 1995) In about one third of CRC cases somatic mutations or frameshift deletions inactivate the TGF-β Receptor 2 (*TGFBR2*) gene. TGF-β signalling can also be abolished by mutations or deletions that inactivate downstream TGF-β pathway components, such as SMAD4 or its partner transcription factors, SMAD2 and SMAD3. (Eppert *et al.,* 1996) Mutations that inactivate the TGF-β pathway often correspond with the transition from adenoma to high-grade dysplasia or carcinoma. (Markowitz and Bertagnolli, 2010)

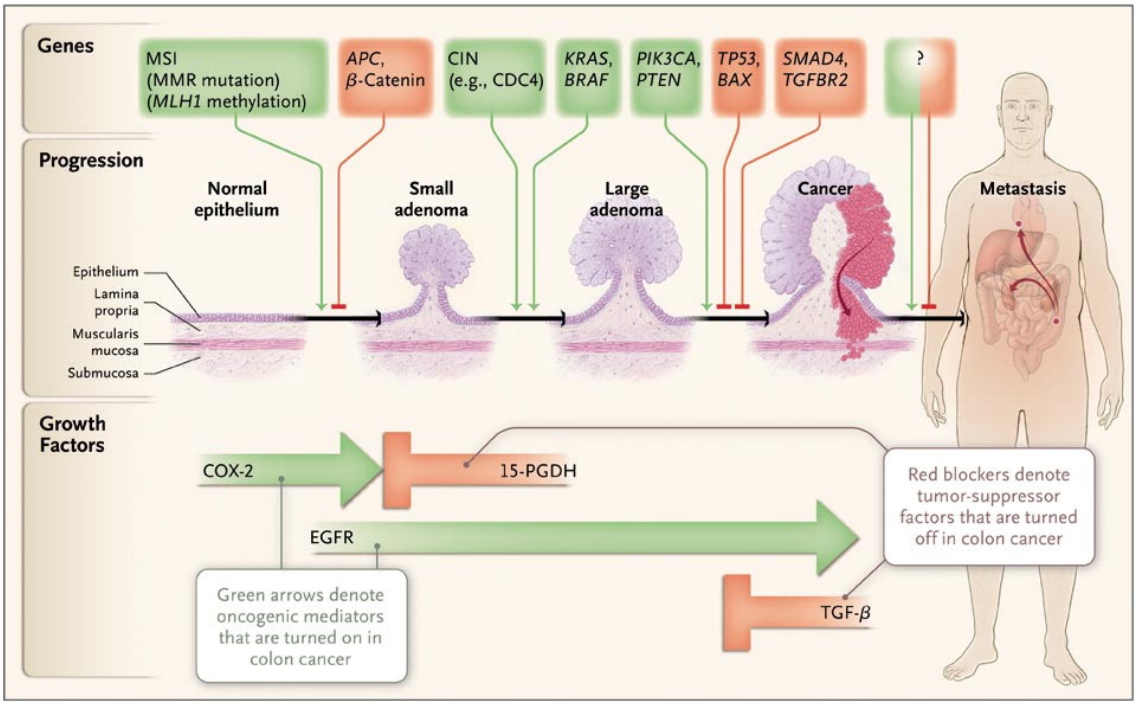

Figure 1.1 Genes and growth factor pathways that drive the progression of colorectal cancer. (Adapted from Markowitz and Bertagnolli, 2010)

In addition to the inactivation of tumour suppressor genes, several oncogenes play key roles in promoting CRC, including KRAS, BRAF, PIK3CA and PTEN. **Table 1.1** lists some of the commonly mutated oncogenes and tumour suppressor genes in CRC. Oncogenic mutations of Ras and BRAF, which activate the mitogen-activated protein kinase (MAPK) signalling pathway, occur in approximately 40% and 5-10% of CRCs respectively. (Bos *et al.*, 1987; Davies *et al.*, 2002) The Ras family of small-G proteins function as molecular switches downstream of multiple different receptor tyrosine kinase (RTK) growth factor receptors, such as the EGFR family. The three Ras family members, KRAS, HRAS and NRAS, are common targets for somatic mutations in many human cancers. (Malumbres and Barbacid, 2003) Mutations in KRAS are most commonly found in CRC, and whilst not required for adenoma initiation, KRAS mutations appear to play a key role in driving the behaviour of advanced CRC cells. (Shirasawa *et al.*, 1993) BRAF is a protein kinase that activates the MAPK effectors MEK1 and MEK2. BRAF mutations have been associated with an altered DNA-methylation phenotype found in CRC, known as CpG island hypermethylation phenotype (CIMP). (Kodama *et al.*, 2002; Jass, 2007)

Phosphatidylinositol-3,4,5-triphosphate (PIP3) is a key second messenger of the phosphatidylinositol 3-kinase (PI3K) pathway which plays a significant role in cellular proliferation, survival and other processes. The formation of PIP3 from PIP2 occurs at the cell membrane by the activity of the class I PI3Ks. (Zhao and Vogt, 2008) Activating somatic mutations of the *PI3KCA* gene occur in approximately 15-25% of CRCs. (Samuels *et al.*, 2004; Wood *et al.*, 2007) PI3KCA encodes the catalytic subunit of PI3K. These mutations activate PIK3CA kinase activity, increasing production of PIP3, allowing for increased cell growth and survival. (Carson *et al.*, 2008)

Less common genetic alterations that may substitute for *PI3KCA* mutations include loss of PTEN protein, a phospholipid phosphatase that mediates de-phosphorylation of PIP3 to PIP2, inhibiting PI3K signalling. (Chalhoub and Baker, 2009) Somatic mutations that inactivate PTEN are found in around 10% of CRCs, however some studies suggest PTEN protein expression may be lost in around 15-20% of CRCs. (Wood *et al.*, 2007; Danielsen *et al.*, 2008) Loss of PTEN expression is observed in both KRAS mutant and KRAS wildtype CRC tumours. (Chalhoub and Baker, 2009; Laurent-Puig *et al.*, 2009; Fearon, 2011)

Gene	Type of mutation	Estimated frequency of alterations
Oncogenes		
KRAS	Point mutations (codons 12, 13, 61)	40% (>75% of mutations are at codon 12)
NRAS	Point mutations (codons 12, 13, 61)	<5%
PIK3CA	Point mutations activating kinase activity	15–25%
BRAF	Point mutations activating kinase activity (e.g., *V600E*)	5–10% (mutations linked to CIMP-positive CRCs)
EGFR	Gene amplification	5–15%
CDK8	Gene amplification	10–15%
CMYC	Gene amplification	5–10%
CCNE1	Gene amplification	5%
CTNNB1	Stabilizing point mutations and in-frame deletions near N terminus	<5%
NEU (*HER2*)	Gene amplification	<5%
MYB	Gene amplification	<5%
Tumour-suppressor genes		
p53	Point mutation, allele loss	60–70% (>95% of point mutations are missense)
APC	Frameshift, point mutation, deletion, allele loss	70–80% (nearly all mutations lead to truncated proteins)
FBXW7	Nonsense, missense, deletion	20%
PTEN	Nonsense, deletion	10%
SMAD4	Nonsense, missense, allele loss	10–15%
SMAD2	Nonsense, deletion, allele loss	5–10%
SMAD3	Nonsense, deletion	5%
TGFβIIR	Frameshift, nonsense	10–15% (>90% of MSI-H CRCs have mutations)
TCF7L2	Frameshift, nonsense	5% (mutations in both MSI-H and MSS CRCs)
ACVR2	Frameshift	10% (>80% of MSI-H CRCs have mutations)
BAX	Frameshift	5% (often one allele in ~50% of MSI-H CRCs)

Table 1.1 Selected recurrent somatic mutations in oncogenic and tumour suppressor genes in CRC. (Adapted from Fearon, 2011)

1.1.2. Genomic Instability: Chromosomal Instability vs. Microsatellite Instability

The acquisition of genomic instability is a crucial feature in CRC tumour development and there are at least 2 distinct pathways in CRC pathogenesis: the chromosomal instability (CIN) and microsatellite instability (MSI) pathways. (Fearon, 2011) Early karyotyping analyses of CRC tumours revealed that many had numerous chromosomal alterations, including frequent losses of chromosomes 18 and 17p, as well as gains of chromosomes 13 and 20. (Muleris *et al.*, 1985; Muleris, Salmon and Dutrillaux, 1990) It was subsequently determined that the majority (~85%) of CRC cases arise through this CIN pathway, which is characterised by widespread imbalances in chromosome number (aneuploidy), loss of heterozygosity and gene deletions or duplications. (Lengauer, Kinzler and Vogelstein, 1997) Key factors that underlie CIN in CRC are poorly defined, but defects in genes that regulate formation of the mitotic spindle, chromosomal segregation and the DNA damage response, contribute to the CIN phenotype. (Leary *et al.*, 2008) Chromosomal instability is an efficient mechanism for causing the loss of a tumour suppressor gene copy, such as APC, p53 and SMAD4. (Grady and Markowitz, 2002; Markowitz and Bertagnolli, 2010)

The MSI pathway is caused by the loss of DNA mismatch repair genes, primarily MLH1 and MSH2, and accounts for the remaining 15% of CRC cases. The inactivation of mismatch repair genes can be inherited, such as in HNPCC, also known as the Lynch syndrome, where patients have germ-line defects in mismatch repair genes. Subsequent inactivation of the second gene allele, gives HNPCC patients an 80% risk of developing CRC within their lifetime. (Bronner *et al.*, 1994; Lynch *et al.*, 2008) Approximately 3% of MSI CRC cases are associated with the Lynch syndrome and the other 12% with sporadic CRC, where methylation-associated silencing of the promotor region of the MLH1 gene inactivates mismatch repair. (Veigl *et al.*, 1998) MSI is characterised by alterations of microsatellite sequences (short tandem repeats of repeated nucleotide sequences ranging in length from 2-7 nucleotides per unit) at many loci across the genome, due to the loss of DNA mismatch repair gene function. High frequency MSI (MSI-H) is characterised by more than 40% of a panel of mononucleotide and dinucleotide sequences. (Thibodeau, Bren and Schaid, 1993) Mutations in microsatellite sequences can inactivate tumour suppressor genes that contain mononucleotide or dinucleotide repeat sequences. The *TGFBR2* gene is inactivated in over 90% of MSI-H CRC cases, due to frameshift mutations of a polyadenine tract in the coding region of the gene. (Markowitz *et al.*, 1995) The majority of CRCs are classified as microsatellite stable (MSS), i.e. they display no microsatellite instability. Some CRC cases

show low-frequency MSI (MSI-L), which have no evidence of mutations of mismatch repair genes. (Vilar and Gruber, 2010) The MSI-L cases do not appear to be significantly different from MSS cases, with regards to tumour pathological features. However, MSI-H CRC tumours have distinct pathological features compared to MSS, including a tendency to arise in the proximal colon, lymphocytic infiltrate (high infiltration with activated CD8+ cytotoxic T-lymphocyte and activated T helper 1 (Th1) cells), and a poorly differentiated, mucinous or signet ring appearance. MSI cases also have improved survival compared to MSS tumours and do not have the same response to chemotherapeutics. (Redston, 2001; Kakar *et al.*, 2004)

Another pathogenic pathway associated with MSI tumours is the CpG island methylator phenotype (CIMP), which is characterised by widespread hypermethylation of CpG islands at several genomic loci. (Issa, Shen and Toyota, 2005) CpG islands is the term used for localised regions of high CpG-dinucleotide content within the genome. The promoter regions of approximately 50% of all genes contain CpG islands. (Issa, 2008) Hypermethylation of CpG islands in the promoter regions of tumour suppressor genes has been linked to their silencing in human malignancies, including CRC. (Esteller, 2008; Berman *et al.*, 2012) The CIMP mechanism suggests that epigenetic events contribute to CRC carcinogenesis. The contribution of epigenetic silencing events to CRC onset/progression remains an ongoing area of study.

1.1.3. The Tumour Microenvironment in Colorectal Cancer

Whilst the emphasis on tumour pathogenesis has previously focused on epithelial cell behaviour and the genetic and epigenetic alterations involved, the importance of the tumour microenvironment and the interaction between stromal and epithelial cells is now widely recognised. During tumour development, a complex tissue is formed composed of cancer cells and multiple distinct cell types, which are derived mainly from the neighbouring mesenchymal stroma. This complex ecology of cells forming the tumour microenvironment, evolves with and provides support to tumour cells during the transition to malignancy, with the functional interactions between tumour and stromal cells sustaining growth and invasion. A major contributor to the tumour microenvironment is inflammation, with chronic inflammation now recognised as both a tumour initiator and promoter. Persistent inflammatory conditions are known to increase the risk of cancer development, e.g. viral infections are related to cervical and liver cancer, and inflammatory bowel diseases such as ulcerative colitis and Crohn's disease increase the risk of developing CRC. (Peddareddigari, Wang and DuBois, 2010; Colangelo *et al.*, 2017)

The tumour microenvironment consists of tumour-infiltrating cells, vasculature, extracellular matrix (ECM) and other matrix associated molecules, as well as an abundance of cytokines and chemokines. The induction of angiogenesis is an important event in the development of most cancers, promoting tumour growth and invasion. In CRC, the microvascular density of a tumour is a prognostic indicator. (Choi *et al.*, 1998) The ECM is composed of macromolecules, including collagen, laminins, fibronectin and proteoglycans, that form a highly organised three-dimensional structure of basement membrane (BM) and interstitial or stromal matrix. The BM is composed of a dense network of collagen type IV and laminin, and acts as a mechanical barrier and organiser of tissue structure. Breakdown of the BM is required for invasive tumour growth, with various types of proteinases involved in ECM turnover, such as matrix metalloproteinases (MMPs). Colon cancer cells can induce secretion of MMP-2 and MMP-9 by stromal cells. (Toda *et al.*, 2006) ECM remodelling is critical for tumour progression and the ECM also provides a reservoir of cytokines and growth factors. (Peddareddigari, Wang and DuBois, 2010)

Local inflammation at the site of a solid malignancy and the secretion of soluble chemoattractants by both cancer and stromal cells results in the infiltration of a large variety

of cells into the tumour microenvironment. CRC tumours are infiltrated by various cell types, such as cancer-associated fibroblasts (CAFs), tumour-associated macrophages (TAMs) and lymphocytes, with the role of these three types in CRC progression described in greater detail in Sections 1.1.3.1-1.1.3.3. Other cell types involved in tumour infiltration include neutrophils, dendritic cells, natural killer (NK) cells, myeloid-derived suppressor cells, endothelial progenitor cells, platelets and mesenchymal stem cells. The dynamic interaction between cancer and stromal cells often promotes tumour cell proliferation, survival and metastasis. The tumour microenvironment can also play a critical role in the development of more advanced and therapy-refractory cancers. Therefore, further understanding of the complex interactions between tumour epithelial and stromal elements will enhance development of therapeutic options and improve clinical outcome in CRC. (Peddareddigari, Wang and DuBois, 2010; Colangelo *et al.*, 2017)

1.1.3.1. Cancer-Associated Fibroblasts (CAFs)

Fibroblasts compose the major stromal population in normal colonic mucosa, responsible for the synthesis and turnover of basement membrane components. (Colangelo *et al.*, 2017) In CRC, the major cellular component of the tumour stroma are CAFs. (Östman and Augsten, 2009) The secretion of factors by cancer cells, such as, platelet-derived growth factor (PDGF), TGF-β, Interleukins 4/6 (IL-4/6) and prostaglandin E (PGE), have been identified as being responsible for fibroblast differentiation into CAFs. (Cirri and Chiarugi, 2011; Hawinkels *et al.*, 2014) Local tissue fibroblasts and fibroblast precursors are generally considered to be the main source of CAFs. However various other cell types, including stellate cells, circulating mesenchymal stem cells and CD34+ fibrocytes, have also been considered as potential sources of CAFs, once recruited into the CRC stroma. (Gascard and Tlsty, 2016) CAFs are still not fully understood, and are mostly defined based on the expression of α-smooth muscle actin (α-SMA), fibroblast activating protein, fibroblast-specific protein-1, platelet-derived growth factor receptors α and β (PDGFR-α, - β) and neuron-glial antigen-2. (Sugimoto *et al.*, 2006; Östman and Augsten, 2009; Augsten, 2014; Chen *et al.*, 2014) CAFs morphologically appear as large, spindle shaped cells with prominent nucleoli and enlarged endoplasmic reticulum and Golgi complex, which reflects

the enhanced secretion of enzymes, growth factors and ECM proteins, involved in tumour microenvironment remodelling. (Paunescu *et al.*, 2011)

CAFs are a source of a large range of growth factors, including TGF-β, epidermal growth factor (EGF), hepatocyte growth factor (HGF), insulin-like growth factor (IGF)-1, IGF-2 and VEGF, that promote tumour growth and invasion. (Östman and Augsten, 2009) CAFs also express chemokines, interleukins, cell-surface molecules like integrin-α11, proteases such as MMP-2 and ECM constituents like osteopontin, that stimulate processes such as inflammation and angiogenesis, and promote tumour cell proliferation, migration, invasion and survival. (Joesting *et al.*, 2005; Yang, Lin and Liu, 2006; Taniwaki *et al.*, 2007; Zhu *et al.*, 2007; Cirri and Chiarugi, 2011) CAF-derived chemokines such as CXCL12 and CXCL14 recruit macrophages and other immune cells into the tumour microenvironment, which also contributes to tumour growth. (Orimo *et al.*, 2005; Östman and Augsten, 2009) CAFs have also been found to mediate tumour cell resistance to chemotherapeutics in CRC. Soluble factors secreted by CAFs trigger a cell signalling cascade, inducing the translocation of AKT, Survivin and p38 to the nucleus of CRC tumour cells, protecting them from the action of conventional chemotherapy used in CRC treatment. (Gonçalves-Ribeiro *et al.*, 2016) CAFs in CRC typically express high levels of PDGFR-β, which is associated with advanced stage of disease and an increased metastatic potential. The blockade of PGFR signalling pathways in tumour-associated stromal cells using drugs such as imatinib, has been shown to inhibit the progressive growth and metastasis of colon cancer cells. (Kitadai *et al.*, 2006)

1.1.3.2. Tumour-Associated Macrophages (TAMs)

TAMs are usually the most abundant immune population found in the tumour microenvironment. (Colangelo *et al.*, 2017) TAMs derive from circulating blood monocytes that are recruited to the tumour site by chemokines such as CCL2/3/4/5/22, cytokines such as colony-stimulating factor-1 (CSF-1), and growth and angiogenic factors such as VEGF-A and PDGF. (Lewis and Pollard, 2006; Sica and Bronte, 2007; Sica, Allavena and Mantovani, 2008) The presence of low IL-12 and high IL-10 levels in the tumour microenvironment induces the differentiation of monocytes into mature TAMs. (Fricke and Gabrilovich, 2006) Macrophages are highly plastic and can polarise into two subtypes with different phenotypes

depending on microenvironment stimuli: classical M1 (anti-tumour) or alternate M2 (pro-tumour). (Mantovani *et al.*, 2004; Martinez and Gordon, 2014; Chanmee *et al.*, 2014)

M1 macrophages are classified as pro-inflammatory and are activated in response to microbial products or interferon-γ (IFN-γ), and produce high levels of IL-12, IL-23, nitric oxide and oxygen intermediates, and promote adaptive immunity through increased antigen presentation and expression of costimulatory molecules. M1 macrophages are part of the Th1 response and are potent effectors against intracellular pathogens and tumour cells. (Chanmee *et al.*, 2014) M2 macrophages are classified as anti-inflammatory and are activated in response to signals such as IL-4, IL-13, IL-10, immunoglobulin complexes and Toll-like receptor (TLR) ligands. M2 macrophages are part of the Th2 response, they downregulate MHC class II expression, stimulate regulatory T-cell differentiation and influence the anti-inflammatory response with increased expression of IL-12 and TGF-β. TAMs with M2 polarisation are a major tumour infiltrating cell population, where they promote tumour growth and metastasis through the induction of angiogenesis by secreting VEGF, and enhance tumour cell invasion by the secretion of MMP-1, -2, -9, and cathepsins B and D, which are involved in ECM breakdown. (Martinez and Gordon, 2014; Stockmann *et al.*, 2014) High TAM density in the tumour microenvironment is now recognised as a poor prognostic sign in various human cancers. (Lewis and Pollard, 2006) However their role in CRC, and whether they exert pro- or anti-tumour activity, is controversial.

Some studies indicate that macrophages have anti-tumour activity in CRC and are associated with improved disease free survival. Whilst other studies indicate that high macrophage infiltration is correlated with tumour growth, progression and aggressiveness. (Ohno *et al.*, 2002; Erreni, Mantovani and Allavena, 2011) Studies on the pro-tumour activity of TAMs in CRC, include a study by Kaler *et al.*, (2009) showing that IL-1β secreted by TAMs promote Wnt signalling in colon cancer cells, supporting tumour growth. TAM-derived IL-6 has been shown to induce STAT3-mediated IL-10 production in tumour cells, which has been correlated with poor prognosis. (Herbeuval *et al.*, 2004) The role of TAMs in CRC seems to depend on their density and localisation within the tumour mass. TAM accumulation along the tumour margin has been most frequently associated with longer patient survival. This could perhaps be due to TAMs at the invasive margin being more likely to be outside of the suppressive tumour microenvironment and may produce cytotoxic molecules such as reactive oxygen species, nitric oxide and tumour necrosis factor-α (TNF-

α). Macrophages along the tumour margin have been shown to induce apoptosis in cancer cells by a Fas ligand-dependent manner. (Sugita *et al.*, 2002) High levels of macrophage infiltration at the invasive front of CRC tumours has been correlated with improvement in both hepatic metastasis and overall survival, indicating a protective role for TAMs in CRC. Conversely, low levels of macrophage infiltration have been associated with more advanced disease and a higher rate of vascular invasion and lymph node metastasis. (Funada and Moouchi, 2003; Forssell *et al.*, 2007; Zhou *et al.*, 2010) However, in contrast with these studies, Bailey *et al.*, (2007) reported that counting macrophages not only at the tumour margin but in all areas within the tumour, including necrotic areas, macrophage accumulation was not a good prognostic indicator.

It therefore appears that macrophages have contradictory roles within the CRC tumour microenvironment, with the localisation of TAMs appearing to be of importance as to whether they exhibit pro- or anti-tumour activity. Macrophages along the tumour margin are likely to have less exposure to cancer cell derived cytokines and are located in a less hypoxic area, perhaps enabling differentiation into an anti-tumour phenotype. Whereas macrophages within the tumour mass, are susceptible to cancer cell signals, creating a positive feedback loop between cancer cells and TAMs, promoting tumour progression.

1.1.3.3. Tumour-Infiltrating Lymphocytes

T-lymphocytes are part of the adaptive immune response, which can shape the development of malignancy and its response to therapy through direct or indirect contact with tumour cells. Antigens expressed by tumour cells can become targets for T-cell-mediated adaptive immune response. Galon *et al.*, (2006) first demonstrated the relevance of specific immune cell populations on prognosis in CRC patients, with the type, density and location of T-cells within the tumour found to be a better predictor of patient survival compared to the histopathological methods currently used to stage CRC. High lymphocyte infiltration of CD8+ cytotoxic T-lymphocytes (CTLs) and T helper 1 (Th1) cells is associated with relapse-free and overall survival in CRC. T helper cells are also known as CD4+ T-cells. They directly interact with MHC class II molecules on the surface of antigen-presenting cells and influence the behaviour of cell types that they "help", including CTLs, B-cells and macrophages. T helper cells can differentiate into several subtypes, including Th1, Th2, Th3,

Th17, Th9 or TFH, which facilitate different types of immune response based on the secretion of different cytokines. The anti-tumour activity associated with the Th1 response is facilitated through IFN-γ secretion and the control of macrophage killing of tumour cells. (Zhu, Yamane and Paul, 2010; Tosolini *et al.*, 2011)

It was subsequently discovered that virtually all primary CRC tumours displaying high infiltration with activated CD8+ CTLs and Th1 cells belong to the MSI phenotype. The density of CTL infiltration was found to positively correlate with the total number of frameshift mutations within the MSI tumours, suggesting that these lead to the production of immunogenic neo-peptides that are recognised by antigen-specific tumour-infiltrating lymphocytes. (Llosa *et al.*, 2015; Maby *et al.*, 2015) The anti-tumour activity of a Th1/CTL-dominant immune response is selectively counterbalanced in MSI tumours by upregulation of multiple immune checkpoints, including cytotoxic T-lymphocyte-associated antigen 4 (CTLA-4), programmed cell death protein 1 (PD-1), and PD1 ligand 1 (PD-L1). This explains why MSI tumours are not naturally eliminated despite a hostile Th1/CTL microenvironment. The blockade of immune checkpoints is an emerging strategy in cancer treatment, with anti-CTLA-4, anti–PD-1 and anti–PD-L1 antibodies shown to induce significant and durable tumour regression in patients with melanoma, renal cancer and non-small-cell lung cancer. (Hodi *et al.*, 2010; Brahmer *et al.*, 2012; Hamid *et al.*, 2013; Topalian *et al.*, 2014) CRC had been considered a non-responding histology to PD-1 pathway blockade, after studies demonstrated a very low response rate to PD-1 or PD-L1 blockade in CRC patient cohorts. However, there was an insufficient number of patients to potentially define subsets of CRC that might be more amenable to checkpoint blockade. Based on the above findings, that suggest blockade of immune checkpoints may be selectively efficacious in the MSI subset of CRC, clinical trials have been initiated to test PD-1 blockade in CRC patients identified as MSI. (Llosa *et al.*, 2015)

Conversely, T-cell infiltrations associated with poor outcomes, include Th17 and regulatory T (Treg) cell infiltration. Th17 cells produce high levels of TNF-α, IL-2, and IFN-γ, with high Th17 cell infiltration in CRC tumours associated with a poor prognosis. (Tosolini *et al.*, 2011) CD4+ T-cells that express the forkhead box P3 (FOXP3) transcription factor, function as Treg cells, pivotal mediators of immune suppression. Treg cells suppress the activation, proliferation and effector functions of a wide range of immune cells, including CD4+ and CD8+ T-cells, NK and B-cells *in vitro* and *in vivo*, hindering an effective immune response

against cancer cells. Treg cells regulate the immune response by a number of mechanisms, including secretion of immunosuppressive molecules (IL-10, TGF-β and IL-35), cytolytic functions via a variety of mediators such as granzyme B, and IL-2 deprivation-mediated apoptosis of effector CD4+ T-cells. (Zhang *et al.*, 2015) The accumulation of Treg cells at tumour sites has been associated with faster angiogenesis through VEGF production. (Facciabene, Motz and Coukos, 2012) CRC tumours infiltrated with Treg cells have significantly worse prognosis. (Saito *et al.*, 2016)

1.2. Pancreatic Cancer

Pancreatic cancer is the fourth leading cause of cancer death in the Western world. Pancreatic ductal adenocarcinoma (PDAC) is the most common pancreatic malignancy, with a median survival lasting months and a dismal 5-year survival rate of just 5%. (Wood and Hruban, 2015) Survival rates have remained relatively unchanged over the past 25 years. This poor prognosis is due to a lack of early symptoms, meaning PDAC is generally not diagnosed until an advanced stage of disease, with presentation of distant metastases. PDAC is also highly resistant to both radiation and chemotherapy. (Hermann *et al.*, 2007) The liver is the most common site of metastasis, followed by the peritoneum and lungs. (Iacobuzio-Donahue *et al.*, 2009) Surgery remains the only treatment with curative potential, however approximately just 20% of patients are eligible for surgical resection at the time of diagnosis. Moreover, those patients who do undergo resection frequently exhibit a high incidence of local recurrence, lymph node and hepatic metastasis, and peritoneal dissemination. (Pierantoni *et al.*, 2008; Birnbaum *et al.*, 2016) The chemotherapeutic drug gemcitabine remains the standard of care for patients with advanced PDAC. Studies on combining gemcitabine with other chemotherapeutics and targeted agents, often gave disappointing results. A chemotherapy regimen combining 5-FU, leucovorin, irinotecan, and oxaliplatin (FOLFIRINOX) was shown to nearly double overall survival compared to gemcitabine, at the expense of a manageable but increased toxicity, limiting its use to good performance status patients. But overall survival was still less than 12 months. (Teague, Lim and Wang-Gillam, 2015) Therefore, there is a desperate need for new and targeted therapeutic strategies that can overcome the drug-resistance of PDAC and improve the clinical outcome for patients. (Iovanna *et al.*, 2012)

1.2.1. Genetics of PDAC

PDAC arises from precursor lesions that develop in the pancreas. Three main pre-invasive lesions have been identified, pancreatic intraepithelial neoplasia (PanIN), intraductal papillary mucinous neoplasms (IPMNs) and mucinous cystadenomas (MCNs). The majority of PDACs arise from PanINs, with IPMN- or MCN-induced PDAC occurring only sporadically. PanINs show a spectrum of divergent morphological alterations relative to normal ducts with increasing cell proliferation and dysplastic growth. PanINs display three different stages of progression before giving rise to PDAC - PanIN-1, PanIN-2 and PanIN-3, which are categorised based on their morphological degree of dysplasia. PanIN-1 and -2 are low grade, with PanIN-3 classified as high grade and is essentially a carcinoma-in-situ. The genetic evolution from early PanIN to invasive PDAC takes approximately 12 years, involving the sequential acquisition of the driver gene mutations that characterise PDAC. **Figure 1.2** shows a representation of the progression from PanIN to PDAC, and the genetic and microenvironmental factors involved. (Bardeesy and DePinho, 2002; Brosens *et al.*, 2015)

The genes most commonly altered in PDAC are KRAS, CDKN2A, TP53 and SMAD4, and are referred to as the four driver genes of PDAC development. (Iovanna *et al.*, 2012) KRAS encodes a small GTPase involved in signal transduction of growth factor mediated signal transduction pathways, such as EGF signalling. Activating KRAS mutations are the earliest genetic change that occur in the progression to PDAC, and are the most commonly mutated oncogene, occurring in >90% of PDACs. Point mutations are found at codons 12, 13 and 61 in KRAS, leading to the generation of a constitutively active form of ras, which binds to GTP, giving uncontrolled stimulation signals to downstream signalling cascades. This has a number of cellular effects, including the induction of proliferation, survival and invasion. (Moskaluk, Hruban and Kern, 1997; Shields *et al.*, 2000; Fokas *et al.*, 2015)

The tumour suppressor gene p16/CDKN2A, which encodes a critical cell cycle regulator, is inactivated in >90% of PDACs. Loss of CDKN2A function can occur by mutation, homozygous deletion or epigenetic silencing by promotor hypermethylation. Loss of CDKN2A typically occurs in moderately advanced, PanIN-2 precursor lesions. (Schutte *et al.*, 1997) Germline mutations in CDKN2A are associated with the familial atypical mole-malignant melanoma (FAMMM) syndrome, which in addition to a very high incidence of

melanoma, also confers a 13-fold increased risk of developing pancreatic cancer. (Borg *et al.*, 2000; Fokas *et al.*, 2015)

Mutations in the tumour suppressor gene TP53 are reported in approximately 75% of PDACs. The p53 protein is a master regulator of genome integrity and plays an important role in cell cycle regulation and induction of apoptosis. Loss of p53 typically occurs through a missense mutation and loss of the second allele, which can lead to uncontrolled cell growth and increased cell survival. (Vogelstein, Lane and Levine, 2000) Inactivation of TP53 occurs later in the malignant progression to PDAC, in PanIN-3 precursor lesions. (Costa, Kern and Hruban, 1994) PDAC tumours have profound aneuploidy and complex cytogenetic rearrangements, and loss of TP53 probably facilitates the widespread genetic instability that occurs in PDAC. (Gorunova *et al.*, 1998; Bardeesy and DePinho, 2002)

Loss of the tumour suppressor gene SMAD4, occurs in approximately 50% of PDACs. (Cowgill and Muscarella, 2003) SMAD4 inactivation occurs by either intragenic mutation and loss of the second allele or by homozygous deletion, and occurs relatively late in pancreatic carcinogenesis, in PanIN-3 lesions. (Yachida and Iacobuzio-Donahue, 2013) SMAD4 encodes a transcriptional regulator that is a key component in the TGF-β signalling cascade. TGF-β inhibits the growth of most normal epithelial cells and promotes apoptosis. Remarkably, the inactivation of SMAD4 abolishes the tumour suppressive functions of TGF-β but maintains some tumour-promoting TGF-β responses, such as epithelial-mesenchymal transition (EMT), which makes cells more invasive. (Massagué, Blain and Lo, 2000) Loss of SMAD4 is more frequent in poorly differentiated PDAC tumours, and is associated with poorer survival and presence of distant metastases. (Levy and Hill, 2005; Iacobuzio-Donahue *et al.*, 2009; Fokas *et al.*, 2015)

However, only a minority of patients have mutations in all four driver genes of PDAC development, highlighting the genetic heterogeneity of PDAC. Several other genes are involved in PDAC formation, such as the tumour suppressor genes BRCA2 and LKB1, and less common genetic alterations in PDAC continue to be described. (Bardeesy and DePinho, 2002) A recent transcriptional classification of PDAC defined 4 subtypes: squamous, pancreatic progenitor, immunogenic and aberrantly differentiated endocrine exocrine (ADEX), that correlate with histopathological characteristics. Squamous tumours are enriched for TP53 and KDM6A mutations, hypermethylation of pancreatic endodermal cell-

fate determining genes and are associated with poor prognosis. Pancreatic progenitor tumours express genes involved in early pancreatic development. ADEX tumours display upregulation of genes involved in KRAS activation, and exocrine and endocrine differentiation. Whilst immunogenic tumours contain upregulated immune networks including pathways involved in acquired immune suppression, such as CTLA-4 and PD-1, inferring therapeutic opportunities with immune checkpoint inhibitors. (Bailey *et al.*, 2016) This shows the importance in identifying the various genetic profiles associated with PDAC, as it could be utilised to help stratify patients to different therapies.

PDACs also overexpress many growth factors and their receptors, including the EGF family, VEGF, fibroblast growth factor (FGF), Cripto-1 growth factor (CRGF), TGF-α and many cytokines such as, TGF-β, TNF-α, and IL-1, -6 and -8. (Fokas *et al.*, 2015) The Sonic hedgehog (Shh) and Notch signalling pathways, are two common pathways involved in pancreatic organogenesis and development, and have been implicated in PanIN initiation and tumour growth. Shh is not expressed in normal adult pancreas but is found in up to 70% of PDAC tumours. Shh promotes cell migration and invasion and also contributes to the formation of stromal desmoplasia by modifying the differentiation of pancreatic stellate cells and fibroblasts. Shh also enhances tumour growth via a paracrine mechanism, whereby Shh secreted by tumour cells induces hedgehog-target genes in the surrounding stromal tissue. (Berman *et al.*, 2003; Feldmann *et al.*, 2007) The multiple alterations in oncogenes and tumour suppressor genes in conjunction with the overexpression of mitogenic and angiogenic growth factors and their receptors that activate aberrant autocrine and paracrine pathways combine to contribute to the biological aggressiveness of PDAC. (Gorunova *et al.*, 1998; Bardeesy and DePinho, 2002)

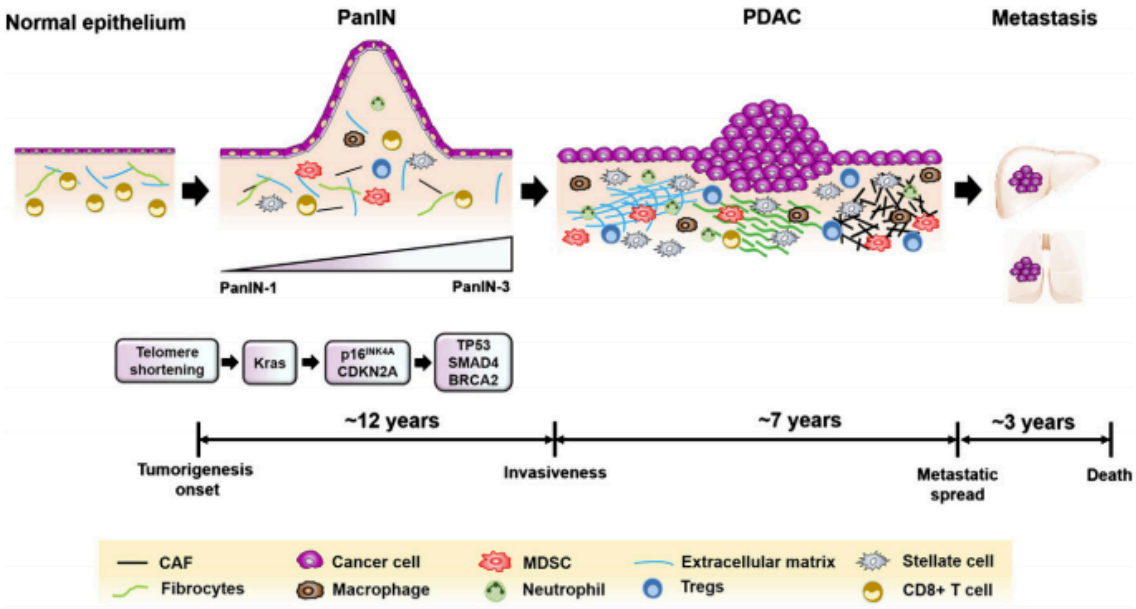

Figure 1.2 Tumour microenvironment and progression in PDAC. PDAC develops from PanIN, a well-defined precursor lesion. Tumour progression is associated with genetic and biological alterations. Telomere shortening and KRAS mutations occur early during pancreatic tumourigenesis (PanIN-1) followed by inactivating mutations of CDKN2A (PanIN-2) and late mutations in TP53, SMAD4 and BRCA2 (PanIN-3). In a similar fashion, progression of PanIN to PDAC is characterised by accumulation of the desmoplastic stroma that drives immunosuppression, tumour growth, invasiveness and metastatic spread. Genetic studies have shown that the average time from early tumourigenesis to patient death from metastatic disease is approximately 22 years. CAF, cancer-associated fibroblast; Treg, regulatory T cell; MDSC, myeloid-derived suppressor cell. (Adapted from Fokas *et al.*, 2015)

1.2.2. The Tumour Microenvironment in PDAC

PDAC is characterised by an intense stromal desmoplastic reaction surrounding the cancer cells, that constitutes more than 80% of the tumour volume. (Kleeff *et al.*, 2007) Desmoplasia results from the extensive proliferation of CAFs and the significant overproduction of ECM, which results in increased stiffness, solid stress and interstitial fluid pressure in the tumour. The PDAC tumour microenvironment is also characterised by a chaotic vascular morphology with low vessel density, and immature, leaky, collapsed vessels. This all contributes to the overall tissue heterogeneity in PDAC, the impaired delivery of oxygen and nutrients, and to chemotherapy and radiation resistance. (Provenzano *et al.*, 2012; Neesse *et al.*, 2013) Other components of the desmoplastic stroma include, pancreatic stellate cells (PSCs), macrophages, inflammatory cells, blood vessels, lymphatic vessels, pericytes, bone marrow-derived cells (BMDCs) and stem cell-like cells. The components of the desmoplastic stroma are displayed in **Figure 1.3**. The complete mechanisms of stroma formation are still being uncovered. PDAC cells produce several modulating growth factors that can alter the adjacent stroma, which in turn release cytokines, pro-tumour growth factors and proteases that form a positive feedback interaction loop to activate both cancer and stromal cells to enhance tumour growth and progression. (Fokas *et al.*, 2015; Nielsen, Mortensen and Detlefsen, 2016)

CAFs are the main effector cells in the desmoplastic reaction, producing a wide variety of ECM molecules and cytokines. They display a myofibroblast-like phenotype, characterised by a spindle shape and the expression of α-SMA. CAFs can originate from different cellular sources, with the most important source in PDAC, considered PSCs. PSCs are also the main effector cells in the fibrotic process of chronic pancreatitis. (Luttenberger *et al.*, 2000; Erkan *et al.*, 2012) PSCs are characterised by their stellate morphology and the presence of vitamin A storing lipid droplets. (Bachem *et al.*, 1998) Quiescent PSCs (qPSCs) in normal pancreas become activated during tissue injury or carcinogenesis, attaining a state called activated PSCs (aPSCs), where they develop a myofibroblast-like phenotype. Factors that activate qPSCs include, PDGF, TGF-β, TNF-α, IL-1, IL-6 and IL-10. (Mews *et al.*, 2002) Other cellular sources of CAFs include resident fibroblasts and BMDCs. (Scarlett, 2013; Augsten, 2014) The cross talk between CAFs and PDAC cells promotes their mutual proliferation and differentiation. CAFs have also been implicated in the metastasis of PDAC cells. CAFs modulate the expression of adhesion molecules and downregulate the expression of E-cadherin, cytokeratin 19 and β-catenin in PDAC cells, increasing their invasiveness.

(Froeling *et al.*, 2009; Kikuta *et al.*, 2010) In a mouse model of PDAC, CAFs followed PDAC cells to the metastatic sites, suggesting CAFs could play a role in the settlement of metastatic PDAC cells. (Xu *et al.*, 2010) CAFs have also been shown to protect PDAC cells from radiation and chemotherapy. (Hwang *et al.*, 2008)

The desmoplastic stroma in PDAC also contains large numbers of inflammatory cells, including macrophages, T-cells, mast cells and neutrophilic granulocytes. Inflammatory cells play multiple opposing roles in PDAC progression, with both anti- and pro-tumour phenotypes. High levels of M2 macrophages and neutrophils are associated with shorter survival in PDAC, whilst high levels of M1 macrophages are associated with longer survival. M2 macrophages express angiogenic and proliferation-promoting cytokines and chemokines which contribute to tumour progression. Large numbers of M2 macrophages correlate with lymph node metastases, which could be explained by their production of VEGF, leading to an increased number of peritumoural lymph vessels. (Schoppmann *et al.*, 2002; Ino *et al.*, 2013) High mast cell infiltration has also been correlated with the number of lymph node metastases in PDAC. (Esposito *et al.*, 2004) Cytotoxic CD8+ T-cells are anti-carcinogenic, resulting in the elimination of PDAC cells. High levels of CD4+ or CD8+ T-cells are associated with longer survival, whilst high levels of Treg cells are associated with shorter survival in PDAC. Treg cell infiltration suppresses the anti-cancer immune response through inhibitory cytokines, inducing immune invasion in PDAC. PDAC cells are suggested to promote the upregulation of Treg cells in part through the secretion of TGF-β. (Liyanage *et al.*, 2002, 2006)

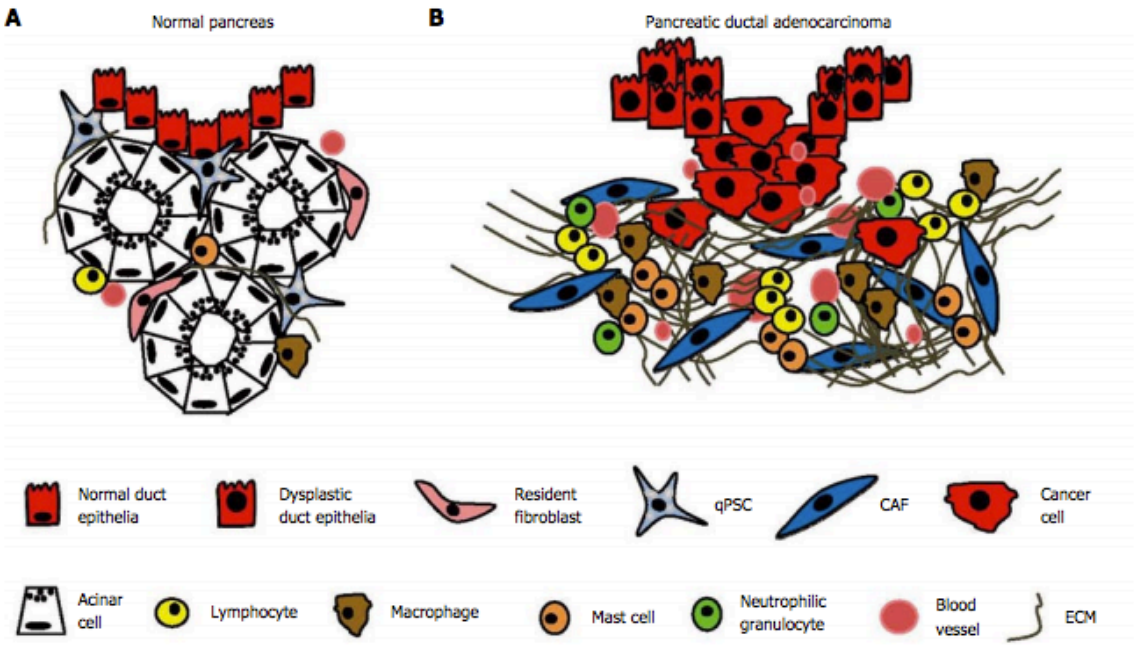

Figure 1.3 Desmoplastic reaction in PDAC. A: Normal pancreas consists of acini with acinar cells and pancreatic ducts lined by epithelial cells. Quiescent pancreatic stellate cells (qPSCs) and interlobular fibroblasts are located in the periacinar space. Small numbers of T-cells are observed, and B-lymphocytes, plasma cells, and eosinophilic and neutrophilic granulocytes are very rare. The extracellular matrix (ECM) is largely limited to thin interlobular septa and pancreatic ducts. **B:** In PDAC, cancer cells permeate the basal membrane of dysplastic pancreatic ducts and invade the surrounding tissue. This invasion is accompanied by a strong desmoplastic reaction in which CAFs, arising mainly from qPSCs, synthesise an abundance of ECM proteins. Lymphocytes, macrophages, and mast cells infiltrate the peritumoural stroma. There is an increased need for oxygen and nutrients, leading to increased angiogenesis. (Adapted from Nielsen, Mortensen and Detlefsen, 2016)

1.2.2.1. Targeting the PDAC Tumour Microenvironment

The standard chemotherapeutic drug used in PDAC treatment has limited effect on patient survival. Numerous studies have documented the tumour-promoting functions of key components of the desmoplastic stroma, leading to significant interest in developing new treatment strategies to target the PDAC microenvironment. However, promising preclinical trials have often not effectively translated into the clinical setting. Subsequent conflicting reports on the precise role of the tumour microenvironment in PDAC, suggests further research is required to effectively target stromal components that will improve clinical outcome for patients.

Due to the observed tumour promoting role of CAFs, it was assumed that a decrease in the CAF population would result in a decrease in PDAC proliferation and migration and an increased response to chemotherapy. However, studies on the consequences of CAF depletion in the PDAC stroma have been conflicting. Olive *et al.*, (2009) first demonstrated the potential in disrupting stromal desmoplasia in a mouse model of PDAC. Treatment with IPI-926, an inhibitor of the Shh pathway, led to depletion of α-SMA positive CAFs and the desmoplastic stroma, increasing tumour vascularisation and drug delivery, and improving overall survival compared to controls. These findings suggest that stromal desmoplasia confers chemoresistance to PDAC, at least partly through decreased drug penetrance. However, phase I and II trials with IPI-926 in combination with FOLFIRINOX or gemcitabine, were closed early due to poor clinical performance, with a shorter median survival indicated in patients receiving the treatment. (Ko *et al.*, 2016) Studies have found that the desmoplastic stroma does not only form a barrier that reduces tumour perfusion and hampers effective drug delivery, it might also reduce the ability of PDAC cells to invade surrounding tissues and metastasise. A smaller number of α-SMA positive CAFs in the PDAC tumour microenvironment has been associated with more invasive tumours and decreased survival. (Özdemir *et al.*, 2014) The Vitamin D analogue calcipotriol, decreases α-SMA expression and induces quiescence in CAFs *in vitro*. In a mouse model of PDAC, the administration of calcipotriol with gemcitabine resulted in a significant reduction in tumour size and increase in median survival. (Sherman *et al.*, 2014) This suggests that stromal reprogramming to a more quiescent state rather than its total depletion could have therapeutic effect in PDAC.

The dense desmoplastic stroma in PDAC is associated with high interstitial pressure and collapsed blood vessels. This hypoxic microenvironment stimulates the production of pro-angiogenic molecules, such as VEGF and FGF, by PDAC cells and stromal cells, such as TAMs and mast cells. (Koong *et al.*, 2000; Büchler *et al.*, 2003) VEGF is an important unfavourable prognostic marker in PDAC, with a significant association found between high VEGF expression and PDAC recurrence. (Niedergethmann *et al.*, 2002) However, clinical trials combining the VEGF inhibitors, Bevacizumab or Axitinib, with gemcitabine found no improvement in overall survival compared to patients receiving gemcitabine alone. (Kindler *et al.*, 2010, 2011) The failure of VEGF inhibitors to improve outcomes in PDAC, could be explained by the poor vascularisation already present in PDAC tumours. Inhibitors of angiogenesis could result in further reduction of chemotherapeutic drug delivery to the tumour. This is supported by studies in mouse models of PDAC, where stromal depletion, resulted in increased tumour vascularisation and drug diffusion, and improved overall survival. (Olive *et al.*, 2009) Therefore, it appears that a more precise modulation of tumour vascularisation is likely required to achieve therapeutic effect in PDAC.

The PDAC tumour microenvironment displays several immunosuppressive properties, suggesting the potential for immune checkpoint therapy in PDAC treatment. Three well described inhibitory checkpoint molecules, CTLA-4, PD-1 and PD-L1, are expressed in the PDAC tumour microenvironment, enabling the tumour to suppress and evade the T-cell mediated immune response. Inhibitors of these immune checkpoints, allow the recognition of tumour cells by T-cells, enabling their elimination. Promising results have been achieved with immune checkpoint inhibitors in the treatment of malignant melanoma, non-small-cell lung cancer and renal cancer, in terms of tumour regression and overall survival. (Sharma and Allison, 2015) Similar strategies are under investigation for PDAC treatment, but have so far achieved limited success. A phase II trial of the anti-CTLA-4 mAb Ipilimumab did not show an acceptable response as a single-agent therapy in PDAC. (Royal *et al.*, 2010) A phase I trial of the PD-LI inhibiting antibody BMS-936559 in patients with selected advanced cancers, showed no objective response in PDAC patients, compared to patients with ovarian cancer, renal cancer, melanoma and non-small-cell lung cancer. (Brahmer *et al.*, 2012) These initial results of immune checkpoint inhibitor treatment in PDAC have not been promising, however studies are still in the relatively early stages, and indicate that further research is needed. Further knowledge on the complex PDAC microenvironment and the identification

of patients most likely to respond to immune checkpoint blockade, could increase the efficacy and response rate to immune checkpoint inhibitors in PDAC. (Nielsen, Mortensen and Detlefsen, 2016)

Other strategies to target the tumour microenvironment and enhance the anti-tumour immune response have shown more promising results. CD40, a member of the TNF-receptor superfamily, is expressed in a wide variety of cells, including monocytes, macrophages, B-cells, dendritic cells and fibroblasts. (van Kooten and Banchereau, 2000) CD40 activation is involved in the T-cell dependent anti-tumour response. Activation of CD40 by agonist antibodies was found to increase the effect of gemcitabine in PDAC, through the activation of macrophages in the tumour stroma. (Beatty *et al.*, 2011) A subsequent phase I trial of CP-870,893, a mAb specific for the agonist CD40, in combination with gemcitabine, was well tolerated in patients with advanced PDAC, and was associated with immune activation and anti-tumour activity. This promising result calls for Phase II studies. (Beatty *et al.*, 2013)

Overall, attempts at targeting the tumour microenvironment in PDAC have been disappointing to date. The precise role of the tumour stroma in PDAC is currently controversial, due to conflicting reports on the activity of various stromal components. Early studies suggested that large numbers of CAFs indicated a poor prognosis in PDAC, whereas more recent studies have indicated that depletion of CAFs promotes tumour aggressiveness. It appears that stromal reprogramming, such as the induction of quiescence in CAFs, rather than stromal depletion, could represent a more appropriate treatment strategy in PDAC. Such strategies might also only be effective at certain stages of PDAC development and progression. Due to the complex interplay of the main components of the tumour stroma, treatment strategies that block single isolated factors are likely to be ineffective. Further understanding is required of the complex interplay of stromal components, and the distinction of various molecular subtypes in PDAC, to identify distinct combination therapies that can be given to increase efficacy and response rate. (Nielsen, Mortensen and Detlefsen, 2016)

1.3. Antibodies in Cancer Therapeutics

Chemotherapy is the main mode of systemic therapy for cancer treatment and can effectively treat advanced cancer, especially when combined with surgery and radiation therapy for locally advanced disease. (Landmann and Weiser, 2005) However, chemotherapeutic agents do not preferentially accumulate in tumours and toxicity to rapidly dividing and other normal cells limit the clinical application of chemotherapeutic drugs. (Krall, Scheuermann and Neri, 2013; Damelin *et al.*, 2015) Molecular targeted therapies, that target specific molecules in cancer cells can overcome some of these limitations. Antibodies have historically been considered as ideal for molecular targeting because of their highly specific binding to antigens. The development of monoclonal antibody (mAb) technology provided the capability to feasibly generate antibodies with required specificities to a molecular target. (Kohler and Milstein, 1975) First generation antibodies were derived from immunised hosts (mainly rodent) that, despite being a significant achievement, had limited clinical application due to their immunogenicity in humans and poor ability to induce human immune effector responses.

The development of genetic engineering approaches and newly developed antibody engineering techniques provided the ability to generate chimeric or humanised antibodies to circumvent these problems. (Winter and Milstein, 1991) They also provided the ability to alter antibody characteristics including size, affinity, half-life and bio-distribution, and to produce structurally modified antibodies, such as bispecific antibodies (BsAbs). Typical antibodies, such as IgG, are divalent but monospecific, with each Fab arm recognising the same epitope of the target antigen. BsAbs exhibit dual functionality, with each Fab arm capable of binding two different epitopes, either of the same or different target antigens. BsAbs can more effectively redirect immune effector cells to tumour cells compared with monospecific antibodies. (Fan *et al.*, 2015) A number of BsAbs have been approved for clinical use including Catumaxomab, which binds to CD3 and EpCAM, and is used for the treatment of malignant ascites in patients with metastatic cancer. (Linke, Klein and Seimetz, 2010) Based on these advancements in antibody engineering techniques, antibody-based therapies have achieved considerable success in recent years, with a range of antibody-based biopharmaceuticals produced to treat major diseases, including cancer, inflammation and autoimmune disorders. The field of antibody-based therapeutics is continuing to grow and evolve. (Scott, Wolchok and Old, 2012; Ayyar, Arora and O'Kennedy, 2016; Gébleux and Casi, 2016)

1.3.1. Unconjugated mAbs

Monoclonal antibodies used in cancer therapy, include unconjugated mAbs, which elicit their effect by binding to soluble or membrane bound antigens, such as growth factors and receptors, thus blocking the target signalling pathway. When the signalling through these pathways is diminished in the tumour, it can result in loss of cellular activity, inhibition of proliferation, activation of apoptosis or cells being re-sensitised to chemotherapeutic agents. (Suzuki, Kato and Kato, 2015) Unconjugated mAbs have been approved for the treatment of both haematological and solid malignancies. Rituximab, targeting CD20, has seen considerable success in the treatment of non-Hodgkin's lymphoma and chronic lymphocytic leukaemia. In solid tumours, unconjugated mAbs have been most successful targeting VEGF and the ERBB family, which includes EGFR and HER2. The HER2 targeting mAb Trastuzumab is approved for use in breast cancer patients with high levels of HER2 expression. (Vogel *et al.*, 2002) Unconjugated mAbs targeting VEGF and EGFR have been approved for use in metastatic CRC patients. Anti-EGFR therapy is limited to CRC patients with wildtype KRAS, as activating KRAS mutations confer innate resistance to anti-EGFR therapies. (Watkins and Cunningham, 2007) The anti-EGFR mAb Cetuximab, selectively binds to EGFR, blocking it from binding to its ligand EGF, and thus blocking signal transduction. Cetuximab has also been approved for use in squamous cell carcinoma of the head and neck. (Harding and Burtness, 2005; Cohen *et al.*, 2013) A second anti-EGFR mAb, Panitumumab has also been approved for use in metastatic CRC. (Amado *et al.*, 2008) VEGF expression is increased in most solid tumours, where it is the main factor that controls angiogenesis, leading to tumour proliferation and metastasis. The anti-VEGF mAb Bevacizumab binds to soluble VEGF in the tumour microenvironment thus preventing it from binding to its receptors, VEGFR-1 and -2. Bevacizumab has been approved for use in a number of cancers, including colon cancer, non–small cell lung cancer and breast cancer. (Lyseng-Williamson and Robinson, 2006)

In general, unconjugated mAbs are most effective when they also engage host defence mechanisms, resulting in antibody-dependent cell-mediated cytotoxicity (ADCC) or complement-dependent cytotoxicity (CDC). In ADCC, after the mAb binds to its tumour antigen, the Fc domain of the mAb binds to Fc gamma receptors on the surface of effector cells, such as macrophages, monocytes, eosinophils and natural killer cells. This triggers the effector cells to secrete various substances such as cytokines, lytic enzymes, perforin and

granzymes that mediate the destruction of the target cell. (Li *et al.*, 2013) CDC is triggered when the C1 complex binds the antibody-antigen complex, activating a cascade of complement proteins which leads to the formation of a membrane attack complex on the surface of the target cells, resulting in cell lysis. (Moore *et al.*, 2010) ADCC and CDC have been demonstrated to play a major role in antibody efficacy, with ADCC shown to be a key mechanism of action of Cetuximab and Trastuzumab. (Scott, Wolchok and Old, 2012) Despite this, unconjugated mAbs are generally not potent enough to be used alone and are used in combination with chemotherapy to treat cancer.

1.3.2. Antibody-Drug Conjugates (ADCs)

ADC technology utilises mAbs to deliver cytotoxic agents specifically to cancer cells. Altered protein expression in cancer cells can involve cell-surface proteins being selectively expressed, overexpressed or mutated, which differentiates them from normal cell-surface proteins, allowing them to be exploited with antibody-based therapeutics. (Damelin *et al.*, 2015; Diamantis and Banerji, 2016) A simple ADC design comprises three main components, a mAb, a linker and a toxic payload. To date, chimeric, humanised and fully human mAbs have been used in ADCs. The antibody isotype is also an important consideration in ADC design, with IgG1 the most commonly used isotype, followed by IgG4. IgG1 antibodies could provide additional anti-tumour activity by engaging effector cells and activating ADCC or CDC. (Goldmacher and Kovtun, 2011) The mAbs are generally covalently conjugated to toxins via linkers that need to be sufficiently stable to maintain the drug-conjugate in circulation until the antibody binds to its specific cancer cell-surface antigen and is internalised, then the linker should be labile enough to release the drug once it reaches the cytoplasm. (Ayyar, Arora and O'Kennedy, 2016) Both cleavable and non-cleavable linkers are currently being utilised in ADC design. Cleavable linkers are designed to be cleaved upon internalisation by lysosomal proteases present in the cell cytoplasm, as shown in **Figure 1.4**. The clinically approved ADC, Brentuximab vedotin utilises a cleavable linker. In non-cleavable linkers, the antibody is completely degraded upon internalisation, releasing the linker with attached toxin into the cell, which is successfully utilised in the ADC, ado-trastuzumab emtansine. (Goldmacher and Kovtun, 2011; Perez *et al.*, 2014)

The cytotoxic payloads of ADCs are extremely potent drugs capable of cell killing with minute quantities. Two classes of cytotoxic drug currently in use are mitotic inhibitor drugs, which interfere with microtubule assembly causing cell cycle arrest and subsequent apoptosis, and DNA-damaging agents, that cause DNA cleavage or bind the minor groove of DNA causing DNA alkylation resulting in cell death. Most ADCs in clinical development use mitotic inhibitor drugs, such as auristatins and maytansinoids, which target rapidly dividing cells more than normal cells. (Alley, Okeley and Senter, 2010; Govindan and Goldenberg, 2012; Ayyar, Arora and O'Kennedy, 2016b)

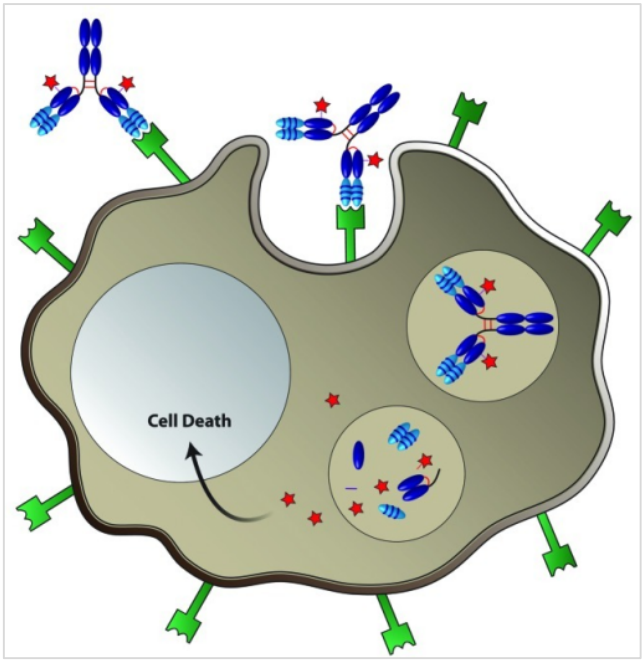

Figure 1.4 Delivery of cytotoxic drugs to cancer cells by ADCs. The mAb component of an ADC selectively binds a cell-surface tumour antigen, resulting in internalisation of the ADC-antigen complex through the process of receptor-mediated endocytosis. This complex then traffics to lysosomal compartments and is degraded, releasing the active cytotoxic drug inside the cell, leading to cell death. (Adapted from Panowski *et al.*, 2014)

1.3.2.1. Target Antigen Selection

In general, optimal targets for ADCs should be homogenously and selectively expressed at high density on the surface of tumour cells and upon antigen recognition and binding the resulting ADC-antigen receptor complex needs to be internalised through receptor-mediated endocytosis, for delivery of the toxic payload. Not all cell-surface molecules will internalise upon antibody binding. The antigen should ideally have low expression on normal tissues, however expression on normal tissues can be tolerated if expression on vital organs is minimal or absent. (Perez *et al.*, 2014) **Figure 1.5** displays some of the critical features deemed necessary for successful ADC design. The internalisation of the ADC-receptor complex was believed to be crucial for ADC therapeutic activity. However non-internalising ADCs have recently been proven to show potent therapeutic activity in mouse models of human cancer. ADCs equipped with peptide-based linker-payload combinations, were shown to efficiently liberate disulphide-linked drugs at the extracellular tumour site, leading to potent anti-cancer activity in preclinical animal models. (Gébleux *et al.*, 2017) This shows promise for the utilisation of molecular targets that may be overexpressed on the surface of cancer cells but do not initiate receptor-mediated endocytosis. In a similar way ADCs that target the tumour stroma or vasculature could show therapeutic benefit by dismantling the tumour microenvironment and exposing the tumour cells to drug indirectly. (Perrino *et al.*, 2014)

Minimal target expression in normal tissues is required to limit off-target toxicities. Target expression on normal tissues can also reduce ADC exposure in the tumour, impacting efficacy as well as safety. However, predicting ADC toxicity based on normal tissue expression is surprisingly challenging. For example, the anti-CD44v6-ADC (Bivatuzumab mertansine) with target antigen expression present in normal skin keratinocytes, caused not surprisingly, toxicity in skin. (Tijink *et al.*, 2006) In contrast, target antigen SLC34A2, has notable expression in normal lung tissue, yet the anti-SLC34A2-ADC has shown encouraging safety and pharmacokinetics in the clinic. (Burris *et al.*, 2014) Various parameters such as the biodistribution of the ADC and the particular normal cell type that expresses the target may determine the translation of target expression to a dose-limiting toxicity. (Damelin *et al.*, 2015)

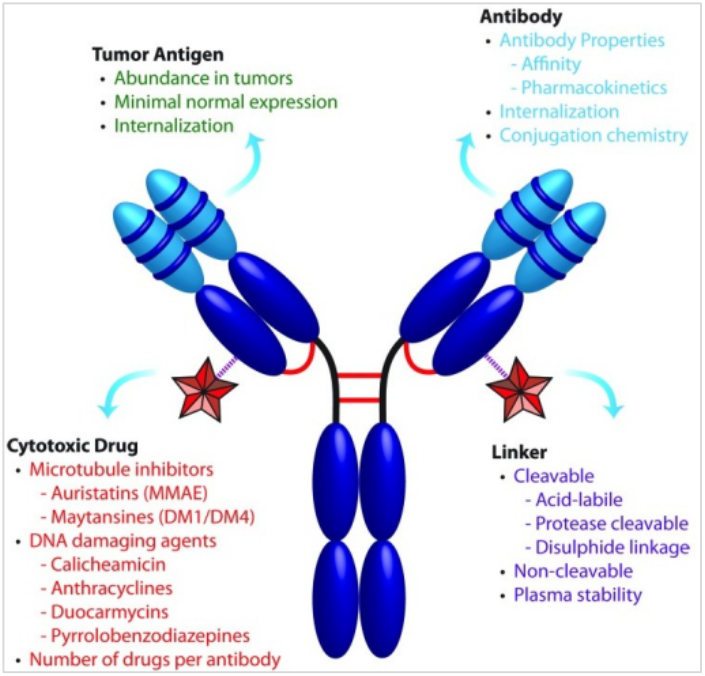

Figure 1.5 Critical factors that influence ADC therapeutics. ADCs consist of a cytotoxic drug conjugated to a mAb by means of a select linker. Optimisation of these components is essential for development of successful conjugates. (Adapted from Panowski *et al.*, 2014)

1.3.2.2. ADCs for Solid Malignancies

There are currently no ADCs approved for the treatment of CRC or PDAC. Until recently only ADCs targeting CD20 or CD33 on haematological malignancies, such as lymphoma and leukaemia, were in clinical use. (Diamantis and Banerji, 2016) Antibody therapeutics for solid malignancies were confined to unconjugated mAbs. However, the ADC ado-trastuzumab emtansine (T-DM1) was recently approved for use in metastatic breast cancer. (Boyraz *et al.*, 2013) This ADC made use of the already established unconjugated mAb Trastuzumab, which targets HER2-overexpression in breast cancer. T-DM1 combines Trastuzumab through a stable non-cleavable linker to the microtubule-inhibitory agent, DM1. This allows intracellular drug delivery specifically to HER2-overexpressing cells and was found to significantly improve overall survival in patients with HER2-positive metastatic breast cancer and further exemplifies the clinical potential of ADCs. (Carvalho *et al.*, 2016)

T-DM1 is one of two currently FDA approved ADCs. The second one is Brentuximab vedotin, a CD30 targeted mAb covalently linked to the synthetic tubulin inhibitor monomethyl auristatin-E (MMAE). It is approved for the treatment of patients with relapsed or refractory Hodgkin's lymphoma or systemic anaplastic large cell lymphoma. (Senter and Sievers, 2012) There are approximately 50 ADCs currently in clinical trials targeting various molecular targets and for application in a wide number of cancers, including gastrointestinal cancers. **Table 1.2** displays several of the ADCs currently in the clinical pipeline.

	Target	**Cytotoxic payload**	**Main indication**	**Phase**
Sacituzumab govitecan (IMMU-132)	TROP2	SN-38	Triple-negative breast cancer	3
Inotuzumab ozogamicin (CMC-544)	CD22	Calicheamicin	Acute lymphoblastic leukaemia	3
Anetumab ravtansine (BAY 94-9343)	Mesothelin	DM4	Mesothelioma	2
Gemtuzumab ozogamicin	CD33	Calicheamicin	Acute myeloid leukaemia, acute promyelocytic leukaemia	2
Depatuxizumab mafodotin (ABT-414)	EGFR	MMAF	Glioblastoma	2
Glembatumumab vedotin (CDX-011)	GPNMB	MMAE	Osteosarcoma, melanoma, triple-negative breast cancer	2
Denintuzumab mafodotin (SGN-CD19A)	CD19	MMAF	Diffuse large B-cell lymphoma	2
Mirvetuximab soravtansine (IMGN-853)	Folate receptor α	DM4	Folate receptor α-positive epithelial ovarian cancer	2
AGS-16C3F	ENPP3	MMAF	Renal cell carcinoma	2
Rovalpituzumab tesirine (Rova-T; SC16LD6.5)	DLL3	Pyrrolobenzodiazepine	Small-cell lung cancer	1/2
(IMMU-130)	CEACAM5	SN-38	Colorectal cancer, epithelial cancers	1/2
BMS-986148	Mesothelin	ND	Mesothelin-expressing cancers	1/2
Humax-TF-ADC	Tissue factor	MMAE	Tissue factor expressing tumours	1/2
Vadastuximab talirine (SGN-CD33A)	CD33	Pyrrolobenzodiazepine	Acute myeloid leukaemia	1/2
TAK-264 (MLN-0264)	Guanylyl cyclase C	MMAE	Gastrointestinal cancers	1/2
Milatuzumab-doxorubicin (CD74-DOX)	CD74	Doxorubicin	Chronic lymphocytic leukaemia, non-Hodgkin lymphoma, multiple myeloma	1/2

Table 1.2 ADCs currently in clinical development. SN-38=active metabolite of irinotecan. DM4=ravtansine. MMAF=monomethyl auristatin F. MMAE=monomethyl auristatin E. ND=not disclosed. (Adapted from Thomas, Teicher and Hassan, 2016)

1.3.3. Immune Checkpoint Inhibitors

Antibodies that restore T-cell responses against tumours have gained considerable attention and success over the past few years. Immune checkpoints are inhibitory receptors and ligands that hold the immune system 'in check' and prevent it from attacking host cells. Tumour cells usually escape the host immune response by up-regulating immune inhibitory signals. Blocking these immune checkpoints allows the recognition of tumour cells by T-cells, and will hopefully lead to their elimination. CTLA-4 and PD-1, along with its ligand PD-L1, are the most actively studied checkpoint proteins for clinical cancer immunotherapy. (Pardoll, 2012) CTLA-4 is expressed exclusively on T-cells and is the immune checkpoint during the early stages of T-cell activation. CTLA-4 primarily counteracts the activity of the T-cell co-stimulatory receptor, CD28, which inhibits T-cell activation resulting in the tumour cell evading cellular immunity. (Rudd, Taylor and Schneider, 2009) PD-1 is a secondary checkpoint because it is expressed on T-cells later, during the effector phase when T-cells become activated. (Ishida *et al.*, 1992) PD-1 binds to its ligands, PD-L1/L2, which are commonly upregulated on tumour cells, inhibiting anti-tumour T-cell mediated responses. The major PD-1 ligand expressed by solid tumours is PD-L1. (Dong *et al.*, 2002; Iwai *et al.*, 2002) PD-1 is also expressed on other activated non-T-lymphocyte subsets, including B-cells and NK cells, reducing their lytic activity. (Fanoni *et al.*, 2011; Terme *et al.*, 2011)

Several mAbs targeting these immune checkpoints are either in development, undergoing trials, or approved for use. Four immune checkpoint inhibitors have so far been approved, Ipilimumab, Pembrolizumab, Nivolumab and Atezolizumab. Ipilimumab targets CTLA-4 and was approved in 2011 based on two phase-III clinical trials that demonstrated improved overall survival in a group of advanced melanoma patients. (Hodi *et al.*, 2010) Ipilimumab is currently undergoing clinical trials in several other cancer types, including small-cell and non-small-cell lung cancer, bladder cancer and prostate cancer. Atezolizumab targets PD-L1 and was granted accelerated FDA approval in 2016 for the treatment of locally advanced or metastatic urothelial carcinoma after failure of cisplatin-based chemotherapy. (Inman *et al.*, 2016) Pembrolizumab and Nivolumab both target the PD-1 receptor. Pembrolizumab was first granted FDA approval in 2014 for the treatment of advanced melanoma, based on results from clinical trials demonstrating an ability to improve progression free survival of Ipilimumab-refractory melanoma patients. (Khoja *et al.*, 2015) Nivolumab was also approved for melanoma and for squamous-cell non-small-cell lung cancer following phase-

III trials that demonstrated improvements in overall survival in comparison with chemotherapy. (Raedler, 2015) Both Pembrolizumab and Nivolumab were subsequently approved for use in several other cancers including head and neck cancer, Hodgkin lymphoma, renal cell carcinoma and urothelial carcinoma. They were recently granted accelerated FDA approval in 2017 for the treatment of metastatic MSI-H cancers, including MSI-H metastatic CRC. Immune checkpoints are selectively upregulated in MSI-H CRC tumours, which account for 15% of all CRC cases. (Llosa *et al.*, 2015) Clinical trials of immune checkpoint inhibitors in PDAC, have shown unpromising results to date. A phase I trial of the PD-LI inhibiting antibody BMS-936559 showed no objective response in PDAC patients. (Brahmer *et al.*, 2012) However, further investigation into molecular subtypes of PDAC may identify patients that would be likely to respond to immune checkpoint blockade, increasing the efficacy of immune checkpoint inhibitors in PDAC.

The results of clinical trials involving immune checkpoint inhibitors suggest better therapeutic potential compared with some conventional therapies in several cancers. However, their success fluctuates with patients' individual immune system response and they are also known to stimulate autoimmunity in normal organs leading to adverse events with varied severity. In most cases, low or moderate adverse effects are observed that are usually reversible. Recent studies are concentrated on combination therapies, including combining two or more immune checkpoint inhibitors against different pathways and combining them with conventional therapies such as chemotherapy. (Pardoll, 2012)

1.3.4. T-cell Receptor Mimic Antibodies

An emerging strategy to circumvent the fact that mutated and overexpressed oncoproteins are typically cytoplasmic or nuclear, and thus not accessible to ADCs, is the development of T-cell receptor mimic (TCRm) mAbs. They are based on the identification of tumour antigens recognized by T-cells in the context of human leukocyte antigen (HLA). Cells can present peptides from intracellular proteins on their cell surface in the context of HLA, which the immune system uses to differentiate between self and non-self cells. Tumour specific antigens can arise from mutated gene products, such as Ras, although the chances that a peptide displaying such a mutation will bind the patient's HLA and be displayed are small, with few documented. However, tumour *associated* antigens, include proteins that are overexpressed in tumour cells, and therefore peptides from these are displayed at a far higher rate on the cell surface. Increases in antigenic peptides presented on cancer cells can distinguish them from normal cells which display low levels. Ideal TCRm targets for cancer therapy therefore are tumour-specific peptide/HLA complexes found in abundance on the cell surface. Peptides are most likely to be presented from overexpressed proteins with short half-lives that are cleaved and processed into peptides with high affinity to the patient's HLA. TCRm antibodies can then be designed to recognise an epitope within the peptide carried by the HLA, recruiting immune cells to mediate cancer cell death or the TCRm mAbs can deliver cytotoxic payloads. (Chang *et al.*, 2016)

However, there are challenges to TCRm antibody efficacy. The general low density of their target peptide/HLA epitopes, with only hundreds to a few thousand expressed on a target cell surface, versus the tens to hundreds of thousands of epitopes targeted by commercially available antibodies is a potential concern. Therefore, strategies should be taken to augment the therapeutic index, such as Fc engineering to enhance antibody-dependent cell-mediated cytotoxicity. MHC molecules do not in general readily or rapidly internalise, reducing the efficacy of drug conjugates, therefore activation of immune effectors will likely be the main mode of cytotoxicity for TCRm antibodies. Also, as has been observed with approved unconjugated mAbs for cancer treatment, TCRm mAb therapy is not likely to be potent enough to eliminate 100% of cells when used as monotherapy, combination with other cancer therapies will likely be necessary. The full potential for TCRm mAb therapy remains to be realised. (Dubrovsky *et al.*, 2016)

1.4. Aims of Thesis:

The aims of this thesis were as follows:

- To identify membrane localised proteins overexpressed in colon cancer vs. normal colon, and to investigate whether they are also overexpressed in other cancer types, including pancreatic and breast cancer.
- To investigate target expression in normal tissues, including the proliferating cells of normal tissues.
- To confirm cell-surface localisation of targets and investigate antibody internalisation upon binding to the target *in vitro*.
- To investigate the functional role of identified overexpressed targets in the cancer cell phenotype by *in vitro* functional analysis, including proliferation, migration and invasion assays.
- To identify target protein-protein interactions to discover potential binding partners and downstream signalling pathways linked to the target proteins.

❖ Based on these findings to assess the potential of identified targets as molecular targets for therapeutic antibody targeting.

Chapter 2. Materials and Methods

2.1. Bioinformatic Analysis of Microarray mRNA Expression Datasets

In order to identify potential membrane cancer targets, colon cancer gene expression arrays available for download from the Gene Expression Omnibus (GEO) database (https://www.ncbi.nlm.nih.gov/geo/) were analysed. The GEO database contains datasets from hundreds of different technologies/platforms, including mRNA gene expression arrays, miRNA arrays and RNA-seq. The criteria for our search of the databases were (1): normal human colon and colon carcinoma tissue sections (excluding cell line data); 2): the microarray platform used was Affymetrix U133 plus 2.0 arrays; (3): the data were presented as gene expression level. With this criteria, and excluding small datasets, a dataset by Skrzypczak *et al.,* (2010) was chosen for analysis. This dataset (accession number: GSE20916) contains whole tissue section samples from 36 colon adenocarcinomas, 45 colon adenomas and 24 normal colon samples. The dataset was generated on Affymetrix GeneChip HG-U133plus2, and processed using two normalisation algorithms: MAS5 and GCRMA with LVS.

For our study the processed CEL file data for this dataset was downloaded from the GEO. Differential gene expression lists were generated using the ebayes function of the limma package (Smyth, 2004) from Bioconductor, to generate lists of genes upregulated in (1) colon adenocarcinoma vs. normal colon and (2) colon adenoma vs. normal colon. A fold change of ≥ 2 and an adjusted p-value of $\leq 1E^{-5}$ were considered significant. The p-values were adjusted using a Bonferroni multiple testing correction. The literature/pathway mining software Pathway Studio Enterprise was then used to identify the genes that express membrane localised proteins. The number of upregulated genes identified in adenoma and adenocarcinoma compared to normal colon are summarised in **Table 2.1.** These lists were generated by Dr. Stephen Madden and Dr. Padraig Doolan, NICB.

	2F UP (Total genes)	2F UP (Membrane localised)
Normal vs. Adenoma	1078	154
Normal vs. Colon adenocarcinoma	1238	127

Table 2.1 Differential gene lists generated from publicly available colon cancer datasets.

2.2. Cell Culture

All cell culture work was carried out in a class II laminar air-flow cabinet (NuAIR), which was cleaned with 70% industrial methylated spirits (IMS) before and after each use. Any items brought into the cabinet were also sterilised with IMS. Only one cell line was worked on at a time in the laminar flow cabinet and upon completion of work with any given cell line, 15 minutes clearance was given to eliminate any possibilities of cross-contamination between the various cell lines. The cabinet was cleaned routinely with Virkon (Antech International, P0550) and IMS. All cells were maintained under standard culture conditions, 5% CO_2 at 37^{o}C. Cells were fed with fresh media or sub-cultured every 2-3 days or as required, in order to maintain active cell growth. Cell lines were maintained in T25; T75; and T175 flasks (Corning).

2.2.1. Cell Lines and Cell Culture Medium

Six colon cancer cell lines, eight PDAC cell lines and eight breast cancer cell lines were used during this study. All cell lines were originally obtained from the American Type Culture Collection (ATCC). **Table 2.2** outlines the details and growth conditions for each cell line. Complete medium was made up by adding appropriate concentration of foetal calf serum (FCS)(PAA) and any required supplements: L-Glutamine (G7513 Sigma). Complete medium was prepared and sterility tested before use by incubating at 37^{o}C for up to 7 days to ensure no bacterial or fungal contamination was present.

Cell Line	Source	Complete Media
SW480	Colorectal adenocarcinoma	RPMI 1640, 5% FCS
SW620	Lymph node metastasis of CRC	RPMI 1640, 5% FCS
HCT116	Colorectal carcinoma	DMEM, 5% FCS, 2mM L-Glutamine
T84	Lung metastasis of CRC	DMEM, 10% FCS, 2mM L-Glutamine
HT29	Colorectal adenocarcinoma	DMEM, 10% FCS, 2mM L-Glutamine
CaCo-2	Colorectal adenocarcinoma	DMEM, 10% FCS, 2mM L-Glutamine
BxPC-3	Pancreas adenocarcinoma	RPMI 1640, 10% FCS
MIA PaCa-2	Pancreas adenocarcinoma	DMEM, 5% FCS, 2mM L-Glutamine
PANC-1	Pancreas adenocarcinoma	DMEM, 10% FCS, 2mM L-Glutamine
HPAC	Pancreas adenocarcinoma	RPMI 1640, 10% FCS
AsPC-1	Ascites PDAC metastatic site	RPMI 1640, 10% FCS
Capan-1	Liver PDAC metastatic site	DMEM, 20% FCS, 2mM L-Glut
Capan-2	Pancreas adenocarcinoma	DMEM, 10% FCS, 2mM L-Glutamine
SW1990	Spleen PDAC metastatic site	DMEM, 10% FCS, 2mM L-Glutamine
MCF-7	Breast	DMEM, 10% FCS, 2mM L-Glutamine
T47D	Pleural effusion metastatic site of breast ductal carcinoma	RPMI 1640, 10% FCS
BT474	Breast ductal carcinoma	RPMI 1640, 10% FCS
MDA-MB-361	Brain metastasis of breast adenocarcinoma	RPMI 1640, 10% FCS
MDA-MB-468	Pleural effusion metastatic site of breast adenocarcinoma	RPMI 1640, 10% FCS
BT20	Breast carcinoma	DMEM, 10% FCS, 2mM L-Glutamine
MDA-MB-157	Breast/medulla carcinoma	RPMI 1640, 10% FCS
MDA-MB-231	Pleural effusion metastatic site of breast adenocarcinoma	RPMI 1640, 10% FCS

Table 2.2 Cell lines and culture medium used in this study.

2.2.2. Subculture of Cell Lines

Waste cell culture medium was removed from the tissue culture flask and discarded into a sterile glass bottle. The flask was then rinsed out with 2-5mls trypsin/EDTA solution (0.25% trypsin, Gibco, 043-05090), 0.01% w/v EDTA (Sigma, E9884) solution in phosphate buffered saline (PBS) (Oxoid, BRI4a) to ensure the removal of any residual media. Depending on the size of the flask, 2-5ml of trypsin was then added to the flask, which was then incubated at 37^{o}C, for approximately 5 mins until all of the cells detached from the inside surface of the flask, monitored by microscopic observation. An equal volume of complete media was added to the flask to deactivate the trypsin. The cell suspension was placed in a sterile universal container (Sterilin, 128A) and centrifuged (Beckman, Allergra™, 6KR centrifuge) at 1000rpm for 5 mins. The supernatant was then discarded from the universal and the pellet was suspended gently in complete medium. A cell count was performed and an aliquot of cells was used to seed a flask at the required density. All cell waste and media exposed to cells were autoclaved before disposal.

2.2.3. Cell Counting

Following the trypsination of cells and resuspension of the cell pellet, an aliquot of cell suspension was applied to the chamber of a glass coverslip-enclosed haemocytometer. For each of the four grids, cells in the 16 squares were counted. The average of the four grids was multiplied by a factor of 10^4 (volume of the grid) and the relevant dilution factor to determine the average cell number per mL in the original cell suspension. The volume of cell suspension for the required cell number could then be calculated.

2.2.4. Cryopreservation of Cells

Cells for cryopreservation were harvested in the mid-log phase of growth. Cell pellets were resuspended in a suitable volume of FCS which had been cooled to 4°C. An equal volume of 10% (v/v) DMSO (Sigma, D2438) in FCS was added drop-wise giving a final concentration of 5% (v/v) DMSO. 1mL of cell suspension was then aliquoted into cryovials (Greiner, 122278) and immediately placed into the -20°C freezer for 2 hrs. The cryovials were then

transferred to -80^{o}C for short term storage, after which the vials were gradually transferred to the liquid phase of liquid nitrogen for long term storage (-196°C).

2.2.5. Thawing of Cryopreserved Cells

A volume of 5mL of fresh culture medium containing serum was added to a sterile universal. The cryopreserved cells were removed from the liquid nitrogen and thawed at 37°C quickly. The cells were removed from the vials and transferred to the aliquoted media (also at 37°C). The resulting cell suspension was centrifuged at 1000rpm for 5 mins. The supernatant was removed and the pellet resuspended in fresh culture medium. Thawed cells were then added to an appropriately sized tissue culture flask with a suitable volume of growth medium and allowed to attach overnight. The following day, flasks were re-fed with fresh media to remove any remaining DMSO and non-viable cells.

2.2.6. Mycoplasma Testing

Mycoplasma testing was carried out every 3 months, using the indirect staining procedure for mycoplasma analysis. Normal rat kidney fibroblast (NRK) cells were seeded onto sterile coverslips in sterile petri dishes (Greiner, 633 185) at a cell density of $2x10^3$ cells/mL and allowed to attach overnight at 37°C in a 5% CO_2 humidified incubator. 1 mL of cell-free supernatant from each test cell line was inoculated onto an NRK petri-dish and incubated as before until the cells reached 20-50% confluency. After this time, the waste medium was removed from the dishes, the coverslips (Chance Propper, 22 x 22 mm) were washed twice with sterile PBS, once with a cold PBS/Carnoys (50/50) solution and fixed with 2 mL of Carnoys solution (acetic acid:methanol, 1:3) for 10 minutes. The fixative was removed and dried coverslips were washed twice in deionised water and stained with 2 mL of Hoechst stain (BDH) (50ng/mL) for 10 minutes. From this point on, work proceeded without direct light to limit quenching of the fluorescent stain. The coverslips were rinsed three times in PBS. They were then mounted in 50% (v/v) glycerol in 0.05 M citric acid and 0.1 M disodium phosphate and examined using a fluorescent microscope with a UV filter. A Mycoplasma infection would be seen as small fluorescent bodies in and sometimes outside the cells. Mycoplasma testing was carried out for all cell lines for possible mycoplasma contamination

in house by Mr. Michael O' Donoghue and Ms. Justine Meiller at the NICB. All cell lines used in this thesis are confirmed to be Mycoplasma free.

2.3. Western Blot Analysis

2.3.1. Preparation of Whole Cell Protein Lysates

Cells were grown to the desired confluency in monolayer culture flasks (T75/T175). Media was removed and cells were washed x3 with sterile ice cold PBS. Excess PBS was removed and 500 µl (per T75cm^2 flask) or 1 mL (per T175cm^2 flask) of RIPA lysis buffer (Sigma, R0278) containing 1X Halt protease/phosphatase inhibitor cocktail (ThermoScientific, 78440) was added to the flask. Flasks were then incubated on ice for 30 mins with regular agitation, to ensure complete cell lysis of the cell culture monolayer by the lysis buffer. The cell lysate was then transferred to a 1.7 mL Eppendorf tube and centrifuged at 16,000 g for 15 minutes at 4°C, and the supernatant was removed and stored at -80°C for future use.

2.3.2. Preparation of Membrane Enriched Cell Fractions

Membrane enrichment was carried out using CALBIOCHEM® ProteoExtract Native Membrane Protein Extraction Kit (Merck Millipore, 444-810KIT). Membrane enrichment was carried out as per manufacturer's recommendations with some modifications. The components of the kit were as follows: Wash Buffer, Extraction Buffer I, Extraction Buffer II and Protease Inhibitor Cocktail. The following protocol outlines the steps taken to obtain a 500 µl membrane protein enriched fraction from ~90% confluent T75 cm^2 adherent culture flask. All reagents were kept on ice except the Protease Inhibitor Cocktail which was stored in DMSO and was allowed to come to room temperature to thaw. Cell culture media was removed and cells were washed x2 with 10mL of ice cold PBS. Extraction Buffer I was prepared by taking 2 mL and adding 10 µl of Protease Inhibitor Cocktail. 2 mL of Extraction Buffer I/Protease Inhibitor Cocktail was added to the washed cells in the flask. The cells were then scraped into the buffer using a sterile disposable cell scraper. The 2 mL cell sample was then divided into two 1 mL volumes in eppendorf tubes and incubated at 4°C for 10 mins. Samples were then centrifuged in a 4°C pre-cooled microcentrifuge at 16,000 x g for 5 mins. The supernatant contains soluble proteins and was discarded. Sample pellets containing the

insoluble membrane proteins were then resuspended in 500 µl Extraction Buffer II/Protease Inhibitor Cocktail + 2.5 µl of Protease Cocktail Inhibitor. Extraction Buffer II solubilises integral membrane and membrane associated proteins. Samples were incubated and agitated at 4°C for 30 mins. To remove any remaining debris the samples were then centrifuged in a 4°C pre-cooled microcentrifuge at 16,000 x g for 15 mins. The supernatant containing solubilised membrane proteins was removed and stored at -80°C for future use.

2.3.3. Preparation of Conditioned Medium (CM)

Cells were seeded in T175cm^2 flasks and cultured until 50-60% confluent. Cells were then washed x 3 in the appropriate serum-free media (SFM) and incubated in SFM for 2 hrs. After this time, cells were washed again x 3 in SFM. This is to ensure the complete removal of FCS proteins from the cells, so that CM containing only proteins secreted by the cells can be collected. 20mL of SFM was then added to the cells and incubated for 72 hrs. The CM was then collected, centrifuged for 5 mins at 1000 rpm and filtered through 0.22µm filter. To concentrate conditioned media, 20mL was added to a Vivaspin20 concentrator with a 5kDa molecular weight cut off (Sartorius, *VS*.0112) and centrifuged at 4°C at 4000rpm (ThermoFisher Scientific, 11175774) until the final volume was reduced x10 (e.g. 10 mL to 1 mL). The sample was removed and then stored in aliquots at -80°C.

2.3.4. Protein Quantification

Protein concentrations in whole cell lysates, membrane enriched fractions and CM were determined using the Pierce™ BCA Protein assay kit (ThermoFisher Scientific, 23225) as per the manufacturer's instructions.

2.3.5. Gel Electrophoresis

Protein samples for Western blotting were separated by SDS-PAGE gel electrophoresis, using 4-12% gradient gels (ThermoFisher Scientific, NP0335, NP0321). Protein samples were prepared for gel electrophoresis by taking the required volume to equalise the protein concentration across a sample set from the protein lysate sample preparation and made up in

4x sample buffer (ThermoFisher Scientific, NP0007) and 10x reducing agent (ThermoFisher Scientific, NP0004). The samples were heated at 95°C for 5 mins on a heating block and allowed to cool to room temperature before being centrifuged. 10-20µg of protein and 5-7ul of pre-stained molecular weight marker (ThermoFisher Scientific, LC5800) were loaded into the wells of a gel. 500 µl of antioxidant (NP0005) was then added to the inner chamber of the Xcell SureLock® minicell (EI0001) electrophoresis gel-rig. The samples were electrophoretically separated at 200 V constant using a 1X MOPS/SDS running buffer (ThermoFisher Scientific, NP001) for 50mins or until the bromophenol blue dye reached the bottom of the gel.

2.3.6. Enhanced Chemiluminescence Detection

Following electrophoresis gels were washed in Ultrapure water (UHP). Proteins were transferred to Polyvinylidene fluoride (PVDF) membranes (ThermoFisher Scientific, IB4010-01) using the iBlot transfer system (ThermoFisher Scientific, IB1001). The membrane was blocked with 5% milk powder (Biorad, 170-6404) in TBS/Tween (1x TBS (Sigma, T5912) and 0.1% Tween20 (Sigma, P1379-500ml)) at room temperature for 2 hrs, then incubated overnight at 4°C in primary antibody diluted with 0.1 % TBS-Tween in 5 % milk powder. The next day the primary antibody was removed and the membrane was given three 30 min washes with 0.5 % TBS-Tween and then incubated at room temperature with secondary antibody in 0.5 % TBS-Tween for 1 hour. **Table 2.3** lists the primary and secondary antibodies used in this study. Secondary antibody was removed and the membrane was given three 30min washes with 0.5 % TBS-Tween. Following the final wash, membranes were incubated for 5mins with a 50:50 mixture of ECL reagent A and ECL reagent B (Amersham, ECL, RPN 2105 or Clarity, BioRad, 170506). The ECL reagent mixture was completely removed and the membrane was covered in a layer of transparent plastic. All excess air bubbles were removed. The membrane was then exposed to autoradiographic film (GE Life Sciences, 95017-681) for various times depending on the intensity of the signal. The exposed autoradiographic film was developed for the appropriate time in developer solution (Kodak, LX24, diluted 1:5 in water) until clear bands developed. The film was then briefly washed in water and transferred to a fixative solution (Kodak, FX-40, diluted 1:5 in water) for 5 mins. The film was washed with water for 5-10 minutes and left to dry at room

temperature. Once dry, the blots were then converted into a digital format using Epson Perfection photo scanner 4990 and Epson Scan software version 3.04a.

Primary Antibody	**Dilution**	**Details**
LY6G6F	0.75µg/ml	Abcam: ab62597
IL1RAPL1	1:5000	Atlas: HPA00564
IL1RAPL1	1:2000	Proteintech: 21609-1-A
IL20RA	1:1000	Abcam: ab135454
BACE2	1:1000	Abcam: ab135778
NTM	1:1000	R+D systems: AF1235
LRRC8E	1:500	Novus: NBP1-82078
EPHX4	1:500	Novus: NBP1-8930
Alpha Tubulin	1:10,000	Abcam: ab4074
Cyclin A	1:1000	Santa Cruz: sc-596
P27	1:1000	Santa Cruz: sc-528
PARP	1:500	Cell signalling: 9542
Phospho-p44/42 MAPK	1:1000	Cell signalling: 4370
Total-p44/42 MAPK	1:1000	Cell signalling: 4695S
Phospho-FAK	1:1000	Cell signalling: 3284S
Total-FAK	1:5000	BD Biosciences: 610088
Secondary Antibody	**Dilution**	**Details**
Anti-Mouse	1:2000	Dako: P0447
Anti-Rabbit	1:2000	Dako: P0448

Table 2.3 List of antibodies and the dilution used in Western blot analysis.

2.4. RNA Interference (RNAi)

RNAi using small interfering RNA (siRNA) was carried out to transiently knockdown /attempt to knockdown the expression of LY6G6F and IL1RAPL1 at the protein level. A number of siRNAs were used for each target from two different companies (Ambion/Life Technologies and Qiagen). These siRNAs were 21-23 bps in length and were introduced to the cells via reverse transfection with Lipofectamine 2000 Transfection Reagent (Life Technologies, 13778075).

2.4.1. Transfection Optimisation

In order to determine the optimal conditions for siRNA transfection, cell concentrations required were first established for each cell line. Cell suspensions were prepared at 7.5×10^4, 1×10^5, 1.5×10^5, 2×10^5 and 1.5×10^5 cells per well in a 6 well plate, and allowed to grow for 72 hrs. This was carried out in order to determine which cell concentration allows the cells to be in late exponential phase at the end of the transfection (i.e. after 72 hrs incubation), ensuring healthy proliferating cells will be used in the follow on functional assays. Transfections were optimised further to determine the optimal Lipofectamine 2000 transfection reagent volume required to efficiently transfect each cell type, by transfecting cells with a range of Lipofectamine 2000 volumes (1-4µl) and 30nM of Negative siRNA and kinesin siRNA, which initiates cell death. Plates were assayed for changes in proliferation after 72 hrs using the acid phosphatase assay described in Section 2.5.1. Optimal conditions for siRNA transfection were determined as the combination of conditions which gave the greatest reduction in cell number with the kinesin siRNA and also the least cell kill in the presence of Lipofectamine 2000 alone. The optimised conditions for the cell lines are shown in **Table 2.4**. The general method used for siRNA transfection is as follows: Solutions of siRNA at their required concentrations were prepared in optiMEM (GibcoTM, 31985047). Separately, a Lipofectamine 2000 solution was made up as a master mix using optiMEM with enough volume required for all transfection samples. Both of these solutions were incubated at room temperature for 10 minutes before being combined together, with the combined siRNA/Lipofectamine solutions incubated for a further 15mins at room temperature. 100 µL of the siRNA/Lipofectamine solutions were added in a drop-wise fashion to each well of a 6-well plate, with each well containing 1.9 mL of a cell suspension

at the required concentration. The plates were mixed gently and incubated at 37°C overnight. After this time, the transfection mixture was removed from the cells and the plates were fed with fresh complete medium.

Cell Line	Cell Number	Lipofectamine 2000
HCT116	2×10^5	2 µl
MIA PaCa-2	2×10^5	2 µl
SW480	1.5×10^5	2 µl
BXPC-3	2×10^5	3 µl

Table 2.4 Optimisation conditions for cell line transfection.

2.4.2. siRNA Transfection for Functional Analyses

Pre-designed siRNAs to the protein targets were purchased from Life Technologies or Qiagen. Three independent LY6G6F siRNAs were used in the functional analysis, with an additional three also used for qRT-PCR analysis. Six independent IL1RAPL1 siRNAs were used in the attempt to achieve protein knockdown of this target. **Table 2.5** lists the siRNAs used in this study. For each set of siRNA transfections carried out, the control groups included: Non-transfected cells only control; Lipofectamine only control cells; and a Negative siRNA transfected cells control. Negative siRNA are sequences that do not have homology to any genomic sequence. The Negative non-targeting siRNA used in this study is commercially produced, and guarantees siRNA with a sequence that does not target any gene product. It has also been functionally proven to have no significant effects on cell proliferation, morphology and viability. Therefore, the effects observed by target siRNA transfection were compared to cells transfected with Negative siRNA. This takes into account any effects due to the siRNA transfection procedure, reagents, and also any random effects of the Negative siRNA. Western blots were used to determine if siRNA had an efficient knockdown effect at the protein level.

Target	siRNA Details Company and Catalog numbers	siRNA Concentration
LY6G6F	Qiagen: SI00331744, SI04136027, SI04253046	30nM (used in functional analysis + qRT-PCR analysis)
LY6G6F	Ambion: s48908, s48909, s48910	30nM (used in qRT-PCR analysis only)
IL1RAPL1	Qiagen: SI00104335, SI00104342, SI00104356, SI03044195. Ambion: s21968, s21969, s21970	30nM qRT-PCR analysis. 10-100nM tested for protein knockdown.
Negative siRNA	Qiagen: 1027310	As required
Negative siRNA A	Ambion: 4390843	As required
Kinesin (Kif11)	Ambion: 16704	As required
AllStars Cell Death	Qiagen: S104381048	As required

Table 2.5 Details of siRNA and concentrations used in this study.

2.5. Functional Analysis

2.5.1. Acid Phosphatase Assay

Following the transfection incubation period of 72 hrs, media was removed from the 6 well plates. Each well was washed x2 with 1 mL of PBS. This was removed and 1 mL of freshly prepared phosphatase substrate (1.5µg/mL p-nitrophenol phosphate (ThermoScientific, 34045) in 0.1 M sodium acetate (Sigma, S8625), 0.1% triton X-100 (BDH, 30632), pH 5.5) was added to each well. The plates were then incubated in the dark at 37°C for 1-2 hours. Colour development was monitored during this time. The enzymatic reaction was stopped by the addition of 500 µl of 1 M NaOH. A 150 µL aliquot of each sample (3 replicates) was transferred to a 96-well plate. The plate was read in a dual beam plate reader at 405 nm with a reference wavelength of 620 nm.

2.5.2. 2D Colony Formation Assay

The cell number was first optimised for each cell line being used in the functional analysis. Cells were seeded at 100-1200 cells/well in a 6 well plate and assessed after 12 days. The optimal cell number chosen was one in which sufficient independent colonies had formed but not started overlapping with each other. The optimal cell number chosen for HCT116 cells was 800 cells/well and for MIA PaCa-2 cells 400 cells/well. For the functional analysis, cells were seeded at the optimal cell number in duplicate, 72 hrs post transfection. Cells were left to form colonies for 12 days. Media was renewed once during this time. After 12 days, wells were washed twice with PBS and colonies fixed in cold Methacare (75% v/v methanol, 25% v/v acetic acid) for 30 mins. The fixative solution was removed and wells washed once with PBS. Fixed colonies were then stained with 1% Crystal violet for 20 mins. Wells were rinsed with UHP and left to air dry. Plates were then scanned as 24-bit colour TIFF images for analysis. Colony area and intensity was quantified using the ImageJ plugin Colony Area. (Guzman *et al.*, 2014) Each assay was performed in biological triplicate.

2.5.3. Invasion Assay

Matrigel (BD Biosciences, 354234) was diluted to a working stock of 1mg/mL in serum-free DMEM. Aliquoted stocks were stored at -20°C for up to 1 year. A volume of 100 µL of Matrigel was placed into each insert (BD Biosciences, 353097) (8.0 µm pore size, 24 well format) and kept at 4°C for 24 hours. The insert and the plate were then incubated for one hour at 37°C to allow the proteins to polymerise. Cells were harvested 72 hrs post transfection and re-suspended and made up to an optimised cell number. Excess media was removed from the inserts, and they were rinsed with 200 µL of culture media. A 100 µL volume of complete cell culture media was added to each insert. A 100 µL volume of cell suspension was added to each insert and 500 µL of culture media was added to the well underneath the insert. Cells were incubated for an optimised amount of time. The optimised cell number and conditions for HCT116 cells: $3x10^5$ cells/insert in serum free culture medium with medium containing 10% FCS in the well underneath the insert to act as a gradient, incubated for 30 hrs. MIA PaCa-2 cells: $1.5x10^5$ cells/insert in culture media containing 5% FCS with the same media in the well underneath the insert, incubated for 40 hrs. Following incubation, the media was removed from the inside of the insert and the insert was wiped with a cotton swab dampened

with PBS. The outer side of the insert was stained with 0.25% crystal violet for 10 mins and then rinsed in UHP and allowed to dry. The inserts were viewed and photographed under the microscope. The invasion assays were quantified by counting cells in 10 random fields within a grid at 40x objective and averaged to get the average number of invaded cells/high power field (HPF). These were then compared to the Negative siRNA cells to calculate % invaded cells compared to Negative siRNA treated cells. Duplicate inserts were set up for each triplicate biological experiment.

2.5.4. Migration Assay

Migration assays were carried out as described in Section 2.5.3 except inserts were not coated with Matrigel. Cell counts were also carried out as for invasion assays.

2.5.5. Statistical Analysis

To compare the effects found in the target siRNA treated cells compared to Negative siRNA treated cells, all functional assays were subjected to statistical analysis using Student's t-tests (2-tailed with unequal variance) on Microsoft Excel. A p-value of ≤ 0.05 (*) was deemed significant, with ≤ 0.01 (**) deemed more significant and ≤ 0.001 (***) deemed highly significant.

2.6. Immunohistochemistry

2.6.1. Tissue Samples

A combination of full-face tissue sections and commercially available tissue microarrays (TMA) were used in this study. For the full-face tissue sections, formalin-fixed, paraffin-embedded (FFPE) tissue blocks were cut into 5μm sections using a microtome and mounted onto poly-l-lysine coated slides. Slides were stored at room temperature until required. Full-face de-identified sections of normal tissues and cancer tissues (colon adenocarcinoma, breast cancer and oesophageal cancer) were obtained courtesy of the Departments of Pathology of St. Vincent's University Hospital (SVUH), Dublin 4 and Royal Victoria Eye

and Ear Hospital (RVEEH), Dublin 2. Of the colon adenocarcinoma tissue sections provided, as well as pathological diagnosis, the KRAS phenotype was known for 18 sections (9 being KRAS wildtype and 9 KRAS mutant phenotype) and the BRAF phenotype was known for 4 sections (2 being BRAF wildtype and 2 BRAF mutant phenotype). Survival data was not available for any of the colon cancer specimens.

The pancreatic cancer patient cohort provided by SVUH consisted of 57 patients diagnosed with pancreatic ductal adenocarcinoma (PDAC) who underwent pancreaticoduodenectomy in SVUH between 2007 and 2013. All tissue specimens were de-identified, with survival data and clinicopathological features including tumour size, differentiation and stage provided for this study. Ethical approval for the use of all tissues was obtained from either SVUH or RVEEH.

The commercial TMAs used in this study contain small 1mm diameter cores of tissue on a single glass slide and were obtained from US Biomax, Accumax and Invitrogen. The commercial TMAs used in this study were as follows:

- Colon disease spectrum TMA (CO2081, US Biomax), containing 17 cases of adenocarcinoma, 17 of mucinous adenocarcinoma, 2 carcinoid, 20 metastatic carcinoma, 5 adenoma and polyp, 8 hyperplasia, 10 inflammation, normal adjacent tissue (NAT) and normal colon tissue, with duplicate cores per case. Tumour, node and metastasis (TNM) and pathology grade data were provided.

- Colon cancer tissue with corresponding normal TMA (Accumax A713 VIII), containing 12 cases of adenocarcinoma and corresponding normal colon in duplicate cores.

- Gastric adenocarcinoma and normal gastric tissue TMA (ST721, US Biomax), containing 18 cases of adenocarcinoma, 3 each of adjacent normal tissue and normal tissue, triplicate cores per case. TNM and pathology grade data were provided.

- Oesophageal carcinoma test TMA (T022a, US Biomax), containing 10 cases of oesophageal cancer (1 carcinoma in situ, 4 squamous cell carcinoma, 2 adenocarcinoma, 1 small cell undifferentiated carcinoma, 1 carcinoma sarcomatodes and 1 carcinosarcoma) and 2 normal oesophagus tissues, with duplicate cores per case. TNM and pathology grade data were provided.

- Pancreas tissue TMA (PAN241a, US Biomax), containing 16 cases of adjacent normal pancreatic tissue, 5 cases of normal pancreatic tissue and 3 adenocarcinoma tissue, single core per case.

- Pancreatic cancer TMA (PA1001, US Biomax), containing 40 cases of pancreatic cancer, 5 cases of adjacent normal pancreatic tissue and 5 cases of normal pancreas tissue, duplicate cores per case. TNM data provided.

- Multiple organ normal tissue TMA (BN242a/b, US Biomax), containing 12 cases of multiple normal organs (stomach, oesophagus, colon, rectum, liver, small intestine, thyroid, spleen, larynx, testis, bladder and trachea), duplicate cores per case.

- Human normal tissue TMA (Catalog No. 75-401, Invitrogen MaxArray), containing 30 normal tissue samples (Lung, Skin, Skeletal Muscle, Heart muscle, Stomach, Oesophagus, Small Intestine, Colon, Liver, Spleen, Pancreas, Salivary Gland, Pituitary Gland, Adrenal Gland, Thyroid Gland, Parathyroid Gland, Thymus Gland, Tonsil, Bone marrow, Breast, Uterus, Cervix, Ovary, Kidney, Prostate Gland, Testis, Omentum, Peripheral Nerve, Cerebral Cortex and Cerebellum). Single cores per case.

2.6.2. Immunohistochemical Staining of Tissue Samples

All Immunohistochemical (IHC) staining was performed using the Dako Autostainer (Dako, S3800). Deparaffinisation and antigen retrieval of FFPE tissue sections was performed using Epitope Retrieval 3-in-1 Solution (pH 6) (Dako, S1699) or the Epitope Retrieval 3-in-1 Solution (pH 9) (Dako, S2375) and the PT Link system (Dako, PT101). For epitope retrieval, slides were heated to 97°C for 20 mins and then cooled to 65°C. The slides were then immersed in wash buffer (Dako, S3006). On the Autostainer, slides were blocked for 10 mins with 200 µl HRP Block (Dako, S2023). Cells were washed with 1 x wash buffer and 200 µl of antibody added to the slides at the optimised dilution and time. The antibodies used in the IHC analysis and their optimised conditions are shown in **Table 2.6**. Slides were washed again with 1 x wash buffer and then incubated with 200 µl Real EnVision (Dako, K4065) for 30 mins. A positive control slide was included in each staining run. Each slide was also run with Negative Control (Antibody Diluent only), to allow evaluation of non-specific staining. All slides were counterstained with haematoxylin (Dako, CS700) for 5 mins, and rinsed with

wash buffer, followed by deionised water. All slides were then dehydrated in graded alcohols (2 x 3 mins each in 70% ethanol, 90% ethanol and 100% ethanol), and cleared in xylene (2 x 5 mins), and mounted with coverslips using DPX mounting medium (Sigma, 44581). Mounted slides were allowed stand overnight before examination under the microscope. Slides were viewed and photographed using Olympus microscope and imaging system. Tissues were then scored for target immunoreactivity. Staining intensity was classified using a scale of 0-3+ as follows: 0, negative; 1+, weakly positive; 2+, moderately positive; 3+, strongly positive. Patients were then stratified into two clinical score categories: high target expression (intensity 2+ or 3+) and low target expression (intensity 0 or 1+). Scoring was carried out by two independent evaluators (AML, EMcA) blinded to specimen and clinical detail. Chi-square tests were carried out using GraphPad Prism (Version 7 GraphPad Software, Inc., USA).

Antibody	**Antibody dilution and incubation time**	**Antigen Retrieval**
LY6G6F (Abcam: ab62597)	11μg/ml 37mins	pH9 20mins
IL1RAPL1 (Atlas: HPA00564)	1:320 37mins	pH6 20mins
IL20RA (Abcam: ab135454)	1:100 30mins	pH6 20mins
BACE2 (Abcam: ab135778)	1:100 30mins	pH6 20mins
NTM (R+D systems: AF1235)	1:6000 30mins	pH6 20mins
Ki67 (Dako)	1:100 30mins	pH6 20mins

Table 2.6 Optimised antibody conditions and antigen retrieval for target IHC.

2.7. Immunocytochemical Analysis on Fixed Cells

Aliquots of 30 µl of cell suspension were seeded directly onto 10 well 7 mm microscope slides (Erie Scientific Company, 465-68X). Cells were allowed to attach overnight. After such time, slides were washed 3 x in PBS and cells were then fixed in cold 4% paraformaldehyde for 5 mins. Immunostaining was carried out using the Dako Autostainer as per Section 2.6.2, without the initial antigen retrieval.

2.8. Immunofluorescence Analysis on Fixed Cells

Cells were seeded onto 10 well microspore slides and incubated as described in Section 2.7. Slides were washed 3 x in PBS and cells were then fixed and permeabilised in either ice-cold methanol alone for 5-10 mins or 4% paraformaldehyde for 7 mins followed by ice-cold methanol for 5 mins. Slides were washed 3x in PBS and in between the wells were then dried using a cotton bud wrapped in lint free tissue, to prevent the primary antibody from running into neighbouring wells. The primary antibody was applied to appropriate wells and incubated overnight at 4°C. After 24 hrs, the slides were washed 3x in PBS and secondary antibody was applied (Alexa Fluor488 goat anti-rabbit; Thermofisher Scientific, A11034) at 1:2000 dilution and incubated for 1 hr at room temperature in the dark. The secondary antibody was removed and cells were washed 3x in PBS. Slides were counterstained using DAPI nuclear stain (Sigma, D9542). Slides were mounted with ProLong Gold mounting medium (ThermoFisher Scientific, P36930) and covered using a glass cover slip. Cells were viewed and photographed using a Nikon phase contrast microscope fitted with an FITC filter.

2.9. Quantitative Real Time-Polymerase Chain Reaction (qRT-PCR)

2.9.1. RNA Extraction

TRIzol Reagent (Thermo Fisher Scientific, 15596-026) was used for RNA extraction from cells in monolayer. 1 mL of TRIzol Reagent was added to each well of a 6-well plate for RNA isolation. These samples were allowed to stand for 5 mins on ice to allow complete lysis of the cells. The TRIzol/lysed cells solution was transferred to a clean Eppendorf tube, and 200 µL of chloroform (Sigma, C2432) was added. Samples were vortexed at high speed

for 15 seconds and allowed to stand for 15 mins at room temperature. The resulting mixtures were centrifuged at 13,684 g in a microcentrifuge for 15 mins at 4ºC. The aqueous layer containing RNA was carefully removed to a clean fresh Eppendorf tube. To this, 500 µL of ice-cold Isopropanol (Sigma, I9516) was added. The samples were mixed and incubated at room temperature for 10 mins, and then centrifuged at 13,684 g for 30 mins at 4ºC to pellet the precipitated RNA. Taking care not to disturb the RNA pellet, the supernatant was removed and the pellet was subsequently washed by the addition of 750 µL of 75% ethanol and vortexed. The samples were centrifuged at 7,500 g for 5 mins at 4ºC. The supernatant was removed and the wash step was repeated. The RNA pellet was allowed to air-dry for 10 mins and then re-suspended in 20 µL of RNase free water.

2.9.2. Determination of DNA/RNA Quantity and Quality

Purified RNA samples were quantified using the Nanodrop® ND-1000 spectrophotometer (NanoDrop Technologies). Before applying the RNA/DNA sample, the pedestal was wiped down using a lint-free tissue dampened with UHP. The programme 'RNA-40' was selected on the NanoDrop software main screen to read the samples at 260nm, and the instrument was blanked with 1 µL of UHP. The concentration of RNA/DNA was calculated by software using the following formula: OD260 nm x Dilution factor x 40 = ng/µL RNA. Samples were checked for quality (i.e. Phenol contamination) by assessing the A260/A280 and A260/A230 ratio values. An A260/A280 ratio ~2, and an A260/A230 of ~1.8-2.2 is indicative of a pure RNA.

2.9.3. High Capacity cDNA Reverse Transcription

Reverse transcription of RNA to cDNA was carried out using the High Capacity cDNA reverse transcription kit (Applied Biosystems, 4368814) in accordance with the manufacturer's specifications. A maximum of 2 µg of RNA was made up to 10 µL in a 0.5 mL PCR tube using nuclease-free water. In a separate 0.5 mL PCR tube, the reverse transcription master mix was prepared. 10 µL of the RT master mix was added to the RNA sample and mixed using a pipette giving a final volume of 20 µL. The temperature profile

and conditions for the reverse transcription reaction carried out using a bench top thermal cycler G-Storm GS1 PCR machine are shown in **Table 2.7.**

	Step1	Step2	Step3	Step 4
Temperature (°C)	25	37	85	4
Time (min)	10	120	5	∞

Table 2.7 Cycling conditions for reverse transcription

2.9.4. Quantitative Real-Time PCR (qRT-PCR)

Taqman® qPCR was used to assess gene expression. Taqman® qPCR involved using individual Taqman® gene expression assays (Applied Biosystems 4453320) for each gene. These assays contain the individual primers and probe for each gene. **Table 2.8** lists the Taqman assays used in this study. These assays were used with Taqman® Fast Advanced Master Mix (Applied Biosystems 4444556) and MicroAmp® Fast Optical 96 well reaction plates (Applied Biosystems 4346907). cDNA sample (from Section 2.9.3) was diluted between 40ng to 100ng per reaction. The cDNA was diluted using nuclease-free water and 1µl was loaded per well with 1µl of Taqman® assay and 10µl of Taqman® Master Mix. The plate was then sealed using MicroAmp® Optical Adhesive Film (Applied Biosystems 4311971) and the cycles listed in **Table 2.9** were performed in Applied Biosystems 7900 Real-Time PCR System. Data was analysed using a Relative Quantification ddCt study. A calibrator sample was selected and set to a value of one, allowing for the comparison of all other samples in relation to the calibrator. For the analysis of target gene and endogenous control amplification, the baseline was set to average, normalised fluorescent signal before detectable increase (usually 3-15 cycles) and the cycle threshold was set in the exponential part of the curve. The Ct standard error was ideally less than +/-0.161 between replicate wells, and Ct errors with values greater than this were removed as outliers. The endogenous control (B2M) was used automatically to normalise the data. When this was achieved for both the target and endogenous control, the relative quantity values for the run were generated and plotted relative to the calibrator samples.

Gene	Catalogue Number
LY6G6F (probe #1)	Hs00222013_m1
LY6G6F (probe #2)	Hs01561205_g1
IL1RAPL1	Hs00990788_m1
B2M	Hs00984230_m1

Table 2.8 TaqMan assays used in this study.

Parameter	Hold	Hold	40 cycles	
Temp. (°C)	50	95	95	60
Time	2min	20sec	1sec	20sec

Table 2.9 Thermal cycling conditions for TaqMan assays.

2.10. Target Overexpression

Overexpression of targets LY6G6F and IL1RAPL1 was carried out using commercial transfection ready cloning vectors (GenScript). These ORF cDNA clones come as protein-coding, expression-ready genes in vectors tagged for protein detection and purification. Both the LY6G6F sequence (Clone ID: OHu03468) and the IL1RAPL1 sequence (Clone ID: OHu19152) are cloned into pcDNA3.1+/C-(K)DYK vectors, with a C-terminal DYKDDDDK tag (FLAG-tag), which will allow confirmation of overexpression by Western blot analysis. An empty pcDNA3.1+/C-(K)DYK vector (containing no target ORF) was also obtained as a negative control. **Figure 2.1** shows the map of the pcDNA3.1+/C-(K)DYK vector. The vector contains Amp and Neo genes for antibiotic selection of bacterial and mammalian transformed cells.

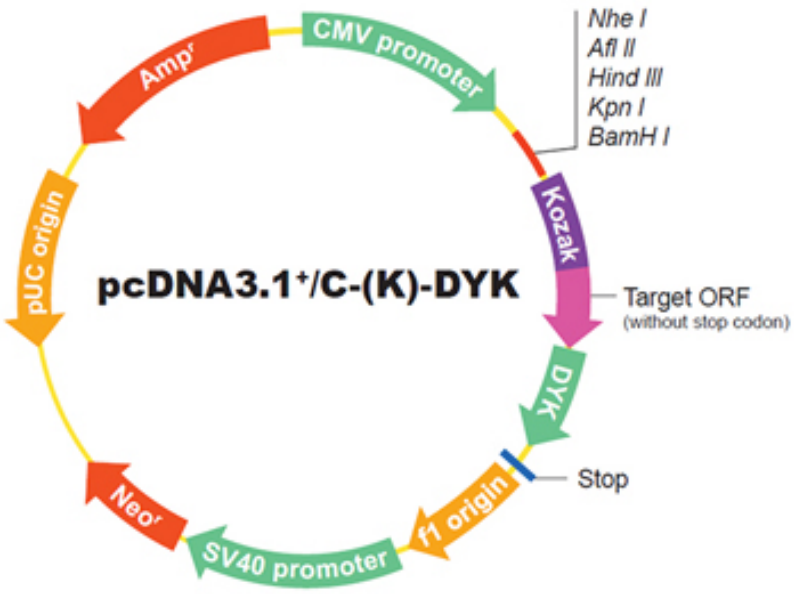

Figure 2.1 Vector map of the cloning vectors used for LY6G6F and IL1RAPL1 overexpression. Gene expression is driven by a CMV promoter. Kozak sequence initiates the mRNA translation process into protein. A C-terminal DYKDDDDK tag (FLAG-tag) is attached to the target sequence.

2.10.1. Optimisation of Vector Transfection Conditions

MIA PaCa-2 and SW480 cells were transfected with overexpression/empty vectors using Lipofectamine 2000 transfection reagent. Prior to this the optimal transfection conditions for vector transformation were determined. The optimal cell number for transfection of these cells was already determined in Section 2.4.1. In order to determine the optimal Lipofectamine 2000 and vector concentration, cells were transfected with varying concentrations of a N44 constitutive GFP expression plasmid (1µg, 2.5µg, 5µg) and varying concentrations of Lipofectamine 2000 (2µl and 3µl), to quickly determine efficiency by looking for GFP expression under fluorescent microscope. 72 hrs post transfection, the cells were assessed for GFP expression under fluorescent microscope, with the optimal conditions taken as those giving maximum GFP expression. The optimal conditions chosen for both cells lines were: 2.5 µg vector + 2 µl Lipofectamine 2000.

2.10.2. G418 Kill Curve

Selection of vector transformed cells is carried out by antibiotic selection. The vectors being used contain the Neo gene, which enables cells to survive in the presence of Neomycin and G418 antibiotics. Therefore prior to target vector transformation of MIA PaCa-2 and SW480 cells, an antibiotic kill curve needed to be carried out to determine the optimal concentration required to kill all cells. Cells were set up in 24 well plates and treated with concentrations of G418 (Sigma: 4727878001) ranging from 200-2000μg/ml. The optimal dose is the lowest antibiotic concentration at which all cells are dead after one week of antibiotic selection. Cells were fed with fresh G418 containing medium every 2-3 days. The optimal G418 dose for SW480 cells was determined to be 1400μg/ml and for MIA PaCa-2 cells, 1600μg/ml.

2.10.3. Generation of Stable Target Overexpression Cell Lines

Following the determination of optimal vector transfection conditions and G418 dose required, SW480 / MIA PaCa-2 cells were set up in 6 well plates and transfected with 2.5μg of LY6G6F/IL1RAPL1/Empty vector. A cells only well was also set up. 48hrs post-transfection cells were placed into G418 antibiotic selection. The cells only well acts as a control showing the length of time it takes for complete cell death of un-transfected cells. Cells that have survived in the transfected wells i.e. that have been successfully transformed with the vector are allowed to grow until confluency in the 6 well plate, kept under continuous G418 selection. When confluent, cells are transferred to T75 flasks for continuous culture. Cells are maintained in G418 selection media for 3 passages to ensure complete selection of stably transformed cells. At this stage cells can be cryopreserved as a new cell line, as the cell line has been changed from the original to a new stable mixed population. Stable cell lines are then grown in regular culture medium, with a routine pulse of G418 containing medium every 3 passages, to ensures that the transgene is retained. Confirmation of target gene overexpression is determined by qRT-PCR analysis as described in Section 2.9. Confirmation of protein overexpression is determined by Western blot analysis as described in Section 2.3, with the presence of the FLAG-tag confirming vector protein expression.

2.11. Co-Immunoprecipitation (Co-IP)

Attempts at Co-IP of targets LY6G6F and IL1RAPL1 were carried out using two independent LY6G6F antibodies (Abcam ab62597 and LSBIO LS-C148408), and two independent IL1RAPL1 antibodies (Proteintech 21609-1-AP and Sigma WH0011141M4). Two different methods of IP were tried – Direct/traditional IP and cross-linked IP. However, neither target protein was successfully immunoprecipitated by either method.

2.11.1. Direct Immunoprecipitation

This method is also known as traditional immunoprecipitation. Proteins were isolated from cell lines using a gentle lysis buffer (Thermo Fisher Scientific, #87787) to preserve protein complexes using the method described in Section 2.3.1. Protein extracts were quantified using as described in Section 2.3.4. Samples were diluted to a concentration of 1 mg/mL in a final volume of 1 mL using the gentle lysis buffer. Protein-G agarose beads (Sigma, P3296) were washed x3 in PBS before being added to the 1 mL test aliquot of protein extract for pre-clearing. 60 µL of Protein-G beads were added to the sample using a cut P-1000 pipette tip to minimise damage to the beads. All samples were incubated for 4 hours at 4°C on a rocking platform for pre-clearing. Beads were removed by spinning at 1000 g for 1 minute at 4°C. Supernatants were removed to clean Eppendorf tubes and divided evenly to represent the test sample and the negative control. The primary antibody of interest was added to the test sample, and IgG matching the host species of the primary antibody was added to the negative control. Antibody/lysate mixtures were incubated at 4°C overnight on a rocking platform. The following day, in order to precipitate the antibody-antigen complex, newly prepared Protein- G agarose beads were added to the samples as before and incubated at 4°C for 4 hours on a rocking platform. Beads were removed by spinning at 1000 g for 1 minute at 4°C, and the supernatant was saved as the 'unbound fraction'. The beads were then washed for 5 x 2-minute periods with gentle lysis buffer and pelleted at 1000 g between each wash for 1 minute. Following the final wash, the sample/bead solution was transferred to a spin column (Sigma, SC1000) before another centrifugation step as before. 70 µL of 2X Laemelli sample buffer was added to both sets of Protein-G beads before being heated to 95°C on a heating block. Samples were spun at 12000 g for 2 minutes and eluted into fresh Eppendorf tubes. Elutions were made to a 1x concentration with PBS and were stored at -20°C until required.

2.11.2. Cross-Linked Immunoprecipitation

Cross Linked IP were carried out using the Pierce Co-Immunoprecipitation Kit (Thermo Fisher Scientific, #26149). 200 µL of AminoLink resin was added to a spin column, and spun down at 1000 g for 1 minute (all subsequent centrifugation steps were at this speed and duration). The resin was washed twice with 0.4 mL of Coupling Buffer, centrifuged and excess solution discarded. The primary antibody of interest was added to the resin, along with 200 mL of Coupling Buffer (same for negative control IgG). 3 µL of Reducing Agent (Sodium Cyanoborohydride) was added to the mixture antibody/resin, which was then incubated at RT for 90 minutes. This step is to facilitate cross-linking of the antibody to the resin. The resin was then centrifuged and washed 2 times with 0.2 mL Coupling Buffer. Following this, 0.2 mL of Quenching Buffer was added to the suspension, centrifuged, and excess solution discarded. 0.4 mL of Quenching Buffer was then added to the gel/antibody complex, along with 3 µL of Reducing Agent. This suspension was incubated with end-over-end mixing, for 30 minutes at room temperature, followed by centrifugation and discarding of any excess solution. The gel was then washed 2 times with 0.2 mL Quenching Buffer, followed by 6 washes in 0.4 mL Wash Solution, with centrifugation following each wash. The protein sample was prepared as described in Section 2.11.1, and added to the resin/antibody complex. This solution was incubated overnight at 4°C on a rocking platform. The following day, the sample was centrifuged, and excess solution discarded. The resin/antibody-antigen complex was then washed 3 times in 0.4 mL Immunoprecipitation Buffer, with centrifugation after each wash. The antigen/antibody complex was then eluted with the addition of 200 µL of a low pH Elution Buffer to the solution, followed by 5-minute incubation at room temperature. The low pH of the buffer was neutralised with the addition of 5 µL of a Tris-HCl, pH 9.5, solution. Elutions were made to a 1x concentration with PBS and were stored at -20°C until required.

Chapter 3. Identification and validation of novel membrane cancer targets

3.1. Identification of Potential Membrane Proteins Overexpressed in Colon Cancer

Background: Colorectal cancer (CRC) is the 3rd most commonly diagnosed cancer worldwide, and also the 4th most common cause of cancer death. There is a huge need for the discovery of new treatment strategies for CRC. This study aimed to identify membrane-localised proteins overexpressed in colon cancer compared to normal colon for investigation as potential molecular targets for therapeutic antibody targeting. Identified proteins would also be examined for increased expression in a number of other cancers, in particular pancreatic ductal adenocarcinoma (PDAC), which has a dismal prognosis with only a 5% 5 year survival rate. There is an urgent unmet need for both a better understanding of the biological phenotype of PDAC and also for new therapeutic targets. There is a current lack of exploitable molecular targets for PDAC.

The search for potential cancer targets began with an analysis of colon cancer gene expression microarray data available for download from the Gene Expression Omnibus (GEO) database, as described in Section 2.1. The GEO database contains datasets from hundreds of different technologies/platforms, including mRNA gene expression arrays, miRNA arrays and RNA-seq. The criteria for our search was for colon cancer datasets with:

1) Normal human colon and colon carcinoma tissue sections used for the analysis (as opposed to cell line data).
2) Data presented as gene expression level.
3) Microarray platform used was Affymetrix U133 plus 2.0 arrays.

With these criteria, a dataset by Skrzypczak *et al.*, (2010) was chosen for analysis. This dataset contains whole tissue section samples from 24 normal colon, 45 colon adenoma and 36 colon adenocarcinoma specimens. From this data, two lists were generated in-house of genes upregulated in (1) colon adenocarcinoma vs. normal colon and (2) colon adenoma vs. normal colon. Genes were then annotated for membrane localisation using Pathway Studio Enterprise software and a fold change of ≥ 2 and an adjusted p-value of $\leq 1E^{-5}$ were considered significant. This produced the final lists of predicted membrane localised genes, with 127 genes found to be upregulated in adenocarcinoma compared to normal colon and 154 genes upregulated in adenoma compared to normal colon.

These gene datasets were then manually curated by literature review and also commercial antibody availability to select genes for validation. The literature mining of targets aimed to eliminate proteins that had already been associated with a functional role in colon cancer or as a potential therapeutic target. Relatively novel cancer targets were sought for validations. With these criteria 7 genes were chosen for validation from across the two lists. They are: Lymphocyte antigen 6 complex, locus G6D/F (LY6G6D/F), Interleukin 1 receptor accessory protein / -like 1 (IL1RAP/L1), Neurotrimin (NTM), Leucine rich repeat containing 8 family, member E (LRRC8E), Epoxide hydrolase 4 (EPHX4), Beta-site APP-cleaving enzyme 2 (BACE2) and Interleukin 20 receptor, subunit Alpha (IL20RA). Whether the genes came from the adenoma list, adenocarcinoma list or both, as well as their relevant fold change is described in **Table 3.1**.

Gene Name	Full Name	Adenoma fold change	Carcinoma fold change
LY6G6D	Lymphocyte antigen 6 complex, locus G6D	9.8	17.6
IL1RAP	Interleukin 1 receptor accessory protein	-	2
NTM	Neurotrimin	-	5.4
LRRC8E	Leucine rich repeat containing 8 family, member E	4.4	3.2
EPHX4	Epoxide hydrolase 4	4.8	8.9
BACE2	Beta-site APP-cleaving enzyme 2	6	2.7
IL20RA	Interleukin 20 receptor, subunit Alpha	4.2	-

Table 3.1 Candidate gene targets selected for protein validation. The up linear fold change for each target in adenoma and carcinoma compared to normal colon is displayed. No number indicates that the candidate target was not present on that list.

3.2. Validation of Candidate Target Protein Expression

As the candidate targets were identified from mRNA overexpression, there is no guarantee that the corresponding protein will be similarly overexpressed. Furthermore, confirmation of the subcellular localisation of these predicted membrane proteins is required. Target protein expression was first examined in a panel of colon cancer cell lines by Western blot analysis, followed by a preliminary Immunohistochemistry (IHC) screen for protein expression in normal colon and colon adenocarcinoma tissue sections. The initial validations were to determine 1) is the protein expressed? and 2) is it expressed at a higher level in colon cancer compared to normal colon (with minimal normal colon expression)?

A panel of 6 colon cancer cell lines (listed in **Table 3.2**) was used to investigate target protein expression. Both the whole cell lysate and a membrane enriched fraction (sample preparation is described in Section 2.3.2) of each cell line were examined for target expression, to determine if the target protein is expressed across these cell lines and, if it is associated with the membrane. The whole cell lysate can be used to determine differences in expression between the cell lines, with alpha-tubulin used as an internal loading control, to confirm equal loading of samples. However, the membrane enriched fraction in this study is being used as a qualitative assessment of whether the protein is membrane associated in the cells. Due to sample preparation variation and the lack of a suitable loading control, the membrane fractions cannot be used to accurately compare membrane localised expression between cell lines, but can validate if target expression is associated with the plasma membrane in these cells. The panel of cell lines represent several different mutations commonly found in CRC (see Table 3.2). An initial IHC screen of formalin-fixed, paraffin-embedded (FFPE) full-face tissue sections of normal colon and colon adenocarcinoma, obtained from St. Vincent's University Hospital, was then carried out. Before this, optimisation of IHC conditions and antibody dilutions for each target was completed, with the final conditions used described in Section 2.6.2. These results would determine whether candidate targets were suitable for wider tissue expression validations and assessment of their functional role, if any, in cancer.

The protein validation results for each of the seven selected candidate targets are shown in Sections 3.2.1-3.2.8. Out of the seven selected candidate targets, only LY6G6F and IL1RAPL1, were observed to be strongly expressed in colon adenocarcinoma tissue sections, with minimal expression in normal colon. The protein expression of targets LRRC8E and

EPHX4 could not be validated in tissue sections by Immunohistochemical analysis. The remaining three targets, NTM, IL20RA and BACE2, all showed similar protein expression levels in normal colon and colon adenocarcinoma tissue sections, indicating no apparent overexpression in cancer vs. normal tissue. Therefore, only LY6G6F and IL1RAPL1 were selected to pursue further for wider tissue expression validations, assessment of any functional role in cancer *in vitro*, and investigation as potential molecular targets for therapeutic antibody targeting.

Cell line	KRAS	BRAF	PIK3CA	PTEN	TP53	Source
SW480*	**G12V**	WT	WT	WT	**R273H; P309S**	Dukes' type B colorectal adenocarcinoma
SW620*	**G12V**	WT	WT	WT	**R273H; P309S**	Dukes' type C colorectal adenocarcinoma, derived from lymph node metastasis
HCT116	**G13D**	WT	**H1047R**	WT	WT	Dukes' type D colorectal carcinoma
T84	**G13D**	WT	**E542K**	WT	WT	Colorectal carcinoma derived from lung metastasis
HT29	WT	**V600E**	**P449T**	WT	**R273H**	Dukes' type C colorectal adenocarcinoma
CaCo-2	WT	WT	WT	WT	**E204X**	Colorectal adenocarcinoma

Table 3.2 Colon cancer cell line panel used in this study, showing some of the common mutations found in CRC and the original source of the cell line. *SW480 and SW620 cell lines are derived from the same patient – SW480 from the primary colon adenocarcinoma tumour and SW620 from a lymph node metastasis. WT, wildtype genotype.

3.2.1. Validation of LY6G6D/F Protein Expression

LY6G6D showed an increased fold change of 17.6 in the colon adenocarcinoma dataset and 9.8 in the adenoma dataset compared to normal colon. The Affymetrix probe set for this gene is stated to not be unique and unable to distinguish between LY6G6D and LY6G6F. The antibody sourced for validations is an anti-LY6G6F antibody (which lists LY6G6D as an alias). There is some confusion in the literature surrounding these genes, with LY6G6F being described as a transcript of the *LY6G6D* gene in some sources. (Calvanese *et al.*, 2008) This will be described in greater detail in Chapter 4, Section 4.1. LY6G6F is a type 1 transmembrane protein, belonging to the immunoglobulin (Ig) superfamily and was first identified as a novel platelet plasma membrane protein. The cytoplasmic tail of LY6G6F is capable of interacting with growth-factor-receptor-bound protein (Grb) 2 and Grb7. (de Vet, Aguado and Campbell, 2003; Macaulay *et al.*, 2007) However, a potential ligand for LY6G6F activation has not yet been discovered.

3.2.1.1. Western Blot Analysis

LY6G6F expression was investigated in the whole cell lysate and membrane enriched fraction of the colon cancer cell line panel. Representative Western blot images of these results are shown in **Figure 3.1**. LY6G6F specific bands were identified at the predicted molecular weight (MW) of 32kDa. LY6G6F is expressed in the whole cell *and* membrane enriched fraction of all of the cell lines probed, indicating an association with the membrane in these colon cancer cells. Highest expression is observed in the T84 and HT29 cell lines. There appears to be no apparent trend of LY6G6F expression towards a particular mutational status in this subset of colon cancer cell lines.

3.2.1.2. Immunohistochemical Analysis

The investigation of LY6G6F expression in normal colon and colon adenocarcinoma tissue sections confirmed the increased expression of LY6G6F at the protein level in colon adenocarcinoma. Negative or weak LY6G6F immunoreactivity was observed in normal colon. In contrast, intense LY6G6F immunoreactivity was observed in colon adenocarcinoma tissue. **Figure 3.2** shows representative photomicrographs of these results.

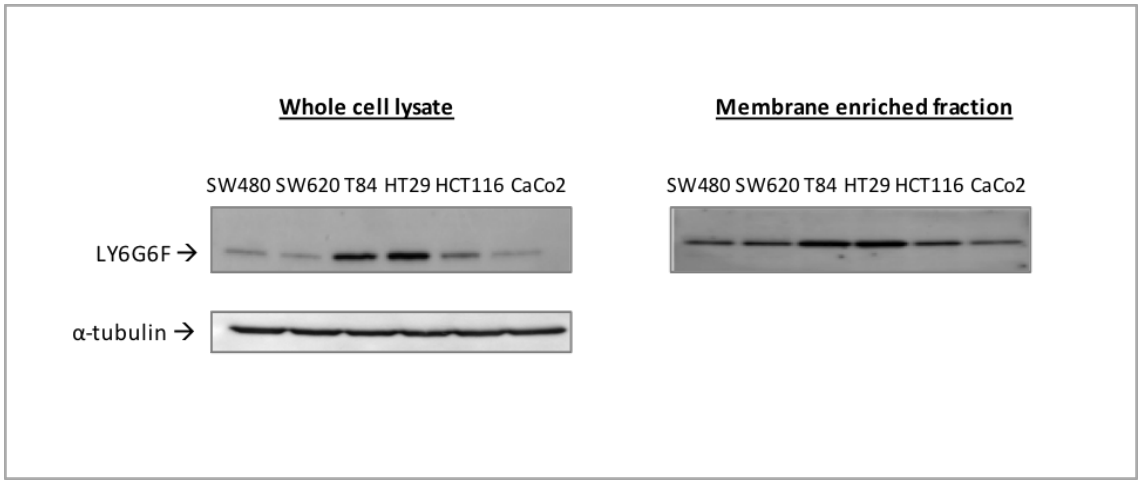

Figure 3.1 Representative Immunoblot showing LY6G6F expression in the whole cell and membrane enriched fractions of a panel of colon cancer cell lines. LY6G6F bands are identified between the 30-40 kDa MW markers, showing the correct MW of ~32kDa. α-tubulin confirms equal loading of total proteins in the whole cell lysate. (n=2)

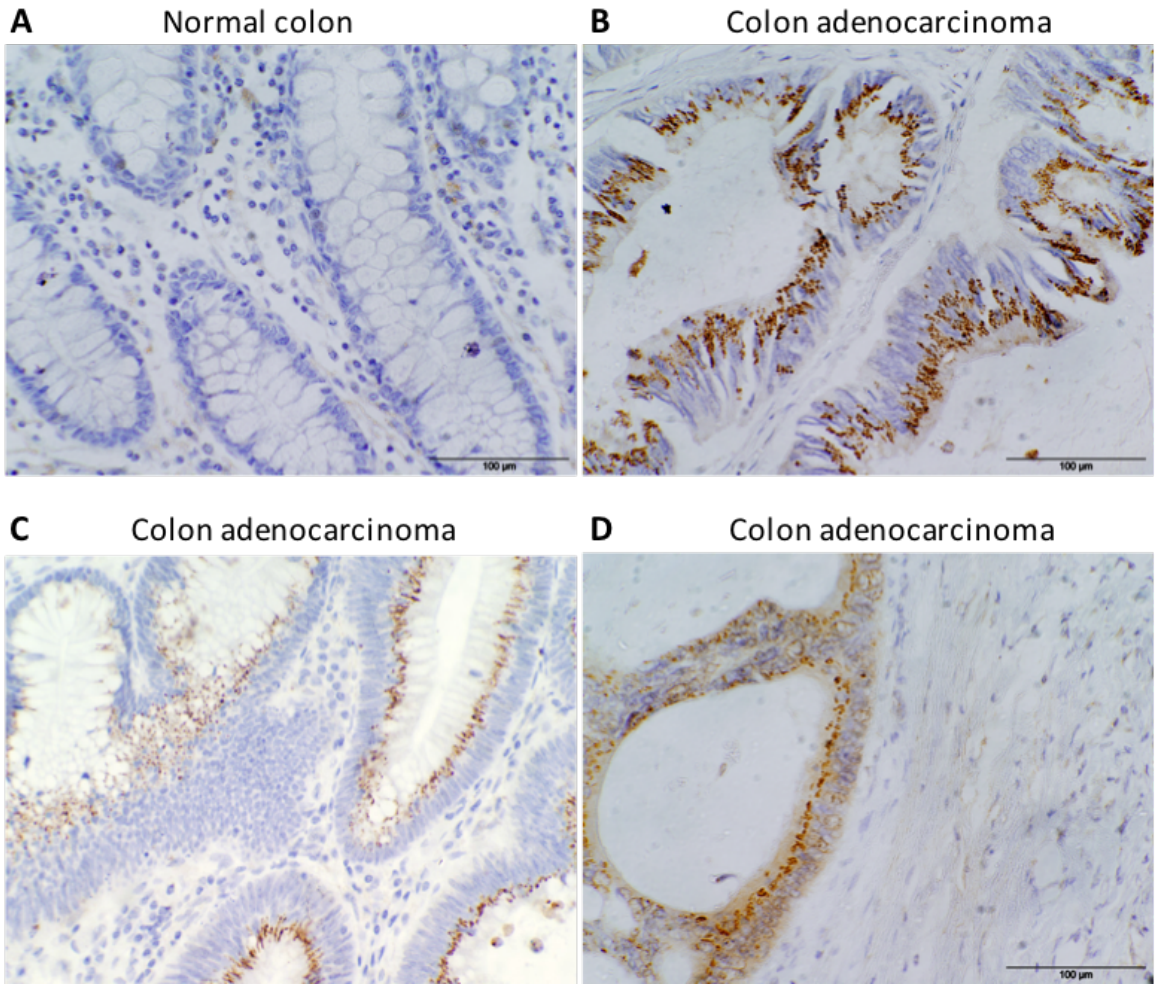

Figure 3.2 IHC analysis of LY6G6F expression in normal and malignant colon. Representative images showing: (**A**) Normal colon with negative immunoreactivity. (n=7) (**B, C, D**) Colon adenocarcinoma with strong granular cytoplasmic immunoreactivity. (n=12) Original magnification 400x. The scale bars represent 100µm.

3.2.2. Validation of IL1RAPL1 Protein Expression

Interleukin 1 receptor accessory protein (IL1RAP) was identified from the datasets, with a 2 fold increase in colon cancer compared to normal colon. However, a transcription error resulted in an antibody against Interleukin 1 receptor accessory protein like 1 (IL1RAPL1) being obtained for validation. IL1RAP and IL1RAPL1 are both members of the interleukin-1 receptor (IL-1R) family. The IL1RAPL1 gene encodes a protein that has homology to IL1RAP, however they have distinct functions. IL1RAP is a necessary accessory protein part of the interleukin 1 receptor complex, which initiates signalling upon IL-1 binding. (Boraschi and Tagliabue, 2013) IL1RAP overexpression has been implicated in a number of haematological malignancies, including myelodysplastic syndrome, acute myeloid leukaemia (AML) and chronic myeloid leukaemia (CML). (Barreyro *et al.*, 2012; Zhao *et al.*, 2014) IL1RAPL1 has been suggested to have a specialised role in physiological processes in the brain, including learning abilities, and mutations in the IL1RAPL1 gene have been identified in patients suffering from nonspecific X-linked intellectual disability. (Chelly *et al.*, 1999; Piton *et al.*, 2008) In this study IL1RAPL1 overexpression was observed in CRC vs. normal colon. IL1RAPL1 is a novel CRC target, with no previous links to CRC described in the literature. Therefore, it was decided to continue with IL1RAPL1 as a candidate target for further validations.

3.2.2.1. Western Blot Analysis

The investigation of IL1RAPL1 expression in the colon cancer cell line panel, revealed bands at ~69kDa, corresponding to the predicted MW of IL1RAPL1. IL1RAPL1 protein is expressed in both the whole cell lysate *and* membrane enriched fraction of all cell lines investigated, indicating an association with the membrane in these cell lines. IL1RAPL1 is expressed at similar levels across the panel, with highest expression observed in the HCT116 cell line. Representative Western blot images are shown in **Figure 3.3.**

3.2.2.2. Immunohistochemical Analysis

The investigation of IL1RAPL1 expression in normal colon and colon adenocarcinoma tissue sections showed increased expression of IL1RAPL1 in colon adenocarcinoma compared to normal colon. Negligible IL1RAPL1 expression was observed in normal colon, with strong IL1RAPL1 immunoreactivity observed in adenocarcinoma tissue, which is shown in **Figure 3.4.** The preliminary IHC validation shows that IL1RAPL1 is overexpressed in CRC compared to normal colon, and as IL1RAPL1 is a novel target in CRC, we decided to pursue it further.

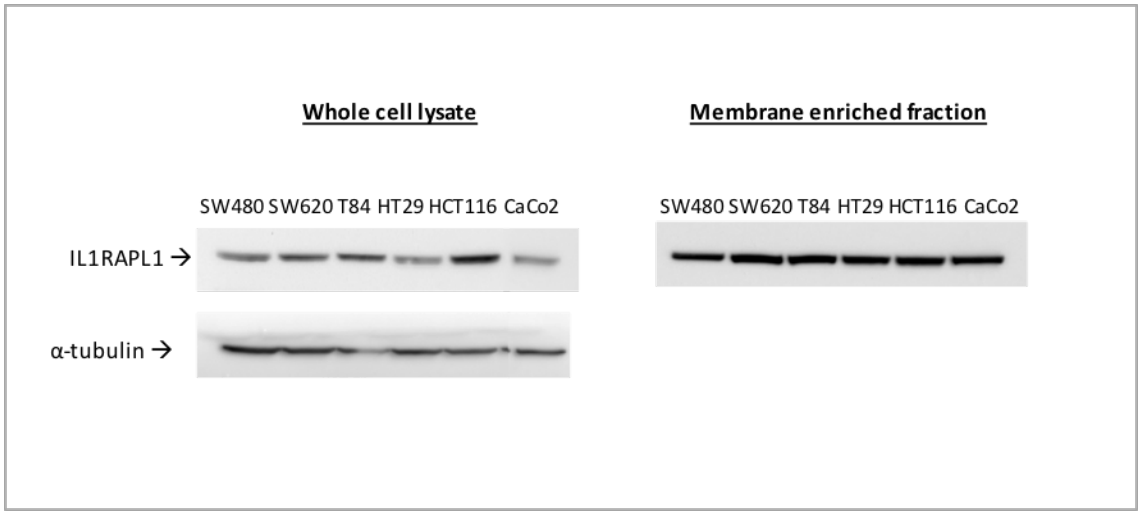

Figure 3.3 Representative Immunoblot showing IL1RAPL1 expression in the whole cell and membrane enriched fraction of a panel of colon cancer cell lines. IL1RAPL1 bands are identified between the 60-80 kDa MW markers, indicating the correct MW of ~69kDa. α-tubulin levels indicate nearly equal loading of total proteins in the whole cell lysate. (n=2)

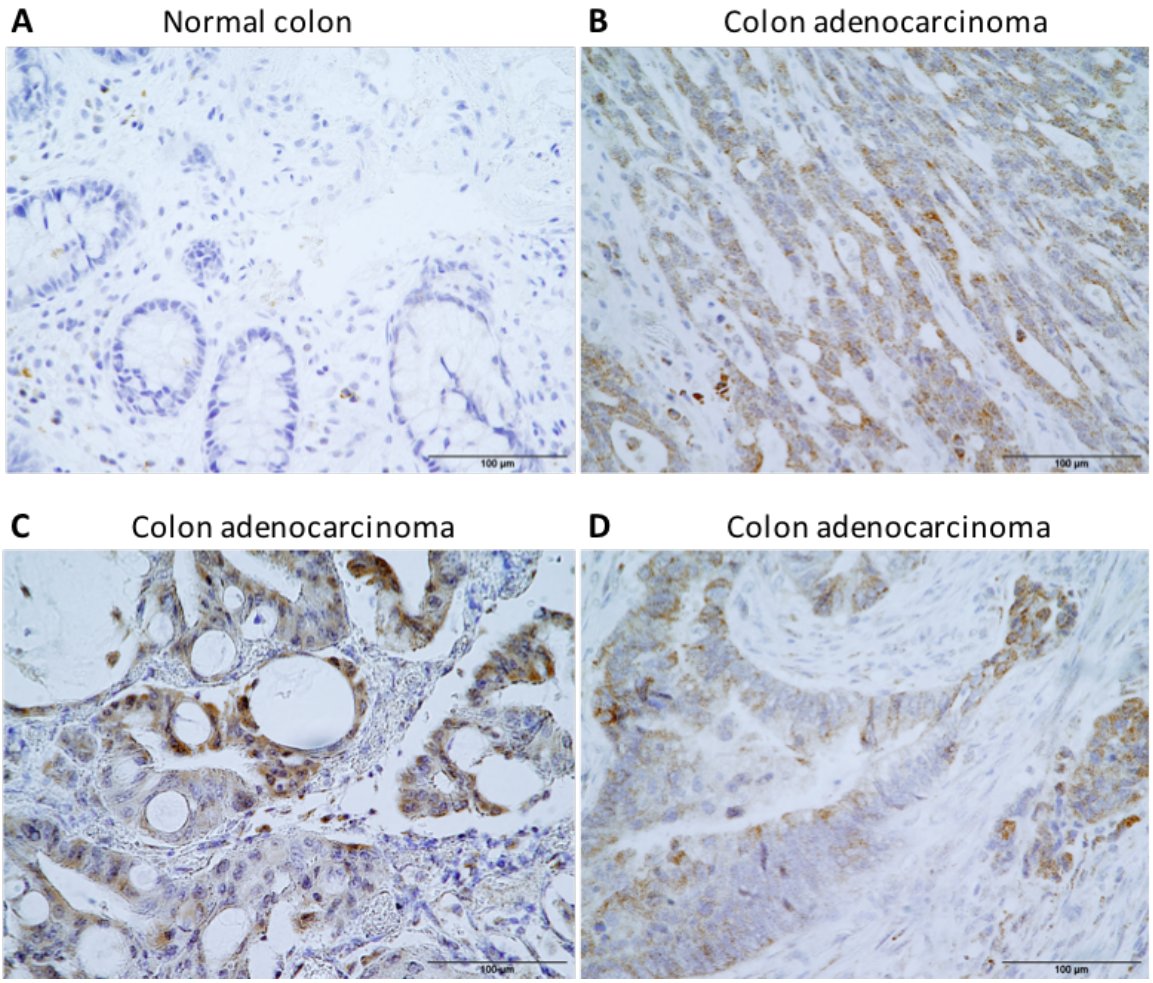

Figure 3.4 IHC analysis of IL1RAPL1 expression in normal and malignant colon. Representative images showing: (**A**) Normal colon with minimal IL1RAPL1 immunoreactivity. (n=7) (**B, C, D**) Colon adenocarcinoma with strong granular cytoplasmic IL1RAPL1 immunoreactivity. (n=12) Original magnification 400x. The scale bars represent 100µm.

3.2.3. Validation of LRRC8E Protein Expression

LRRC8E (Leucine-rich repeat-containing protein 8E) is a multi-pass membrane protein which contains 13 LRR (leucine-rich) repeats, and is a component of the volume-regulated anion channel (VRAC), an anion channel required to maintain a constant cell volume in response to extracellular or intracellular osmotic changes. (Ng and Xavier, 2011) LRRC8E showed a 4.4 fold increase in expression in the adenoma dataset and 3.2 fold increase in the adenocarcinoma dataset compared to normal colon.

3.2.3.1. Western Blot Analysis

The investigation of LRRC8E expression in the colon cancer cell line panel by Western blot analysis, revealed bands at ~90kDa, the predicted MW of LRRC8E. LRRC8E is expressed at similar levels across the whole cell line panel, and is also present in the membrane fraction of all cell lines analysed. These results are shown in **Figure 3.5**.

3.2.3.2. Immunohistochemical analysis

The optimisation of LRRC8E antibody for IHC analysis was unsuccessful. No LRRC8E immunoreactivity was detected in normal colon or colon adenocarcinoma, even with high antibody dilutions used. (Data not shown)

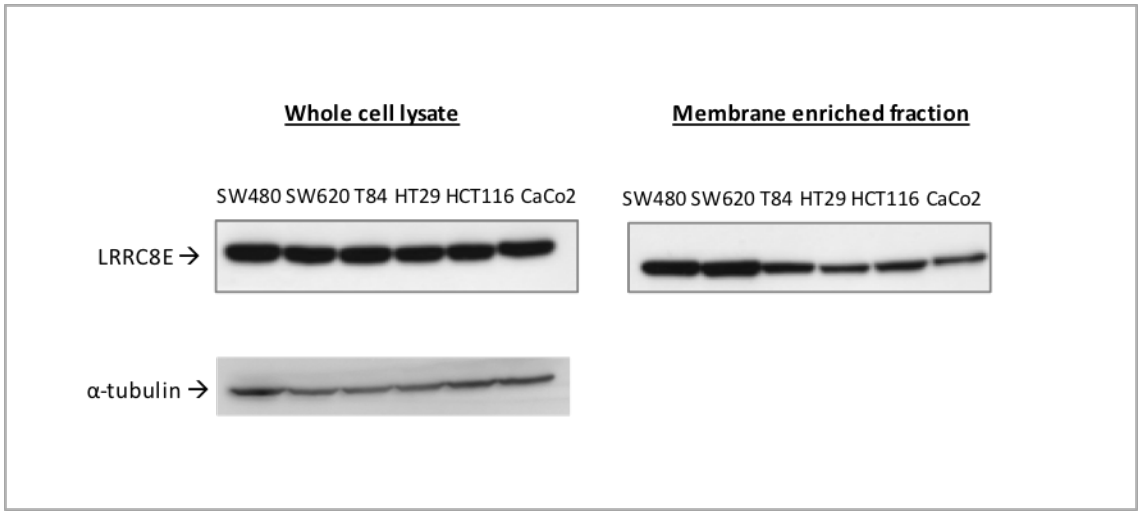

Figure 3.5 Western blot analysis showing LRRC8E expression in the whole cell and membrane enriched fraction of a panel of colon cancer cell lines. LRRC8E bands are identified between the 80-110 kDa MW markers, indicating the correct MW of ~90kDa. α- tubulin levels indicate nearly equal loading of total proteins in the whole cell lysate. (n=1)

3.2.4. Validation of EPHX4 Protein Expression

Epoxide hydrolase 4 (EPHX4) is expressed at a 4.8 fold higher level in the adenoma cohort, increasing to 8.9 fold higher in the adenocarcinoma cohort, compared to normal colon. EPHX4 is a single pass type II transmembrane protein. Epoxide hydrolases are critical biotransformation enzymes that activate and detoxify epoxides. (Omiecinski, Yang and Laurenzana, 2012)

3.2.4.1. Western Blot Analysis

The investigation of EPHX4 expression in the colon cancer cell line panel by Western blot analysis, revealed bands at ~40kDa, the predicted MW of EPHX4. EPHX4 is expressed in both the whole cell lysate *and* the membrane enriched fraction of every cell line analysed. EPHX4 is expressed at similar levels across the whole panel. **Figure 3.6** shows the results of the Western blot analysis.

3.2.4.2. Immunohistochemical Analysis

The IHC analysis to investigate EPHX4 expression in normal colon and colon adenocarcinoma sections was unsuccessful. No EPHX4 immunoreactivity was detected in tissue sections, including positive control tissues, even using high antibody concentrations. The antibody may not have been working correctly or EPHX4 protein was not expressed in the tissues analysed. (Data not shown)

Figure 3.6 Western blot analysis showing EPHX4 expression in the whole cell and membrane enriched fraction of a panel of colon cancer cell lines. EPHX4 bands are identified around the 40kDa MW marker, the predicted MW of EPHX4. α- tubulin levels indicate nearly equal loading of total proteins in the whole cell lysate (n=1)

3.2.5. Validation of NTM Protein Expression

Neurotrimin (NTM) is a glycosylphosphatidylinositol (GPI)-anchored membrane protein belonging to the IgLON family of neural cell adhesion molecules. IgLONs have been identified primarily in the central nervous system, where they are the most abundantly expressed GPI-anchored proteins. Ntougkos *et al.*, (2005) investigated the expression profiles of the IgLON family in ovarian cancer, and found that NTM expression is increased in tumour samples in relation to non-malignant ovary. NTM displayed a 5.4 fold increase in gene expression in colon adenocarcinoma compared to normal colon in the gene microarray datasets.

3.2.5.1. Western Blot Analysis

NTM is described as having 4 isoforms produced by alternative splicing by Uniprot; isoform 1: 38kDa, isoform 2: 38kDa, isoform 3: 35kDa and isoform 4: 39kDa. Additionally, a glycosylated form at ~58kDa has also been reported in the literature. Western blot analysis for NTM expression in the colon cancer cell line panel produced very poor results, as shown in **Figure 3.7.** Multiple bands and high background made it impossible to correctly identify the NTM protein band. A second anti-NTM antibody was also tested, but this was also unable to reliably detect the correct band.

3.2.5.2. Immunohistochemical Analysis

Investigation of NTM expression in normal colon and colon adenocarcinoma, showed high expression in some normal colon tissues, with similar expression in the adenocarcinomas analysed. Therefore, NTM does not appear to be upregulated at the protein level in colon tumours compared to normal colon. **Figure 3.8** shows some representative photomicrographs of these results.

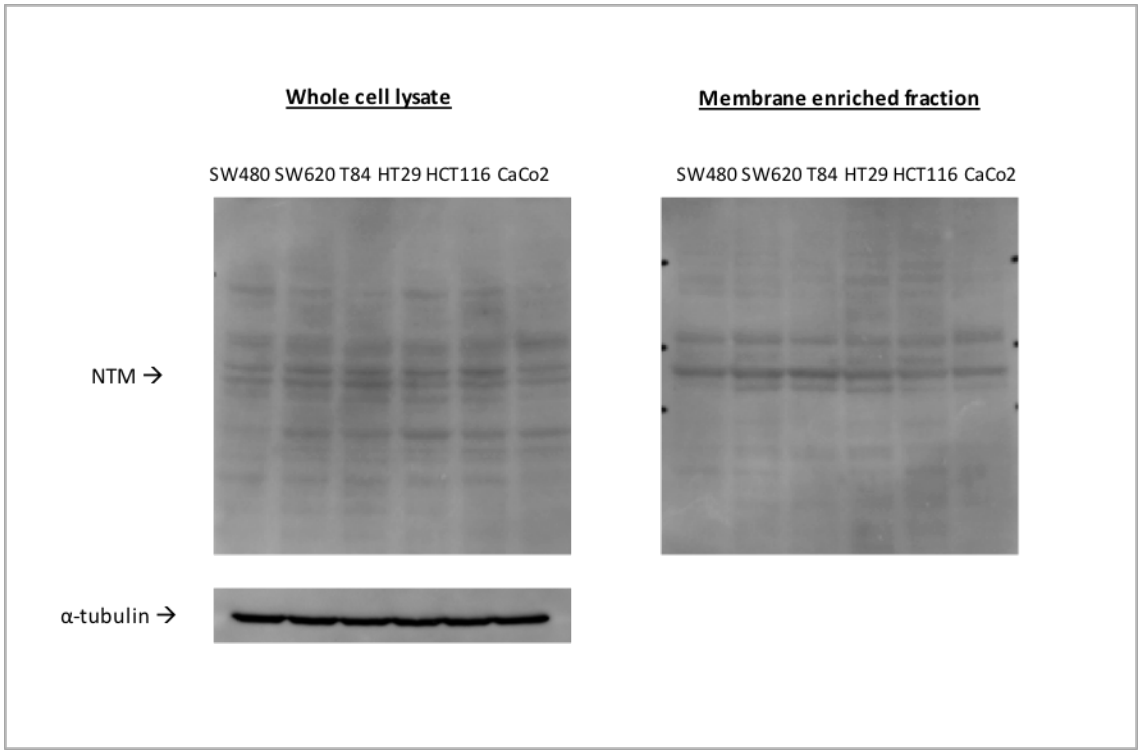

Figure 3.7 Western blot showing the whole cell and membrane enriched fraction of a panel of colon cancer cell lines probed for NTM. Multiple bands and high background prevented the identification of the correct NTM band. α-tubulin shows equal loading of total proteins in the whole cell lysate. (n=1)

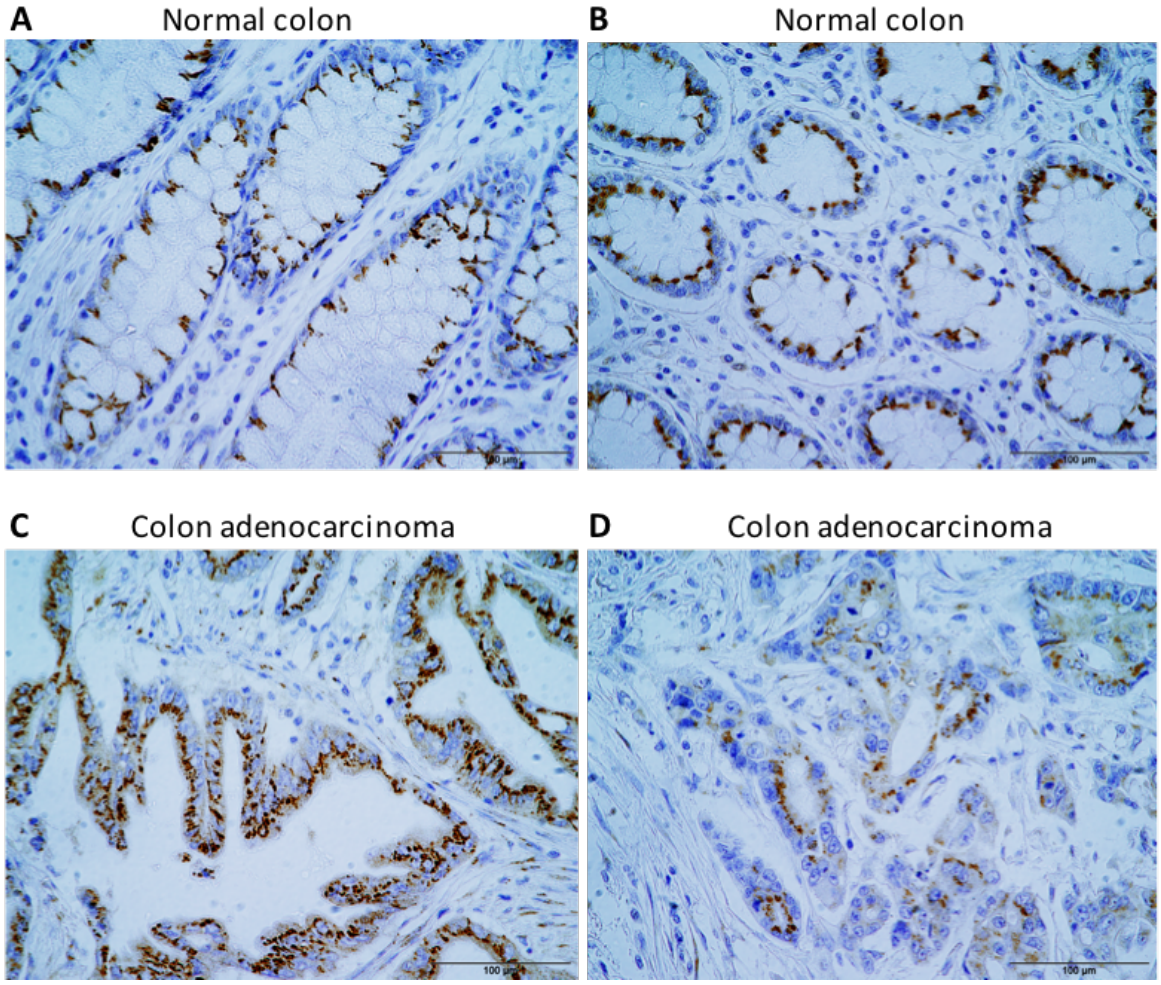

Figure 3.8 IHC analysis of NTM expression in normal and malignant colon. Representative images showing: (**A, B**) Normal colon with moderate to strong granular cytoplasmic immunoreactivity. (n=16) (**C, D**) Colon adenocarcinoma with strong granular cytoplasmic immunoreactivity. (n=12) Original magnification 400x. The scale bars represent 100µm.

3.2.6. Validation of IL20RA Protein Expression

IL20RA is a single pass type 1 membrane protein that forms a receptor complex with IL20RB for IL-20. It is also capable of forming a complex with IL10R2 for IL-26. IL20RA was found to be 4.2 fold up in the adenoma dataset compared to normal colon, but was not identified in the adenocarcinoma dataset. However, we still sought to validate its expression, as it may represent a potential marker for progression from normal colon to adenoma and then adenocarcinoma and a role for IL20RA in CRC has not been described to date to our knowledge. Elevated levels of IL-20, IL20RA and IL20RB are found in psoriasis and rheumatoid arthritis. IL20RA and IL20RB mRNA was also found to be expressed in colon, colonic supepithelial myofibroblasts and colonic epithelial cell lines. The expression of IL-20 and its receptors has also been linked to atherosclerosis. (Blumberg *et al.*, 2001; Wei *et al.*, 2006; Wegenka, 2010)

3.2.6.1. Western Blot Analysis

The investigation of IL20RA expression in the colon cancer cell line panel, revealed bands at ~62kDa, corresponding to the predicted MW of IL20RA. IL20RA is expressed across all cell lines analysed, in both the whole cell *and* membrane enriched fractions, as shown in **Figure 3.9.** Considerably higher expression is observed in the metastatic SW620 cell line compared to the primary tumour cell line, SW480, derived from the same patient. IL20RA also displays higher expression in the T84 cell line, which is derived from a lung metastasis, compared to some of the other cell lines. Therefore, IL20RA expression could have a potential association with metastatic colon adenocarcinomas.

3.2.6.2. Immunohistochemical Analysis

IHC analysis of IL20RA expression in normal colon and colon adenocarcinoma tissue sections, showed intense membrane immunoreactivity in adenocarcinoma tissue. A tissue section of colon cancer metastasised to liver, showed intense IL20RA membrane immunoreactivity in the colon cancer metastasis with low levels of IL20RA in surrounding liver tissue. However strong immunoreactivity was also observed in normal colon. **Figure 3.10** shows representative photomicrographs of these results. Therefore, this preliminary IHC

study shows that there does not appear to be differential expression of IL20RA at the protein level between normal colon and colon adenocarcinoma.

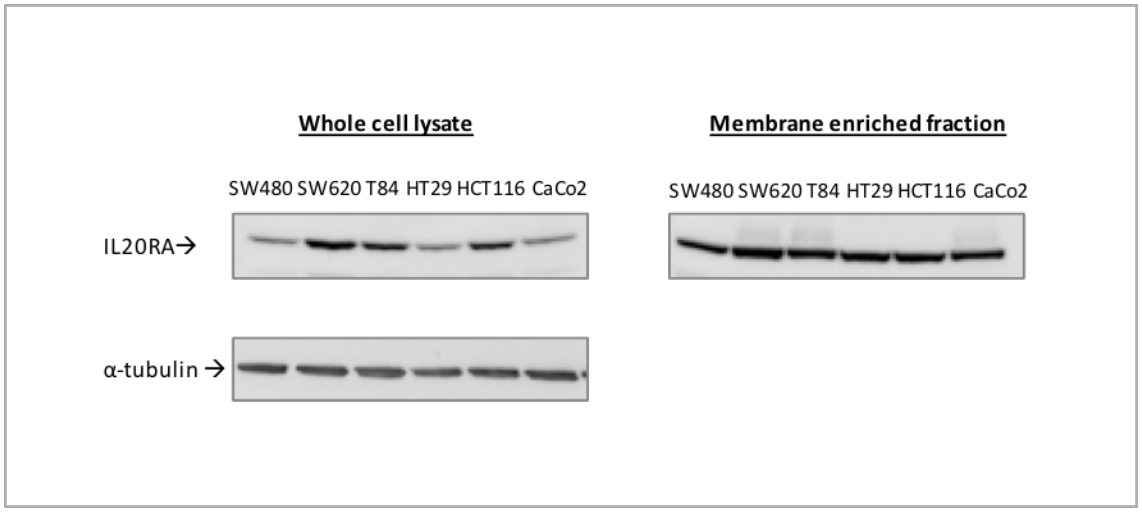

Figure 3.9 Western blot analysis showing IL20RA expression in the whole cell and membrane enriched fraction of a panel of colon cancer cell lines. IL20RA bands are identified between the 60-80 kDa MW markers, indicating the correct MW of ~62kDa. α-tubulin shows equal loading of total proteins in the whole cell lysate. (n=1)

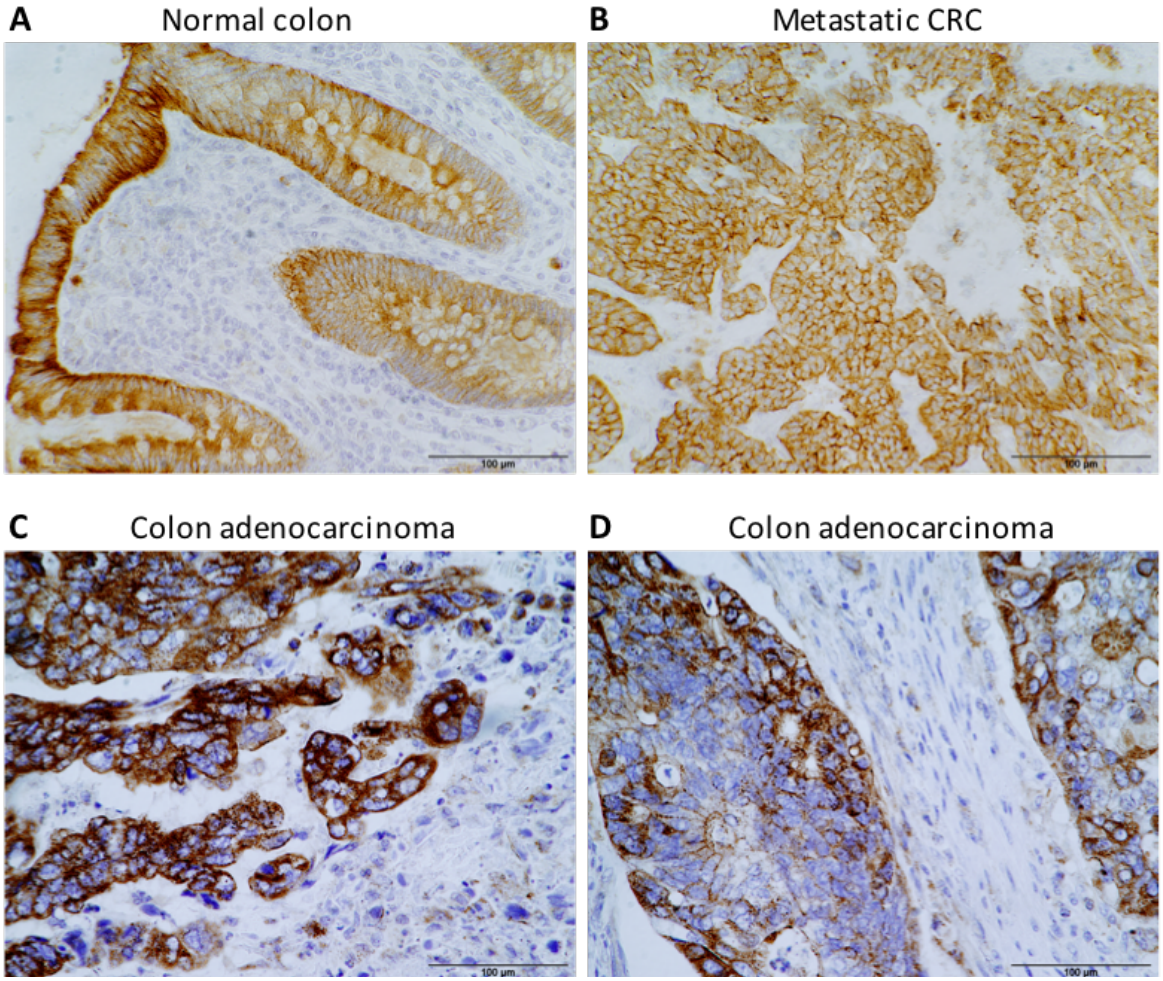

Figure 3.10 IHC analysis of IL20RA expression in normal and malignant colon. Representative images showing: (**A**) Normal colon with strong cytoplasmic and membranous immunoreactivity. (n=2) (**B**) CRC that has metastasised to liver with intense membrane immunoreactivity. (n=1) (**C, D**) Colon adenocarcinoma with strong cytoplasmic and membranous immunoreactivity. (n=4) Original magnification 400x. The scale bars represent 100μm.

3.2.7. Validation of BACE2 Protein Expression

BACE2 is an aspartyl protease that is involved in the production of amyloid-β protein, the principal component of the senile plaques that are an early and critical feature of Alzheimer's disease and a frequent complication of Down syndrome. (Farzan *et al.*, 2000) BACE2, an integral membrane glycoprotein, showed a 6 fold increase in expression in the adenoma dataset and 2.7 fold increase in the adenocarcinoma dataset compared to normal colon.

3.2.7.1. Western Blot Analysis

The investigation of BACE2 expression in the colon cancer cell line panel by Western blot analysis, revealed bands at ~56kDa, the predicted MW of BACE2. BACE2 is expressed in all of the colon cancer cell lines analysed, with highest expression observed in the whole cell lysate of the SW620 cell line, showing higher expression in the metastatic tumour compared to primary (SW480) tumour derived from the same patient. BACE2 is also associated with the membrane of all cell lines, as shown in **Figure 3.11**.

3.2.7.2. Immunohistochemical Analysis

The IHC analysis of BACE2 confirmed expression in colon adenocarcinoma tissue sections. However, the expression in normal colon was also quite high. **Figure 3.12** shows some representative photomicrographs of this result. Therefore, BACE2 may not be sufficiently overexpressed in colon adenocarcinoma compared to normal colon, to warrant further investigation as a potential molecular target for therapeutic antibody targeting.

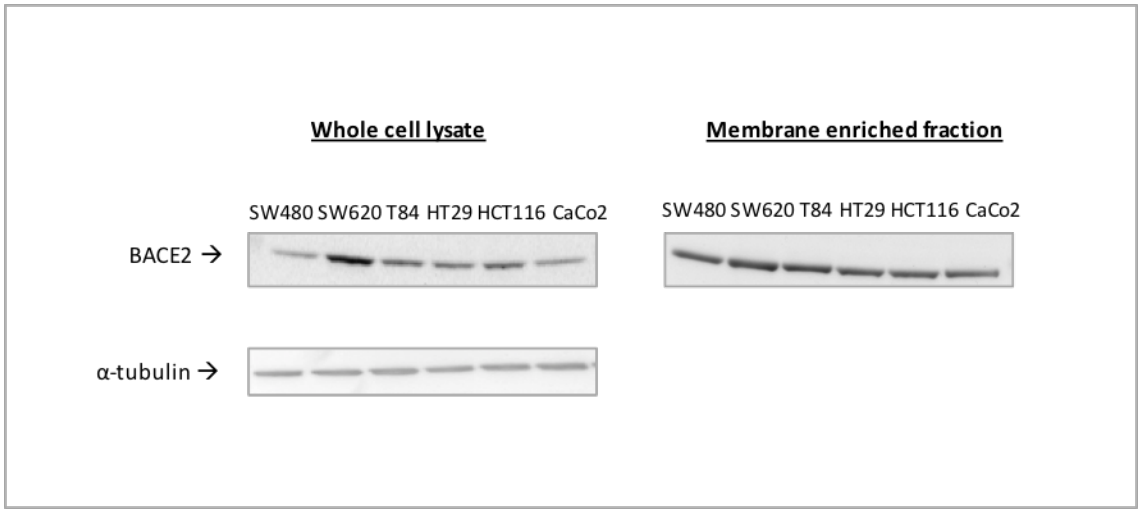

Figure 3.11 Western blot analysis showing BACE2 expression in the whole cell and membrane enriched fraction of a panel of colon cancer cell lines. BACE2 reactive bands are identified between the 50-60 kDa MW markers, indicating the correct MW of ~56kDa. α- tubulin levels confirm equal loading of total proteins in the whole cell lysate. (n=1)

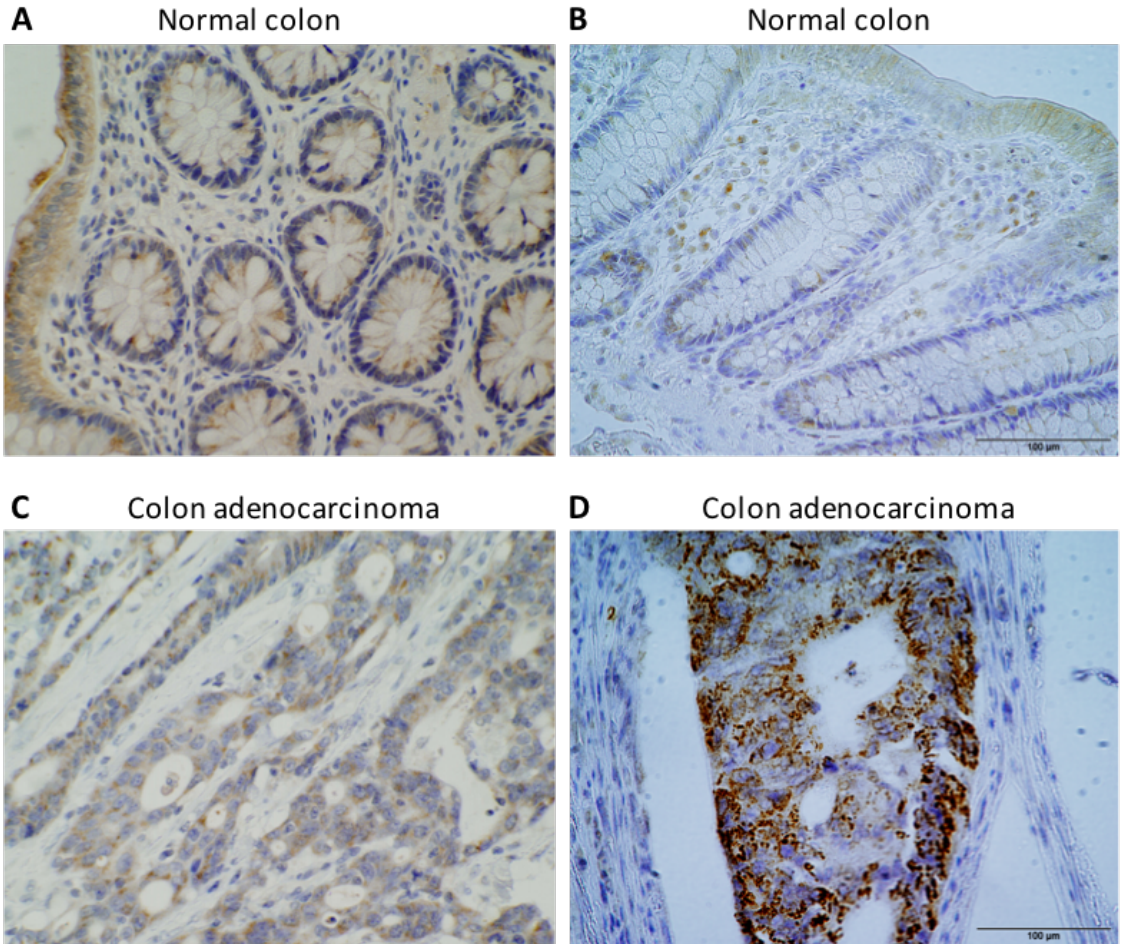

Figure 3.12 IHC analysis of BACE2 expression in normal and malignant colon. Representative images showing: (**A, B**) Normal colon with moderate cytoplasmic immunoreactivity in areas. (n=3) (**C, D**) Colon adenocarcinoma with moderate to strong granular cytoplasmic immunoreactivity. (n=5) Original magnification 400x. The scale bars represent 100µm.

3.2.8. Further preliminary investigation of IL20RA and BACE2 expression

The protein expression of targets IL20RA and BACE2 was validated in both the colon cancer cell line panels and in colon adenocarcinoma tissue sections (Sections 3.2.6 and 3.2.7). However, the immunoreactivity observed in normal colon tissues, was similar to the levels observed in colon adenocarcinoma, indicating that IL20RA and BACE2 are not overexpressed in colon cancer compared to normal colon at the protein level. As IL20RA and BACE2 both represent potential novel cancer targets, it was decided to carry out some further analysis of these targets to investigate their expression in other tissues also. Immunohistochemical analysis was carried out to assess their expression in a limited number of normal tissues and also in PDAC and oesophageal cancer, to determine if they display any relevance in other cancer types, which would warrant further investigation of IL20RA and BACE2 as potential molecular targets for therapeutic antibody targeting.

Table 3.3 and **Table 3.4** outline the results of the IHC analysis for BACE2 and IL20RA. BACE2 was found to be expressed in all normal colon tissues analysed, with intensity ranging from weak to moderate depending on the area of the tissue and only displayed strong immunoreactivity in 2/5 CRC tissues analysed. BACE2 expression was assessed in PDAC by analysing a commercial TMA that contained 10 normal pancreas and 39 PDAC cores (PA1001, US Biomax Inc). BACE2 showed strong cytoplasmic and membrane immunoreactivity in 43.6% of the PDAC specimens. However strong cytoplasmic immunoreactivity was also observed in 50% of the normal pancreas tissues analysed. Normal oesophagus and oesophageal cancer both showed weak BACE2 immunoreactivity. Normal gastric tissue had negligible BACE2 expression and normal duodenum showed weak expression. **Figure 3.13** shows some representative images of this IHC analysis.

IL20RA showed strong membrane immunoreactivity in CRC, however normal colon also had strong expression. A similar result was observed in PDAC, with strong membrane immunoreactivity observed in PDAC tissues, but strong cytoplasmic immunoreactivity also observed in the small cohort of normal pancreas analysed. IL20RA also showed strong expression in normal duodenum and tonsil, with weak expression observed in normal gastric tissue and liver. Normal oesophagus and oesophageal cancer both showed weak and diffuse IL20RA immunoreactivity. **Figure 3.14** shows some representative images of this IHC

analysis. This preliminary IHC analysis showed no apparent overexpression of BACE2 or IL20RA in the cancer types examined, therefore these targets were not pursued further.

BACE2 expression	
Normal tissue	**Corresponding cancer tissue**
Duodenum (1/1 some weak expression)	-
Gastric (0/1 negligible expression)	-
Colon (3/3 weak to moderate in different areas of tissue)	CRC (3/5 weak; 2/5 strong expression)
Pancreas (5/10 weak; 5/10 strong)	PDAC (22/39 weak; 17/39 strong)
Oesophagus (1/1 weak diffuse)	Oesophageal cancer (1/1 weak)

Table 3.3 BACE2 expression in normal and cancer tissues. The number of sections that showed positive BACE2 immunoreactivity out of the total number analysed is listed in brackets.

IL20RA expression	
Normal tissue	**Corresponding cancer tissue**
Duodenum (2/2 strong expression)	-
Gastric (1/1 weak expression)	-
Liver (1/1 weak diffuse)	-
Colon (2/2 strong in epithelial layer)	CRC (5/5 strong expression)
Pancreas (2/2 strong diffuse)	PDAC (5/5 moderate to strong membrane immunoreactivity)
Oesophagus (1/1 weak diffuse)	Oesophageal cancer (1/1 weak diffuse)
Tonsil (8/8 strong)	-

Table 3.4 IL20RA expression in normal and cancer tissues. The number of sections that showed positive IL20RA immunoreactivity out of the total number analysed is listed in brackets.

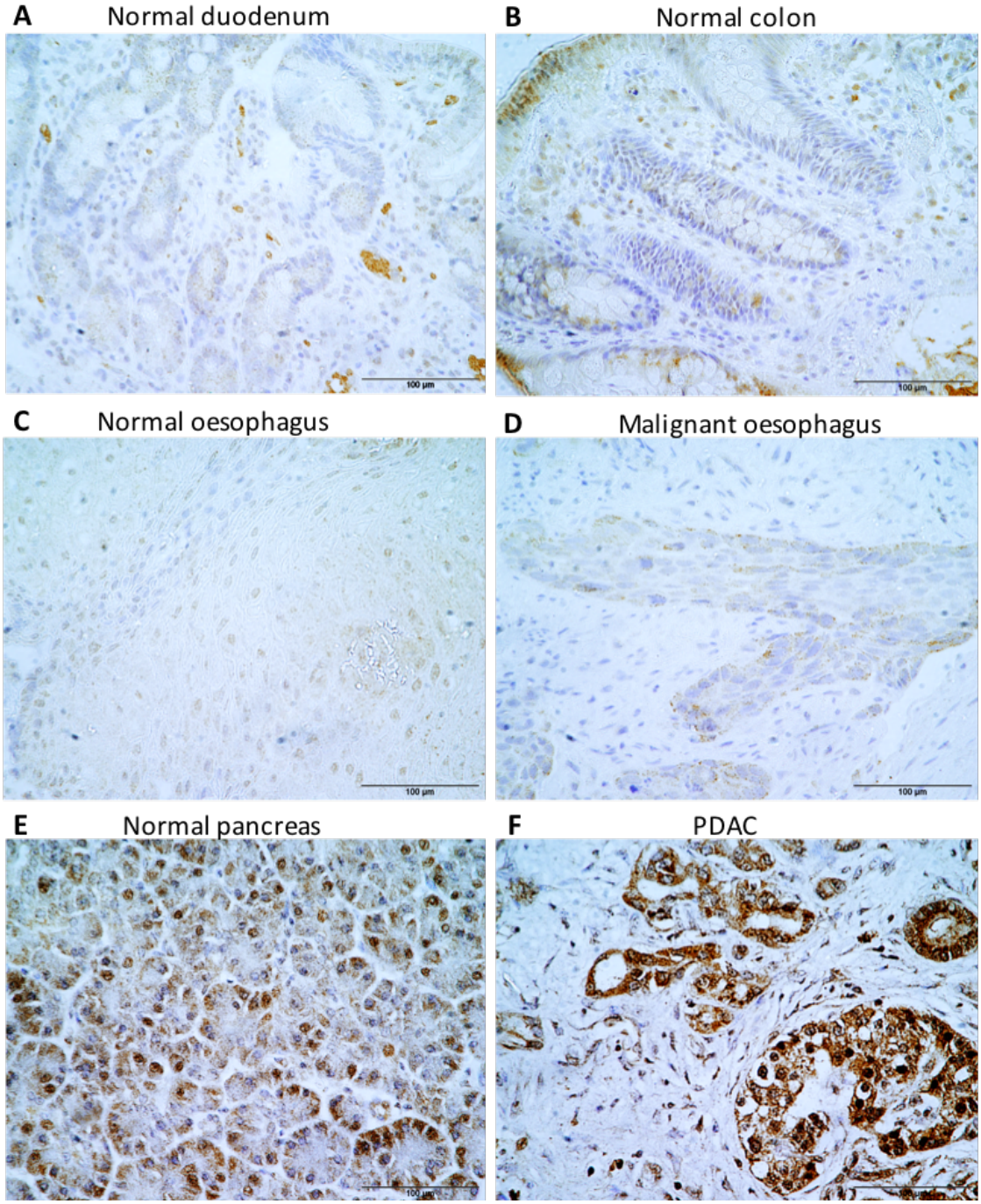

Figure 3.13 IHC analysis of BACE2 expression in normal and cancer tissues. Representative images showing: (**A**) Normal duodenum with some weak immunoreactivity. (n=1) (**B**) Normal colon with weak to strong BACE2 immunoreactivity depending on the area. (n=3) (**C**) Normal oesophagus with weak and diffuse BACE2 immunoreactivity. (n=1) (**D**) Malignant oesophagus with weak immunoreactivity. (n=1) (**E**) Normal pancreas with strong diffuse cytoplasmic immunoreactivity. (n=10) (**F**) PDAC with strong cytoplasmic BACE2 immunoreactivity. (n=39) Original magnification 400x. The scale bars represent 100µm.

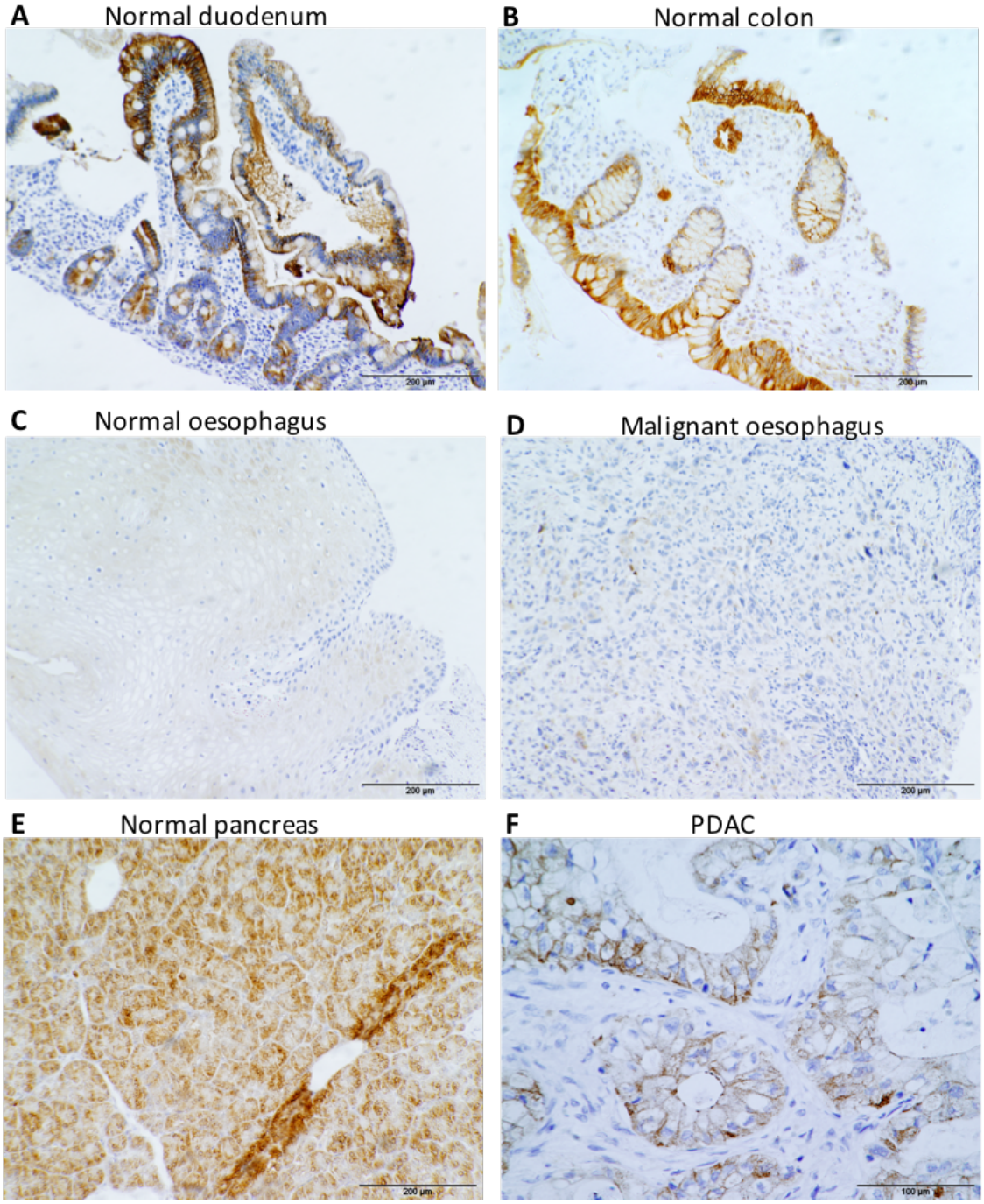

Figure 3.14 IHC analysis of IL20RA expression in normal and cancer tissues. Representative images showing: (**A**) Normal duodenum with strong immunoreactivity. (n=2) (**B**) Normal colon with strong immunoreactivity in the epithelial layer. (n=2) (**C**) Normal oesophagus with weak and diffuse immunoreactivity. (n=1) (**D**) Malignant oesophagus with weak/negligible immunoreactivity. (n=1) (**E**) Normal pancreas with strong diffuse cytoplasmic immunoreactivity. (n=2) (**F**) PDAC with strong membrane IL20RA immunoreactivity. (n=5) Original magnification of A-E: 200x, scale bars represent 200µm; F: 400x, scale bars represent 100µm.

3.3. Summary

Out of the seven candidate gene targets chosen for validation at the protein level in normal colon and colon adenocarcinoma tissue sections, only two targets, LY6G6F and IL1RAPL1, met the criteria of 1) the protein is expressed and 2) the protein is expressed at a higher level in colon cancer vs. normal colon. The IHC analysis confirmed LY6G6F protein is overexpressed in colon adenocarcinoma vs. normal colon tissue sections. Minimal expression was observed in normal colon, with strong LY6G6F immunoreactivity observed in the cancer tissues. Similarly, IL1RAPL1 was found to be strongly expressed in colon adenocarcinoma tissues with negative or minimal expression in normal colon. IL1RAPL1 protein expression has been exclusively described in neuronal cells to date, with no links to CRC. Additionally, both LY6G6F and IL1RAPL1 protein expression was confirmed in the panel of colon cancer cell lines, which will enable *in vitro* functional analysis. Therefore, LY6G6F and IL1RAPL1 were selected to pursue for further validation and investigation as potential molecular targets for therapeutic antibody targeting.

Two candidate targets (EPHX4 and LRRC8E) could not be pursued further due to the inability to validate protein expression by IHC analysis. Due to the unconvincing IHC results for NTM (similar levels of expression observed in normal colon and CRC tissues) and the poor Western blot results, it was decided not to pursue NTM further as a candidate target at this stage. The expression of IL20RA was confirmed at the protein level and was the only target validated to show distinct membrane localisation in both CRC and PDAC tumours (an important feature for molecular targets to be utilised as ADC targets). However, IL20RA expression was also found to be high in normal colon and pancreatic tissues. BACE2 exhibited a similar pattern, with strong expression observed in some CRC and PDAC tumours, but also in corresponding normal tissues. These results indicate that IL20RA and BACE2 are endogenously expressed at high levels in these tissue types, and as no distinct overexpression in the cancer tissues was observed, it appears that they would be unsuitable molecular targets for therapeutic targeting of these cancers. Therefore, IL20RA and BACE2 were not selected to pursue further.

Further validation of the expression of targets LY6G6F and IL1RAPL1 in colon cancer and also other cancer types, in particular PDAC, which has a high unmet need for new treatment strategies, is described in Chapters 4 and 5. The tissue expression pattern and cellular localisation of LY6G6F and IL1RAPL1 will be assessed, to establish if they represent molecular targets that may be amenable to therapeutic antibody targeting.

Chapter 4. LY6G6F

4.1. LY6G6F

LY6G6D/F was identified from the gene microarray datasets as being significantly overexpressed in colon adenoma and colon adenocarcinoma compared to normal colon (Section 3.2.1). The preliminary IHC analysis with a commercial antibody specifically directed against LY6G6F confirmed this result at the protein level, with strong LY6G6F immunoreactivity observed in colon adenocarcinoma and minimal to weak expression observed in normal colon, see Section 3.2.1.2. On the basis of this observed differential expression in normal and cancer tissue, LY6G6F was selected to follow up for more extensive validation and investigation.

The confusion in the literature surrounding the inability to distinguish between genes LY6G6D and LY6G6F, stems from the gene discovery and annotation. Both were originally annotated as G6D and G6F, and discovered as novel surface molecules encoded within the class III region of the human major histocompatibility complex (MHC). They are members of two different super-families, with G6D belonging to the lymphocyte antigen-6 superfamily and LY6G6F to the immunoglobulin (Ig) superfamily. (Ribas, Neville and Campbell, 2001) **Figure 4.1** shows the genomic structure of G6F and G6D, with G6F consisting of 6 exons, G6D of 3 exons and they are separated by the gene LY6G6E. The confusion arises after they were annotated, LY6G6F and LY6G6D. A splice variant was discovered by Beliakov, Karakasheva and Mazurenko (2009), that contained exons from both G6F and G6D. They called this the MEGT1 transcript that consists of exons 1-4 of G6F, which then splice to exons 2 and 3 of G6D. This led them to annotate LY6G6D as one gene, containing transcripts G6F, G6D and MEGT1. There was considerable confusion from then on, with these genes listed as aliases of one another, and making it difficult to ascertain which transcript was being referred to when talking about LY6G6D.

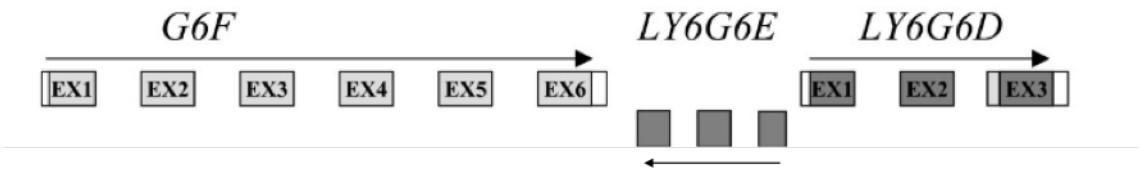

Figure 4.1 Genomic structure of the G6F, LY6G6E and LY6G6D genes. (Adapted from Calvanese *et al.*, 2008)

However, this MEGT1 transcript has not been characterised and does not have its own gene accession number. The general consensus now when talking about these genes, refers to the original discovery of the distinct genes, with LY6G6F consisting of exons 1-6, LY6G6D of 1-3, with no exons in common between the two genes. However, the persistence of the aliases for these genes (i.e. LY6G6D is listed as an alias of LY6G6F) still leads to considerable confusion. **Table 4.1** shows the approved name, the chromosomal location and exon number for these genes. (Loughner *et al.*, 2016)

To clarify, the gene investigated in this study, is LY6G6F (Gene ID: 259215) with an exon count of 6, corresponding to the mRNA transcript for LY6G6F (Accession number: NM_00100369), which is 898bp in length, translating to a 297 amino acid (AA) long protein. With the confusion over aliases, it was ensured that all siRNA, antibodies, Taqman probes etc. used in this study correspond to this gene or protein transcript.

Approved gene symbol (NCBI Gene ID #)	**Gene Name**	**Aliases**	**Genomic Location**	**Number of exons**
LY6G6D (58530)	Lymphocyte antigen 6 complex, locus G6D	G6D; NG25; LY6-D; MEGT1; C6orf23	6p21.3	3
LY6G6F (259215)	Lymphocyte antigen 6 complex, locus G6D	G6f; NG32; LY6G6D; C6orf21	6p21.33	6

Table 4.1 Name, chromosomal location and number of exons for human LY6G6D and LY6G6F genes. (Adapted from Loughner *et al.*, 2016)

LY6G6F is a type 1 transmembrane protein and as already described belongs to the Ig superfamily. LY6G6F contains two extracellular domains, the most N-terminal of which is a putative V-type Ig domain and contains a cytoplasmic tail that could be involved in signal transduction. (Ribas, Neville and Campbell, 2001; de Vet, Aguado and Campbell, 2003) G6F was identified as a novel megakaryocyte (MK) plasma membrane protein, with a suggested activatory role in platelet and MK signalling. Expression of G6F on the platelet surface was confirmed by flow cytometry on fixed platelets. (Macaulay *et al.*, 2007) In another study the G6f protein was shown to be capable of interacting with both Grb2 and Grb7 (where Grb stands for growth-factor-receptor-bound protein), linking to downstream signal transduction pathways. They established that the cytoplasmic tail of G6f can bind the signalling adaptor proteins Grb2 and Grb7 and that these interactions are dependent on the phosphorylation of Y281 of G6f. The coupling of G6f with the Ras-MAP kinase pathway is strongly suggested following its interaction with Grb2. This pathway is involved in a variety of functions such as proliferation, differentiation, survival and apoptosis. The downstream pathways that connect with Grb7 are not well defined although its association with focal adhesion kinase (FAK) in a cell-adhesion-dependent manner suggests a role for Grb7 in integrin signalling. Further work is required to fully elucidate the effect of LY6G6F activation on cellular function, and a potential extracellular ligand for LY6G6F is yet to be discovered. (de Vet, Aguado and Campbell, 2003)

In relation to cancer, LY6G6F gene expression has been listed as being significantly differentially expressed within microsatellite instable (MSI) colon tumours vs. microsatellite stable (MSS) tumours, being down-regulated in MSI tumours. (Slattery *et al.*, 2015) LY6G6F was also reported as one of 29 proteins giving a Mucin 5AC (MUC5AC) hyposecretory phenotype in the human colonic adenocarcinoma cells HT29-18N2. (Mitrovic *et al.*, 2013) Mucin genes, including MUC5AC, have been shown to be up-regulated in MSI tumours. (Pastrello *et al.*, 2005)

4.2. Preliminary Analysis of LY6G6F Expression in PDAC, Oesophageal Cancer and Breast Cancer

LY6G6F expression was confirmed to be overexpressed in a small number of colon adenocarcinomas compared to normal colon, as described in Section 3.2.1, which led to LY6G6F being selected for further investigation as a candidate cancer target. The next step was to investigate LY6G6F expression in a larger number of colon cancers, to determine if this overexpression compared to normal colon can be deemed significant. Before this a preliminary screen of other cancer types, including pancreatic cancer and breast cancer, was also carried out to determine if LY6G6F shows any differential expression in other cancer types, that would warrant further investigation. The results of this preliminary screen are described below.

4.2.1. Immunohistochemical Analysis

We had access to a limited number of tissue sections from a variety of different cancers, as well as normal tissue sections from those organs. **Figure 4.2** shows representative photomicrographs of the results obtained for IHC analysis of LY6G6F expression in PDAC, breast cancer and oesophageal cancer. In the PDAC sections analysed, LY6G6F showed intense immunoreactivity in all cases, with negative or minimal immunoreactivity in normal pancreas. Some weak LY6G6F positive expression was observed in the ducts of normal breast, with a similar weak expression level observed in the majority of invasive breast cancer tissue sections analysed. Similarly, normal oesophagus displayed a negative/weak diffuse expression pattern for LY6G6F and the expression in the malignant oesophagus section analysed was also very weak. Therefore, increased expression of LY6G6F does not appear to be present in breast cancer or oesophageal cancer. However further investigation of LY6G6F expression was warranted in PDAC, as strong expression in PDAC compared to normal pancreas was observed.

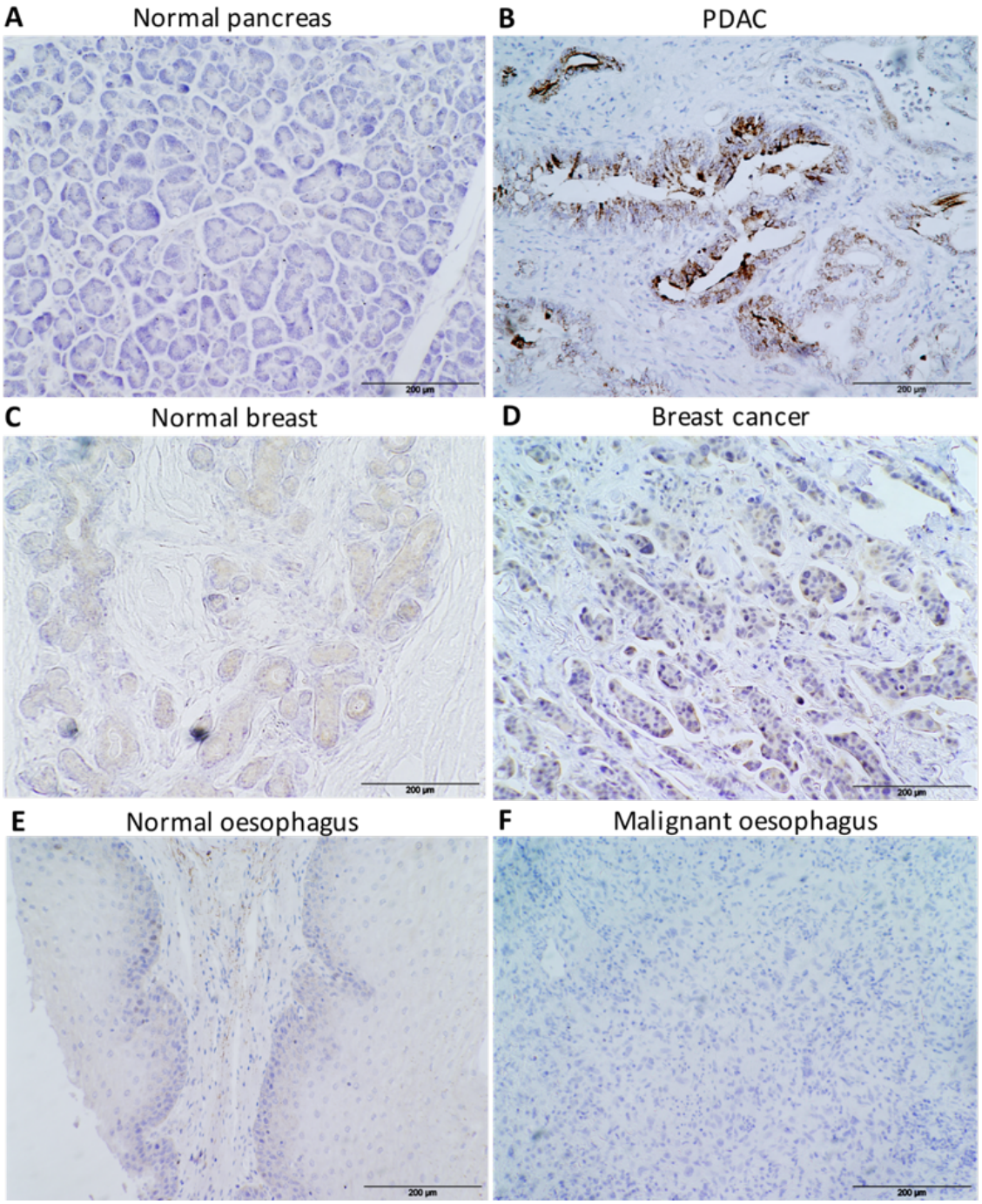

Figure 4.2 IHC analysis of LY6G6F expression in normal and cancer tissues. Representative images showing: (**A**) Normal pancreas with negative LY6G6F immunoreactivity. (**B**) PDAC with strong LY6G6F immunoreactivity. (**C**) Normal breast with some weak and diffuse LY6G6F immunoreactivity in ductal tissue. (**D**) Breast cancer with moderate cytoplasmic immunoreactivity in areas. (**E**) Normal oesophagus with negligible LY6G6F immunoreactivity. (**F**) Malignant oesophagus with negligible immunoreactivity. Original magnification 200x. The scale bars represent 200µm.

4.2.2. LY6G6F Expression in PDAC and Breast Cancer Cell Line Panels

LY6G6F expression in both the whole cell and membrane enriched fractions of colon cancer cell lines was confirmed, see Section 3.2.1.1. The expression of LY6G6F in a panel of PDAC cell lines and breast cancer cell lines was also investigated by Western blot analysis. A panel of eight PDAC cell lines was used in this study. **Table 4.2** lists the original source of these cell lines, as well as indicating if mutations in the four major driver genes associated with PDAC – KRAS, TP53, p16 and SMAD4 are present in these cell lines. KRAS activating mutations are found in approximately 90% of PDAC tumours. One cell line in the panel is KRAS wildtype, the BXPC-3 cell line. Collisson *et al.*, (2011) defined three pancreatic cancer subtypes, denoted as classical, quasi-mesenchymal (QM) and exocrine-like, based on their interpretation of subtype specific gene expression in tumour samples. The classical subtype had high expression of adhesion-associated and epithelial genes, the QM subtype had high expression of mesenchyme associated genes and the exocrine-like subtype showed relatively high expression of digestive enzyme genes. When they examined these subtypes in pancreatic cancer cell lines, they found no representative for the exocrine-like subtype, hypothesising that this subtype may have been an artefact of normal adjacent pancreas tissue in their analysis. Of the cell lines used in this study, three cell lines (BXPC-3, HPAC and Capan-2) represent the classical subtype, and the remainder (PANC-1, MIA PaCa-2, AsPC-1, Capan-1 and SW1990) represent the QM subtype. **Figure 4.3** shows the results of the Western blot analysis. There is no apparent association between LY6G6F expression and any mutational status or subtype classification. Higher LY6G6F expression is observed in the KRAS WT BXPC-3 cell line, along with Capan-2, Capan-1 and AsPC-1. Lower expression is observed in MIA PaCa-2, PANC-1 and SW1990 cell lines. LY6G6F is also detected in the membrane enriched fraction of all cell lines.

A panel of eight breast cancer cell lines was also used in this study. **Table 4.3** lists the original source of these cell lines and some of the subtype classifications associated with breast cancer. Four of the cell lines (MDA-MB-468, BT20, MDA-MB-157 and MDA-MB-231) are Basal-like/triple negative, lacking the ER, PR and HER receptors. Two cell lines represent the Luminal A and HER2 amplified subtype (BT474 and MDA-MB-361), with the remaining two the Luminal B subtype (MCF-7 and T47D**). Figure 4.4** shows the results of the Western blot analysis. LY6G6F is detected in the whole cell lysate and membrane enriched fraction of all cell lines, with a lower level of expression in all four Basal subtype

cell lines compared to the other four Luminal subtype cell lines, which have a similar expression level.

Cell line	KRAS	TP53	p16	SMAD4	Source
BxPC-3	WT	MT	WT	MT	Pancreas adenocarcinoma
MIA PaCa-2	G12C	MT	MT	WT	Pancreas adenocarcinoma
PANC-1	G12D	MT	MT	WT	Pancreas adenocarcinoma
HPAC	G12D	WT	MT	WT	Pancreas adenocarcinoma
AsPC-1	G12D	MT	WT	WT	Ascites metastatic site of pancreas adenocarcinoma
Capan-1	G12V	MT	MT	MT	Liver metastasis of pancreas adenocarcinoma
Capan-2	G12V	WT	WT	WT	Pancreas adenocarcinoma
SW1990	G12D	WT	MT	WT	Spleen metastasis of pancreas adenocarcinoma

Table 4.2 Pancreatic cancer cell line panel showing the original source of the cell lines and their mutational status in the four major driver genes associated with PDAC. Mutations in TP53, p16 and SMAD4 are inactivating gene mutations; KRAS is an activating mutation. WT, wildtype genotype; MT, mutant genotype.

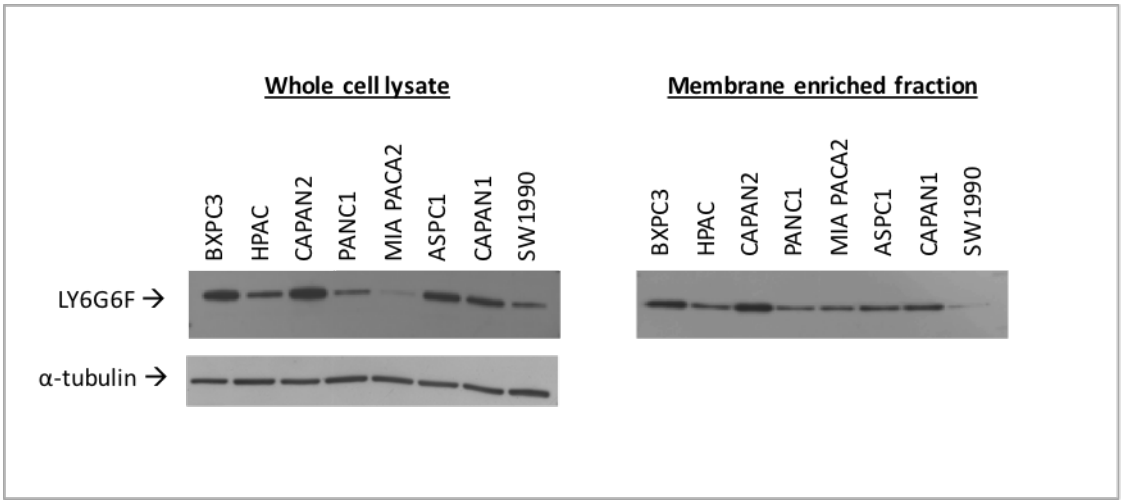

Figure 4.3 Representative Immunoblot showing LY6G6F expression in the whole cell and membrane enriched fraction of a panel of PDAC cell lines. LY6G6F has a MW of ~32kDa. α-tubulin confirms equal loading of total proteins in the whole cell lysate. (n=2)

Cell line	Classification	Source
MCF-7	Luminal A (ER^+, $PR^{+/-}$, $HER2^-$)	Pleural effusion metastatic site of breast adenocarcinoma
T47D	Luminal A (ER^+, $PR^{+/-}$, $HER2^-$)	Pleural effusion metastatic site of breast ductal carcinoma
BT474	Luminal B (ER^+, $PR^{+/-}$, $HER2^+$)	Breast ductal carcinoma
MDA-MB-361	Luminal B (ER^+, $PR^{+/-}$, $HER2^+$)	Brain metastasis of breast adenocarcinoma
MDA-MB-468	Basal A (ER^-, PR^-, $HER2^-$)	Pleural effusion metastatic site of breast adenocarcinoma
BT20	Basal A (ER^-, PR^-, $HER2^-$)	Breast carcinoma
MDA-MB-157	Basal B (ER^-, PR^-, $HER2^-$)	Breast/medulla carcinoma
MDA-MB-231	Basal B (ER^-, PR^-, $HER2^-$)	Pleural effusion metastatic site of breast adenocarcinoma

Table 4.3 Breast cancer cell line panel showing the original source of the cell lines and some of the classifications associated with them.

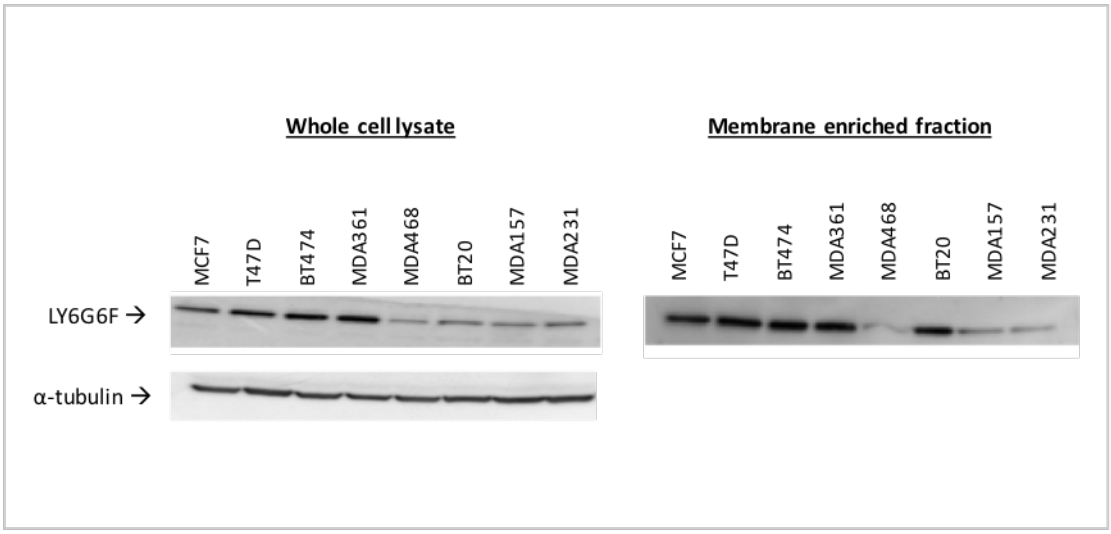

Figure 4.4 Western blot analysis showing LY6G6F expression in the whole cell and membrane enriched fraction of a panel of breast cancer cell lines. Lower LY6G6F expression is observed in the Basal subtype cell lines. α-tubulin confirms equal loading of total proteins in the whole cell lysate. (n=1)

4.2.3. Summary of Analysis of LY6G6F Expression across Various Cancer Types

In addition to CRC, further IHC validation studies indicated LY6G6F is highly expressed in PDAC. Intense LY6G6F immunoreactivity was observed in PDAC tumours with minimal expression in normal pancreas. Despite no apparent overexpression observed in breast cancer in the IHC analysis, Western blot analysis showed that LY6G6F may have differential expression associated with different subtypes of breast cancer. However, for our purpose of identifying targets upregulated in cancer vs. normal tissues that could have potential as therapeutic targets, CRC and PDAC cancer types will be investigated further for LY6G6F expression.

4.3. LY6G6F Expression in Normal Colon and CRC Tissues

In order to investigate LY6G6F expression in a larger patient cohort of CRC by Immunohistochemical analysis, a combination of commercial tissue microarray (TMA) and full-face tissue sections was used. TMAs contain small 1mm diameter cores of tissues on a single glass slide, enabling rapid analysis of large patient cohorts for target expression. The full-face tissue sections contain much larger pieces of tissue and can give a broader picture of target expression in the tumour and surrounding tissue. We had access to a small number of full-face colon adenocarcinoma tissue sections obtained from our collaboration with St. Vincent's University Hospital – 9 KRAS mutant (MT) phenotype and 9 KRAS wildtype (WT) colon adenocarcinoma sections, as well as 2 each of BRAF MT and BRAF WT tissue sections. A number of normal colon sections were also available.

A colon disease spectrum TMA (CO2081, Biomax US) was used to investigate LY6G6F expression across a broad spectrum of colon disease, from benign to cancerous tissues. This TMA includes colon adenocarcinoma, which the majority of CRCs are classified as, as well as mucinous adenocarcinoma and carcinoid tumours. Mucinous colon carcinoma is a distinct form of CRC, accounting for 10-15% of cases, and has been associated with inferior response to treatment compared to adenocarcinoma. Carcinoid tumours arise from neuroendocrine cells of the colon, and are a much rarer form of CRC. Colon cancers from lymph node metastases are also on the TMA. The benign spectrum is represented with cores from normal colon, normal cancer adjacent tissue (NAT), chronic inflammation of mucosa, hyperplasia of glandular epithelium, polyps and adenomas. The layout of this TMA is shown in **Figure 4.5**. In addition, a small TMA with 12 colon adenocarcinoma and 12 matched normal cancer adjacent colon specimens (Accumax A713 VIII) was also analysed. Some cores of TMAs can be missing from the slide, therefore the combined numbers of CRC, benign, and normal sections analysed (from the full-face tissue sections and TMAs) are displayed in **Table 4.4.** The pathological grade diagnosis was available for some of the full-face colon adenocarcinoma tissue sections, as well as the cancer specimens on the TMAs. However, no survival data was available for any of the cancer specimens.

Normal and Benign Spectrum Specimens	Cancer Specimens
Normal Colon - 21	Adenocarcinoma – 50 (includes the KRAS and BRAF MT and WT specimens)
NAT Colon - 21	Mucinous Adenocarcinoma - 15
Chronic Inflammation – 10	Carcinoid - 2
Hyperplasia - 7	Metastatic Adenocarcinoma – 19
Polyps - 6	
Adenoma - 5	

Table 4.4 Total number of normal, benign and colon cancer specimens analysed for LY6G6F expression.

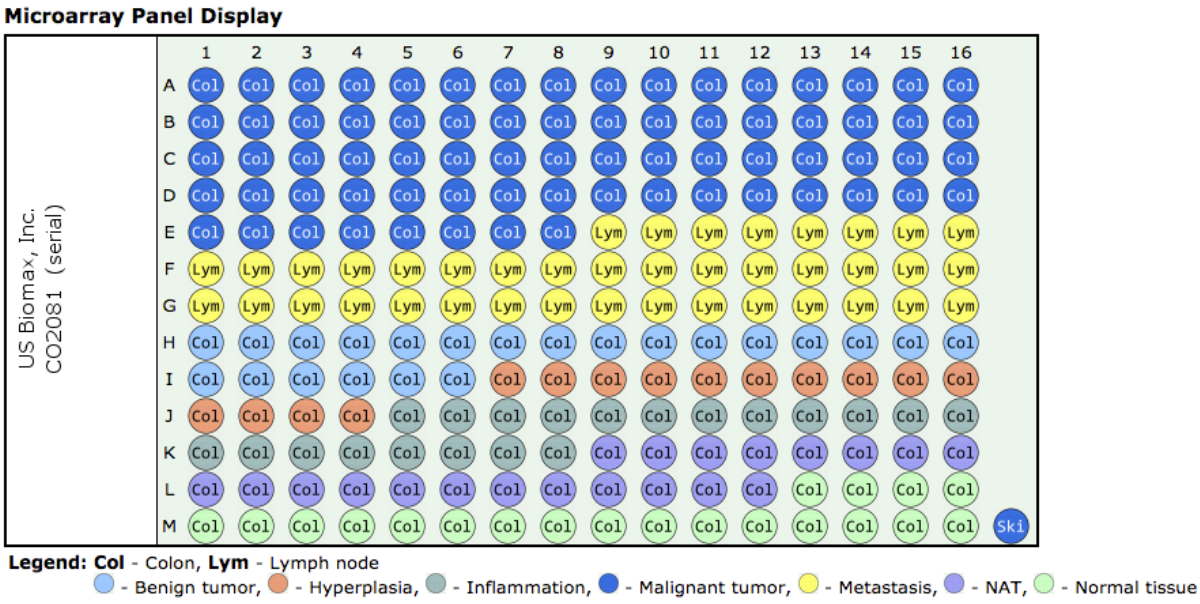

Figure 4.5 CO2081 colon disease spectrum (colon cancer progression) tissue array. Duplicate cores of each case are present. NAT: Normal cancer adjacent tissue. (US Biomax, Inc)

The tissue sections were analysed by IHC for LY6G6F expression, as described in Section 2.6. Sections were then scored for intensity of LY6G6F immunoreactivity in the tumour cells or normal tissues, as outlined in **Table 4.5**. Slides were scored by two independent examiners (EMC, AML). These scores were then grouped into those tumours with negative or low levels of LY6G6F expression (0-1+) and those tumours showing high LY6G6F expression (2-3+) for analysis. **Table 4.6** shows the LY6G6F expression results for the colon cancer progression spectrum analysed. Normal colon and normal cancer adjacent colon were negative for LY6G6F or displayed weak diffuse stain in the majority of cases. A small number showed some strong LY6G6F immunoreactivity. 47.6% (10/21) of normal colon scored as 0 for LY6G6F immunoreactivity, 23.8% (5/21) scored as 1+, 23.8% (5/21) scored as 2+ and 4.8% (1/21) scored as 3+. 47.6% (10/21) of NAT colon scored as 0 for LY6G6F, 42.8% (9/21) scored as 1+, 4.8% (1/21) scored as 2+ and 4.8% (1/21) scored as 3+. In order to determine if there is any significant association between the low expression found in normal colon (including NAT colon) and the expression levels found in both the benign and cancer spectrum, a Chi-square test to compare the expression of every other specimen with normal colon was carried out. The p-value results for this test are also listed in **Table 4.6.**

Score	**Level of target immunoreactivity**
0	Negative staining
1+	Weak staining
2+	Moderate staining
3+	Strong (intense) staining

Table 4.5 Scoring system used for target IHC immunoreactivity.

		LY6G6F expression		
Specimen:	**No. of cases**	**Low (0-1+)**	**High (2-3+)**	**p-value**
Normal colon	21	15 (71.4%)	6 (28.6%)	
NAT colon	21	19 (90.5%)	2 (9.5%)	
Chronic Inflammation	10	7 (70%)	3 (30%)	NS
Hyperplasia	7	0	7 (100%)	<0.0001
Polyps	6	0	6 (100%)	<0.0001
Adenoma	5	1 (20%)	4 (80%)	0.0031
Adenocarcinoma	50	15 (30%)	35 (70%)	<0.0001
- KRAS MT	9	0	9 (100%)	
- KRAS WT	9	1 (11.1%)	8 (88.9%)	
- BRAF MT	2	0	2 (100%)	
- BRAF WT	2	0	2 (100%)	
Mucinous adenocarcinoma	15	11 (73.3%)	4 (26.7%)	NS
Carcinoid	2	2 (100%)	0	NS
Metastatic adenocarcinoma	19	12 (63.2%)	7 (36.8%)	NS

Table 4.6 LY6G6F expression in the colon disease spectrum. The number of each specimen that scored as LY6G6F low and LY6G6F high expressing is listed. The association between expression levels observed in normal colon specimens (including NAT colon) and all of the other cases both benign and cancerous was estimated for significance by Chi-square test. P-values are noted for those with significant correlations. NS = not significant.

4.3.1. LY6G6F Expression in Normal Colon vs. Colon Cancer Spectrum

Four different colon cancer types have been assessed for LYG6F expression – Colon adenocarcinoma, mucinous adenocarcinoma, carcinoid and metastatic adenocarcinoma. The initial scoring revealed that 86% (43/50) of adenocarcinomas express LY6G6F, with 14% (7/50) scored as 0. In mucinous adenocarcinoma this drops to 60% (9/15) of cases expressing LY6G6F, with 40% (6/15) scored as 0. There were only 2 carcinoid cores for analysis, with 50% (1/2) scored as 0 and 50% (1/2) scored as 1+, indicating low LY6G6F expression in this rare subtype of CRC. Metastatic adenocarcinoma (derived from lymph nodes) showed 63.2% (12/19) expressed LY6G6F, with 36.8% (7/19) scored as 0.

The grouped scores of low (0-1+) and high (2-3+) LY6G6F expression for analysis then, as shown in **Table 4.6,** shows that the majority (70%) of adenocarcinomas analysed express high levels of LY6G6F. LY6G6F is significantly overexpressed in colon adenocarcinoma vs. normal colon, as determined by Chi-square test (p-value <0.0001). In contrast the majority (73.3%) of mucinous adenocarcinomas show low LY6G6F expression. The sample size of carcinoid tumours was very small (n=2), with 100% of these showing low LY6G6F expression. Finally, in the metastatic adenocarcinoma group, 63.2% display low LY6G6F expression. Therefore, the majority of mucinous adenocarcinoma, carcinoid and metastatic adenocarcinomas show low LY6G6F expression, with no significant correlation found between these and the expression in normal colon, as determined by Chi-square test.

Therefore, LY6G6F overexpression appears to be a characteristic of adenocarcinomas, irrespective of KRAS or BRAF mutational status, as both the wildtype and mutated KRAS/BRAF specimens showed high (2-3+) LY6G6F expression in the majority of cases. (**Table 4.6)** High LY6G6F expression is not associated with metastatic adenocarcinoma, mucinous adenocarcinoma or carcinoid tumours. As well as being significantly overexpressed compared to normal colon, LY6G6F is also significantly overexpressed in adenocarcinoma compared to these other 3 cancer types, with a p-value of 0.0027 found in this comparison by Chi-square test. Strong granular cytoplasmic LY6G6F immunoreactivity is observed in colon adenocarcinomas. Whereas in normal colon, if LY6G6F immunoreactivity is present, it tends to be weak and diffuse. **Figure 4.7** shows representative photomicrographs of this pattern of LY6G6F immunoreactivity observed in the colon disease spectrum.

4.3.2. LY6G6F Expression in Normal Colon vs. Benign Disease

The benign spectrum includes normal cancer adjacent colon, chronic inflammation of mucosa, polyps, hyperplasia of glandular epithelium and adenoma. The normal adjacent colon showed low LY6G6F expression in 90.5% (19/21) of cases, showing similar expression to normal colon. In some instances, normal cancer adjacent tissue can be affected by close proximity to the tumour microenvironment. The majority of sample tissues representing chronic inflammation of mucosa (70%) also exhibited low LY6G6F expression. In contrast, the majority of polyps (100%), hyperplasia of glandular epithelium (100%) and adenoma (80%) had high LY6G6F expression (2-3+ score). LY6G6F is significantly overexpressed in polyps (p-value <0.0001), hyperplasia (p-value <0.0001) and adenoma (p-value 0.0031), as determined by Chi-square test, and shown in **Table 4.6**. Representative photomicrographs of the pattern of LY6G6F stain observed in the colon disease spectrum are shown in **Figure 4.6.**

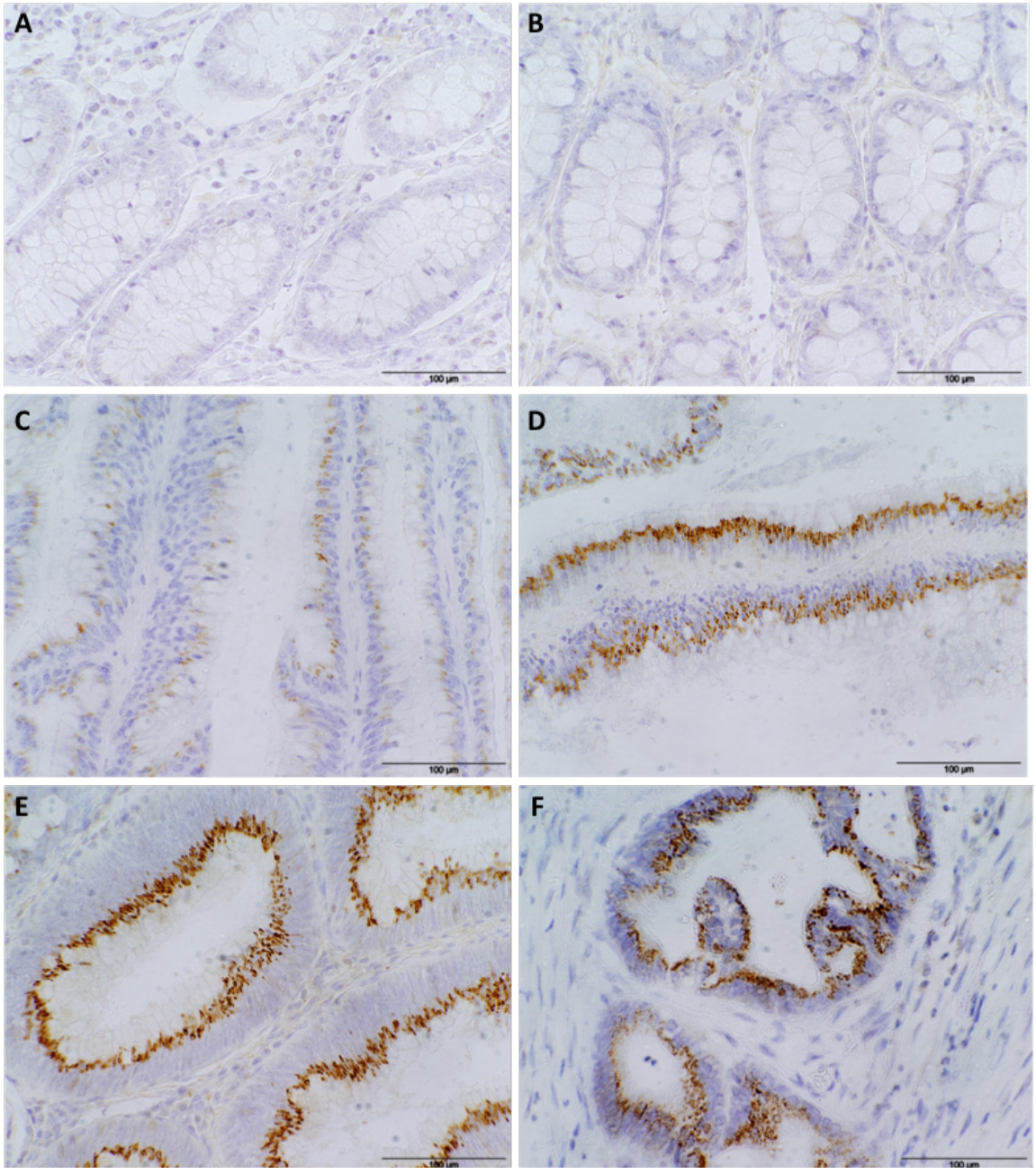

Figure 4.6 IHC analysis of LY6G6F expression in normal, diseased and malignant colon. Representative images showing: (**A**) Normal colon exhibiting negative immunoreactivity. (**B**) Chronic inflammation of colon mucosa exhibiting negative immunoreactivity. (**C**) Adenoma exhibiting weak LY6G6F immunoreactivity. (**D**) Adenoma showing strong granular cytoplasmic immunoreactivity. (**E**) Hyperplasia of glandular epithelium with strong granular cytoplasmic immunoreactivity. (**F**) Colon adenocarcinoma (KRAS MT, moderately differentiated) with strong granular cytoplasmic immunoreactivity in tumour cells. Original magnification 400x. The scale bars represent 100μm.

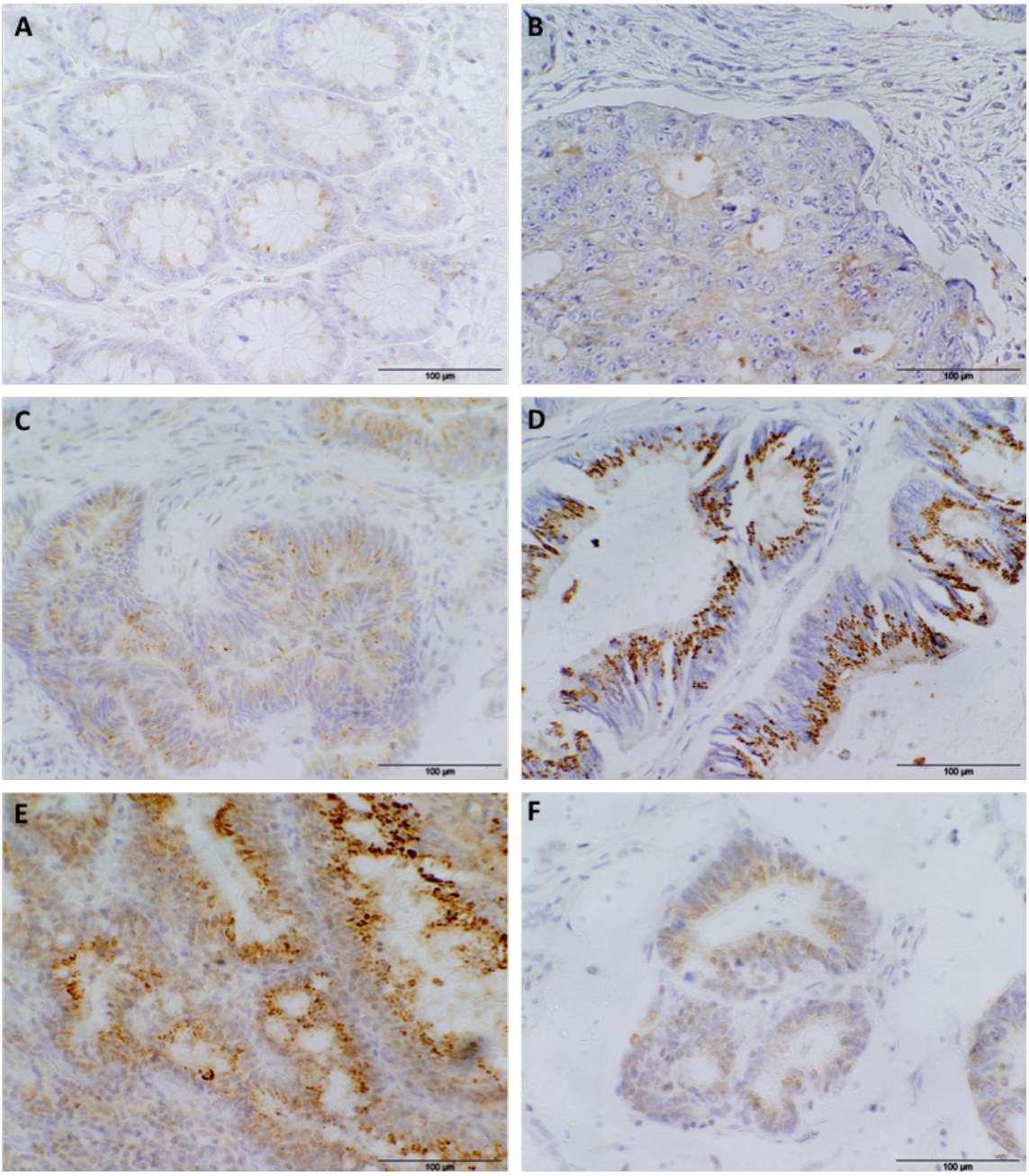

Figure 4.7 IHC analysis of LY6G6F expression in normal and malignant colon. Representative images showing: (**A**) NAT colon with minimal LY6G6F immunoreactivity observed. (**B**) Moderately differentiated colon adenocarcinoma (KRAS WT) showing weak LY6G6F immunoreactivity. (**C**) Colon adenocarcinoma (BRAF WT) with moderate LY6G6F immunoreactivity. (**D**) Moderately differentiated colon adenocarcinoma (KRAS MT) showing strong granular cytoplasmic immunoreactivity. (**E**) Colon adenocarcinoma (BRAF MT) showing strong granular cytoplasmic immunoreactivity. (**F**) Metastatic colon adenocarcinoma with weak-moderate immunoreactivity. Original magnification 400x. The scale bars represent 100µm.

4.3.3. Association between LY6G6F Expression and CRC Tumour Grade

In order to determine if LY6G6F expression correlates with the histopathological grade of CRC, the score was analysed in the specimens that this information was available for. Tumours are pathologically diagnosed from Grade 1-3; Grade 1 or well differentiated denotes tumours with cells that appear normal and are not rapidly growing; Grade 2 or moderately differentiated denotes tumours with cells that appear slightly different than normal; Grade 3 or poorly differentiated denotes tumours with cells that appear abnormal and tend to grow and spread more aggressively. The grade diagnosis was known for 63 of the cancer specimens analysed: 30 adenocarcinomas, 15 mucinous adenocarcinomas and 18 metastatic adenocarcinomas. Combining the score for all of these and grouping into Grades 1-3, showed that the majority (55.6%) of tumours analysed were Grade 2, followed by Grade 3 at 31.7% and Grade 1 representing 12.7% of tumours. **Table 4.7** shows the LY6G6F expression pattern for the three grades across these combined colon cancer types. There appears to be no correlation with LY6G6F expression and tumour grade, with a fairly even distribution between low and high LY6G6F expression in all three grades.

As high LY6G6F expression has been shown to significantly correlate with colon adenocarcinoma, with low expression observed in the majority of both mucinous and metastatic adenocarcinoma, the correlation between grade and LY6G6F expression was also assessed for each of these cancer types separately. These results are shown in **Table 4.8**. LY6G6F expression does not correlate to grade in adenocarcinoma, with a similar level of high expression shown in Grade 1, 2 and 3. There similarly appears to be no correlation in metastatic adenocarcinoma, with similar percentages of low and high expression observed in both Grade 2 and 3 (no Grade 1 present). Mucinous adenocarcinoma, which shows low LY6G6F expression in the majority (73.3%) of cases, does show some differences in the LY6G6F expression pattern between grades. The level of LY6G6F expression appears to increase as the grade increases, with 0% of Grade 1 tumours showing high expression, 22.2% of Grade 2 showing high expression and then 66.7% of Grade 3 tumours showing high LY6G6F expression, however this trend wasn't deemed significant by a Chi-square test.

		LY6G6F expression	
Grade	**No of cases**	**Weak (0-1+)**	**Strong (2-3+)**
1	8	4 (50%)	4 (50%)
2	35	17 (48.6%)	18 (51.4%)
3	20	8 (40%)	12 (60%)

Table 4.7 Association between LY6G6F expression and CRC tumour grade. (Results for adenocarcinoma, mucinous and metastatic adenocarcinoma combined)

Adenocarcinoma (n=30)			
Grade	**No of cases**	**Weak (0-1+)**	**Strong (2-3+)**
1	5	1 (20%)	4 (80%)
2	16	4 (25%)	12 (75%)
3	9	2 (22.2%)	7 (77.8%)
Mucinous Adenocarcinoma (n=15)			
Grade	**No of cases**	**Weak (0-1+)**	**Strong (2-3+)**
1	3	3 (100%)	0
2	9	7 (77.8%)	2 (22.2%)
3	3	1 (33.3%)	2 (66.7%)
Metastatic Adenocarcinoma (n=18)			
Grade	**No of cases**	**Weak (0-1+)**	**Strong (2-3+)**
1	0	-	-
2	10	6 (60%)	4 (40%)
3	8	5 (62.5%)	3 (37.5%)

Table 4.8 Association between LY6G6F expression and tumour grade in each CRC subtype.

4.3.4. Summary of LY6G6F Expression in Colon Disease Spectrum

- LY6G6F expression is either absent or weak in the majority of normal colon tissues.
- LY6G6F is significantly overexpressed in colon adenocarcinoma vs. normal colon (p-value <0.0001), irrespective of tumour grade or KRAS/BRAF mutational status.
- However, LY6G6F is weakly expressed in the metastatic adenocarcinoma cohort.
- LY6G6F is weakly expressed in chronic inflammation of colon tissues, but is significantly overexpressed in the rest of the benign spectrum – hyperplasia, polyps and adenoma, indicating an association between LY6G6F expression and the adenocarcinoma progression profile.
- LY6G6F shows weak expression in mucinous adenocarcinoma, with no significance in expression compared to normal colon.
- LY6G6F is also weakly expressed in the rare carcinoid tumour subtype.

4.4. LY6G6F Expression in Normal Pancreas and PDAC

The preliminary analysis in Section 4.2, showed high LY6G6F expression in PDAC compared to normal pancreas, warranting investigation in a larger patient cohort. Specimens obtained from 57 patients undergoing pancreaticoduodenectomy in St. Vincent's University Hospital between 2007 and 2013 for PDAC were available for this study. Information on the pathological features and survival rates for this cohort was also provided. All specimens are PDAC, which accounts for ~95% of pancreatic cancer cases, and were all located in the head of the pancreas. To assess the expression of LY6G6F in normal pancreas alongside this cohort, 3 full-face tissue sections of normal pancreas were used and a commercially sourced TMA (PAN241a, US Biomax) containing 4 normal pancreas cores and 16 normal adjacent tissue (NAT) cores, which are derived from cancer adjacent normal tissue, giving a total of 7 normal pancreas and 16 NAT pancreas for analysis.

Tissues were stained for LY6G6F expression and assigned an intensity score from 0-3+, as described in Table 4.5. Slides were scored by two independent examiners (EMC, AML). It was observed that LY6G6F strongly stained the stroma of a number of the PDAC specimens. Therefore, the score for LY6G6F stain in both the tumour cells and the stroma was noted, as outlined in **Table 4.9**. Overall LY6G6F expression is either absent or displays a weak and diffuse cytoplasmic pattern of expression in normal pancreas and normal cancer adjacent pancreas. In contrast, high LY6G6F expression is observed in the majority of PDAC tumour ducts, with 78.9 % (45/57) scored 2-3+. Only 5.3% (3/57) showed no LY6G6F expression, and 15.8% (9/57) scored as 1+. LY6G6F overexpression in PDAC compared to normal pancreas is highly significant, with a p-value of <0.0001 obtained by Chi-square test. LY6G6F expression in the PDAC tumours is for the most part, observed as granular cytoplasmic-like staining, localised to the apical membrane (the membrane that faces inward to the lumen) of ducts. A combination of membrane-like, and cytoplasmic-like stain is observed in a small number of specimens, with membrane–like immunoreactivity more likely to be observed in smaller tumour ducts or tumour buds. Tumour budding is where individual malignant cells and/or small clusters of malignant cells are found in the tumour stroma at the invasive front of the tumour and is an adverse prognostic factor in PDAC. (Karamitopoulou *et al.*, 2013) Strong stromal LY6G6F immunoreactivity was observed in 40.4% (23/57) of the PDAC specimens analysed. A small number of normal pancreas (3/7) and normal cancer adjacent pancreas (2/16) also displayed some strong LY6G6F immunoreactivity in the

stroma, but to a much smaller extent than that observed in PDAC. The difference in LY6G6F stromal expression between normal pancreas and PDAC was not deemed significant (by Chi-square test). **Figure 4.8** and **Figure 4.9** show some representative photomicrographs of LY6G6F immunoreactivity observed in normal pancreas and PDAC.

		Score of LY6G6F immunoreactivity in pancreatic tumour ducts and normal pancreas tissue			
Specimen:	**No. of cases**	**0**	**1+**	**2+**	**3+**
Normal Pancreas	7	4 (57.1%)	3 (42.9%)	0	0
NAT pancreas	16	4 (25%)	12 (75%)	0	0
PDAC	57	3 (5.3%)	9 (15.8%)	24 (42.1%)*	21 (36.8%)*
		Score of LY6G6F immunoreactivity in the stroma of PDAC and normal pancreas			
Specimen:	**No. of cases**	**0**	**1+**	**2+**	**3+**
Normal Pancreas	7	4 (57.1%)	0	3 (42.9%)	0
NAT pancreas	16	14 (87.5%)	0	2 (12.5%)	0
PDAC	57	12 (21%)	22 (38.6%)	7 (12.3%)	16 (28.1%)

Table 4.9 LY6G6F expression in normal pancreas and PDAC. The IHC score is outlined for normal pancreas, normal cancer adjacent (NAT) pancreas and PDAC specimens. The LY6G6F immunoreactivity score is described for both the tumour ducts / normal pancreas tissue and also for stromal immunoreactivity observed in these tissues. *LY6G6F is significantly overexpressed in PDAC tumours vs. normal pancreas (p-value: <0.0001; estimated by Chi-square test)

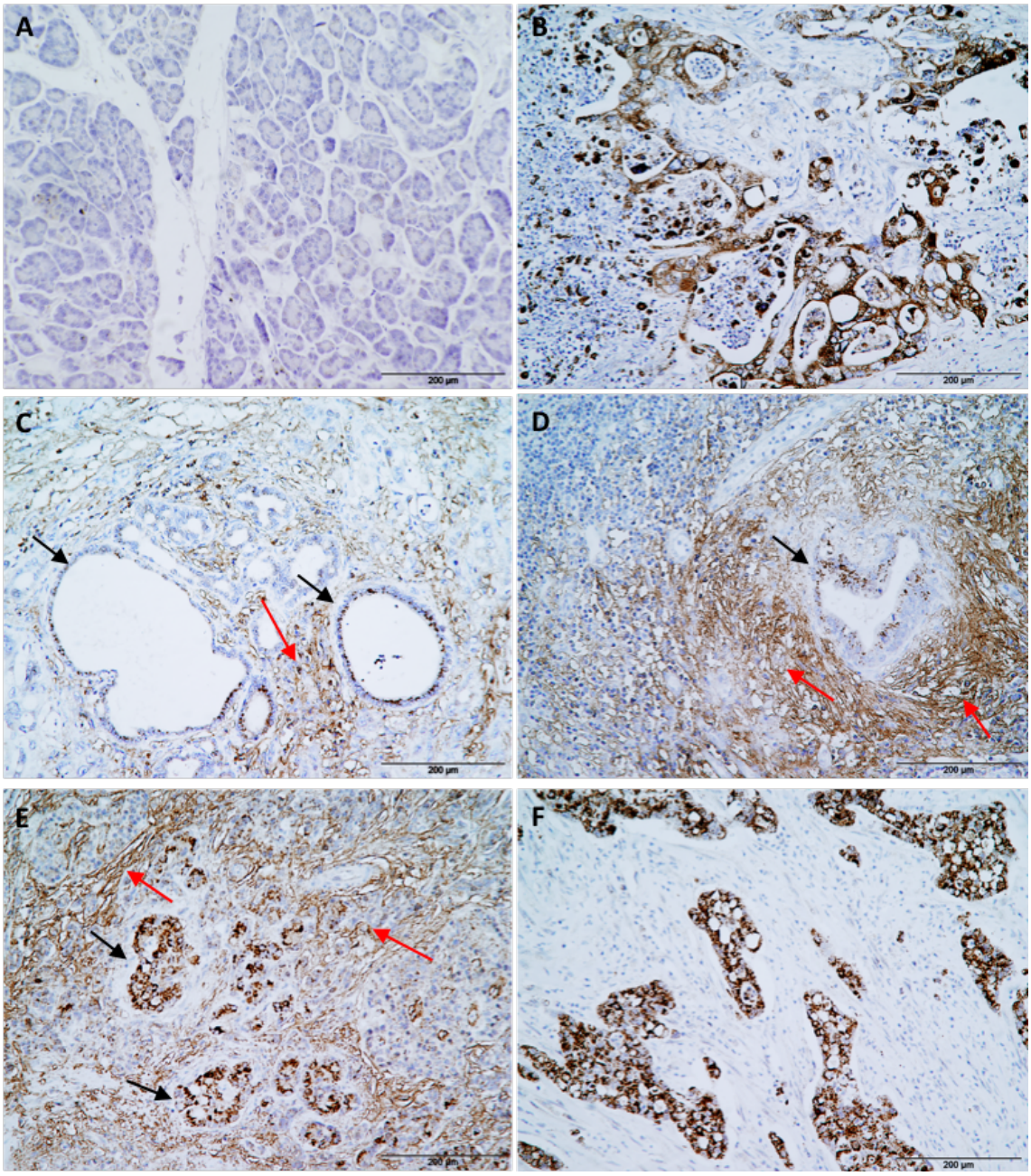

Figure 4.8 IHC analysis of LY6G6F expression in normal pancreas and PDAC. Representative images showing: (**A**) Normal pancreas with negative LY6G6F immunoreactivity. (**B**) PDAC exhibiting strong cytoplasmic and membrane-like LY6G6F immunoreactivity. (**C-E**) PDAC tumours surrounded by stroma with strong LY6G6F immunoreactivity. Black arrows indicate the tumour ducts and red arrows the surrounding stroma. Weaker LY6G6F immunoreactivity is observed in the ducts of C and D, with strong immunoreactivity in the tumour ducts in E. Strong immunoreactivity is observed in the stroma of all. (**F**) PDAC with strong cytoplasmic and membrane-like LY6G6F immunoreactivity. Original magnification 200x. The scale bars represent 200µm.

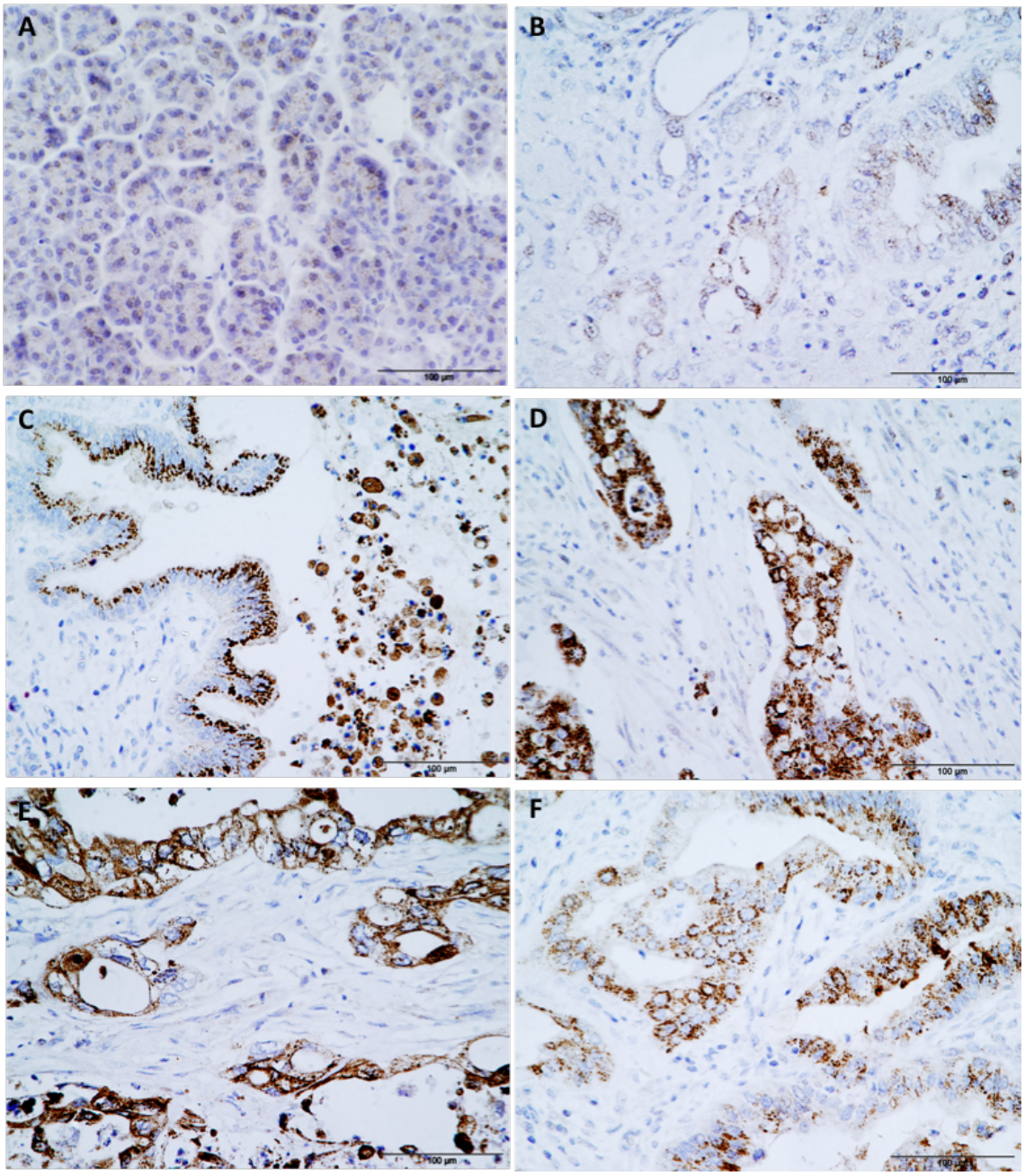

Figure 4.9 IHC analysis of LY6G6F expression in normal pancreas and PDAC. Representative images showing: (**A**) Normal pancreas with very weak and diffuse LY6G6F immunoreactivity. (**B**) PDAC showing weak LY6G6F immunoreactivity. (**C**) PDAC exhibiting strong granular cytoplasmic LY6G6F immunoreactivity localised to the apical membrane side of a malignant duct. (**D**) PDAC with strong cytoplasmic and membrane-like LY6G6F immunoreactivity observed in tumour ducts. (**E**) Small clusters of PDAC tumour ducts showing strong cytoplasmic and membranous LY6G6F immunoreactivity. (**F**) PDAC exhibiting moderate-strong cytoplasmic LY6G6F immunoreactivity. Original magnification 400x. The scale bars represent 100µm.

4.4.1. Association between LY6G6F Expression and PDAC Clinicopathological Features

Information on the clinicopathological features associated with PDAC was available for the 57 patient cohort. The mean age at time of diagnosis was 62.6 years in this group. 64.4% (37/57) of patients were male and 35.1% (20/57) were female. The majority (84.9%) of the tumours were moderately differentiated, with 26.3% poorly differentiated and 8.8% well differentiated. The average maximum pathological tumour axis was 2.98cm. The tumour staging ranged from T1-3, where the higher the number indicates the larger the tumour has grown and extended into nearby tissues; 89.4% (51/57) were T3, 5.3% were T2 and 5.3% were T1. 68.4% of cases were diagnosed as N1 stage and 31.6% as N0, where N1 indicates the presence of regional lymph node metastasis and N0 indicates no cancer is present in the regional lymph nodes. Lymphovascular invasion (LVI) was present in 63% (36/57) of cases and perineural invasion (PNI) was present in 82.5% (47/57) of cases. Portal vein involvement (PVI) was present in only 3.5% (2/57) of cases.

LY6G6F expression in this cohort was grouped into LY6G6F low (0-1+ IHC score) and LY6G6F high (2-3+ IHC score) expression for analysis. **Table 4.10** shows the association between LY6G6F expression and the clinicopathological features of this PDAC cohort. Overall, LY6G6F is highly expressed in this PDAC patient cohort, with 78.9% displaying strong LY6G6F immunoreactivity. No significant correlation was found between LY6G6F expression and any of the clinicopathological features examined. There are some notable differences in expression in some of the clinicopathological features despite not being deemed significant. T3 stage tumours highly express LY6G6F in 80.4% of cases, whilst 66.7% of T1-2 stage tumours highly express LY6G6F. LY6G6F is more highly expressed in cases where lymphovascular invasion is present (83.3%) compared to cases where it is absent (71.4%) and it is also more highly expressed in the cases with perineural invasion – 81% have high LY6G6F expression, compared to 70% of cases where PNI is absent having high LY6G6F expression. The sample size is very small for those with portal vein involvement (2/57), with 100% of these showing high LY6G6F expression, compared to 78.2% in cases without PVI. There is some differential expression observed across the different histological grades, with 100% of well differentiated tumours highly expressing LY6G6F, 81% of moderately differentiated and 67% of poorly differentiated tumours highly expressing LY6G6F.

Feature		LY6G6F expression		
	No. of patients	**Low (0-1+)**	**High (2-3+)**	p-value*
Overall	57	**n=12 (21.1%)**	**n=45 (78.9%)**	
Sex				0.132
Male	37	10 (27%)	27 (73%)	
Female	20	2 (10%)	18 (90%)	
Age (years)				0.443
< 60	23	6 (26.1%)	17 (73.9%)	
≥ 60	34	6 (17.6%)	28 (82.4%)	
Tumour size				0.569
< 4 cm	44	10 (22.7%)	34 (77.3%)	
≥ 4 cm	13	2 (15.4%)	11 (84.6%)	
Tumour differentiation				0.247
Well	5	0	5 (100%)	
Moderate	37	7 (19%)	30 (81%)	
Poor	15	5 (33%)	10 (67%)	
pT stage				0.435
T1-2	6	2 (33.3%)	4 (66.7%)	
T3	51	10 (19.6%)	41 (80.4%)	
pN stage				0.581
N0	18	3 (16.7%)	15 (83.3%)	
N1	39	9 (23.1%)	30 (76.9%)	
Lymphovascular invasion				0.288
Absent	21	6 (28.6%)	15 (71.4%)	
Present	36	6 (16.7%)	30 (83.3%)	
Perineural invasion				0.445
Absent	10	3 (30%)	7 (70%)	
Present	47	9 (19%)	38 (81%)	
Portal vein involvement				0.457
Absent	55	12 (21.8%)	43 (78.2%)	
Present	2	0	2 (100%)	
R-status				0.592
R0	54	11 (20.4%)	43 (79.6%)	
R1	3	1 (33.3%)	2 (66.7%)	

Table 4.10 Association between LY6G6F expression in PDAC and the clinicopathological features of pancreatic cancer. T, tumour; N, lymph node. *Significance estimated with Chi-square test.

4.4.2. Correlation between LY6G6F Expression and Survival in PDAC

Survival analysis was carried out for the PDAC patient cohort comparing those with LY6G6F low (0-1+) and LY6G6F high (2-3+) expressing tumours. At the time of analysis 66.7% (38/57) of patients had succumbed to PDAC and 33.3% (19/57) of patients were alive. The median survival for those that died from PDAC was 532 days. **Figure 4.10** shows the Kaplan-Meier survival analysis for LY6G6F low and high expression in the whole patient cohort. There is a distinct trend towards patients with high LY6G6F expression having a poorer prognosis compared to those with low LY6G6F expression. However, this was not found to be a statistically significant correlation (p=0.182). The median survival for LY6G6F low expressing tumours was 1305 days. The median survival for LY6G6F high expressing tumours was 628 days. Therefore, even though not deemed significant, there is a trend towards the tumours exhibiting higher levels of LY6G6F immunoreactivity having poorer survival than the LY6G6F low expressing tumour cohort.

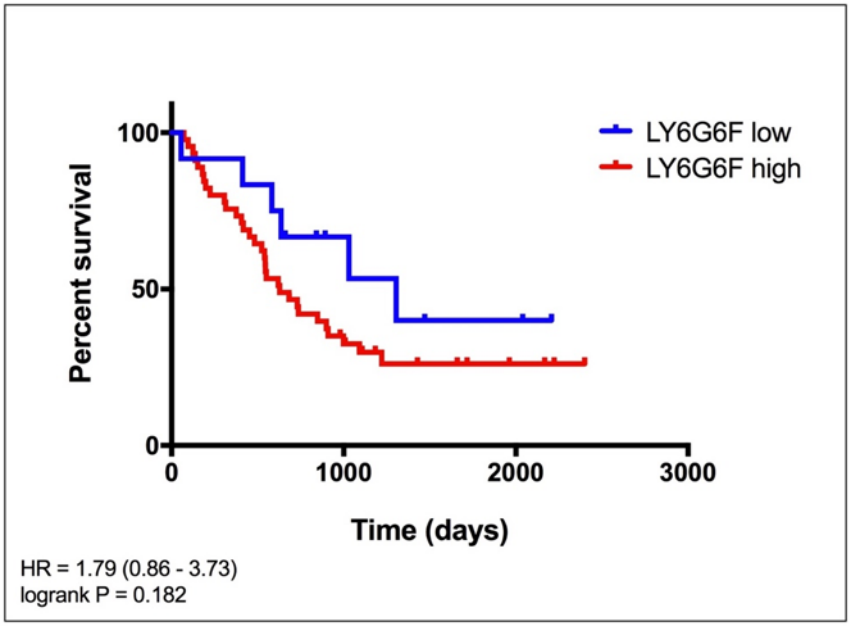

Figure 4.10 Kaplan-Meier survival analysis of PDAC patients after surgical resection grouped according to LY6G6F expression. (n=57) Patients with high LY6G6F expression show poorer survival vs. patients with low LY6G6F expression. LY6G6F low = (0-1+ score); LY6G6F high = (2-3+ score). (p=0.182; logrank test) Survival analysis performed using GraphPad Prism version 7.

4.4.3. Summary of LY6G6F Expression in Normal Pancreas and PDAC

- LY6G6F expression is absent in the majority of normal pancreas, and shows weak and diffuse expression in the cases where it is present.
- LY6G6F is highly expressed in the majority (78.9%) of PDAC and this was found to be a highly significant overexpression (p-value <0.0001) compared to normal pancreas.
- Strong LY6G6F expression was also observed in the stroma of 40.4% of the PDAC cases analysed.
- LY6G6F was observed to be more highly expressed in cases where lymphovascular invasion, perineural invasion and portal vein involvement were present.
- There is a trend towards higher LY6G6F expression being associated with poorer survival in this PDAC patient cohort (n=57).

4.5. LY6G6F Expression in Gastric Cancer

The preliminary IHC analysis of normal oesophagus and malignant oesophagus (Section 4.2) showed no apparent overexpression of LY6G6F in oesophageal cancer. However, we wanted to assess LY6G6F expression in other cancers of the gastrointestinal (GI) tract. High LY6G6F gene expression was shown to be significantly associated with poorer survival in gastric cancer patients, using the KM plotter website analysis. (Szász *et al.*, 2016) **Figure 4.11** shows the corresponding Kaplan-Meier survival analysis for LY6G6F low and high mRNA expression based on data from 631 gastric cancer patients. Therefore, to investigate LY6G6F expression at the protein level in gastric cancer tumours, a small gastric adenocarcinoma and normal gastric tissue TMA (ST721, US Biomax, Inc) was examined for LY6G6F expression. In addition, we also had 8 normal gastric epithelium tissue sections available for analysis. This gave a total of 16 gastric adenocarcinomas, 3 normal cancer adjacent and 11 normal gastric epithelium specimens for analysis.

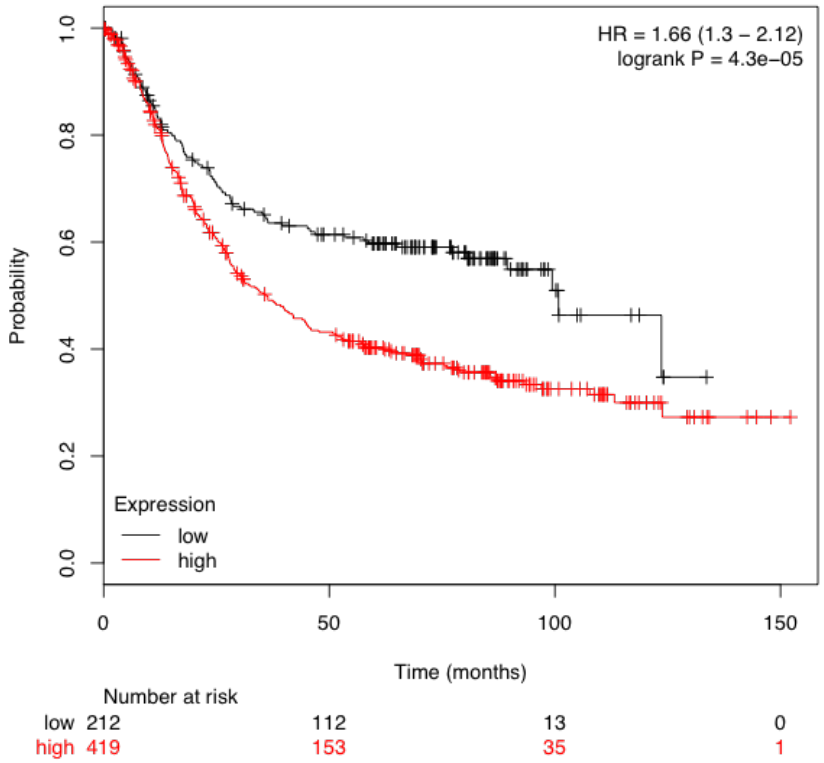

Figure 4.11 Kaplan-Meier overall survival analysis for LY6G6F low and high gene expression in gastric cancer. **(n=631)** High LY6G6F gene expression is significantly associated with poorer survival in gastric cancer. (kmplot.com)

The sections were scored for LY6G6F expression, as previously described in Table 4.5. The results obtained are shown in **Table 4.11**. Normal gastric and normal cancer adjacent tissue both showed some weak LY6G6F immunoreactivity (as shown in **Figure 4.12**), 9/11 normal stomach and 3/3 NAT stomach scored as 1+, with this characterised as weak diffuse staining. **Table 4.12** shows the two normal scores combined and along with the adenocarcinoma score, grouped into low LY6G6F and high LY6G6F expression for analysis. Compared to normal gastric epithelium, which showed weak diffuse LY6G6F immunoreactivity in the majority of cases, 50% of the gastric adenocarcinomas showed high LY6G6F immunoreactivity. An estimation of the significance of this result, by Chi-square test, showed higher LY6G6F expression is significantly correlated with gastric adenocarcinoma vs. normal gastric tissue (p-value 0.002), as high LY6G6F expression was not observed in any of the normal gastric tissues analysed. The LY6G6F immunoreactivity observed in gastric adenocarcinoma was a combination of granular cytoplasmic staining, with some membrane localisation observed in some specimens. **Figure 4.12** shows representative images of LY6G6F immunoreactivity observed in normal gastric tissue and gastric adenocarcinoma.

Out of the 16 gastric adenocarcinomas analysed, 18.75% (3/16) were classified as Grade 2 and 81.25% (13/16) as Grade 3 tumours, however there was no significant association found between LY6G6F expression and grade in this small sample size. 66.7% (2/3) of Grade 2 tumours had low LY6G6F expression (0-1+), with high LY6G6F expression in 33.3% (1/3) of cases. Grade 3 tumours had high LY6G6F expression in 53.8% (7/13) of cases and low LY6G6F in 46.2% (6/7). Therefore, there is a trend towards higher expression in the higher grade tumours.

		LY6G6F Score			
Specimen:	**No. of cases**	**0**	**1+**	**2+**	**3+**
Normal Gastric	**11**	2	9	0	0
NAT Gastric	**3**	0	3	0	0
Gastric Adenocarcinoma	**16**	5	3	4	4

Table 4.11 LY6G6F expression by IHC score in normal gastric tissue, cancer adjacent normal gastric tissue and gastric adenocarcinoma.

		LY6G6F expression	
Specimen:	**No of cases**	**Weak (0-1+)**	**Strong (2-3+)**
Normal Gastric + NAT Gastric	14	14	0
Gastric Adenocarcinoma	16	8	8 **

Table 4.12 Association between LY6G6F expression in gastric cancer vs. normal gastric tissue. High LY6G6F expression is associated with gastric cancer; ** p-value 0.002 as estimated by Chi-square test.

4.5.1. Summary of LY6G6F Expression in Normal Gastric Tissue and Gastric Cancer

- The majority of normal gastric epithelium displays some weak and diffuse LY6G6F immunoreactivity.
- LY6G6F was found to be highly expressed in 50% of gastric cancer specimens, a significant overexpression vs. normal gastric tissue (p-value 0.002).
- Kaplan-Meier survival analysis (kmplot.com) shows that high LY6G6F gene expression is significantly associated with poorer survival compared to low LY6G6F gene expression in gastric cancer.

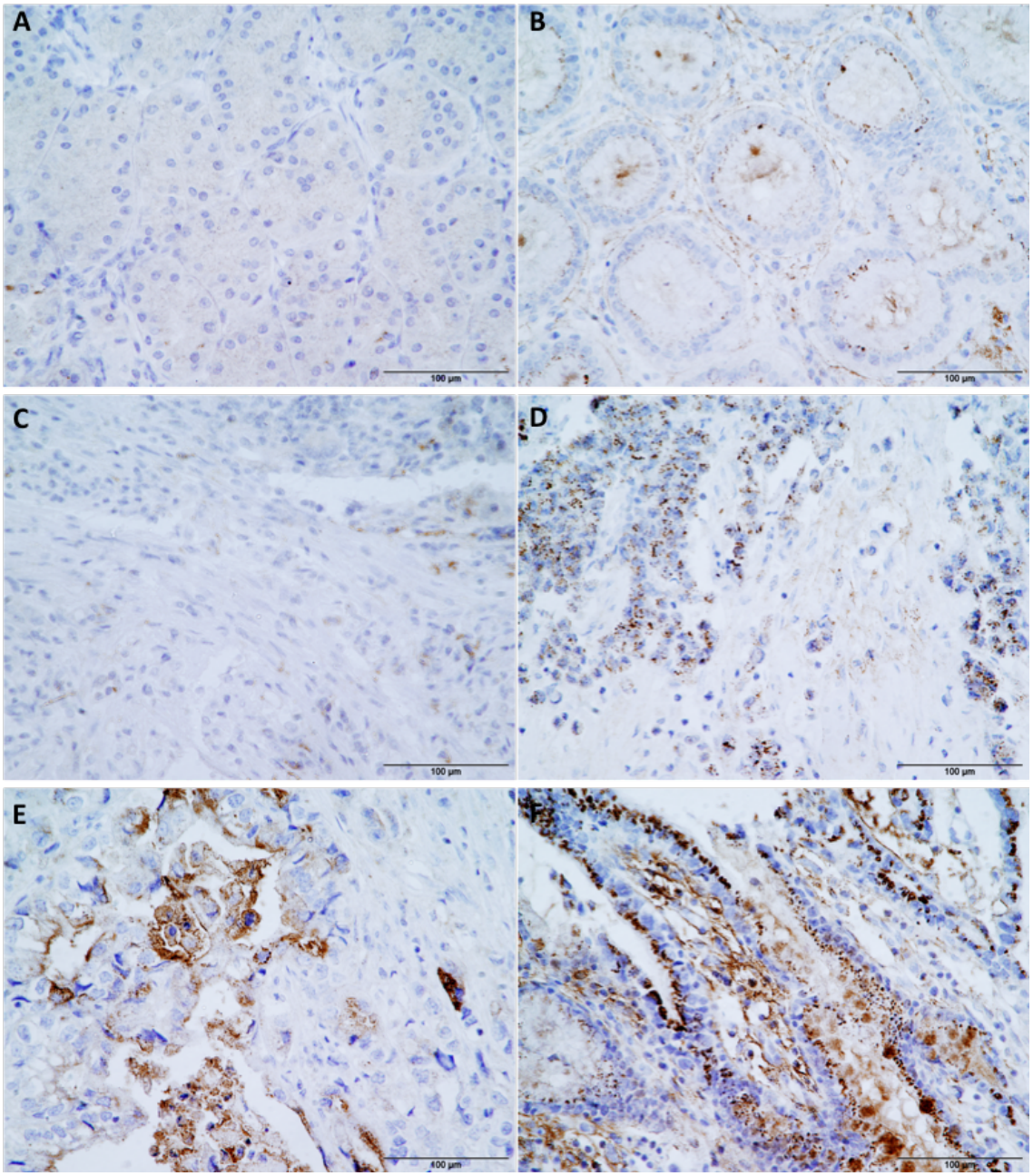

Figure 4.12 IHC analysis of LY6G6F expression in normal and malignant gastric tissue. Representative images showing: (**A**) Normal gastric epithelium with negligible LY6G6F immunoreactivity. (**B**) Normal cancer adjacent gastric tissue with weak immunoreactivity. (**C**) Gastric cancer with negative immunoreactivity. (**D**) Gastric cancer with moderate cytoplasmic immunoreactivity. (**E**) Gastric cancer with strong cytoplasmic and membrane-like immunoreactivity. (**F**) Gastric cancer with strong granular cytoplasmic and membrane-like immunoreactivity. Original magnification 400x. The scale bars represent 100μm.

4.6. LY6G6F Expression in Normal Tissues

The expression pattern of LY6G6F in normal tissues will be an important factor in assessing its potential as a molecular target for potential therapeutic antibody targeting. An excellent candidate target would ideally have negative expression in normal tissues, particularly vital organs, with expression exclusively in cancer cells. However, it is very difficult to find proteins with such an expression pattern. Therefore, minimal target expression can be tolerated in some normal tissues, if the target candidate has a much stronger expression pattern in cancer cells. The absence or minimal expression of target in the proliferating cells of normal tissues is also required, to minimise off target toxicities.

To investigate LY6G6F expression in normal tissues, a number of TMAs with normal tissues (described in Section 2.6.1), as well as full-face tissue sections, if available, were analysed for LY6G6F expression. **Table 4.13** displays the results of LY6G6F expression in the range of normal tissues analysed. In general, if LY6G6F was expressed in normal tissues it showed weak or diffuse cytoplasmic staining. The only exception is normal colon, where a small number (8/42) of cases did show some strong LY6G6F expression. Then as previously noted in some normal pancreas specimens and more so in PDAC, LY6G6F strongly stained the stroma of some normal tissues analysed, with these results also displayed in **Table 4.13**. LY6G6F expression was observed in the stroma of normal bladder, kidney, larynx, salivary gland and pancreas tissue. **Figure 4.13** shows representative images of LY6G6F immunoreactivity observed in some normal tissues.

To investigate LY6G6F expression in highly proliferating cells of normal tissues, serial tissue sections of a range of proliferative tissues, including colon, duodenum, tonsil and skin, were stained for LY6G6F and Ki67, a cellular marker of proliferation. **Figure 4.14** shows some of the representative results of this analysis. In general, LY6G6F did not appear to be present in the same cells as those stained for Ki67. However, in some of the serial sections it was a bit more difficult to determine the exact same cellular location. A dual IHC set up, where a single section is stained for both LY6G6F and Ki67 would be required for absolute determination of localisation.

Normal tissues with negative or minimal LY6G6F immunoreactivity				
Colon (14/42)*	Pancreas (15/23)	Duodenum (0/3)	Stomach (12/14)	Oesophagus (3/3)
Tonsil (8/10)	Liver (2/4)	Breast (2/2)	Lung (0/2)	Thyroid (1/3)
Spleen (2/3)	Uterus (0/1)	Cervix (0/2)	Ovary (0/1)	Skin (3/3)
Testis (1/2)	Prostate (2/2)	Pituitary gland (1/1)	Adrenal gland (1/1)	Parathyroid gland (1/1)
Bone marrow (1/1)	Placenta (2/3)	Muscle, skeletal (0/1)	Heart muscle (1/1)	Omentum (0/1)
Peripheral nerve (0/1)	Cerebellum (0/1)	Thymus (0/1)	Cerebral cortex (1/1)	
Normal tissues with strong LY6G6F immunoreactivity in the stroma				
Bladder (1/1)	Kidney (1/1)	Larynx (1/1)	Salivary gland (2/2)	Pancreas (5/23)

Table 4.13 LY6G6F expression in normal tissues. The number of sections that stained out of the total number analysed is listed. Tissues that displayed strong stromal stain had negative / weak LY6G6F expression in the glandular tissue. * Normal colon also showed some strong expression in 8/42 cases.

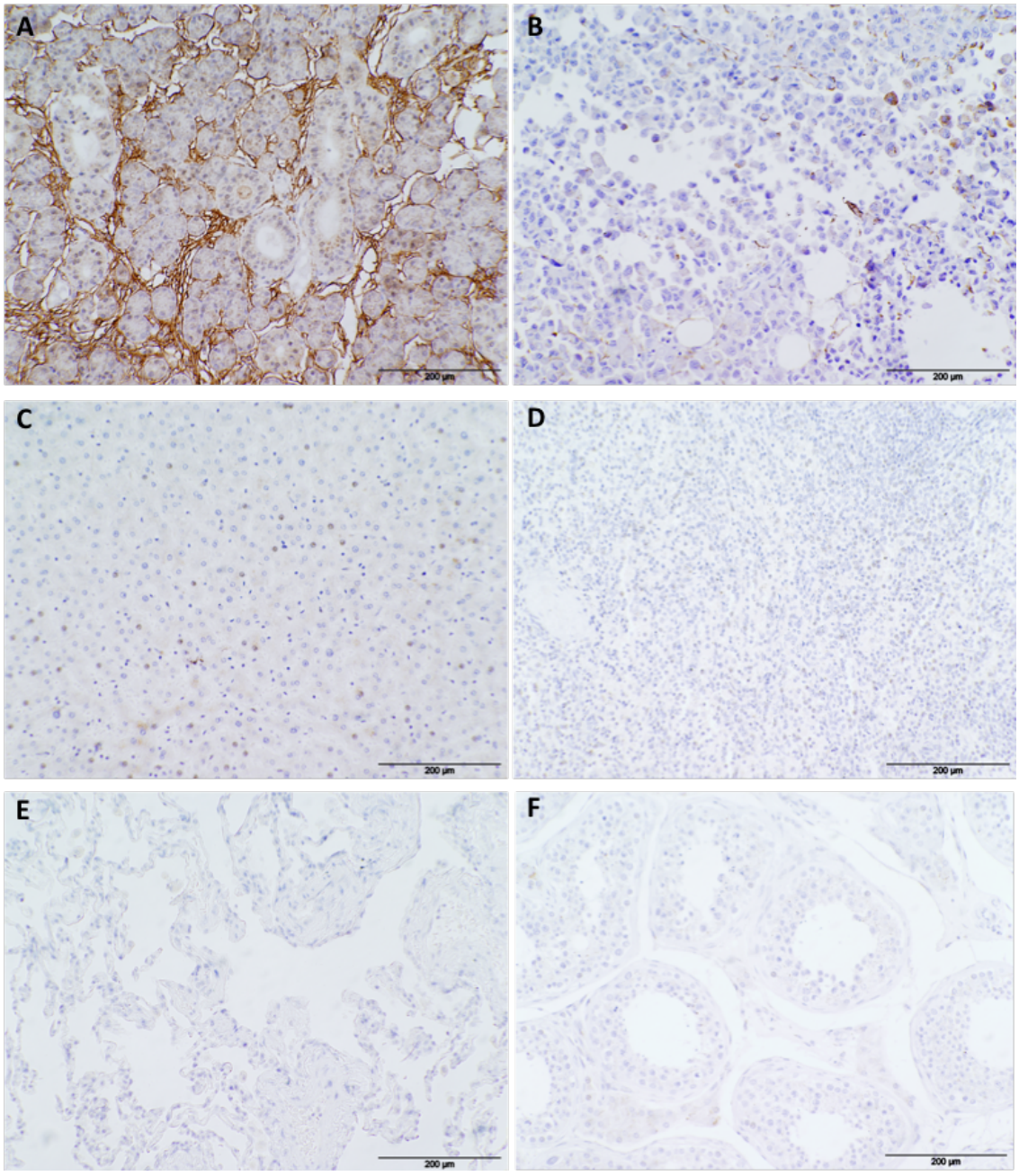

Figure 4.13 IHC analysis of LY6G6F expression in normal tissues. Representative images showing: (**A**) Salivary gland with strong LY6G6F immunoreactivity in the stroma. (**B**) Thyroid with negligible immunoreactivity. (**C**) Liver with very weak and diffuse immunoreactivity. (**D**) Spleen with negative immunoreactivity. (**E**) Lung with negative immunoreactivity. (**F**) Testis with negative immunoreactivity. Original magnification 200x. The scale bars represent 200µm.

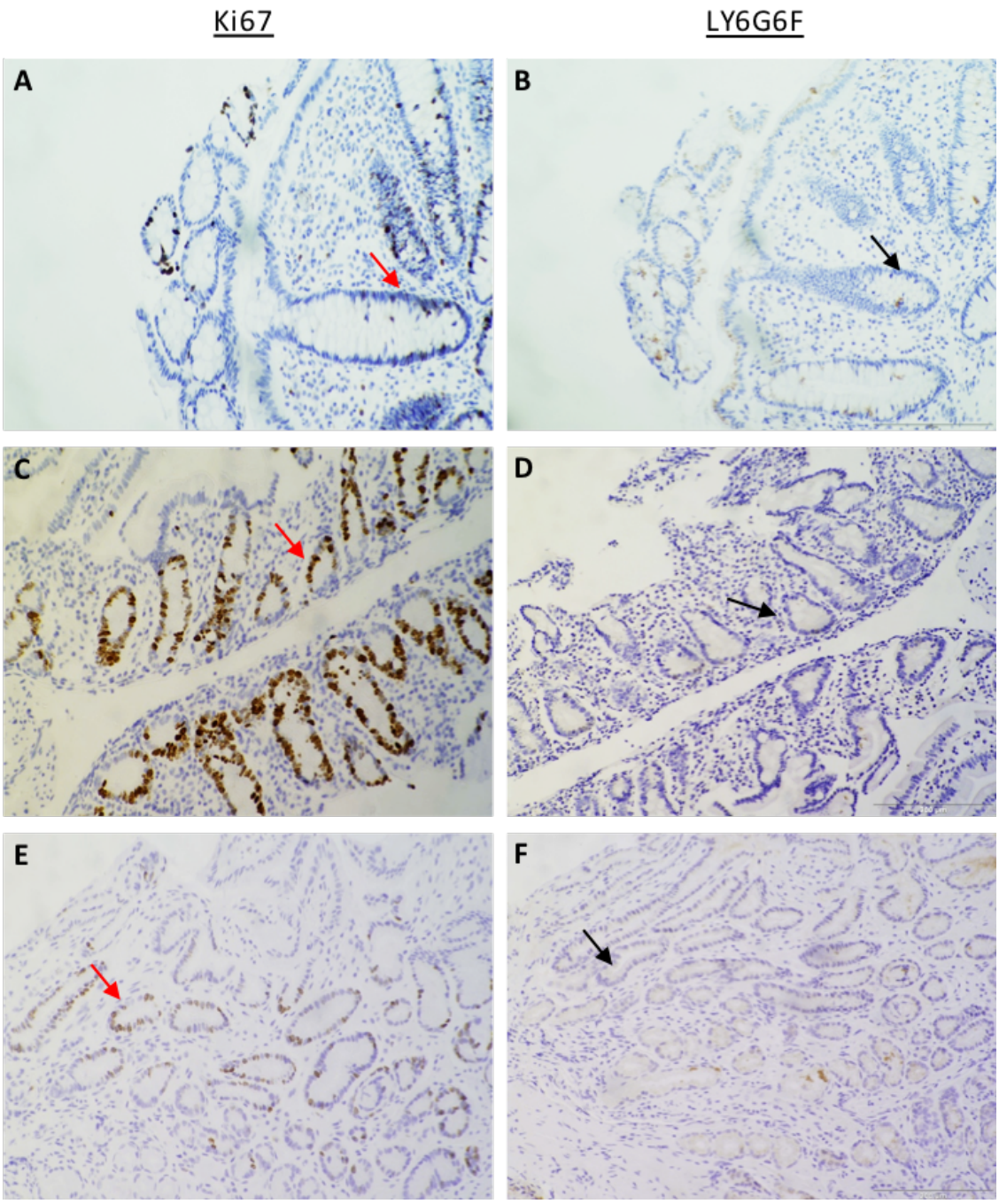

Figure 4.14 IHC analysis of LY6G6F expression in proliferating cells of normal tissues. Representative images of colon, duodenum and gastric epithelium stained for Ki67 and LY6G6F. (**A-B**) Normal colon (**C-D**) Normal duodenum. (**E-F**) Normal gastric epithelium. Red and black arrows indicate the approximate same location in the Ki67 and LY6G6F stained serial sections. LY6G6F immunoreactivity appears to be absent or minimal in proliferating cells. Original magnification 200x. The scale bars represent 200µm.

4.7. Imaging of LY6G6F in Cancer Cell Lines

In order to further investigate the localisation of LY6G6F in cancer cell lines, Immunofluorescence and Immunocytochemical staining for LY6G6F in the MIA PaCa-2 cell line was carried out as described in Sections 2.7-2.8. Cells were fixed and permeabilised with methanol for both methods. **Figure 4.15** shows representative images of the Immunofluorescent analysis. The LY6G6F stain was visualised with a green-fluorescent dye labelled secondary antibody and the cells nuclei were stained blue with DAPI. These two images were then merged, to allow better interpretation of the cellular localisation of LY6G6F. The Immunofluorescent analysis shows mainly cytoplasmic LY6G6F staining in this cell line, with some perinuclear stain also observed, and possibly some plasma membrane immunoreactivity. Similarly, in the Immunocytochemical analysis shown in **Figure 4.16**, cytoplasmic stain is observed in the majority of MIA PaCa-2 cells, with no distinct membrane localisation observed. Further optimisation of these methods is required to determine if a better picture of LY6G6F subcellular location in colon cancer and PDAC cell lines can be determined, and whether the cell-surface localisation of LY6G6F can be confirmed in these cancer cell lines.

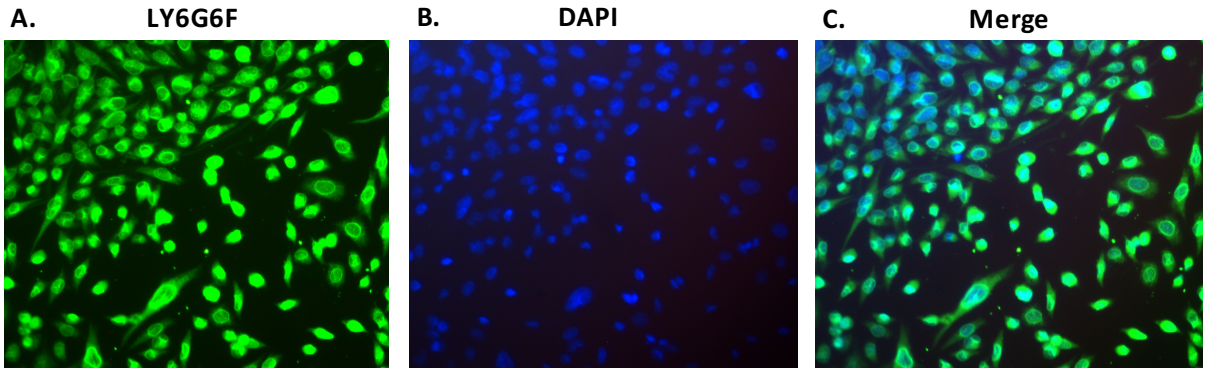

Figure 4.15 Immunofluorescent analysis of LY6G6F expression in MIA PaCa-2 cells. Representative images showing: (**A**) MIA PaCa-2 cells fixed with methanol and stained for LY6G6F. (**B**) The nuclei were stained blue with DAPI. (**C**) The merged LY6G6F and DAPI image. Cytoplasmic, perinuclear and possibly some membranous LY6G6F staining is observed in these cells. Original magnification 400x.

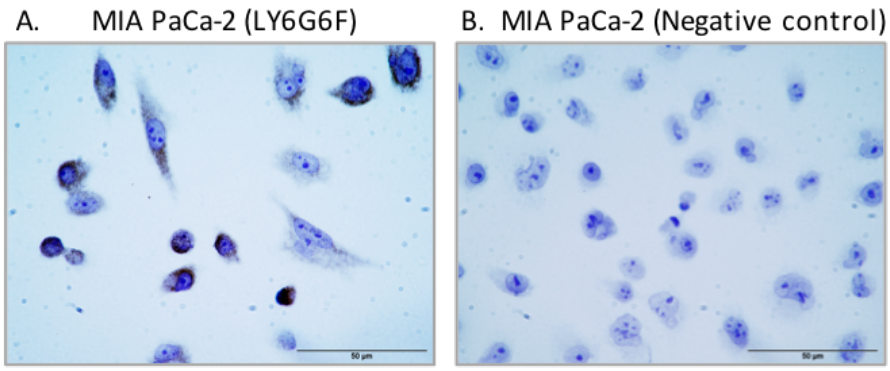

Figure 4.16 Immunocytochemical analysis of LY6G6F expression in MIA PaCa-2 cells. Representative images show (**A-B**) MIA PaCa-2 cells fixed with methanol and stained for LY6G6F and a negative control (no primary antibody). LY6G6F cytoplasmic immunoreactivity is observed in some cells, with no immunoreactivity observed in the negative control. Original magnification 600x. Scale bars represent 50μm.

4.8. Functional Analysis of LY6G6F Knockdown by RNAi

LY6G6F has been found to be significantly overexpressed in CRC and PDAC tumours compared to normal colon and pancreas by IHC analysis. Therefore, to investigate the functional role of LY6G6F in the colon cancer and pancreatic cancer cell phenotype, siRNA mediated knockdown (KD) of LY6G6F was carried out *in vitro*. The HCT116 colon cancer cell line and MIA PaCa-2 PDAC cell line were selected for functional analysis. Transfection conditions were optimised for each cell line, as described in Section 2.4.1. The siRNA target LY6G6F mRNA for destruction, leading to protein knockdown, and the effect this has on the cells is then assessed by a number of different functional assays. Three different LY6G6F siRNAs (#1, #2 and #3) were used in this analysis. Controls for the comparison of LY6G6F knockdown, include cells only control (no transfection reagents) and cells transfected with a Negative siRNA (siRNA that does not code for any known mRNA sequence).

4.8.1. Knockdown of LY6G6F in the Colon Cancer Cell Line HCT116

The HCT116 cell line was chosen for functional analysis as it shows a moderate level of LY6G6F expression in the colon cancer cell line panel (see Figure 3.1) and it also has a suitable level of migration and invasion, for assessing any effect LY6G6F KD has on these phenotypes. HCT116 cells transfected with siRNAs were assayed for protein knockdown after 72hrs by Western blot analysis. **Figure 4.17** shows a representation of the amount of protein knockdown achieved in these cells, with a bar chart of densitometry analysis visualising the approximate LY6G6F protein levels relative to cells only control. Complete protein knockdown was never achieved for this target, and further optimisations did not increase the amount of protein KD observed. Therefore, cells were set up for functional assays at the 72hr time point, to determine what effect the partial protein knockdown has on proliferation, 2D colony formation, migration and invasion of these cells.

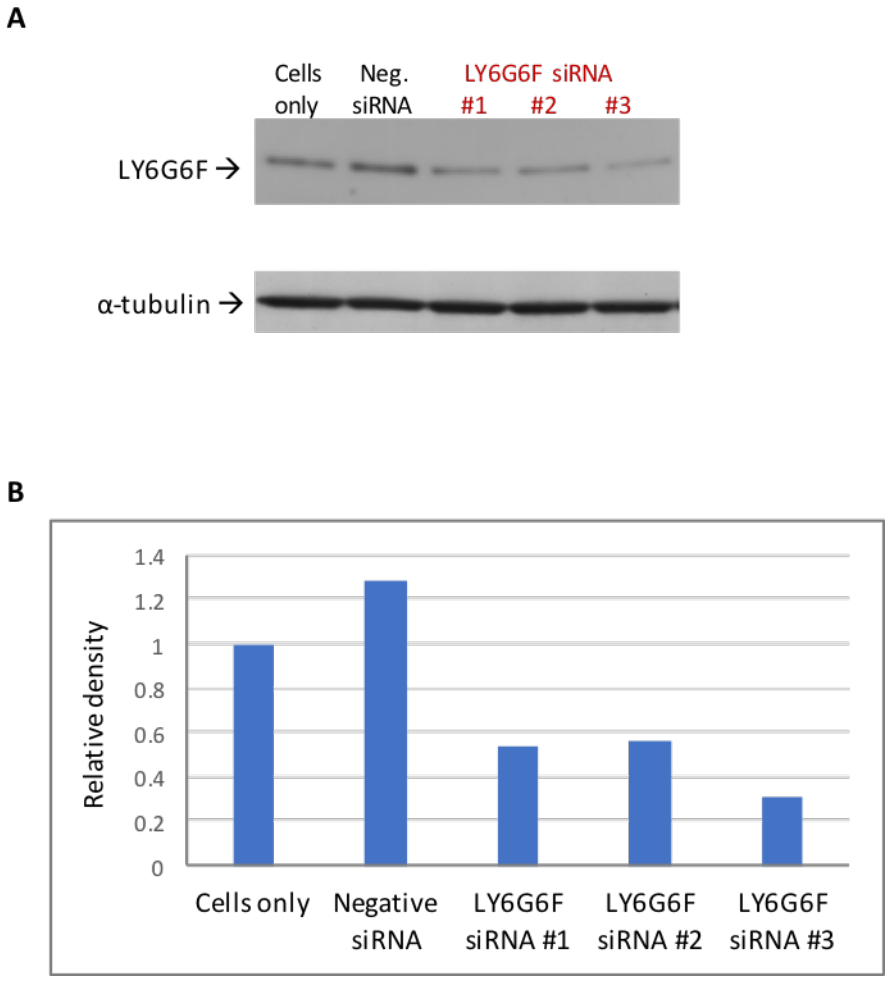

Figure 4.17 LY6G6F expression in HCT116 cells following siRNA treatment. A: Representative Immunoblot showing HCT116 cells probed for LY6G6F in cells only control, Negative siRNA transfected cells, and cells transfected with LY6G6F siRNA #1, 2, 3 (30nM siRNA concentration). α-tubulin was used as a loading control. **B**: Densitometry analysis of the representative blot shown in A, with results graphed as relative density of bands compared to cells only. Analysis performed using ImageJ software.

4.8.1.1. Proliferation of HCT116 Cells post LY6G6F Knockdown

Proliferation of HCT116 cells was measured 72hrs post transfection by the acid phosphatase assay as described in Section 2.5.1. **Figure 4.18** shows the percentage proliferation of cells relative to the Negative siRNA transfected cells. The transfection procedure (Lipofectamine only cells; and Negative siRNA treated cells) had negligible effects on proliferation compared to cells only. Knockdown of LY6G6F was found to significantly reduce proliferation compared to the Negative siRNA, with all 3 siRNAs used. LY6G6F siRNA #3 transfected cells had a 21% reduction in proliferation compared to the Negative control. Whilst LY6G6F siRNA #1 and #2 transfected cells showed an even bigger decrease, with a 36% and a 38% growth inhibition.

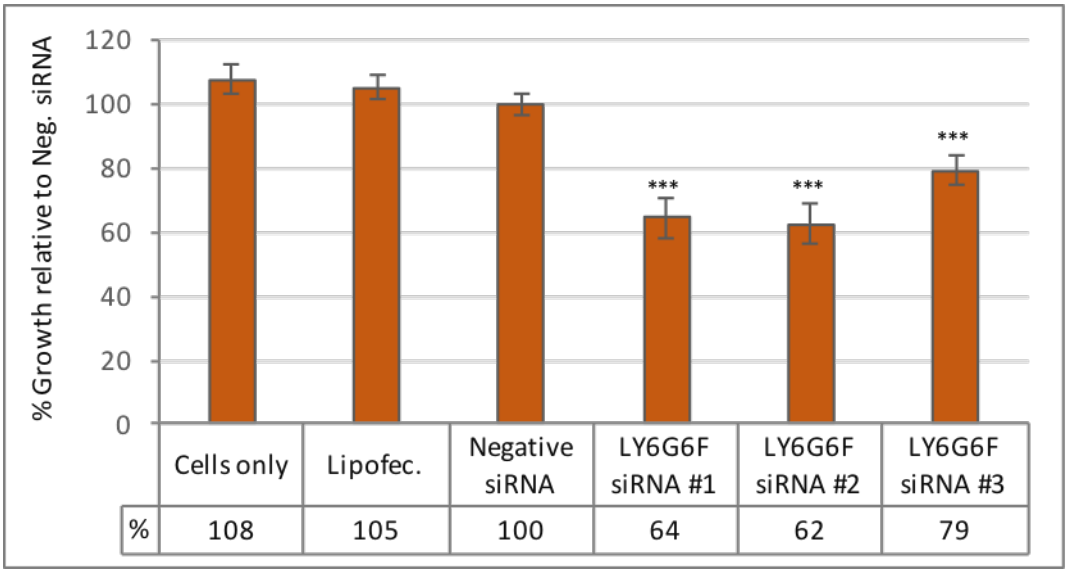

Figure 4.18 Proliferation assay on HCT116 cells following LY6G6F knockdown. Results graphed as % survival (mean ± SD) relative to the Negative control siRNA. (n=5) The proliferation of HCT116 cells was significantly reduced after LY6G6F knockdown compared to the Negative control. (siRNA #1 p-value: 0.0002, #2 p-value: 0.00017, #3 p-value: 0.00059. Students t-test unequal variance)

4.8.1.2. 2D Colony Formation of HCT116 Cells post LY6G6F Knockdown

The 2D colony formation assay assesses the ability of single cells to survive and proliferate into colonies. Cells are set up at an optimised cell number in 6 well plates, as described in Section 2.5.2, 72hrs post transfection. Colony formation is then assessed after 12 days, by fixing cells and staining with crystal violet. Clonogenic assays are commonly manually counted, however the data presented in this study uses a plugin for ImageJ software, which calculates the percentage area of the 6 well covered by colonies and also the intensity stain. These calculations equate to the number of colonies formed (area covered) and also the size of colonies (with stronger intensity indicating more cells in a colony). Therefore using these parameters, the effect of LY6G6F protein knockdown compared to Negative siRNA treated cells can be determined.

Figure 4.19 shows representative results of this analysis, with representative images of the colony formation in 6 well plates and the percentage area covered and percentage intensity of colonies relative to the Negative siRNA transfected cells graphed. All three LY6G6F siRNA treated cells showed a decrease in both the area covered and intensity of colonies formed compared to the Negative siRNA, with siRNA #1 showing the biggest decrease, with a 58.4% decrease in colony area and 59.9% decrease in intensity, indicating fewer and smaller colonies formed, compared to the Negative siRNA treated cells. The average decrease observed in LY6G6F siRNA #2 and #3 treated cells was smaller, with a 25.9% decrease in colony area for #2 and a 29.4% decrease in area for #3. However due to the high standard deviations between triplicate experiments, these reductions were not deemed significant for any of the siRNAs. However, there is a trend towards a decrease in colony forming ability following knockdown with all 3 siRNAs.

A

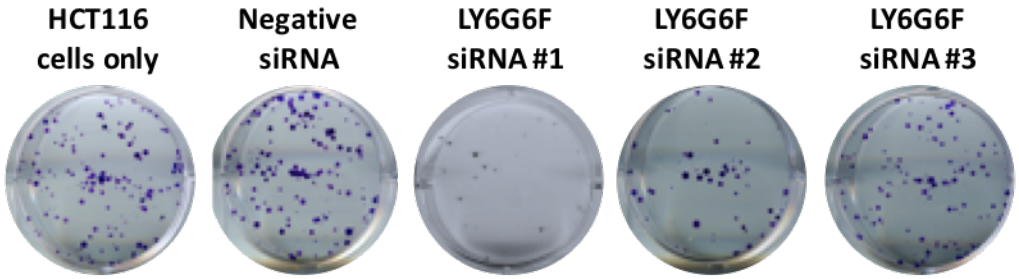

B

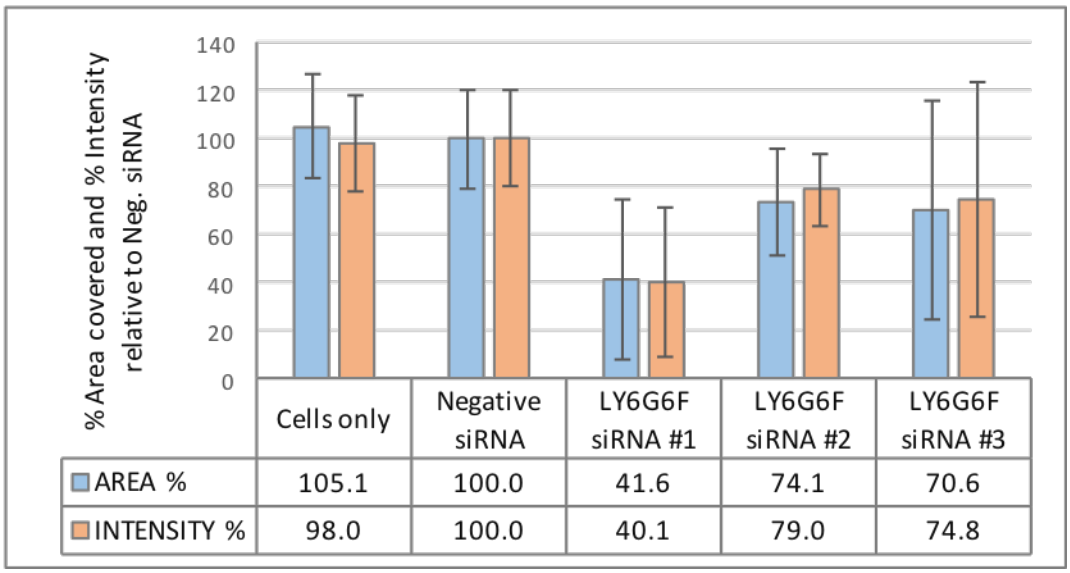

Figure 4.19 2D colony formation of HCT116 cells following LY6G6F knockdown. (**A**) Representative images showing the 2D colony formation in 6 well plates of HCT116 cells only, cells transfected with Negative siRNA and LY6G6F siRNAs #1, 2 and 3. (**B**) Results graphed as % area covered and % intensity of colonies (mean ± SD) relative to the Negative control siRNA. (n=3) The 2D colony formation of HCT116 cells was reduced after LY6G6F knockdown compared to the Negative control. (Not significant, Students t-test unequal variance)

4.8.1.3. Migration of HCT116 Cells post LY6G6F Knockdown

Migration assays were set up 72hrs post transfection and carried out as described in Section 2.5.4, with cells allowed to migrate through the membrane for 30hrs before being fixed and stained with crystal violet. **Figure 4.20** shows these results graphed as percentage migration relative to the Negative siRNA treated cells. A significant reduction in migration was observed for 2 out of the 3 siRNAs used in the analysis. LY6G6F siRNA #2 treated cells had a 73% significant reduction in migration, with siRNA #1 showing a 48% significant reduction. Although the effect caused by siRNA #3 was not found to be significant, it does follow the same trend towards a decrease, with an average 54% reduction in migration. The higher SD in this case possibly prevented significance. As 2/3 siRNAs show a significant result, it can be concluded that knockdown of LY6G6F significantly reduces the migratory ability of HCT116 cells.

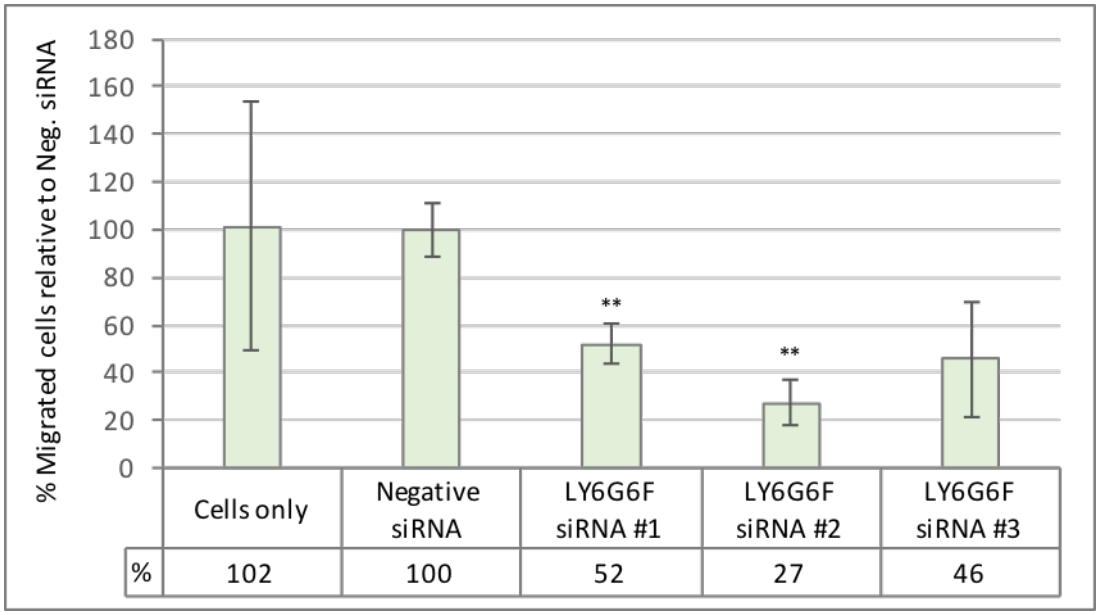

Figure 4.20 Migration assay results for HCT116 cells following LY6G6F knockdown. Results graphed as % migration (± SD) relative to the Negative siRNA. (n=3) The migration of HCT116 cells was significantly reduced after LY6G6F knockdown compared to the Negative control. Statistics: unpaired t-test (siRNA #1 p-value: 0.006, #2 p-value: 0.005, #3 p-value: 0.06)

4.8.1.4. Invasion of HCT116 Cells post LY6G6F Knockdown

Invasion assays were set up 72hrs post transfection and carried out as described in Section 2.5.3, with cells allowed to migrate through the Matrigel coated membrane for 30hrs before being fixed and stained with crystal violet. High variability between replicates was found in this assay. The Negative siRNA control appeared to increase invasion compared to control cells only, however the effect of LY6G6F knockdown was still compared to the Negative siRNA in this experiment to test for significance, as it was deemed the most appropriate control. **Figure 4.21** shows the percentage invasion of cells relative to the Negative siRNA treated cells. A significant reduction in invasion was observed for 2 out of the 3 siRNAs used in the analysis. Both LY6G6F siRNA #2 and #1 treated cells showed a significant reduction in invasion levels, with a 70% and 59% reduction in invasion observed for each respectively. The higher variability observed for siRNA #3 resulted in a lack of significance, however it does follow the same trend towards a decrease in invasion, with a 33% average decrease in invasion. Therefore as 2/3 siRNAs show significance, it appears that LY6G6F knockdown significantly inhibits invasion of HCT116 cells.

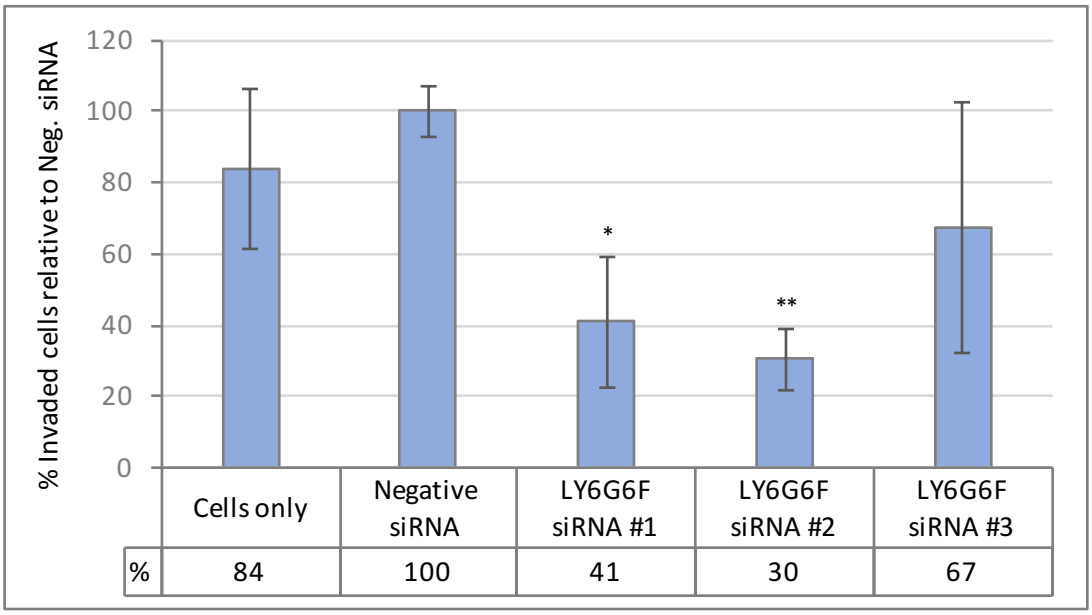

Figure 4.21 Invasion assay results for HCT116 cells following LY6G6F knockdown. Results graphed as % invasion (± SD) relative to the Negative siRNA (n=3). The invasion of HCT116 cells was significantly reduced after LY6G6F knockdown compared to the Negative control. Statistics: unpaired t-test (siRNA #1 p-value: 0.03, #2 p-value: 0.006, #3 p-value: 0.28)

4.8.2. Knockdown of LY6G6F in the PDAC Cell Line MIA PaCa-2

Attempts were made to achieve protein knockdown of LY6G6F in the BxPC-3 PDAC cell line, one of the more highly LY6G6F expressing cell lines, as shown in Figure 4.3. However, no obvious protein knockdown was observed, therefore the MIA PaCa-2 cell line, one of the more lowly LY6G6F expressing cell lines was selected for functional analysis. The MIA PaCa-2 cell line displays sufficient levels of migration and invasion for analysis, with some of the other PDAC cells lines being very lowly invasive or display a clumpy growth morphology that would make counting migrated cells very difficult. Similar to the HCT116 cell line, complete knockdown of LY6G6F protein was not achieved in the MIA PaCa-2 cell line. **Figure 4.22** shows a representation of the amount of protein knockdown achieved in these cells 72hrs post transfection, with a bar chart of densitometry analysis visualising the approximate LY6G6F protein levels relative to cells only control. Cells were set up for functional assays at the 72hr time point, to determine what effect the partial protein knockdown has on proliferation, 2D colony formation, migration and invasion of these cells.

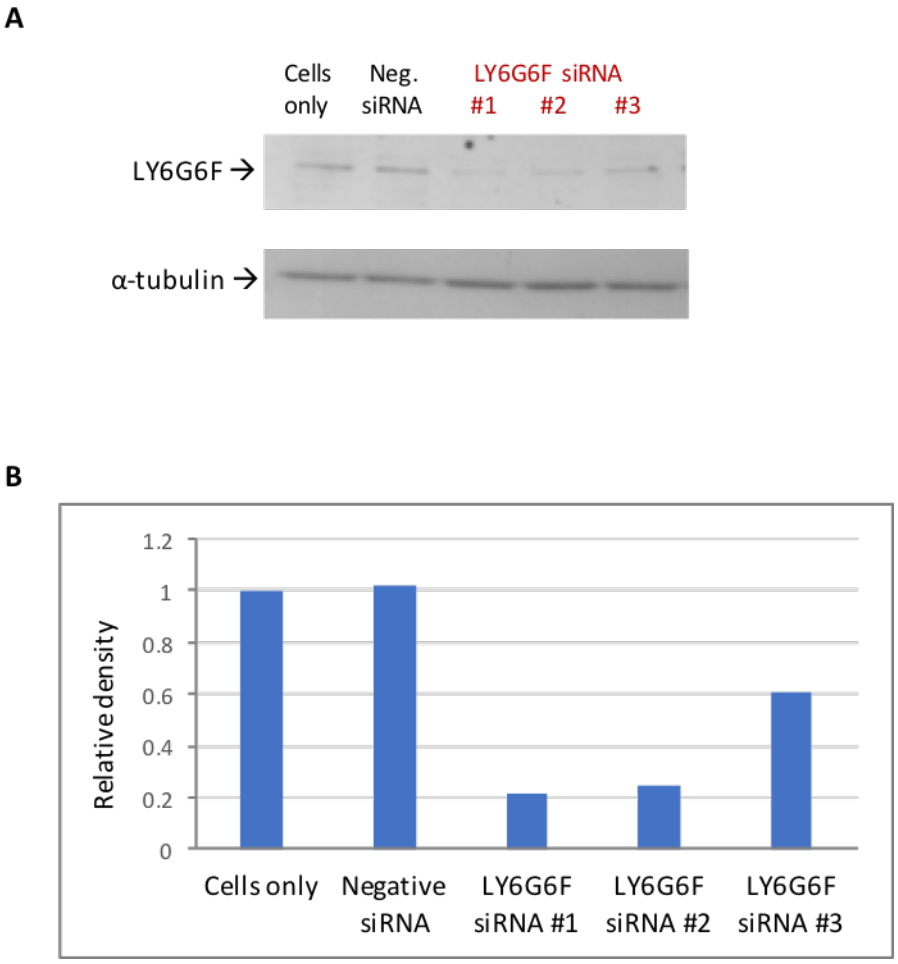

Figure 4.22 LY6G6F expression in MIA PaCa-2 cells following siRNA treatment. A: Representative Immunoblot showing MIA PaCa-2 cells probed for LY6G6F in cells only control, Negative siRNA transfected cells, and cells transfected with LY6G6F siRNA #1, 2, 3 (30nM siRNA concentration). α-tubulin was used as a loading control. **B**: Densitometry analysis of the representative blot shown in A, with results graphed as relative density of bands compared to cells only. Analysis performed using ImageJ software.

4.8.2.1. Proliferation of MIA PaCa-2 Cells post LY6G6F Knockdown

Proliferation of MIA PaCa-2 cells was measured 72hrs post transfection by the acid phosphatase assay as described in Section 2.5.1. **Figure 4.23** shows the percentage proliferation of cells relative to the Negative siRNA transfected cells. Knockdown of LY6G6F was found to significantly reduce proliferation compared to the Negative siRNA, with all 3 siRNAs used. The reduction in proliferation was minimal from 11% decrease with siRNA #2 to 20% with siRNA #1, and the largest decrease of 24% observed in siRNA #3 treated cells.

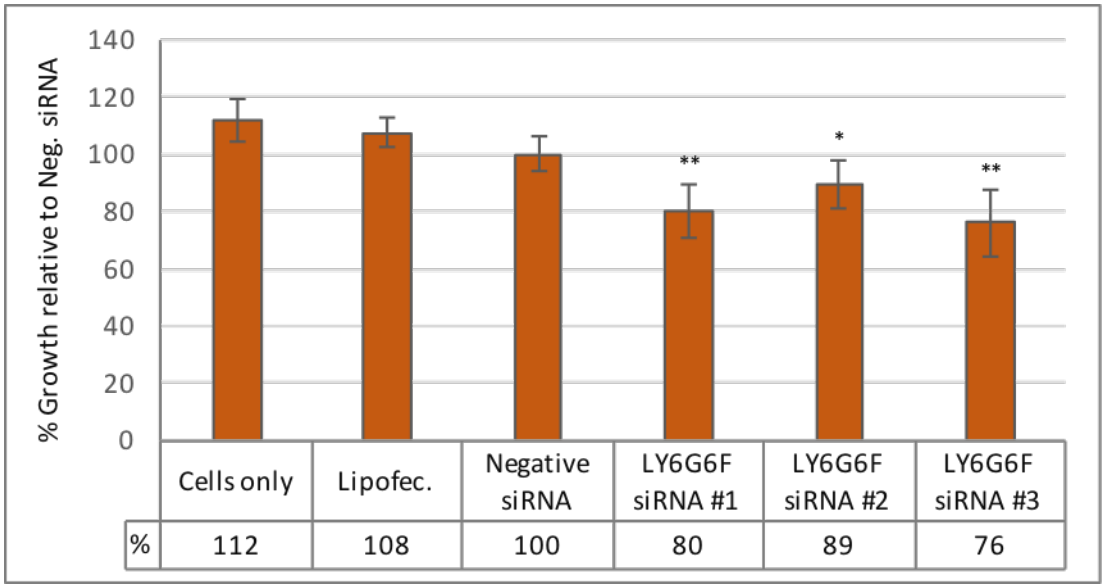

Figure 4.23 Proliferation assay on MIA PaCa-2 cells following LY6G6F knockdown. Results graphed as % survival (mean ± SD) relative to the Negative control siRNA. (n=5) The proliferation of MIA PaCa-2 cells was significantly reduced after LY6G6F knockdown compared to the Negative control. (siRNA #1 p-value: 0.0085, #2 p-value: 0.045, #3 p-value: 0.01. Students t-test unequal variance)

4.8.2.2. 2D Colony Formation of MIA PaCa-2 Cells post LY6G6F Knockdown

2D colony formation assays were set up 72hrs post transfection, and colony formation analysed after 12 days. **Figure 4.24** shows representative results of this analysis, with representative images of the colony formation in 6 well plates and the percentage area covered and percentage intensity of colonies relative to the Negative siRNA transfected cells graphed. Knockdown of LY6G6F with two of the siRNAs was found to significantly decrease the colony forming ability of MIA PaCa-2 cells, with both the area and intensity of colonies reduced. The results for both LY6G6F siRNA #1 and #3 were deemed significant. LY6G6F siRNA #1 showed a 51.1% decrease in colony area and a 48.9% decrease in intensity. LY6G6F siRNA #3 gave a 31.7% decrease in colony area and a 40.4% decrease in intensity. Whilst the results for siRNA #2 were not found to be significant (due to high SD between replicates), it does follow the same trend with an average decrease of 30.4% in colony area and a 36.4% decrease in colony intensity. Therefore as 2/3 siRNAs show significance, it appears that knockdown of LY6G6F in the MIA PaCa-2 cell line, significantly reduces both the number (area) and size (intensity) of colonies formed compared to Negative siRNA treated cells.

A

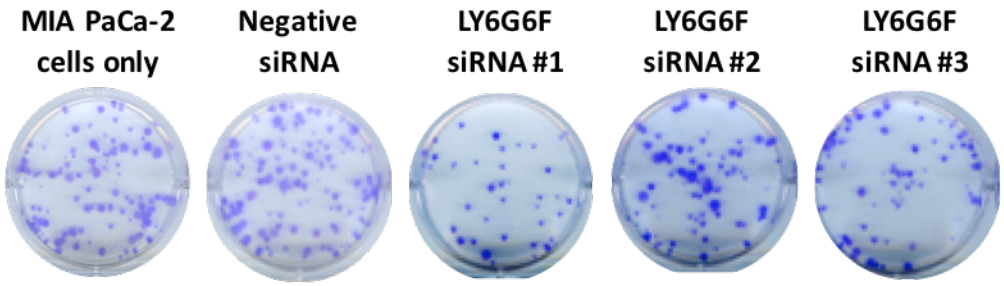

B

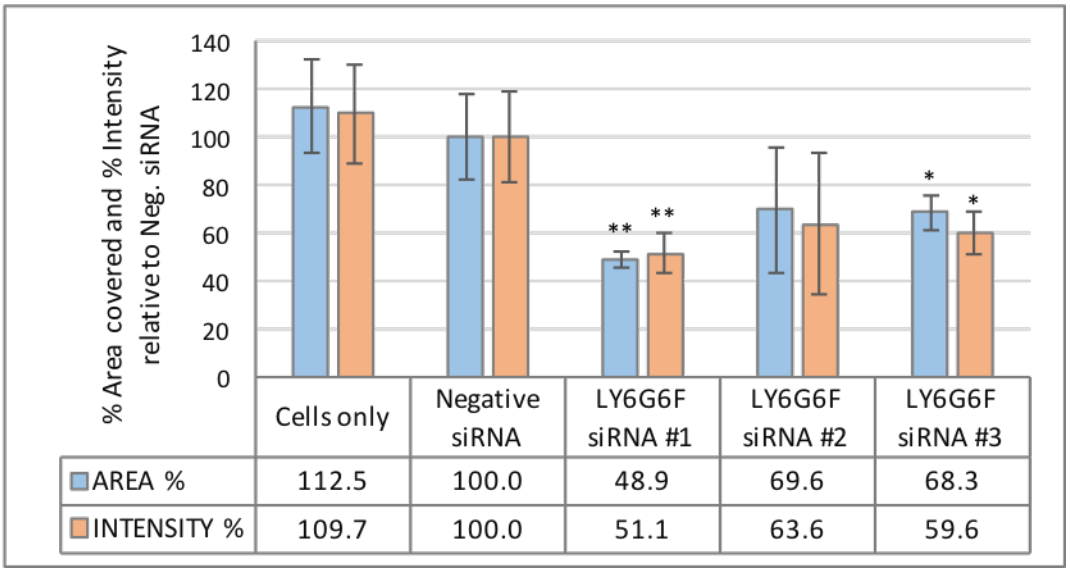

Figure 4.24 2D colony formation of MIA PaCa-2 cells following LY6G6F knockdown. (**A**) Representative images showing the 2D colony formation in 6 well plates of MIA PaCa-2 cells only, cells transfected with Negative siRNA and LY6G6F siRNAs #1, 2 and 3. (**B**) Results graphed as % area covered and % intensity of colonies (mean ± SD) relative to the Negative control siRNA. (n=3) The 2D colony formation of MIA PaCa-2 cells was significantly reduced after LY6G6F knockdown compared to the Negative control. (siRNA #1: area p-value: 0.0014, intensity p-value 0.009; #3 area p-value: 0.016, intensity p-value: 0.015. Students t-test unequal variance)

4.8.2.3. Migration of MIA PaCa-2 Cells post LY6G6F Knockdown

Migration assays were set up 72hrs post transfection and carried out as described in Section 2.5.4, with cells allowed to migrate through the membrane for 40hrs before being fixed and stained with crystal violet. **Figure 4.25** shows these results graphed as percentage migration relative to the Negative siRNA treated cells. No overall significant effect on the migration of these cells was observed. A significant reduction of 15% compared to the Negative siRNA was found for LY6G6F siRNA #3. However, siRNA #1 and 2 had no effect. Therefore, it appears that LY6G6F knockdown has no effect on MIA PaCa-2 cell migration.

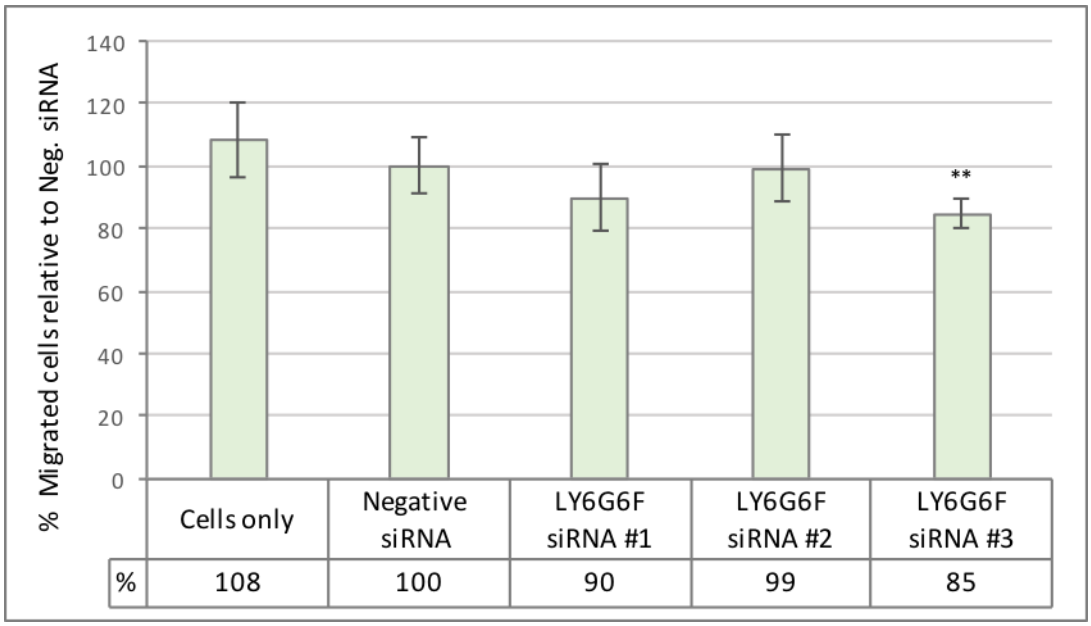

Figure 4.25 Migration assay results for MIA PaCa-2 cells following LY6G6F knockdown. Results graphed as % migration (± SD) relative to the Negative siRNA. (n=3) The migration of MIA PaCa-2 cells was significantly reduced after LY6G6F knockdown with siRNA #3 compared to the Negative control. However, no significant difference was found between LY6G6F siRNAs #1 and #2 and the Negative control, indicating that overall the migration of MIA PaCa-2 cells is not affected by LY6G6F knockdown. Statistics: unpaired t-test (siRNA #1 p-value: 0.2, #2 p-value: 0.9, #3 p-value: 0.01)

4.8.2.4. Invasion of MIA PaCa-2 Cells post LY6G6F Knockdown

Invasion assays were set up 72hrs post transfection and carried out as described in Section 2.5.3 with cells allowed to migrate through the Matrigel coated membrane for 40hrs before being fixed and stained with crystal violet**. Figure 4.26** shows these results graphed as percentage invasion relative to the Negative siRNA treated cells. A significant reduction in invasion was observed for 2 out of the 3 siRNAs used in the analysis, with siRNA #3 showing the biggest decrease of 34%, followed by #1 showing a 26% decrease in invasion. LY6G6F siRNA #2 also showed a similar decrease of 25%, however this was not found to be significant. However as 2/3 siRNAs show significance, it appears that LY6G6F knockdown significantly inhibits invasion of MIA PaCa-2 cells.

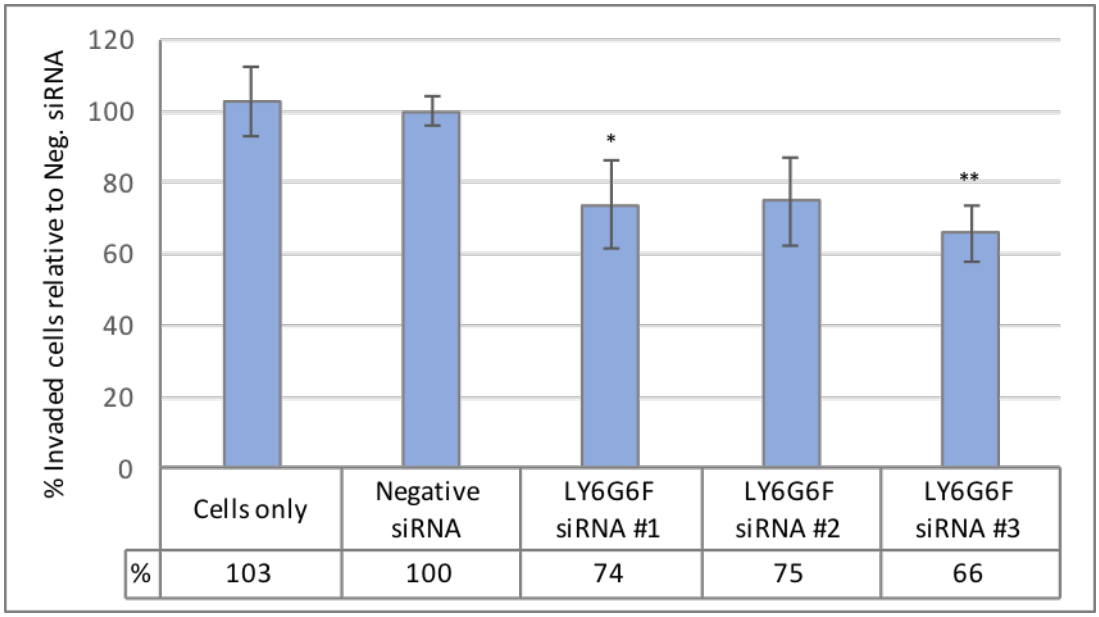

Figure 4.26 Invasion assay results for MIA PaCa-2 cells following LY6G6F knockdown. Results graphed as % invasion (± SD) relative to the Negative siRNA. (n=3) The invasion of MIA PaCa-2 cells was significantly reduced after LY6G6F knockdown compared to the Negative control. Statistics: unpaired t-test (siRNA #1 p-value: 0.048, #2 p-value: 0.07, #3 p-value: 0.01)

4.8.3. Effect of LY6G6F Knockdown on FAK Activation and PARP Cleavage in HCT116 and MIA PaCa-2 Cells

LY6G6F protein knockdown was found to significantly decrease the proliferation, migration and invasion of HCT116 and MIA PaCa-2 cells, as described in the previous Sections 4.8.1-4.8.2. Therefore, it was decided to next examine various signalling pathways that may be affected and contributing to these phenotypic changes, in particular the activation of the p44/42 MAPK signalling pathway and the activation of FAK, as previous studies have strongly suggested the coupling of LY6G6F with these pathways. In order to determine the effect of LY6G6F knockdown on p44/42 MAPK and FAK activation, antibodies specific to phosphorylated forms and total protein were used for Western blot analysis 72hrs post LY6G6F siRNA transfection. In both cell lines, the effect of LY6G6F knockdown on the levels of phosphorylated p44/42 MAPK were inconsistent across triplicate experiments. (Data not shown) However, there was a marked decrease in the levels of phosphorylated-FAK in both the HCT116 and MIA PaCa-2 cell lines, compared to the stable levels of total FAK, following knockdown of LY6G6F, as shown in **Figure 4.27**. A decrease in FAK activation was observed for all three LY6G6F siRNAs in the HCT116 cell line, and predominantly with just siRNA #1 and #3 in the MIA PaCa-2 cell line. This is consistent with the functional assay results for MIA PaCa-2 cells, were siRNAs #1 and #3 gave a higher and more significant reduction in proliferation, migration and invasion compared to the results for siRNA #2.

Furthermore, to examine whether the decrease in proliferation observed in both cell lines is due to an increase in apoptotic cell death or cell cycle arrest, the expression of a small number of apoptotic and cell cycle markers was also assessed by Western blot analysis. The levels of the cell cycle markers, Cyclin A, which is expressed at a higher level in the G1/S phase transition of the cell cycle and p27, which controls cell cycle progression at G1, showed no apparent difference or inconsistent differences in expression between control cells and LY6G6F siRNA treated cells. (Data not shown) Therefore no conclusion can be made on whether LY6G6F knockdown leads to cell cycle arrest in these cell lines. To examine whether LY6G6F knockdown leads to an increase in apoptotic cell death, an antibody that recognises both full length (116kDa) Poly(ADP-ribose) polymerase (PARP) and also the 89kDa fragment of cleaved PARP was used for Western blot analysis. PARP cleavage is a marker of cells undergoing apoptosis. These results are also shown in **Figure 4.27**. An

increase in the levels of cleaved PARP was observed in both cell lines, with LY6G6F siRNAs #1and #2 showing the biggest increase in the HCT116 cell line and LY6G6F siRNAs #1and #3 showing the biggest increase in the MIA PaCa-2 cell line vs. Negative siRNA treated cells. These results are consistent with the proliferation assay results for both cell lines, where siRNAs #1and #2 gave the biggest decrease in proliferation in the HCT116 cell line and siRNAs #1and #3 gave the biggest decrease in the MIA PaCa-2 cell line.

Overall, LY6G6F knockdown has been shown to decrease FAK activation and increase apoptosis levels in the HCT116 and MIA PaCa-2 cell lines, indicating that the inhibitory effects observed on cell growth, migration and invasion may potentially be mediated by these pathways.

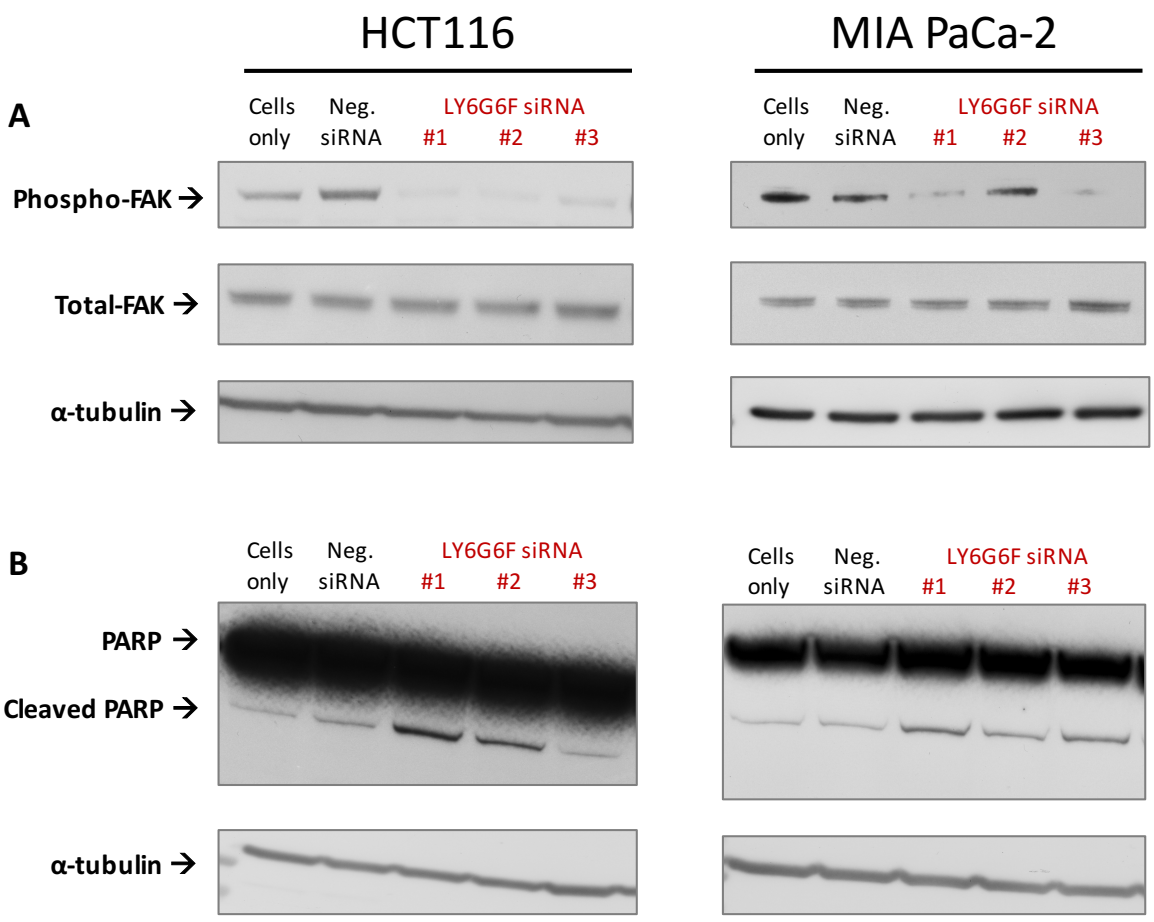

Figure 4.27 The effect of LY6G6F knockdown on FAK activation and PARP cleavage in HCT116 and MIA PaCa-2 cells. Representative Immunoblots showing the levels of phosphorylated and total FAK (**A**) and cleaved PARP (**B**) in HCT116 and MIA PaCa-2 cells transfected with LY6G6F siRNAs #1,2,3. (n=3) The levels of phosphorylated FAK are decreased with all three LY6G6F siRNAs in the HCT116 cell line, and reduced in LY6G6F siRNA #1 and #3 treated cells in the MIA PaCa-2 cell line compared to Negative siRNA treated cells. There is an increase in the levels of cleaved PARP in LY6G6F siRNA #1 and #2 treated HCT116 cells and in LY6G6F siRNA #1 and #3 treated MIA PaCa-2 cells compared to the Negative siRNA control cells.

4.8.4. Summary of Functional Analysis of LY6G6F Protein Knockdown

- LY6G6F protein knockdown was found to significantly decrease the proliferation of both HCT116 and MIA PaCa-2 cells, as determined by both the acid phosphatase assay and the 2D colony formation assay. This decrease in proliferation was significant for both the acid phosphatase assay and 2D colony formation assay in the MIA PaCa-2 cell line. In the HCT116 cell line, the decrease found in the acid phosphatase assay was significant, with the 2D colony formation assay showing a trend towards decreased colony formation.
- A significant reduction in the migration and invasion of HCT116 cells was observed.
- No overall effect was observed on the migration of MIA PaCa-2 cells, but a significant reduction in invasion was observed.
- A decrease in FAK activation, and an increase in apoptosis (as determined by the presence of increased PARP cleavage), was observed in both the HCT116 and MIA PaCa-2 cell lines following LY6G6F knockdown, indicating that these are some of the mechanisms of action mediating the phenotypic effects observed.

- Taken together with the IHC analysis, which showed a significant increase in LY6G6F expression in colon adenocarcinoma and PDAC tumours compared to normal tissues, with decreased survival observed in the PDAC patients with high LY6G6F expression vs. low LY6G6F expression, a role for LY6G6F in the growth and survival of these cancers is implicated.

4.9. LY6G6F mRNA Expression

4.9.1. LY6G6F mRNA Expression in HCT116 and MIA PaCa-2 Cells post LY6G6F siRNA Transfection

The amount of LY6G6F protein knockdown achieved in the HCT116 and MIA PaCa-2 cell lines was often variable. Therefore qRT-PCR was used to determine what effect the LY6G6F siRNAs have on the mRNA levels in these cell lines. Total mRNA was extracted from cells 48hrs post transfection as described in Section 2.9.1, and converted to cDNA template for qRT-PCR. The LY6G6F siRNAs #1, 2, 3 and the Negative siRNA that were used in the functional analysis in Section 4.8, as well as siRNAs sourced from another company (Ambion), labelled Negative siRNA A, LY6G6F siRNAs A1, A2 and A3, were used in this analysis. **Table 4.14** shows the Ct (threshold cycle) values obtained for each of these samples with a concentration of 40ng cDNA per well. The Ct values indicate the number of cycles it took to detect a real signal from the sample, with higher Ct values indicating lower amounts of target nucleic acid in the sample. The Ct values for cells only of both HCT116 and MIA PaCa-2 are quite high (>35). In general samples with a Ct of 30 or higher are not considered reliable data, or indicate that if the transcript is present, it's at low levels.

However as shown in **Table 4.14** there are some differences in Ct values for the siRNA treated samples, with all LY6G6F siRNA treated cells having higher Ct values than cells only (some are not determined: CT > 40). The relative quantitation (RQ) of LY6G6F expression was calculated in the samples compared to cells only and normalised to the endogenous control gene B2M. **Figure 4.28** shows this RQ for each sample in the HCT116 cell line graphed as fold change (FC) relative to cells only (LY6G6F siRNA #1 was undetermined, Ct >40; therefore, this is not represented on the graph). These results show that whilst both of the Negative siRNAs analysed show LY6G6F mRNA levels similar to cells only, there is a decrease in the amount of LY6G6F mRNA detected in all of the LY6G6F siRNA treated cells. **Figure 4.29** shows the FC results for the MIA PaCa-2 cell line (LY6G6F siRNA #3 was undetermined and siRNA A1 was not tested, therefore these are not graphed). Combined with the Negative siRNA result there is no apparent change in LY6G6F mRNA level with siRNAs #1 and #2. There is however a decrease with the second set of siRNAs, A2 and A3. These results represent only one biological experiment.

Sample	HCT116 Ct value	MIA PaCa-2 Ct value
Cells only	36.1	36.8
Negative siRNA	36.3	37.7
LY6G6F siRNA #1	Undetermined	37.1
LY6G6F siRNA #2	36.7	37.4
LY6G6F siRNA #3	37.6	Undetermined
Negative siRNA A	36	37.1
LY6G6F siRNA A1	36.2	-
LY6G6F siRNA A2	37.5	37.9
LY6G6F siRNA A3	37.5	38.7

Table 4.14 Results from qRT-PCR analysis of LY6G6F mRNA expression, showing the average Ct values for HCT116 and MIA PaCa-2 cells only and cells treated with Negative siRNAs and LY6G6F siRNAs. (n=1)

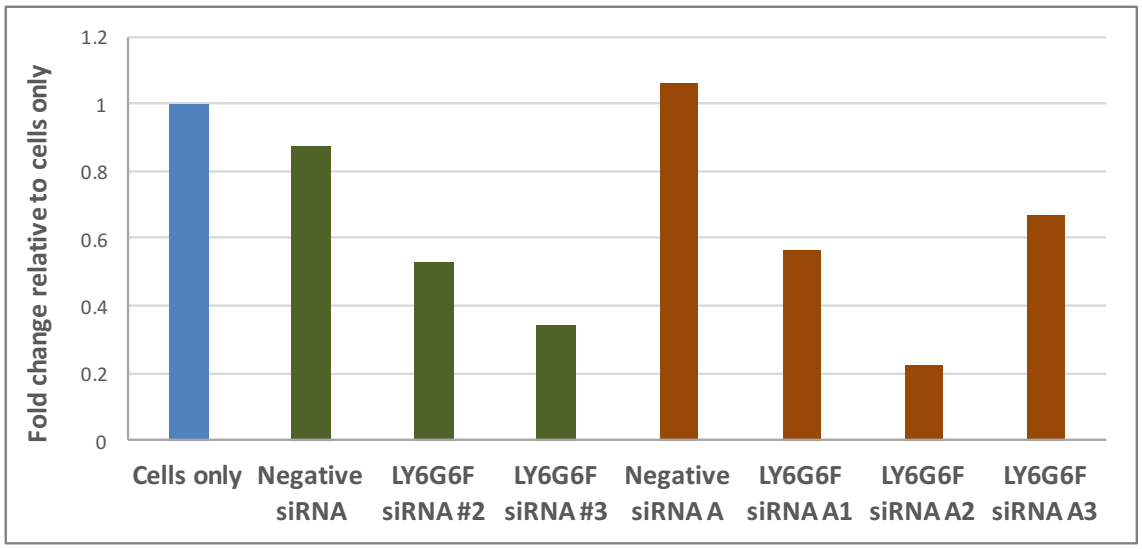

Figure 4.28 Relative quantitation of LY6G6F mRNA in HCT116 siRNA transfected cells compared to cells only and normalised to B2M by qRT-PCR. (Results represent one biological experiment)

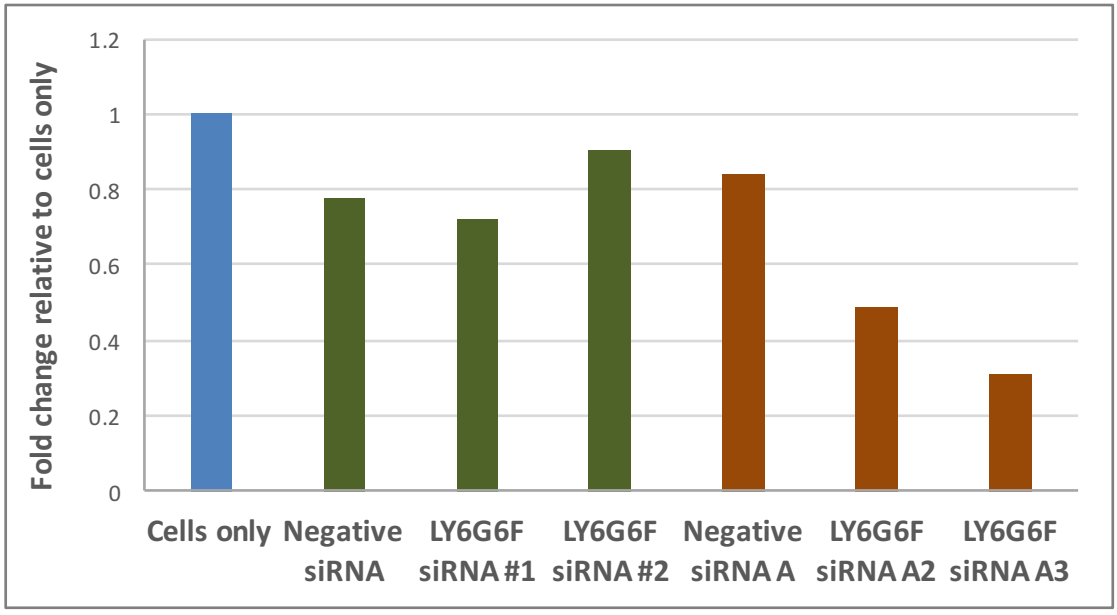

Figure 4.29 Relative quantitation of LY6G6F mRNA in MIA PaCa-2 siRNA transfected cells compared to cells only and normalised to B2M by qRT-PCR. (Results represent one biological experiment)

These results are not conclusive as the Ct values are >30 and the RQ was carried out for 1 biological experiment. However, the increased Cts observed in the LY6G6F siRNA treated cells could indicate that LY6G6F mRNA transcript is present and being reduced by siRNA treatment. To determine if lower Ct values could be obtained, the amount of cDNA template for HCT116 and MIA PaCa-2 cells only samples was increased from 40ng to 140ng cDNA per PCR reaction well. (100ng was actually the maximum amount indicated to use in the mastermix protocol) These results are shown in **Table 4.15** and indicate that even though the Ct values are >30, LY6G6F mRNA transcript is present in the cells, as the Ct value decreases upon the addition of more cDNA template. The Ct values decrease by 2 in both cell lines (36.8 to 34.8 in MIA PaCa-2; 36.1 to 34.1 in HCT116), which is what could be expected upon the addition of 3.5 times the amount of template, as 1 Ct value is roughly equivalent to a doubling in template cDNA.

Additionally, the no template control (NTC) sample did not give a signal in the qRT-PCR reaction (undetermined result), which increases confidence that the signal observed for LY6G6F is due to the transcript being present and not a non-specific signal. The NTC contains all of the reagents in the qRT-PCR reaction minus the cDNA template. A signal from this sample could indicate contamination or primer-dimer formation. The No RT control (everything except reverse transcriptase enzyme) also detected no signal in the qRT-PCR reaction. This suggests that LY6G6F mRNA is present at low abundance in HCT116 and MIA PaCa-2 cells, which makes it difficult to detect knockdown at the mRNA level. However, the preliminary RQ does show a decrease in LY6G6F mRNA with all siRNAs in the HCT116 cell line, and some of the siRNAs in the MIA PaCa-2 cell line.

Sample	Ct value
MIA PaCa-2 (40ng cDNA)	36.8
MIA PaCa-2 (140ng cDNA)	34.8
HCT116 (40ng cDNA)	36.1
HCT116 (140ng cDNA)	34.1

Table 4.15 LY6G6F mRNA expression in MIA PaCa-2 and HCT116 cells determined by qRT-PCR analysis. The average Ct values for MIA PaCa-2 and HCT116 cells are shown, when the amount of cDNA template is increased from 40-140ng in the PCR reaction.

4.9.2. LY6G6F mRNA Expression in Cell Lines

To ensure that the low level of LY6G6F mRNA detected in HCT116 and MIA PaCa-2 cells wasn't due to inefficiency of the LY6G6F Taqman assay used, a second LY6G6F assay was obtained for analysis. These Taqman assays contain primers specific to LY6G6F for amplification and fluorescent probes specific to different areas of the LY6G6F mRNA sequence. The release of these probes upon LY6G6F amplification is what gives the gene expression signal in the qRT-PCR analysis. The PDAC cell lines MIA PaCa-2 and BXPC-3, the colon cancer cell lines SW480 and HT29, and the CML cell line K562 (a LY6G6F expressing cell line according to the literature), were analysed for LY6G6F mRNA expression using both probes by qRT-PCR. **Figure 4.30** shows the Ct values obtained in this analysis. Both probes give nearly the same result in the MIA PaCa-2 cell line (34.4 with probe 1 and 32.8 with probe 2) indicating that LY6G6F mRNA is lowly abundant in this cell line. LY6G6F mRNA appears to be lowly abundant in the BXPC-3, SW480 and HT29 cell lines using probe 1 also, with probe 2 giving a similar result in the HT29 cell line. However, probe 2 does differ from probe 1 in the Ct values obtained for BXPC-3 and SW480 cells. The second probe gives a Ct value <30 for both cell lines. This discrepancy between probes could perhaps be due to varying primer efficiency rates. Both probes detect LY6G6F mRNA in the K562 cell line at a similar level, with a Ct value of 28. Therefore, LY6G6F mRNA appears to be present at low levels in the PDAC and colon cancer cell lines analysed.

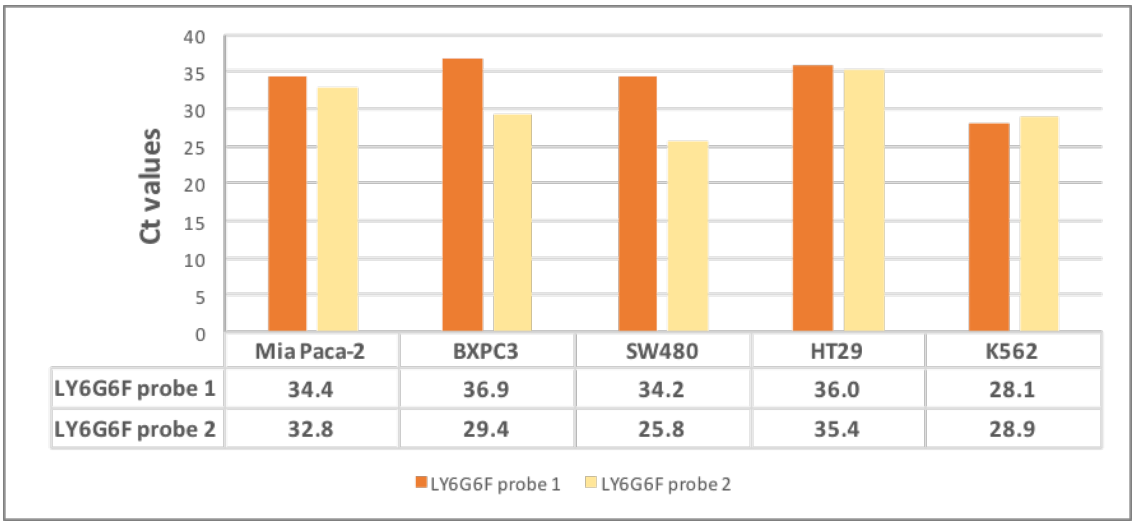

Figure 4.30 LY6G6F mRNA expression in a cell line panel determined by qRT-PCR analysis. The average Ct values obtained using two independent LY6G6F Taqman assays are shown for five cell lines: MIA PaCa-2, BXPC-3, SW480, HT29 and K562. (100ng cDNA/well; Results represent one biological experiment)

4.10. Overexpression of LY6G6F in MIA PaCa-2 and SW480 Cell Lines

To further investigate the functional role of LY6G6F in the CRC and PDAC cancer cell phenotype, it was decided to overexpress LY6G6F by vector transformation. A commercial transfection ready cloning vector containing the LY6G6F sequence (Acc no: NM_001003693) was obtained (GenScript). **Figure 4.31** shows the map of the vector used. The vector contains Amp and Neo genes for antibiotic selection of bacterial and mammalian transformed cells. The LY6G6F overexpressed protein will contain a C-terminal DYKDDDDK tag **(**FLAG-tag), which will allow confirmation of overexpression by Western blot analysis. An anti-FLAG-tag antibody should detect a band at the corresponding MW of the target protein i.e. at ~ 32kDA for LY6G6F. An empty vector control – the same vector containing everything except target ORF sequence was also obtained.

The PDAC cell line MIA PaCa-2 and the CRC cell line SW480 were chosen for overexpression as they both express lower levels of LY6G6F protein (see Figure 4.3 and Figure 3.1). Overexpression of LY6G6F in these cell lines followed by *in vitro* functional analysis will enable us to determine if overexpression of LY6G6F has any effect on the phenotype of these cells. LY6G6F overexpressing cells can also be used as a positive control for qRT-PCR analysis. Transfection optimisation was carried out as described in Section 2.10.1. Following vector transfection cells were placed under G418 antibiotic selection, with the optimal concentration for each cell line having been previously determined by setting up a kill curve (Section 2.10.2).

Following selection qRT-PCR analysis of the MIA PaCa-2 and SW480 empty vector (E.V.) and LY6G6F overexpression (O.E.) cell lines was carried out as described in Section 2.9. The two independent LY6G6F Taqman assays, described in Section 4.9.2, were used. **Figure 4.32** shows the Ct value results of this analysis for the MIA PaCa-2 cell line. Both probes confirm overexpression of LY6G6F mRNA compared to both cells only and E.V. control, with a big increase in the amount of LY6G6F mRNA in the overexpression cells. In the SW480 cell line the two independent Taqman assays had given different results, as shown in Figure 4.30. The Ct value results of the overexpression in this cell line are shown in **Figure 4.33**, with the varying Ct values between the two assays again observed for cells only and E.V samples. LY6G6F probe 2 gives a substantially lower Ct value in these samples compared to probe 1 (~9 Cts lower). Both probes then give a similar result in the O.E.

samples. They both confirm overexpression of LY6G6F mRNA, yielding Ct values of 18.2 and 19.3 respectively. It is not clear why they also do not differ by ~9 Ct values, like the other samples. But regardless overexpression has been confirmed.

LY6G6F mRNA overexpression was confirmed in both cell lines, however overexpression at the protein level was not. **Figure 4.34** shows representative Western blot images of MIA PaCa-2 cells only, E.V. and LY6G6F O.E. cell lysates, and SW480 E.V. and LY6G6F O.E cell lysates probed for LY6G6F. Western blot images of these samples probed for FLAG-tag is also shown. No increase in LY6G6F protein was observed in either the MIA PaCa-2 or SW480 cell lines (in duplicate biological experiments). It could not be confirmed whether the vector expressed version of LY6G6F protein was present at all in the samples, as the FLAG-tag blot gave inconclusive results. The FLAG-tag is attached to the C-terminal end of LY6G6F overexpressed protein, therefore a band around the same MW as LY6G6F should appear (the FLAG-tag is so small it shouldn't visibly effect the MW of LY6G6F). However, the FLAG-tag probed blot gave a strange result, with multiple bands appearing in all samples. Samples were only probed for FLAG-tag once, the antibody may need to be diluted to give a better result.

Therefore, without a clear FLAG-tag result, it cannot be concluded if following overexpression, the LY6G6F vector derived protein is being expressed or not. The Western blot analysis does not show any increase in LY6G6F protein, despite high LY6G6F mRNA overexpression in these cells. Preliminary functional analysis of the effect of LY6G6F mRNA overexpression on proliferation of MIA PaCa-2 cells is shown in **Figure 4.35**, with no effect observed on the proliferation rate compared to cells only. Post-translational regulation could be inhibiting the translation of the overexpressed mRNA into protein. The FLAG-tag analysis needs to be repeated to try and get a conclusive result.

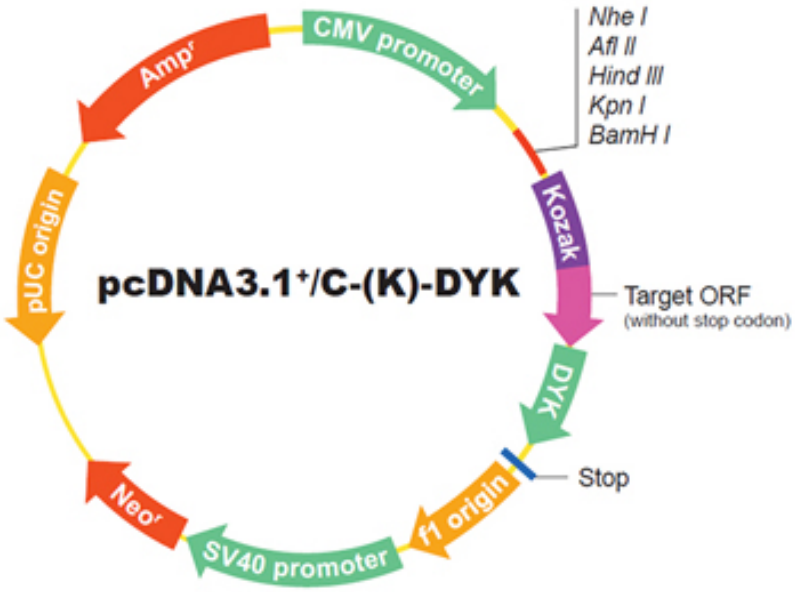

Figure 4.31 Vector map of the LY6G6F overexpression vector. The target ORF (LY6G6F; NM_001003693) expression is driven by a CMV promoter. Kozak sequence initiates the mRNA translation process into protein. A C-terminal DYKDDDDK tag (FLAG-tag) is attached to the LY6G6F sequence.

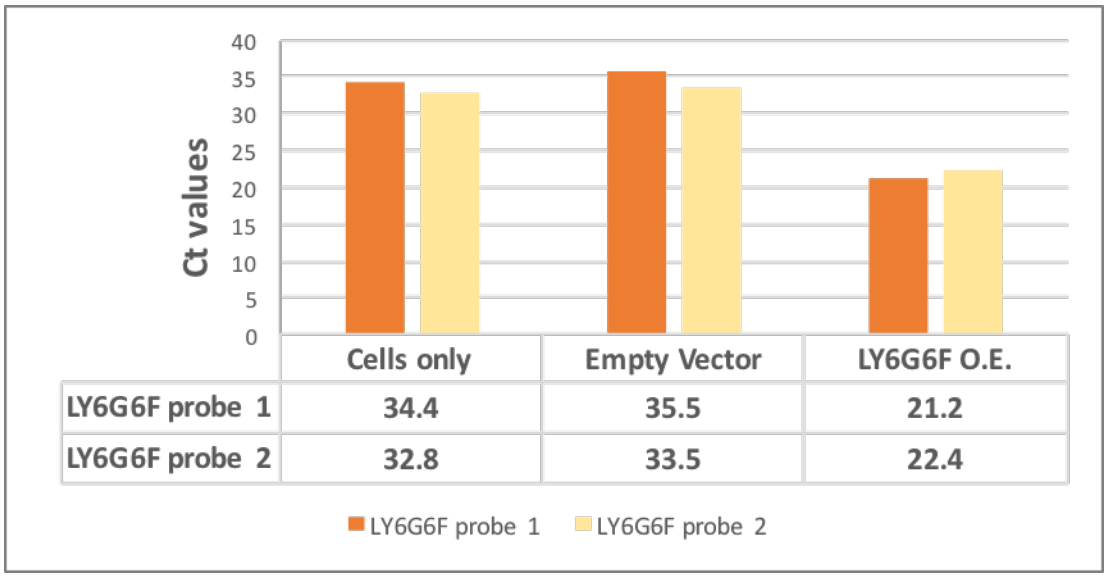

Figure 4.32 LY6G6F mRNA expression in MIA PaCa-2 cells only and cells transfected with an empty vector and LY6G6F overexpression vector, determined by qRT-PCR analysis. The average Ct values obtained using two independent LY6G6F Taqman assays are shown. (100ng cDNA/well; Results represent one biological experiment)

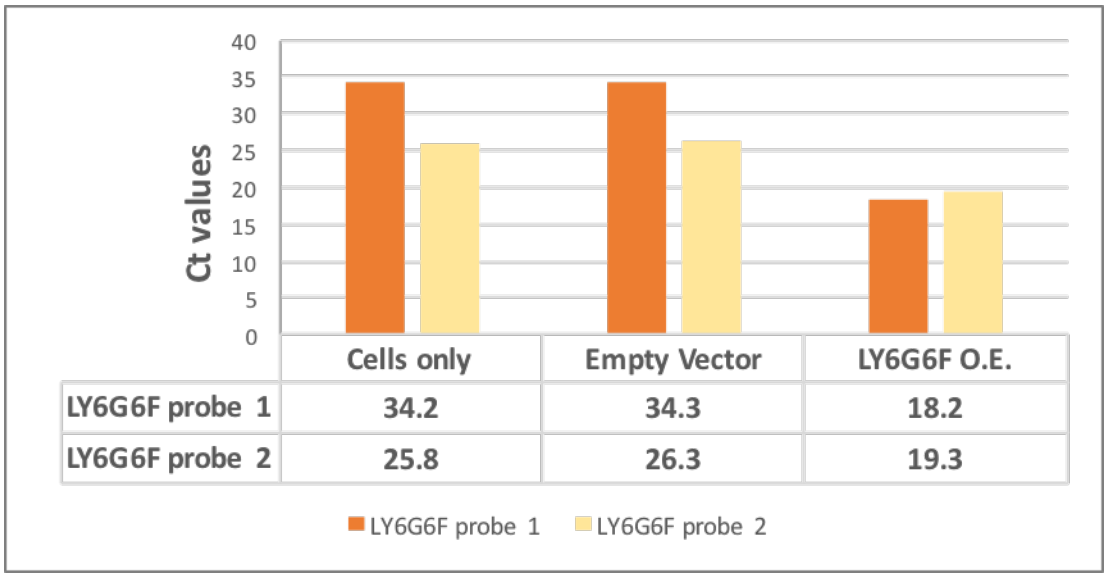

Figure 4.33 LY6G6F mRNA expression in SW480 cells only and cells transfected with an empty vector and LY6G6F overexpression vector, determined by qRT-PCR analysis. The average Ct values obtained using two independent LY6G6F Taqman assays are shown. (100ng cDNA/well; Results represent one biological experiment)

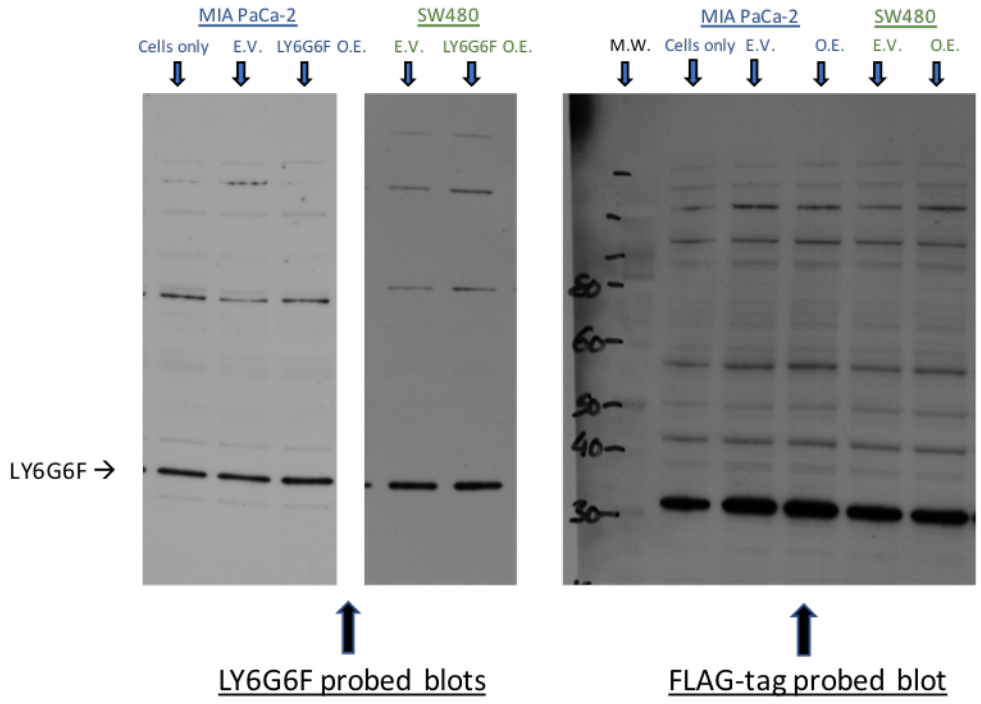

Figure 4.34 Representative Western blot probing for LY6G6F and FLAG-tag. Results are shown for MIA PaCa-2 cells only, E.V. and LY6G6F O.E. on the first blot and SW480 E.V. and LY6G6F O.E. on the second blot, both probed for LY6G6F, with no apparent protein overexpression of LY6G6F observed. The same samples probed for FLAG-tag, which should only be detected at LY6G6F MW in the LY6G6F O.E. samples, gave an inconclusive result, as multiple bands are visible in all wells. (n=2)

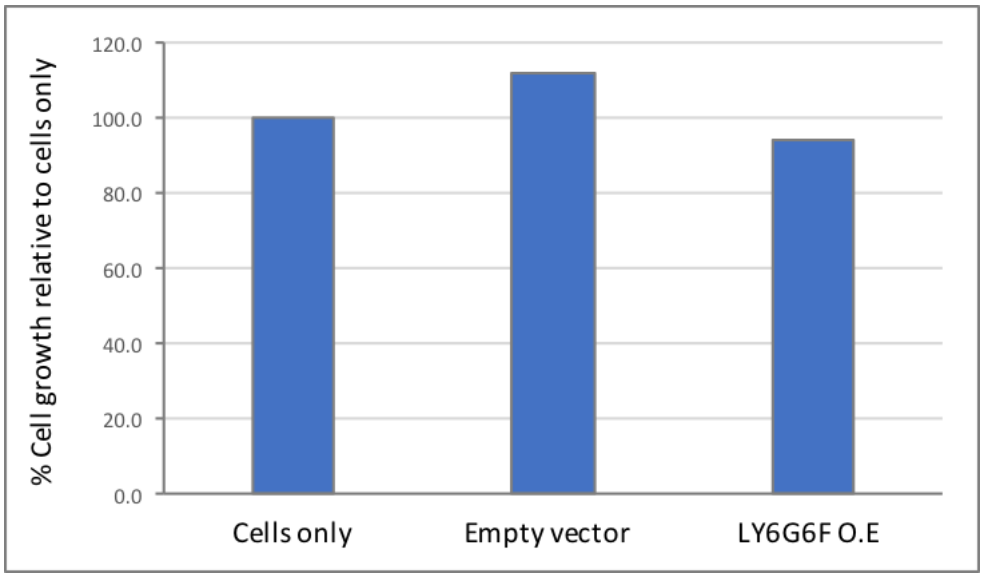

Figure 4.35 Proliferation assay on MIA PaCa-2 cells only and MIA PaCa-2 E.V. and LY6G6F O.E cells. Results graphed as % proliferation relative to cells only. (n=1)

4.11. Attempted Immunoprecipitation of LY6G6F

To further investigate the role of LY6G6F in the cancer cell phenotype, co-immunoprecipitation (Co-IP) of LY6G6F was attempted. Co-IP involves using a specific antibody to a target to isolate it from a complex mixture (e.g. cell lysate) along with any interacting proteins or ligands that may be bound to the target protein. Co-IP can identify complex partners, signalling molecules, structural proteins etc. that are bound to the protein of interest. An IP lysis buffer is used which will effectively solubilise cellular proteins but won't disrupt protein complexes. Two different methods were used in the attempt to immunoprecipitate LY6G6F from both MIA PaCa-2 and HCT116 cell lysates: cross-linked Co-IP and traditional Co-IP, which were carried out as described in Section 2.11.

Traditional Co-IP involves the use of Protein A/G (immunoglobulin binding proteins) agarose beads, to isolate the antibody-protein of interest complex. This method results in both the antibody and the protein of interest (and any interacting proteins) ending up in the elution. The contaminating antibody in the elution, results in antibody heavy chain (55kDa) and light chain (25kDa) fragments showing up in Western blot analysis, which can be a problem for target protein detection, if it has a similar MW. The cross-linked Co-IP method involves covalently immobilising the antibody by cross-linking to an agarose resin in a column. This allows target protein isolation and elution without antibody contamination, and the antibody column can also be reused.

Both methods however were unsuccessful in LY6G6F precipitation from MIA PaCa-2 and HCT116 lysates. Two independent LY6G6F antibodies were used (neither listed IP as a proven application). LY6G6F was never detected in the elutions by either method. **Figure 4.36** shows a representative blot of traditional Co-IP of MIA PaCa-2 cells. LY6G6F was detected in the control lysate, confirming the antibody can detect LY6G6F protein from cells lysed with a less stringent lysis buffer. However, in the LY6G6F elutions, no LY6G6F band was detected. As the LY6G6F antibody was produced in rabbit, a rabbit IgG control antibody was also used, to confirm that any proteins isolated were not from non-specific rabbit IgG interactions. Strong heavy and light chain antibody fragments were observed in the LY6G6F and Rabbit IgG elutions.

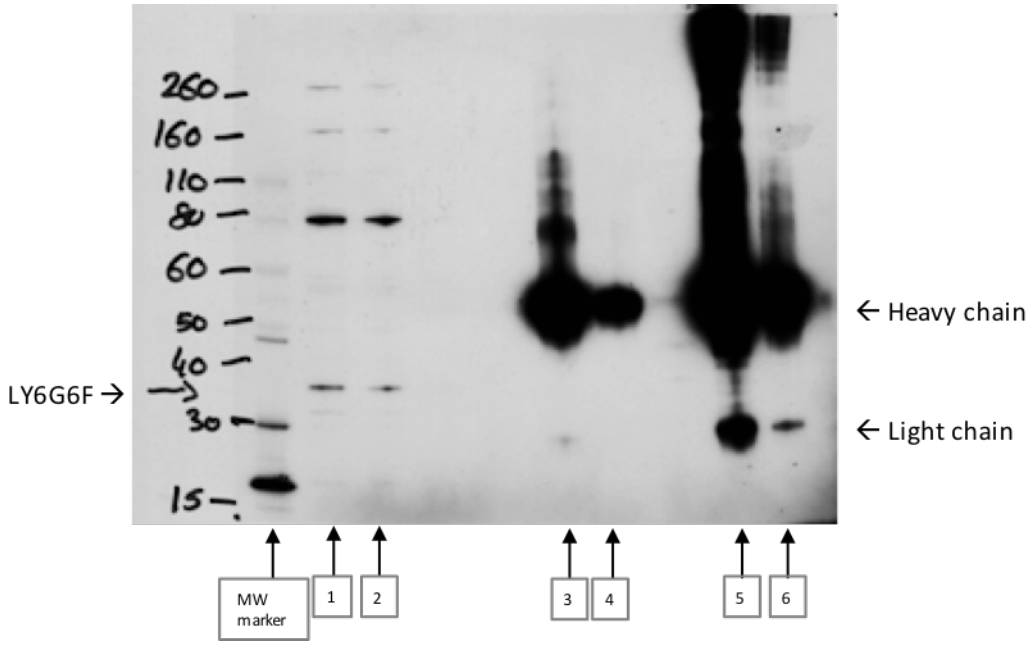

Figure 4.36 Western blot probing for LY6G6F in MIA PaCa-2 samples following traditional IP with Protein G agarose beads. Lanes **1** and **2** show MIA PaCa-2 IP lysate control, with LY6G6F detected in between 30 and 40kDa. Non-specific bands higher up, are also observed. Lanes **3** and **4** show the first and second elution from LY6G6F Co-IP, with no LY6G6F band detected. Lanes **5** and **6** show the first and second elution from the Rabbit IgG control. Heavy and light chain antibody fragments at 55kDa and 25kDa are visible in LY6G6F and Rabbit IgG elutions.

4.12. Summary

LY6G6F has been found to be significantly overexpressed in colon adenocarcinoma, PDAC and gastric adenocarcinoma compared to corresponding normal tissues. Weak expression was observed in the small number of breast cancer and oesophageal cancer specimens analysed. LY6G6F is significantly overexpressed in colon adenocarcinoma, irrespective of KRAS or BRAF mutational status vs. normal colon. LY6G6F is also significantly overexpressed in the benign spectrum that precedes cancer, with strong expression observed in hyperplasia, polyps and adenoma vs. normal colon. Weak LY6G6F expression was observed in the majority of the other CRC subtypes analysed: mucinous adenocarcinoma, carcinoid cancer and metastatic adenocarcinoma.

In PDAC, LY6G6F is highly expressed in the majority of tumours, with intense immunoreactivity observed compared to negative or weak immunoreactivity in normal pancreas. Strong LY6G6F immunoreactivity has also been observed in the stroma of PDAC specimens. The majority of normal gastric epithelium specimens analysed did show some weak and diffuse LY6G6F immunoreactivity. However the strong expression observed in 50% of the gastric adenocarcinomas analysed was found to be a significant overexpression compared to normal tissue expression.

High LY6G6F expression has been associated with poorer survival in both gastric cancer and PDAC. Data from the online KM plotter analysis showed that high LY6G6F gene expression is significantly associated with poorer survival in gastric cancer patients. Our data of LY6G6F protein expression in PDAC patients showed a trend towards high LY6G6F expression and poorer survival in this patient cohort, compared to patients with low LY6G6F expression, this did not reach significance however.

The analysis of LY6G6F expression in normal tissues showed a predominantly negative or weak expression pattern, with no apparent expression in highly proliferating cells of normal tissues. In a small subset of normal tissues (pancreas, bladder, kidney, larynx and salivary gland) some stronger LY6G6F immunoreactivity was observed in the stroma of the tissues.

LY6G6F was shown to be expressed in all CRC and PDAC cell lines analysed, with expression also detected in the membrane enriched fraction of these cells lines. Expression was also detected in a panel of breast cancer cell lines, with lower expression observed in the

Basal subtype. In the Immunohistochemical analysis, the localisation of LY6G6F was mainly observed as strong granular cytoplasmic immunoreactivity, with membrane-like immunoreactivity only observed in a small number of specimens. Immunofluorescence and Immunocytochemical analysis of MIA PaCa-2 cells, to further investigate the cellular localisation of LY6G6F, also showed mainly cytoplasmic localisation in these cells.

Transient protein knockdown of LY6G6F in the HCT116 and MIA PaCa-2 cell lines, followed by functional analysis, showed a significant decrease in proliferation in both cell lines. There was also a significant decrease in the 2D colony formation of MIA PaCa-2 cells, with a decrease also observed in the HCT116 cell lines, which failed to reach significance, due to high variability between biological replicates. LY6G6F protein knockdown was also found to decrease the migration and invasion of both cell lines. In the HCT116 cell line, a significant reduction was observed in both the migration and invasion of cells. In the MIA PaCa-2 cell line, a significant decrease was found in the invasion of cells, and a trend towards a decrease in migration. Subsequently, the potential mechanism of action of these observed phenotypic effects, was determined to be due to a decrease in FAK activation and an increase in apoptotic cell death in these cells following LY6G6F knockdown. This indicates a potential role for LY6G6F in FAK activation and apoptosis regulation.

Analysis of LY6G6F mRNA expression levels in these cell lines was not carried out until after functional analysis had been started, and unexpectedly showed that LY6G6F appears to have quite low mRNA abundance levels in these cells. The analysis indicates LY6G6F mRNA is present at low levels, but the protein knockdown observed by Western blot analysis, indicates that the LY6G6F siRNAs are sufficiently targeting LY6G6F mRNA for destruction, with the effect this has on HCT116 and MIA PaCa-2 cells shown in the functional analysis.

Attempts to determine the effect LY6G6F protein overexpression has on the functional phenotype of SW480 and MIA PaCa-2 cells, by transfection with a LY6G6F overexpression vector, could not be completed. High overexpression of LY6G6F mRNA was confirmed in these cells by qRT-PCR analysis, however protein overexpression was not observed. Unfortunately, time did not allow for optimisation, therefore functional analysis could not be carried out. Attempts at further investigation of the functional role of LY6G6F in the cancer cell phenotype by Co-IP, to try and identify protein-protein interactions involving LY6G6F,

also proved unsuccessful. LY6G6F was not successfully immunoprecipitated, which may have been due to the commercial antibodies used, with none listing IP as a proven application.

Chapter 5. IL1RAPL1

5.1. IL1RAPL1

IL-1 receptor accessory protein-like 1 (IL1RAPL1) was first identified as a novel member of the IL-1R family, in a search of DNA sequence databases for genes involved in mental retardation and named for its homology to IL-1 receptor accessory protein (IL1RAP). IL1RAPL1 is located on chromosome Xp and encodes a protein of 696 amino acids and has structural and sequence homology with other molecules of the IL-1R family, except for an unusually long intracytoplasmic portion. A 150 amino acid long C-terminal extension specific to IL1RAPL1 was found to have no significant homology with any protein of known function. IL1RAPL1 was originally found to not bind any of the IL-1 family cytokines and did not show IL-1R like signalling capacity. (Chelly *et al.*, 1999; Born *et al.*, 2000; Bahi *et al.*, 2003)

IL1RAPL1 is abundantly expressed in the brain, in particular in the structures of the hippocampal memory system, leading to a hypothesis for a potential role in brain development and/or physiological processes underlying memory and learning. Mutations in IL1RAPL1 were found to be associated with X-linked intellectual disability, autism and schizophrenia. (Piton *et al.*, 2008) Studies in an artificial cell transfection system showed that alone IL1RAPL1 is unable to activate pathways classically involved in IL-1 signalling, such as, NF-κB, or the MAP kinases ERK and p38, but was able to activate JNK. (Khan *et al.*, 2004) Further studies of the activation of JNK by IL1RAPL1 suggest it is independent of the TIR domain, as truncation mutants missing part of or even the entire TIR domain were found to be able to activate JNK to the same extent as the full-length receptor. IL1RAPL1 may be able to activate JNK by recruiting other molecules through its extracellular domain. IL1RAPL1 was shown to be present in dendritic spine, where it interacts with PSD-95, a major scaffold protein of excitatory post-synaptic density. IL1RAPL1 is reported to regulate the synaptic localisation of PSD-95 by controlling JNK activity and PSD-95 phosphorylation. Despite previous reports suggesting IL1RAPL1 is not capable of binding IL-1, it has subsequently been shown that the activation of the JNK pathway in neurons by IL-1 is mediated by IL1RAPL1. (Pavlowsky *et al.*, 2010; Boraschi and Tagliabue, 2013)

The 150 amino acid C-terminal extension of IL1RAPL1 was later found to interact with the neuronal calcium sensor 1 (NCS-1) protein (which is upregulated in schizophrenic and bipolar patients). Via the NCS-1 interaction, IL1RAPL1 plays a role in the down-regulation

of voltage-dependent calcium channels activity, in calcium-dependent exocytosis and nerve growth factor (NGF)-induced neurite outgrowth. IL1RAPL1 was shown to be an important regulator of synapse formation and stabilisation in cortical neurons. Therefore IL1RAPL1 has an important role in cognitive functions. (Khan *et al.*, 2004; Piton *et al.*, 2008)

IL1RAPL1 has been reported as being a common fragile site (CFS) gene contained within the FRAXC CFS region. Common fragile sites (CFSs) are large regions of profound genomic instability found in all individuals. They are biologically significant due to their role in a number of genomic alterations that are frequently found in many different types of cancer. IL1RAPL1 is abundantly expressed in normal brain but was found to be dramatically underexpressed in every brain tumour cell line and xenograft, derived from an intracranial model of glioblastoma multiforme (GBM), examined in one study. (Smith *et al.*, 2006; McAvoy *et al.*, 2007) However another study that classified GBM into different subtypes, linked IL1RAPL1 expression to the proneural subtype. (Cruceru *et al.*, 2013) In summary, IL1RAPL1 has mainly been linked with cognitive impairments due to mutations in the gene. It has been reported as both downregulated in brain tumours and associated with a particular genetic subset, the proneural subtype. IL1RAPL1 expression in other types of cancer has not been widely reported on.

5.2. Preliminary Analysis of IL1RAPL1 Expression in PDAC, Oesophageal Cancer and Breast Cancer

IL1RAPL1 was found to be overexpressed in a small cohort of colon adenocarcinomas vs. normal colon, as described in Section 3.2.2. In addition to investigating the expression of IL1RAPL1 further in CRC, a preliminary screen of several other cancers was also carried out, to determine if IL1RAPL1 is differentially expressed in any of those. The results of this preliminary screen are described below.

5.2.1. Immunohistochemical Analysis

As described already in Section 4.2.1, we had access to a limited number of tissue sections from a variety of different cancers, as well as normal tissue sections from those organs, enabling a screen for IL1RAPL1 expression across these cancer types by IHC analysis. IL1RAPL1 expression was examined in breast cancer (n=4), oesophageal cancer (n=1) and PDAC (n=7). **Figure 5.1** shows some representative photomicrographs of the results obtained. IL1RAPL1 showed negative immunoreactivity in normal oesophagus (n=1) but was strongly expressed in a malignant oesophagus tissue section. Some weak IL1RAPL1 positive expression was observed in the ducts of normal breast (n=3), with stronger expression observed in one of the invasive breast cancer specimens analysed, but the majority of breast cancer sections did not show stronger expression vs. normal breast. Normal pancreas (n=2) displayed negative to weak diffuse immunoreactivity in some areas, with the majority of PDAC sections analysed showing negative-weak IL1RAPL1 expression. Therefore, increased expression of IL1RAPL1 does not appear to be present in breast cancer or PDAC. However, the strong expression in oesophageal cancer compared to negative expression in normal oesophagus, suggests further investigation of IL1RAPL1 expression in this cancer types should be carried out.

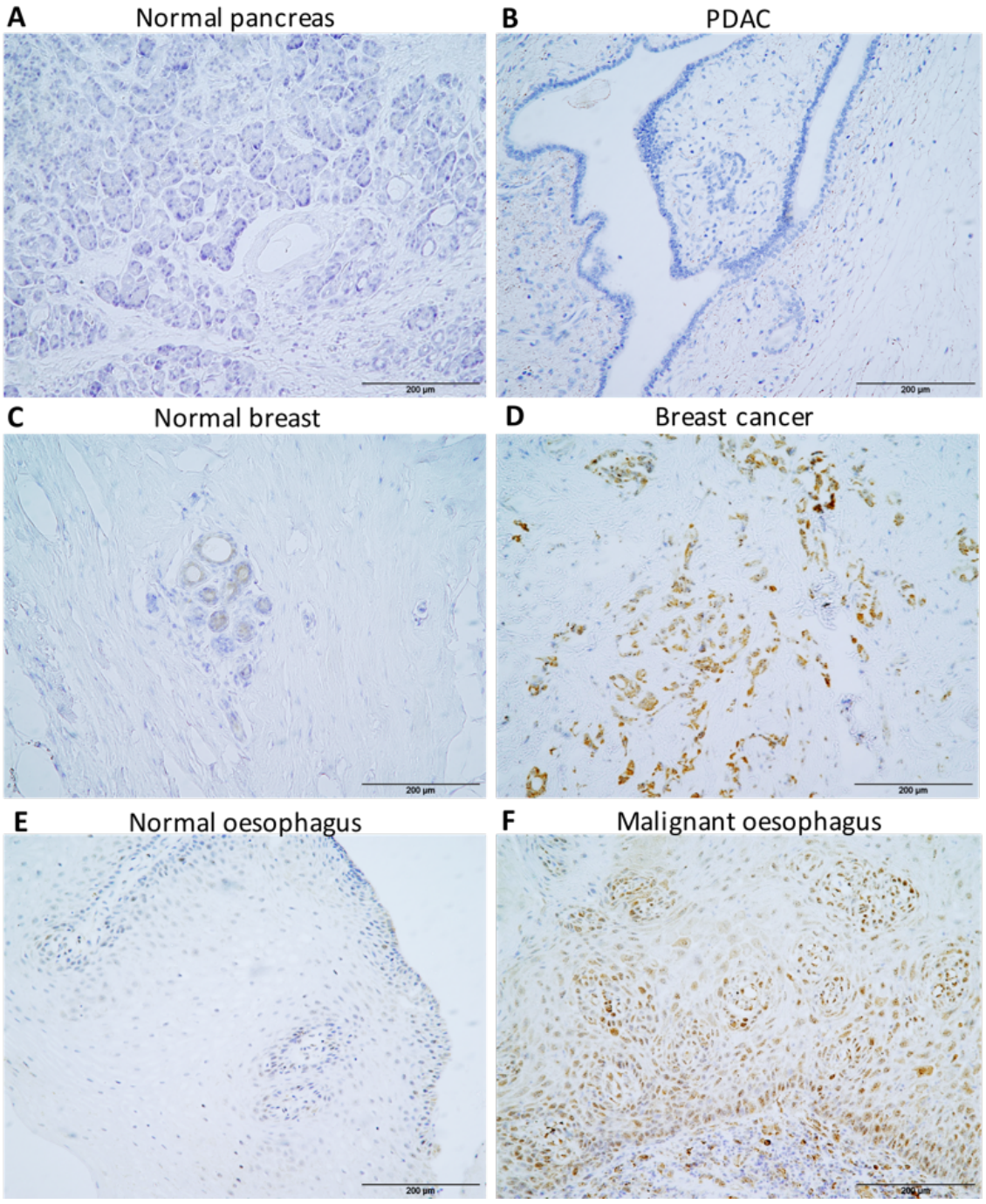

Figure 5.1 IHC analysis of IL1RAPL1 expression in normal and cancer tissues. Representative images showing: (**A**) Normal pancreas with negative IL1RAPL1 immunoreactivity. (**B**) PDAC with negative immunoreactivity. (**C**) Normal breast with weak immunoreactivity in ducts. (**D**) Breast cancer with strong cytoplasmic immunoreactivity. (**E**) Normal oesophagus with negligible IL1RAPL1 immunoreactivity. (**F**) Malignant oesophagus with strong immunoreactivity. Original magnification 200x. The scale bars represent 200µm.

5.2.2. IL1RAPL1 Expression in PDAC and Breast Cancer Cell Line Panels

IL1RAPL1 expression in both the whole cell and membrane enriched fraction of colon cancer cell lines has already been confirmed, see Section 3.2.2.1. The expression of IL1RAPL1 in a panel of PDAC cell lines and breast cancer cell lines was also investigated by Western blot analysis, refer to Table 4.1 and Table 4.2 for information on the source and mutational status of these cell lines. **Figure 5.2** shows the results of the Western blot analysis of the breast cancer cell line panel. IL1RAPL1 is expressed in the whole cell *and* membrane enriched fraction of all cell lines analysed, with no apparent differential expression according to subtype.

Figure 5.3 shows the results of the Western blot analysis for some of the PDAC cell line panel and also includes conditioned medium (CM) samples from MIA PaCa-2 and BXPC-3 cells on the end of each blot. The CM was prepared as described in Section 2.3.3, and contains proteins that are secreted by the cell lines. IL1RAPL1 is observed in the whole cell *and* membrane enriched fraction of all PDAC cell lines analysed at the expected MW of ~69kDa, with no apparent differential expression. A second lower band (in between the 50 and 60kDa MW marker) is also observed in the whole cell lysate of all cell lines, and corresponds to the single band observed in the CM samples. This indicates a secreted form of IL1RAPL1 is produced by these cells.

The original Western blot analysis of the colon cancer cell line panel did not reveal a second lower band, however repeat analysis, shown in **Figure 5.4**, detected the lower band in three of the cell lines, SW480, SW620 and CaCo-2. Therefore, the lower band identified in the Western blot analysis could be a soluble form of IL1RAPL1.

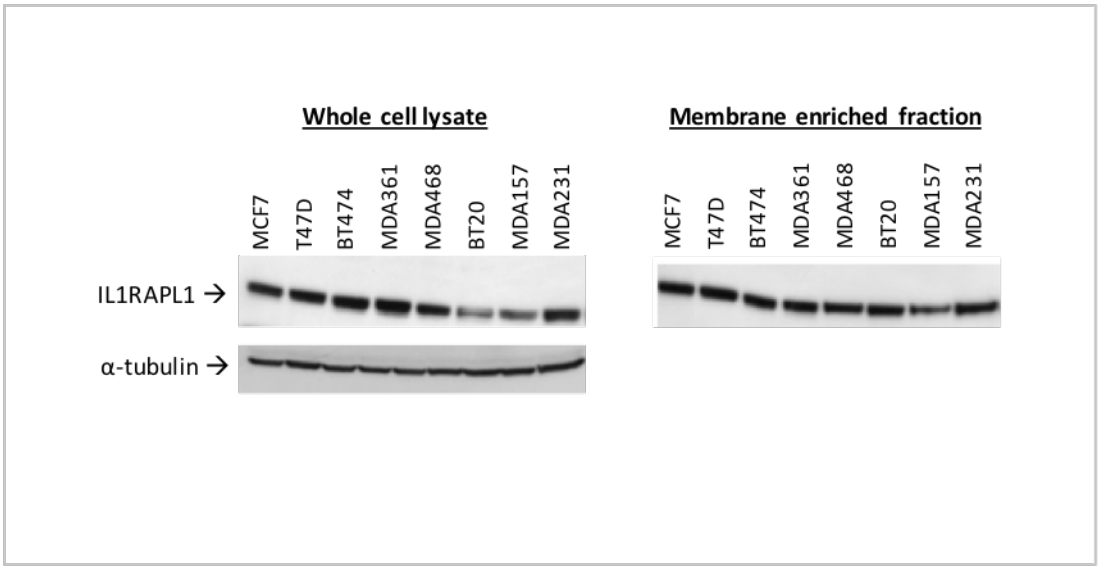

Figure 5.2 Western blot analysis showing IL1RAPL1 expression in the whole cell and membrane enriched fraction of a panel of breast cancer cell lines. α-tubulin confirmed equal loading of total proteins in the whole cell lysate. (n=1)

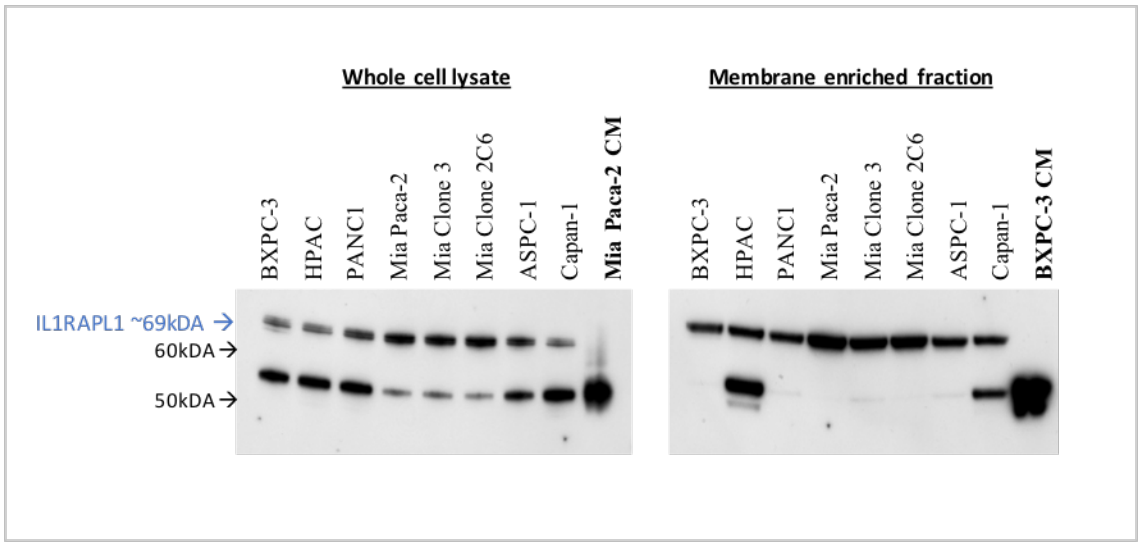

Figure 5.3 Western blot analysis showing IL1RAPL1 expression in the whole cell and membrane enriched fraction of a panel of PDAC cell lines and CM from MIA PaCa-2 and BXPC-3 cells. IL1RAPL1 is detected at the predicted MW of ~69kDA. A lower band that is the only one present in CM samples, indicates a secreted form of IL1RAPL1 is expressed by these cell lines. α-tubulin confirmed equal loading of total proteins in the whole cell lysate (blot not shown). (n=1)

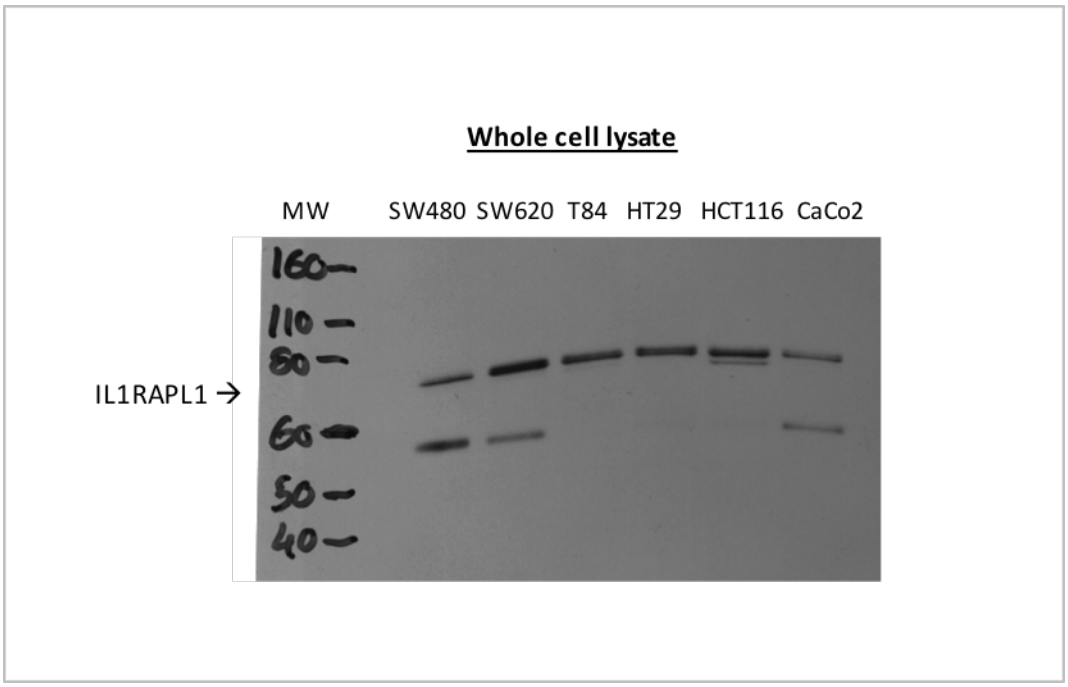

Figure 5.4 Representative Immunoblot showing IL1RAPL1 expression in the whole cell lysate of a panel of colon cancer cell lines. IL1RAPL1 bands are detected at the predicted MW of ~69kDA, in between the 60 and 80 kDa MW marker. A second lower band, in between 50 and 60kDA, is also detected in the SW480, SW620 and CaCo2 cell lines. This is potentially a secreted isoform of IL1RAPL1.

5.2.3. Summary of Analysis of IL1RAPL1 Expression across Various Cancer Types

In addition to CRC, further IHC validation studies indicated IL1RAPL1 is highly expressed in oesophageal cancer, compared to negligible expression in normal oesophagus. IL1RAPL1 does not appear to be highly expressed in PDAC tissues, however it was found to be expressed in all PDAC cell lines analysed. Western blot analysis revealed a potential soluble/secreted isoform of IL1RAPL1 expressed in all of the PDAC cell lines and some of the colon cancer cell lines. IL1RAPL1 is expressed in all breast cancer cell lines analysed, with some breast cancer tissues showing strong expression. However, with the majority of breast cancer sections showing weak immunoreactivity, it was decided to focus on CRC and oesophageal cancer in this study, (both gastrointestinal malignancies), for further investigation of IL1RAPL1 expression.

5.3. IL1RAPL1 Expression in Normal Colon and CRC

In order to investigate IL1RAPL1 expression in a larger patient cohort of CRC by Immunohistochemical analysis, a combination of commercial tissue microarray (TMA) and full-face tissue sections was used, as described in Section 4.3. The same commercial TMAs - colon disease spectrum TMA (CO2081, Biomax US) and the small CRC TMA (Accumax A713 VIII), that was used in the LY6G6F analysis, was used in the IL1RAPL1 analysis. The colon cancer disease spectrum TMA contains samples from normal colon, normal cancer adjacent (NAT) colon, chronic inflammation of mucosa, hyperplasia of glandular epithelium, polyps, adenoma, colon adenocarcinoma, mucinous adenocarcinoma, carcinoid tumours and metastatic adenocarcinoma, as outlined in Figure 4.4. The full-face tissue sections consisted of: 9 KRAS MT phenotype, 9 KRAS WT, 2 BRAF MT and 2 BRAF WT colon adenocarcinoma tissue sections. A number of normal colon sections were also available. Tissues were scored for IL1RAPL1 immunoreactivity as outlined in Table 4.4. The total number of each specimen analysed and their IL1RAPL1 immunoreactivity score from 0-3+ is outlined in **Table 5.1**. The majority of normal colon and NAT colon were negative for IL1RAPL1 expression. Combining these two groups, 66.7% (28/42) of normal colon were negative for IL1RAPL1 immunoreactivity, 28.6% (12/42) scored as 1+ and just 4.7% (2/42) scored as 3+. The scores for the whole spectrum were grouped into those specimens with negative or low levels of IL1RAPL1 expression (0-1+) and those showing high IL1RAPL1 expression (2-3+) for analysis. The expression levels observed in the benign and cancer spectrum were compared to the expression in normal colon (including NAT colon) by Chi-square test, to determine whether there is any significant association between IL1RAPL1 expression in any of the specimens. These results are shown in **Table 5.2**.

Specimen:	No. of cases	IL1RAPL1 Score			
		0	1+	2+	3+
Normal colon	**20**	12	6	-	2
NAT colon	**22**	16	6	-	-
Chronic Inflammation	**10**	8	2	-	-
Hyperplasia	**7**	3	4	-	-
Polyps	**6**	3	3	-	-
Adenoma	**5**	2	3	-	-
Adenocarcinoma	**51**	2	15	18	16
- KRAS MT	**9**	-	3	3	3
- KRAS WT	**9**	-	1	5	3
- BRAF MT	**2**	-	-	-	2
- BRAF WT	**2**	-	-	-	2
Mucinous adenocarcinoma	**15**	2	6	5	2
Carcinoid	**2**	-	-	-	2
Metastatic adenocarcinoma	**19**	-	10	8	1

Table 5.1 IL1RAPL1 expression by IHC score in the colon disease spectrum.

		IL1RAPL1 expression		
Specimen:	**No. of cases**	**Low (0-1+)**	**High (2-3+)**	**p-value**
Normal colon + NAT colon	42	40 (95.2%)	2 (4.8%)	
Chronic Inflammation	10	10 (100%)	0	NS
Hyperplasia	7	7 (100%)	0	NS
Polyps	6	6 (100%)	0	NS
Adenoma	5	5 (100%)	0	NS
Adenocarcinoma	51	17 (33.3%)	34 (66.7%)	<0.0001
- KRAS MT	9	3 (33.3%)	6 (66.7%)	
- KRAS WT	9	1 (11.1%)	8 (88.9%)	
- BRAF MT	2	0	2 (100%)	
- BRAF WT	2	0	2 (100%)	
Mucinous adenocarcinoma	15	8 (53.3%)	7 (46.7%)	0.0001
Carcinoid	2	0	2 (100%)	<0.0001
Metastatic adenocarcinoma	19	10 (52.6%)	9 (47.2%)	<0.0001

Table 5.2 IL1RAPL1 expression in the colon disease spectrum. The number of each specimen that scored as IL1RAPL1 low and high expressing is listed. The association between expression levels observed in normal colon specimens and all of the other cases both benign and cancerous was estimated for significance by Chi-square test. P-values are noted for those with significant correlations. NS = not significant.

5.3.1. IL1RAPL1 Expression in Normal Colon vs. Benign Disease

The majority of normal colon (including NAT colon) was negative for IL1RAPL1 immunoreactivity (66.7%), and where IL1RAPL1 expression was present it showed mainly weak and diffuse immunoreactivity (28.6%). Only 2 normal colon specimens (4.6%) showed some strong IL1RAPL1 immunoreactivity in areas. The benign spectrum includes chronic inflammation of mucosa, polyps, hyperplasia of glandular epithelium and adenoma. All specimens from the benign spectrum showed negative or weak IL1RAPL1 immunoreactivity. The majority of sample tissues representing chronic inflammation of mucosa (80%) were negative for IL1RAPL1 immunoreactivity, with the remainder (20%) showing weak expression. Hyperplasia of glandular epithelium was negative for IL1RAPL1 expression in 42.9% of specimens, with 57.1% showing weak immunoreactivity. The polyp specimens had weak IL1RAPL1 immunoreactivity in 50% of cases, with negative expression in the remainder. Adenoma specimens were negative for IL1RAPL1 in 40% of cases, with the rest showing weak expression. Representative photomicrographs of IL1RAPL1 expression in some of the benign specimens are shown in **Figure 5.5**.

5.3.2. IL1RAPL1 Expression in Normal Colon vs. Colon Cancer Spectrum

IL1RAPL1 was found to be significantly overexpressed in all of the cancer specimens analysed, as shown in **Table 5.2**. 96.1% of adenocarcinomas analysed express IL1RAPL1, with 66.7% showing high IL1RAPL1 expression, a significant upregulation compared to normal colon (p-value <0.0001). Within colon adenocarcinoma, IL1RAPL1 expression does not appear to correlate with KRAS or BRAF mutational status, with 66.7% of KRAS MT and 88.9% of KRAS WT specimens showing strong IL1RAPL1 immunoreactivity, and 100% of both BRAF MT and BRAF WT showing strong expression. In the mucinous adenocarcinoma specimens, 86.7% express IL1RAPL1, 46.7% highly, which is a significant overexpression compared to normal colon (p-value 0.0001). The number of carcinoid tumour specimens analysed was quite low (n=2), however 100% of these showed strong IL1RAPL1 immunoreactivity, which was deemed significant by Chi-square test compared to normal colon (p-value <0.0001). 100% of metastatic adenocarcinoma express IL1RAPL1, with 47.2% showing high expression, which was deemed significant compared to normal colon (p-value <0.0001).

IL1RAPL1 has been observed as having mainly cytoplasmic immunoreactivity in the majority of cancer specimens, with some membranous immunoreactivity possibly observed in a small number of specimens. It was also observed in some cancer specimens that IL1RAPL1 expression may potentially be associated with immune cells in CRC. The observation by a pathologist examining one section, was that inflammatory cells that are responding to the tumour stained strongly for IL1RAPL1 (Refer to image B in **Figure 5.6**). This potential immune cell cohort showing strong IL1RAPL1 immunoreactivity was subsequently observed in other CRC sections and single immune cells in some normal colon specimens were also observed to show strong IL1RAPL1 immunoreactivity. As this cell type hasn't been confirmed to be a particular immune cell, for the moment they are hypothesised "immune" cells. **Figure 5.6** shows representative photomicrographs of the pattern of IL1RAPL1 immunoreactivity observed in CRC tumours and also in the "immune" cells of some specimens.

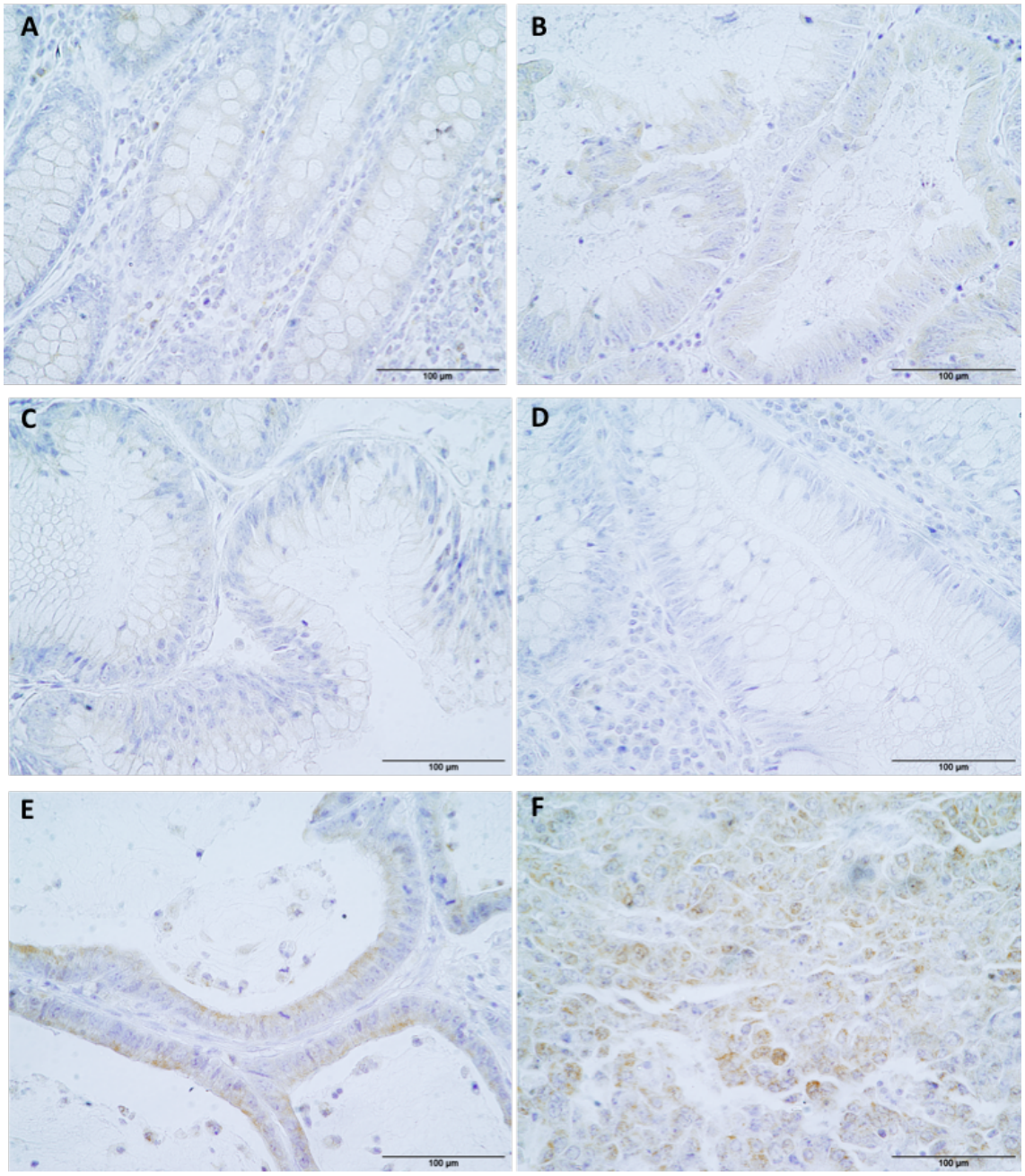

Figure 5.5 IHC analysis of IL1RAPL1 expression in diseased and malignant colon. Representative images showing: (**A**) Chronic inflammation of colon mucosa with negative IL1RAPL1 immunoreactivity. (**B**) Inflammatory polyp with negligible immunoreactivity. (**C**) Hyperplasia of glandular epithelium with negative immunoreactivity. (**D**) Adenoma with negative immunoreactivity. (**E**) Mucinous colon adenocarcinoma with weak-moderate IL1RAPL1 immunoreactivity. (**F**) Carcinoid tumour with strong cytoplasmic IL1RAPL1 immunoreactivity. Original magnification 400x. The scale bars represent 100µm.

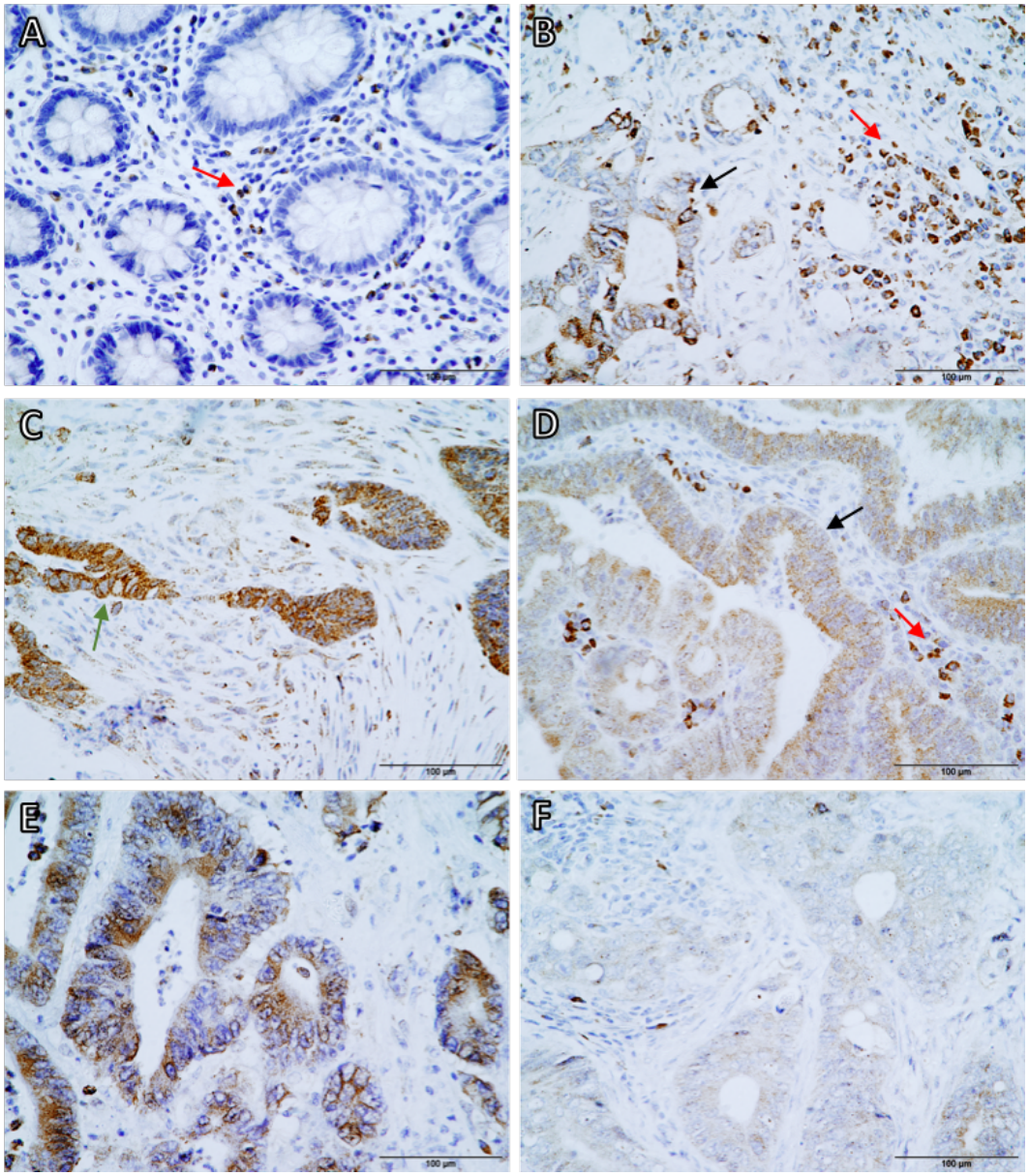

Figure 5.6 IHC analysis of IL1RAPL1 expression in normal and malignant colon. Representative images showing: (**A**) Normal colon with IL1RAPL1 immunoreactivity in "immune" cells (red arrow). (**B**) Moderately differentiated colon adenocarcinoma with strong cytoplasmic and membrane-like immunoreactivity in the tumour (black arrow) and also in "immune" cells (red arrow) responding to the tumour. (**C**) Colon adenocarcinoma (BRAF WT) with strong cytoplasmic and membrane-like IL1RAPL1 immunoreactivity (green arrow). (**D**) Colon adenocarcinoma (BRAF MT) with moderate-strong cytoplasmic immunoreactivity in the tumour (black arrow) and strong immunoreactivity in "immune" cells (red arrow). (**E**) Moderately differentiated colon adenocarcinoma (KRAS MT) with strong cytoplasmic immunoreactivity. (**F**) Poorly differentiated colon adenocarcinoma (KRAS WT) with weak cytoplasmic immunoreactivity. Original magnification 400x. The scale bars represent 100μm.

5.3.3. Association between IL1RAPL1 Expression and CRC Tumour Grade

In order to determine if IL1RAPL1 expression correlates with the histopathological grade of CRC, the score was analysed in the specimens that this information was available for. The grade diagnosis was known for 63 of the cancer specimens analysed – 30 adenocarcinomas, 15 mucinous adenocarcinomas and 18 metastatic adenocarcinomas. Combining the score for all of these and grouping into Grades 1-3, showed that the majority (55.6%) of tumours analysed were Grade 2, followed by Grade 3 at 31.7% and Grade 1 representing 12.7% of tumours. **Table 5.3** shows the IL1RAPL1 expression pattern for the three grades across the combined colon cancer types. There is a small increase in the number of Grade 3 tumours strongly expressing IL1RAPL1 compared to Grade 1 and 2, with 65% of Grade 3 tumours strongly expressing IL1RAPL1, 57.1% of Grade 1 and 55.5% of Grade 2 strongly expressing IL1RAPL1. This was not deemed a significant correlation however.

Table 5.4 shows the result of IL1RAPL1 expression in the three grades for each cancer type separately. IL1RAPL1 expression does not significantly correlate with tumour grade in any of the cancer types examined – adenocarcinoma, mucinous adenocarcinoma or metastatic adenocarcinoma, as determined by Chi-square test. In adenocarcinoma 88.9% of Grade 3 tumours strongly express IL1RAPL1, with 58.8% of Grade 2 and 75% of Grade 1 tumours strongly expressing IL1RAPL1. In mucinous adenocarcinoma Grade 2 tumours most highly express IL1RAPL1 (55.6%), with 33.3% of both Grade 1 and Grade 2 tumours strongly expressing IL1RAPL1. IL1RAPL1 expression is split 50:50 between low and high expression in Grade 2 and Grade 3 tumours in metastatic adenocarcinoma.

		IL1RAPL1 expression	
Grade	**No of cases**	**Weak (0-1+)**	**Strong (2-3+)**
1	7	3 (42.9%)	4 (57.1%)
2	36	16 (44.4%)	20 (55.5%)
3	20	7 (35%)	13 (65%)

Table 5.3 Association between IL1RAPL1 expression and CRC tumour grade. (Results for adenocarcinoma, mucinous and metastatic adenocarcinoma combined)

Adenocarcinoma (n=30)			
Grade	**No of cases**	**Weak (0-1+)**	**Strong (2-3+)**
1	4	1 (25%)	3 (75%)
2	17	7 (41.2%)	10 (58.8%)
3	9	1 (11.1%)	8 (88.9%)
Mucinous Adenocarcinoma (n=15)			
Grade	**No of cases**	**Weak (0-1+)**	**Strong (2-3+)**
1	3	2 (66.7%)	1 (33.3%)
2	9	4 (44.4%)	5 (55.6%)
3	3	2 (66.7%)	1 (33.3%)
Metastatic Adenocarcinoma (n=18)			
Grade	**No of cases**	**Weak (0-1+)**	**Strong (2-3+)**
1	0	-	-
2	10	5 (50%)	5 (50%)
3	8	4 (50%)	4 (50%)

Table 5.4 Association between IL1RAPL1 expression and tumour grade in each CRC subtype.

5.3.4. Summary of IL1RAPL1 Expression in Colon Disease Spectrum

- IL1RAPL1 expression is absent in the majority of normal colon tissues analysed and shows mainly weak expression in the remainder of specimens.
- IL1RAPL1 is not upregulated in the benign spectrum of colon disease – chronic inflammation of mucosa, hyperplasia, polyps and adenoma all showed negative or weak IL1RAPL1 expression.
- IL1RAPL1 is significantly overexpressed in the colon cancer spectrum.
    - Colon adenocarcinoma vs. normal colon (p-value <0.0001)
    - Mucinous adenocarcinoma vs. normal colon (p-value 0.0001)
    - Carcinoid tumours vs. normal colon (p-value <0.0001)
    - Metastatic adenocarcinoma vs. normal colon (p-value <0.0001)

5.4. IL1RAPL1 Expression in Normal Oesophagus and Oesophageal Cancer

The preliminary analysis in Section 5.2 showed high IL1RAPL1 expression in oesophageal cancer compared to normal oesophagus, in a very small sample size (n=1). Therefore, to assess IL1RAPL1 expression in a larger cohort, a commercially sourced oesophageal cancer test TMA (T022a, US Biomax Inc) was obtained for analysis. This small TMA contains 12 cases – 2 normal oesophagus, 1 carcinoma in situ, 4 squamous cell carcinoma, 2 adenocarcinoma, 1 small cell undifferentiated carcinoma, 1 carcinoma sarcomatodes, and 1 carcinosarcoma. Three other normal oesophagus sections were available to us for analysis, giving a combined number of 5 normal oesophagus specimens. The two main subtypes of oesophageal cancer are squamous cell carcinoma, which arises from the epithelial cell lining of the oesophagus and adenocarcinoma, which arises from glandular cells in the lower part of the oesophagus.

Table 5.5 shows the IL1RAPL1 IHC immunoreactivity score from 0-3+ in this cohort. Normal oesophagus does show some weak IL1RAPL1 expression, with 60% (3/5) of cases showing some weak and diffuse immunoreactivity, with the remainder negative. There was only one specimen each of carcinoma in situ, small cell undifferentiated carcinoma, carcinoma sarcomatodes and carcinosarcoma, which all showed negative or weak IL1RAPL1 immunoreactivity. The two adenocarcinoma specimens both showed weak IL1RAPL1 immunoreactivity. IL1RAPL1 is distinctly strongly expressed in only one group, squamous cell carcinoma. **Table 5.6** shows the scores grouped into those specimens with negative or low levels of IL1RAPL1 expression (0-1+) and those showing high IL1RAPL1 expression (2-3+) for analysis. The results are grouped into all oesophageal cancers combined, and also squamous cell carcinoma by itself, as this is the only group that appears to show differential expression compared to normal oesophagus. Combining all cancer types shows no significant correlation between IL1RAPL1 expression in cancer vs. normal, with 40% of cancers highly expressing IL1RAPL1. However, 100% (4/4) of squamous cell carcinoma specimens highly express IL1RAPL1, compared to 100% of normal oesophagus specimens showing negative or weak expression. This was found to be a significant overexpression (p-value 0.0027), as determined by Chi-square test. IL1RAPL1 showed strong cytoplasmic and in some areas membrane-like immunoreactivity in squamous cell carcinoma. **Figure 5.7** shows representative photomicrographs of IL1RAPL1 immunoreactivity observed in normal oesophagus and oesophageal cancer.

		IL1RAPL1 Score			
Specimen:	**No. of cases**	**0**	**1+**	**2+**	**3+**
Normal Oesophagus	**5**	2	3	0	0
Carcinoma in situ	**1**		1		
Squamous cell carcinoma	**4**			3	1
Adenocarcinoma	**2**		2		
Small cell undifferentiated carcinoma	**1**	1			
Carcinoma sarcomatodes	**1**	1			
Carcinosarcoma	**1**		1		

Table 5.5 IL1RAPL1 expression by IHC score in normal oesophagus and cancer spectrum

		IL1RAPL1 expression	
Specimen:	**No of cases**	**Weak (0-1+)**	**Strong (2-3+)**
Normal Oesophagus	5	5 (100%)	0
Oesophagus carcinoma (all types)	10	6 (60%)	4 (40%)
Squamous cell carcinoma	4	0	4 (100%) **

Table 5.6 IL1RAPL1 expression in normal oesophagus and oesophageal cancer. The number of each specimen that scored as LY6G6F low and high expressing is listed. The association between expression levels observed in the whole cancer cohort and squamous cell carcinoma by itself was estimated for significance by Chi-square test. (** IL1RAPL1 is significantly overexpressed in squamous cell carcinoma vs. normal oesophagus; p-value 0.0027)

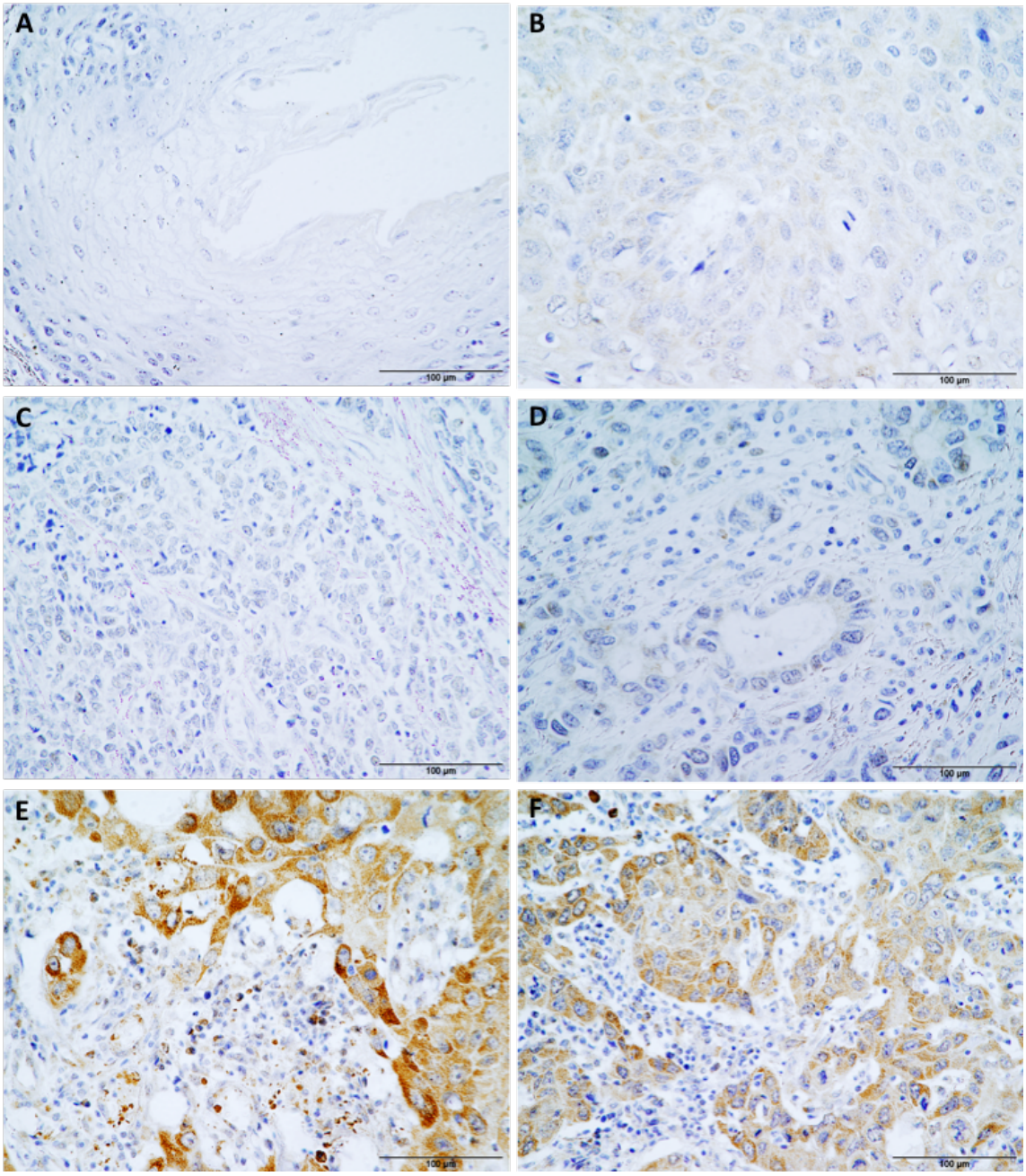

Figure 5.7 IHC analysis of IL1RAPL1 expression in normal and malignant oesophagus. Representative images showing: (**A**) Normal oesophagus with negative IL1RAPL1 immunoreactivity. (**B**) Carcinoma in situ with weak diffuse immunoreactivity. (**C**) Small cell undifferentiated oesophageal cancer with negative immunoreactivity. (**D**) Oesophagus adenocarcinoma with negative to weak immunoreactivity. (**E**) Squamous cell carcinoma with strong cytoplasmic and membrane-like IL1RAPL1 immunoreactivity. (**F**) Squamous cell carcinoma with strong cytoplasmic and membrane-like immunoreactivity. Original magnification 400x. The scale bars represent 100μm.

5.4.1. Summary of IL1RAPL1 Expression in Normal Oesophagus and Oesophageal Cancer

- IL1RAPL1 expression is absent or shows weak and diffuse immunoreactivity in the normal oesophagus specimens analysed.
- IL1RAPL1 is not strongly expressed in oesophageal carcinoma in situ, small cell undifferentiated carcinoma, carcinoma sarcomatodes, carcinosarcoma, or adenocarcinoma specimens, with all showing negative or weak expression.
- IL1RAPL1 is strongly expressed in all oesophageal squamous cell carcinoma specimens analysed and was found to be significantly overexpressed in this cancer type vs. normal oesophagus (p-value 0.0027).
- However, sample size was very small, and investigation of IL1RAPL1 expression in a larger cohort of normal oesophagus and the different oesophageal cancer subtypes is required, to determine if high IL1RAPL1 expression is associated specifically with the squamous cell carcinoma subtype in a larger patient cohort

5.5. IL1RAPL1 Expression in Normal Tissues

In order for a protein to be a potential candidate therapeutic target, it must have no or minimal expression in normal tissues, particularly in vital organs. The absence or minimal expression of target in the proliferating cells of normal tissues is also required, to minimise off target toxicities. IL1RAPL1 expression in normal tissues was examined in a number of normal tissue TMAs, as well as full-face tissue sections, if they were available by Immunohistochemical analysis. **Table 5.7** lists the tissues that had negative or weak IL1RAPL1 immunoreactivity. Some normal tissues did display some stronger IL1RAPL1 immunoreactivity in some specimens and these are listed in **Table 5.8**. The majority of normal colon were negative for IL1RAPL1 expression, however a small number (2/42) did show some stronger immunoreactivity. All of the normal duodenum and gastric epithelium specimens analysed showed IL1RAPL1 expression, with 1/4 duodenum specimens showing some strong immunoreactivity. Strong IL1RAPL1 immunoreactivity was observed in certain collections of individual cells in 3/5 gastric epithelium tissues. Cerebral cortex and bone marrow (only n=1) showed some strong IL1RAPL1 immunoreactivity in isolated cells. Salivary gland displayed weak-moderate cytoplasmic immunoreactivity. Representative images of IL1RAPL1 immunoreactivity in some of the normal tissues analysed are shown in **Figure 5.8**.

To investigate IL1RAPL1 expression in highly proliferating cells of normal tissues, serial tissue sections of a range of proliferative tissues, including colon, tonsil and gastric tissue, were stained for IL1RAPL1 and Ki67, a cellular marker strictly associated with proliferation. **Figure 5.9** shows representative images for the results of this analysis in normal colon, duodenum and gastric epithelium. In general, if IL1RAPL1 immunoreactivity is observed in normal colon it is not in the proliferating cells of colonic crypts. The normal duodenum tissue shown in **Figure 5.9** shows strong Ki67 immunoreactivity in the cells lining the crypts of the duodenum. Strong IL1RAPL1 immunoreactivity is observed in the luminal space of these crypts, therefore IL1RAPL1 could be expressed in the same cells. The gastric epithelium shows some weak IL1RAPL1 immunoreactivity, but it is more difficult to determine the same cellular location of Ki67 positive cells in this tissue. Overall, in normal colon IL1RAPL1 does not appear to be expressed in the proliferating cells. It is more difficult to determine the exact same cellular location in the other tissues. Further investigation is

required, such as a dual IHC set up, where a single section is stained for both IL1RAPL1 and Ki67, as this would enable a more accurate determination of the same cell localisation.

Normal tissues with negative or minimal IL1RAPL1 immunoreactivity				
Oesophagus (3/3)	Pancreas (2/2)	Kidney (2/2)	Liver (2/3)	Tonsil (7/10)
Breast (2/3)	Lung (0/3)	Thyroid (2/3)	Larynx (0/1)	Bladder (0/1)
Spleen (1/3)	Uterus (0/1)	Cervix (1/2)	Ovary (1/1)	Skin (0/1)
Testis (0/1)	Prostate (0/1)	Placenta (2/3)	Adrenal gland (1/1)	Parathyroid gland (1/1)
Thymus (0/1)	Cerebellum (0/1)	Muscle, skeletal (0/1)	Heart muscle (0/1)	Omentum (0/1)
Peripheral nerve (0/1)				

Table 5.7 Normal tissues that showed negative or weak IL1RAPL1 expression. The number of sections that stained out of the total number analysed is listed.

Normal tissues displaying weak to strong IL1RAPL1 immunoreactivity			
Tissue	**No. negative**	**No. weak**	**No. strong**
Colon	28/42 negative	12/42 weak diffuse	2/42 some strong granular positivity
Duodenum	-	3/4 weak diffuse	1/4 strong positivity
Gastric	-	2/5 weak diffuse	3/5 some strong positivity in certain cells
Salivary gland	-	1/2 weak diffuse	1/2 stronger cytoplasmic diffuse
Pituitary gland	-	-	1/1 strong granular diffuse
Cerebral cortex	-	-	1/1 isolated cells stained strongly
Bone marrow	-	-	1/1 strong stain in isolated cells

Table 5.8 Normal tissues that showed strong IL1RAPL1 expression in some specimens. The normal tissues that displayed strong IL1RAPL1 immunoreactivity in some specimens is listed, with the number of sections that positively stained out of the total number analysed indicated. The number for each specimen that showed negative or weak IL1RAPL1 immunoreactivity is also indicated.

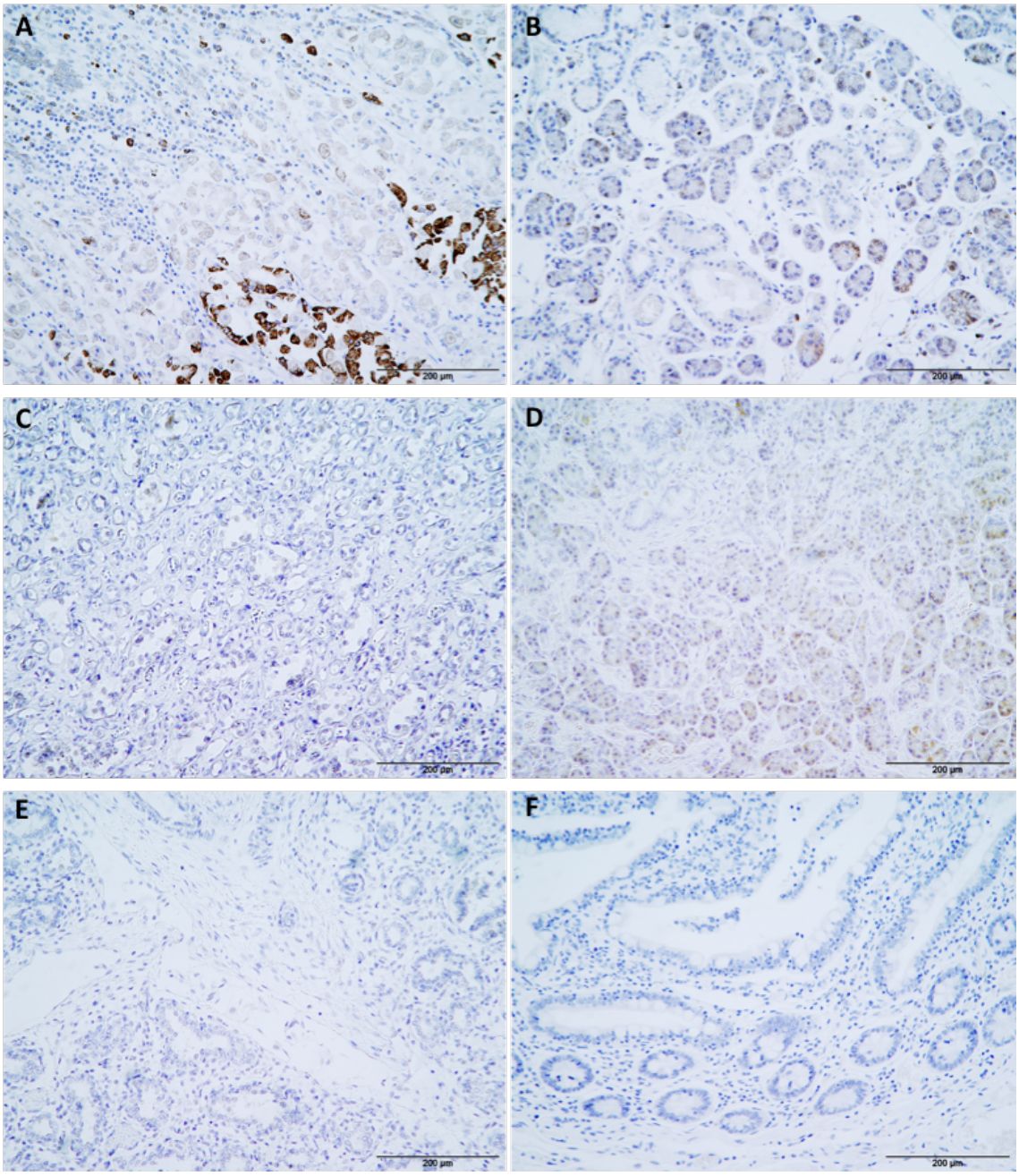

Figure 5.8 IHC analysis of IL1RAPL1 expression in normal tissues. Representative images showing: (**A**) Gastric epithelium with strong IL1RAPL1 immunoreactivity in certain cell populations. (**B**) Salivary gland with weak immunoreactivity. (**C**) Kidney with negative immunoreactivity. (**D**) Pancreas with weak diffuse immunoreactivity. (**E**) Lung with negative immunoreactivity. (**F**) Small intestine with negative immunoreactivity. Original magnification 200x. The scale bars represent 200µm.

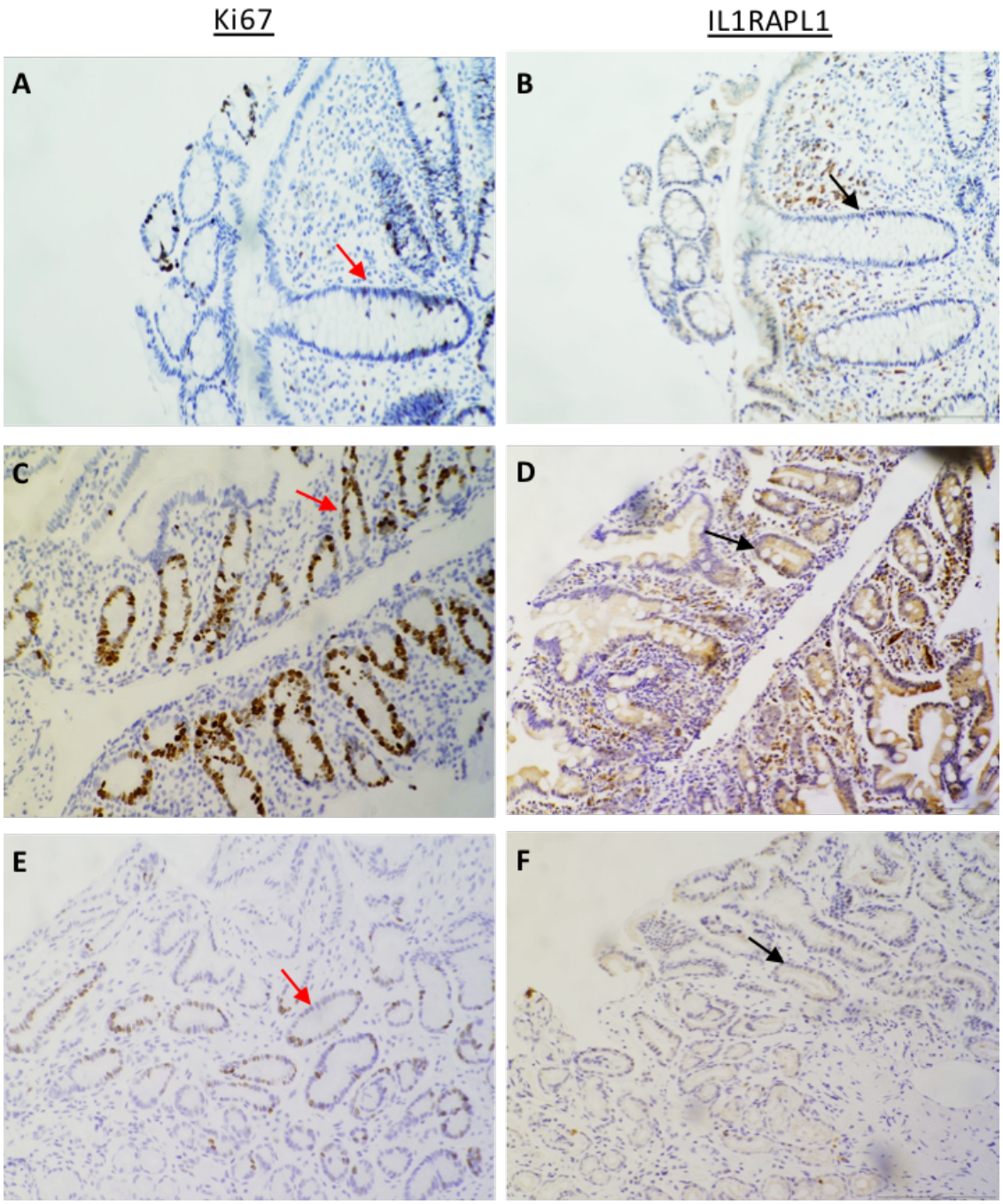

Figure 5.9 IHC analysis of IL1RAPL1 expression in proliferating cells of normal tissues. Representative images of colon, duodenum and gastric epithelium stained for Ki67 and IL1RAPL1, with red and black arrows indicating the approximate same location in the Ki67 and IL1RAPL1 stained serial sections. (**A-B**) Normal colon showing negligible IL1RAPL1 immunoreactivity in proliferating cells. (**C-D**) Normal duodenum showing strong Ki67 and IL1RAPL1 immunoreactivity, potentially in the same cells. (**E-F**) Normal gastric epithelium showing weak IL1RAPL1 immunoreactivity, which could potentially be in some proliferating cells. Original magnification 200x. The scale bars represent 200μm.

5.6. Imaging of IL1RAPL1 in Cancer Cell Lines

IL1RAPL1 protein expression was confirmed in colon cancer and PDAC cell lines by Western blot analysis, with expression in the membrane fractions suggesting an association with membrane localisation. To further investigate the localisation of IL1RAPL1 in some of these cancer cell lines, Immunocytochemical analysis staining for IL1RAPL1 in the HCT116 and MIA PaCa-2 cell lines was carried out as described in Section 2.7. Cells were fixed and permeabilised with either methanol alone or formalin followed by methanol. Immunofluorescent analysis staining for IL1RAPL1 was carried out in the HCT116 and SW480 cell lines (formalin and methanol fixed) as described in Section 2.8. Negative controls (secondary antibody only) were included in both analyses.

Figure 5.10 shows representative images of the Immunocytochemical analysis. Strong cytoplasmic IL1RAPL1 stain is observed in both the MIA PaCa-2 and HCT116 cells. The strong nuclear stain observed in some HCT116 cells appears to be non-specific stain due to the fixation procedure. **Figure 5.11** shows representative images of the Immunofluorescent analysis. Again, strong cytoplasmic stain is observed, with possibly some membranous staining in both the HCT116 and SW480 cell lines. Live cell immunofluorescence was attempted to try and confirm IL1RAPL1 localisation on the cell surface, however this was unsuccessful to date. Therefore, IL1RAPL1 was shown to be located in the cytoplasm, with no exclusive membrane localisation observed in these cells.

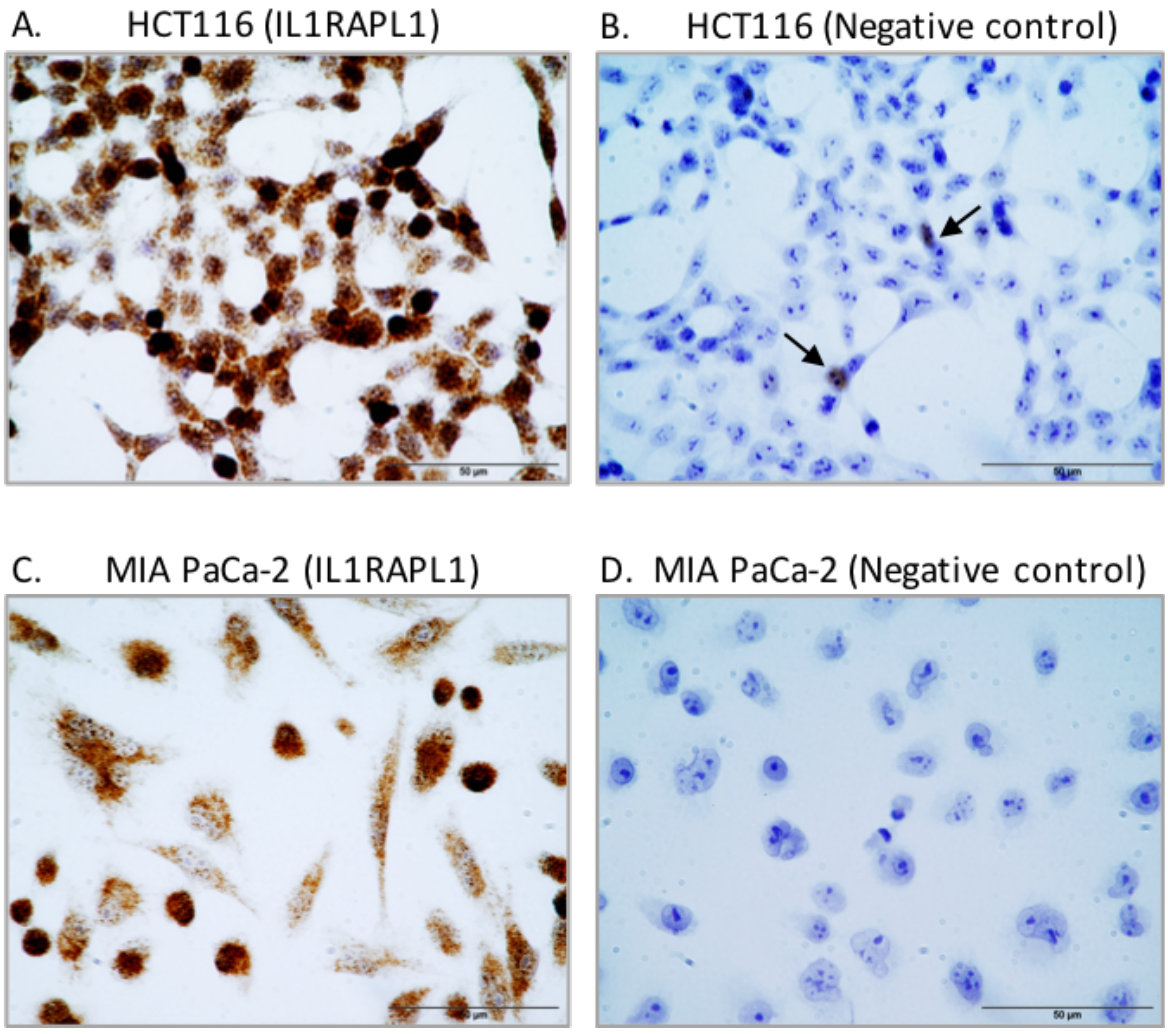

Figure 5.10 Immunocytochemical analysis of IL1RAPL1 expression in HCT116 and MIA PaCa-2 cells. Representative images show (**A**) HCT116 cells stained with IL1RAPL1 and (**B**) HCT116 cells negative control (no primary antibody). HCT116 cells were fixed with formalin and methanol. Some non-specific nuclear stain is observed in the negative control from this fixation method (black arrows). Therefore, discounting this nuclear stain, granular cytoplasmic IL1RAPL1 stain is observed in HCT116 cells. (**C-D**) MIA PaCa-2 cells fixed with methanol and stained for IL1RAPL1 and negative control. Cytoplasmic IL1RAPL1 immunoreactivity is observed. No immunoreactivity is observed in the negative control. Original magnification 600x. Scale bars represent 50μm.

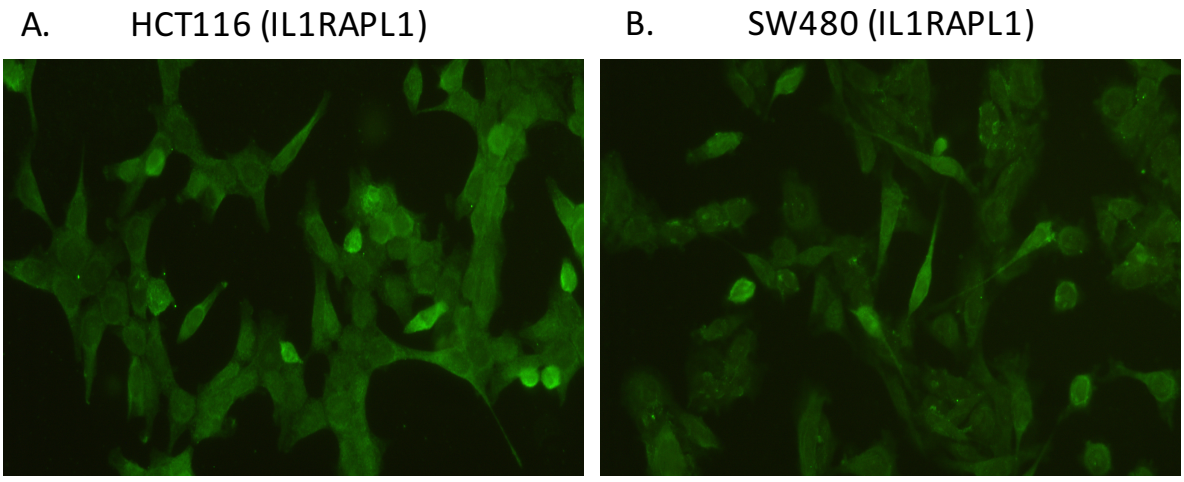

Figure 5.11 Immunofluorescent analysis of IL1RAPL1 expression in HCT116 and SW480 cells. Representative images show (**A**) HCT116 cells and (**B**) SW480 cells stained for IL1RAPL1. Negative controls (secondary antibody only) showed no immunofluorescence (images not shown). IL1RAPL1 is observed as having cytoplasmic and possibly some membranous localisation in these cells. (Formalin and methanol fixation of cells) Original magnification 400x.

5.7. Attempted Functional Analysis of IL1RAPL1 Knockdown by RNAi

IL1RAPL1 has been found to be significantly overexpressed in CRC tumours compared to normal colon by IHC analysis. Therefore, to investigate the functional role of IL1RAPL1 in the colon cancer cell phenotype, siRNA mediated protein knockdown of IL1RAPL1 was attempted in the SW480 and HCT116 colon cancer cell lines, to be followed by *in vitro* functional analysis of the effect on proliferation, 2D colony formation, migration and invasion of these cells. However, protein knockdown of IL1RAPL1 was never observed by Western blot analysis. Attempts were also made in the PDAC cell line MIA PaCa-2. Transfection optimisation was carried out as described in Section 2.4.1, with a number of optimisations carried out in the attempt to achieve IL1RAPL1 protein knockdown.

A total of six independent IL1RAPL1 siRNAs were used in this analysis, with optimisations involving increasing the siRNA concentration (a range from 10nM-100nM was tested), as well as assaying for protein knockdown at various time-points post transfection (48hrs, 72hrs and 93hrs). However, no obvious protein knockdown was observed in either the 69kDa MW protein or the identified soluble form (~58kDa) of IL1RAPL1, if it was present, in any of the cell lines examined by Western blot analysis. To determine if the siRNAs were sufficiently reducing IL1RAPL1 mRNA levels, qRT-PCR analysis was carried out on MIA PaCa-2 cells transfected with all six siRNAs and taken down 48hrs post transfection. The relative quantitation (RQ) of IL1RAPL1 mRNA in siRNA treated cells (IL1RAPL1 and Negative siRNA at 30nM concentration) compared to untreated cells is shown in **Figure 5.12**. This analysis was only carried out once, but shows that the IL1RAPL1 siRNAs are decreasing the mRNA levels, to varying degrees. The biggest reduction is observed with siRNA #3, however protein knockdown was still not achieved with the most effective siRNAs determined from the qRT-PCR analysis. **Figure 5.13** shows representative Western blots of MIA PaCa-2 cells assayed for protein knockdown 48, 72 and 93hrs post transfection, with no reduction in the amount of IL1RAPL1 protein observed. Therefore unfortunately, the effect of IL1RAPL1 protein knockdown on the functional phenotype of colon cancer could not be determined.

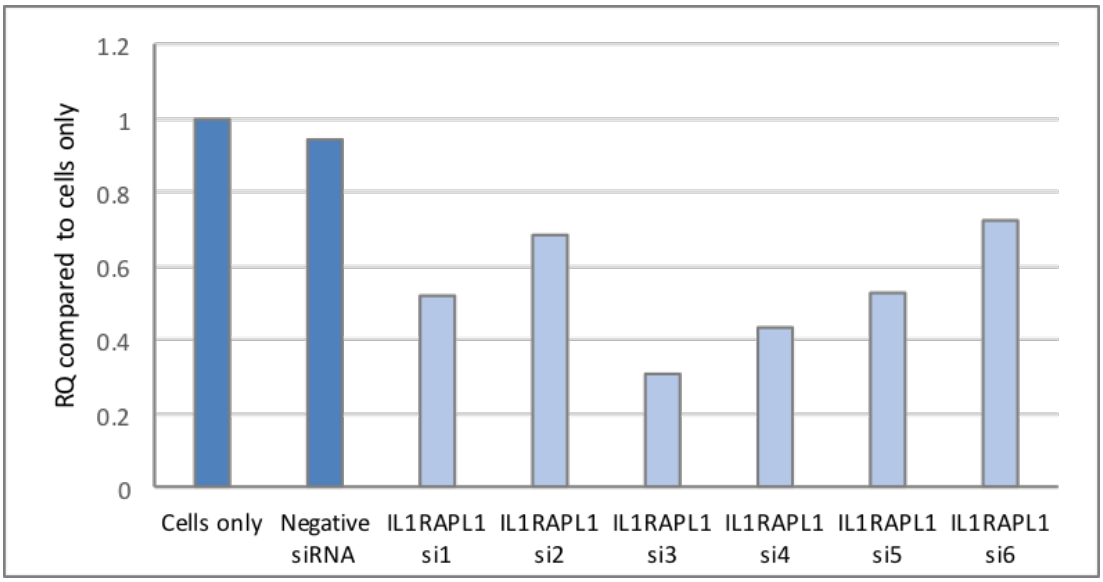

Figure 5.12 Relative quantitation of IL1RAPL1 mRNA in MIA PaCa-2 siRNA transfected cells compared to cells only and normalised to B2M by qRT-PCR. (30nM siRNA, assayed 48hrs post transfection) (Results represent one biological experiment)

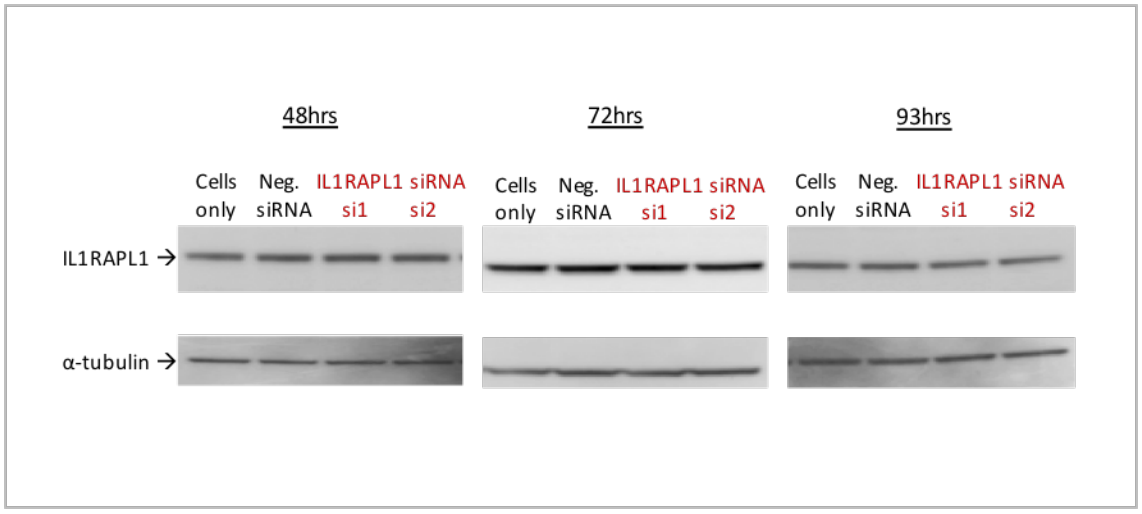

Figure 5.13 Western blot analysis showing MIA PaCa-2 cells probed for IL1RAPL1 in cells only control, cells transfected with Negative siRNA and IL1RAPL1 siRNA (si1 and si2) treated cells, assayed at 48hrs, 72hrs and 93hrs post transfection. (30nM siRNA) α-tubulin was used as a loading control. No protein knockdown is observed.

5.8. Overexpression of IL1RAPL1 in SW480 Cells

As the attempts to knockdown IL1RAPL1 protein in cancer cells were unsuccessful, it was decided to try IL1RAPL1 protein overexpression, to determine if any functional role for IL1RAPL1 in the CRC cell phenotype could be determined this way. The colon cancer cell line SW480 was selected for IL1RAPL1 overexpression, as it expresses IL1RAPL1 at a lower level compared to some of the other cell lines (Figure 3.3). As described in Section 4.10, a commercial transfection ready cloning vector containing the IL1RAPL1 sequence (Acc no: NM_014271.3) was obtained (GenScript), with the vector map shown in Figure 4.31. Transfection optimisation is described in Section 2.10.1.

Following antibiotic selection, qRT-PCR analysis of the SW480 empty vector (E.V.) and IL1RAPL1 overexpression (O.E.) cell lines, as well as a cells only control, was carried out as described in Section 2.9. **Table 5.9** shows the Ct value results of this analysis. An accurate determination of whether IL1RAPL1 is overexpressed at the mRNA level could not be carried out, as the Ct value for the endogenous control gene (B2M) was higher in the IL1RAPL1 O.E. cells compared to cells only and E.V. cells. IL1RAPL1 overexpression could possibly be affecting B2M levels. Excluding the B2M result, the Ct values for IL1RAPL1 do decrease in the O.E. cells compared to cells only and E.V., indicating some mRNA overexpression could be present (Ct of 22 compared to 26). However, this was only carried out once, the qRT-PCR needs to be repeated with a different endogenous control, to determine if IL1RAPL1 mRNA overexpression can be confirmed.

Western blot analysis to determine if IL1RAPL1 overexpression can be detected at the protein level is shown in **Figure 5.14**. This was only carried out once to date and no IL1RAPL1 protein overexpression was observed. Similar to the overexpression of LY6G6F in Section 4.10, the FLAG-tag blot gave inconclusive results, with multiple bands observed in all lanes. Therefore, it could not be confirmed whether the vector expressed version of IL1RAPL1 protein was present at all in the samples. Without confirmation of IL1RAPL1 protein overexpression, functional analysis could not be carried out. The qRT-PCR analysis first needs to be repeated to accurately determine if mRNA overexpression is present, and if so, the Western blot analysis needs to be repeated to confirm if this is translated into protein. Then functional analysis can be carried out.

Sample	IL1RAPL1 Ct value	B2M Ct value
SW480 cells only	26.8	17.8
SW480 Empty Vector	26.7	18.3
SW480 IL1RAPL1 O.E.	22.9	23.7

Table 5.9 Results of qRT-PCR analysis of IL1RAPL1 and B2M mRNA expression in SW480 cells. The average Ct values for IL1RAPL1 and the endogenous control B2M in SW480 cells only, E.V. and IL1RAPL1 O.E. cells are shown. (n=1)

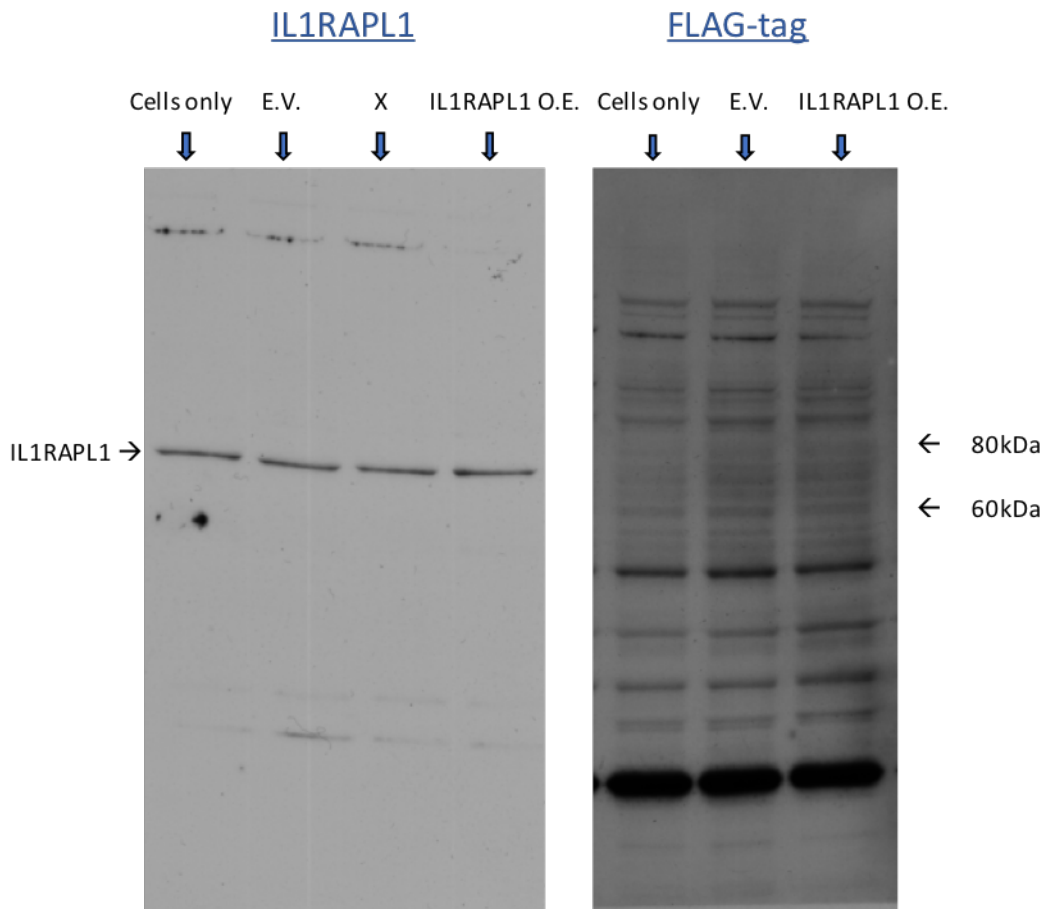

Figure 5.14 Western blot probing for IL1RAPL1 and FLAG-tag. Results are shown for SW480 cells only, E.V. and IL1RAPL1 O.E. cells. (The X lane on the IL1RAPL1 probed blot is a different protein O.E. cell line) No apparent protein overexpression of IL1RAPL1 is observed. The same samples probed for FLAG-tag, which should only be detected at IL1RAPL1 MW in the IL1RAPL1 O.E. sample, gave an inconclusive result, as multiple bands are visible in all wells. (n=1)

5.9. Attempted Immunoprecipitation of IL1RAPL1

To try and identify a functional role for IL1RAPL1 in the cancer cell phenotype, co-IP was carried out as described similarly for LY6G6F in Section 4.11. Both traditional and cross-linked IP with two independent IL1RAPL1 antibodies were used for Co-IP in the attempt to isolate IL1RAPL1 and any associated proteins from the cell lysate of a number of cell lines (including HCT116 and MIA PaCa-2). However, IL1RAPL1 was not successfully immunoprecipitated using either method.

Figure 5.15 shows representative Western blot analysis of the result obtained from cross-linked IP of IL1RAPL1 from MIA PaCa-2 cell lysate. A mouse IL1RAPL1 antibody was used for the IP, therefore a mouse IgG was used as a negative control. The Western blot was probed with a different rabbit IL1RAPL1 antibody, for detection of IL1RAPL1 in the cell lysate and IP elutions. IL1RAPL1 is detected in the MIA PaCa-2 IP buffer lysate, confirming the antibody can detect IL1RAPL1 from cell lysate made with a less stringent lysis buffer. IL1RAPL1 is also detected in the unbound fractions of both IL1RAPL1 and Mouse IgG control, with no band detected in the first or second elution from the IL1RAPL1 column. This shows that IL1RAPL1 protein was not pulled out from the cell lysate with the antibody used.

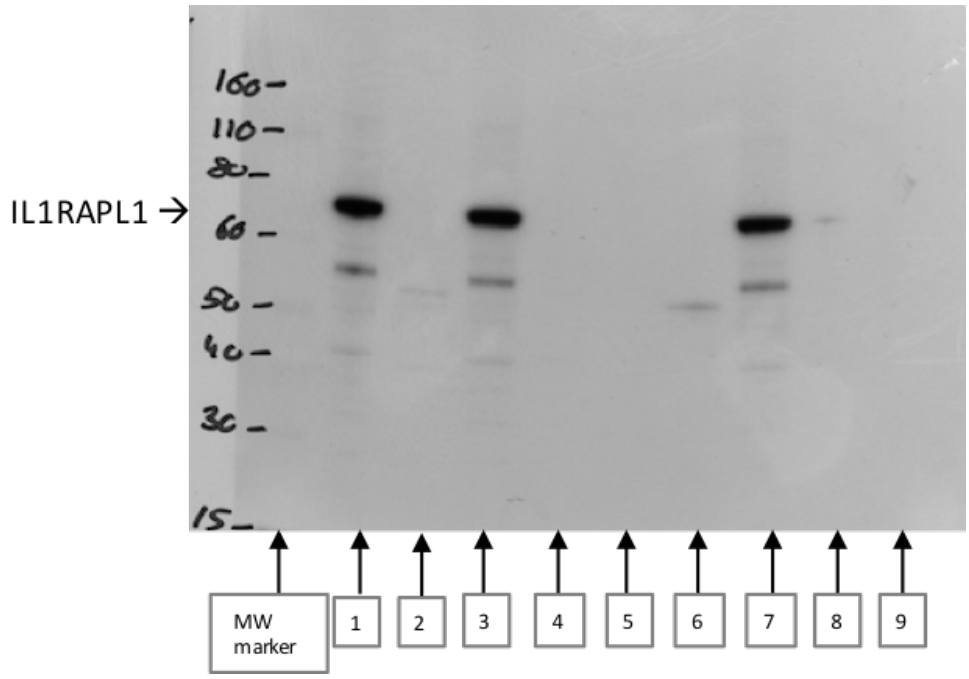

Figure 5.15 Western blot analysis probing for IL1RAPL1 in MIA PaCa-2 samples following cross-linked Co-IP. Lane **1**: MIA PaCa-2 control IP lysate. Lane **2**: Flow-through following IL1RAPL1 antibody coupling to column. Lane **3**: IL1RAPL1 Co-IP unbound fraction. Lanes **4** and **5**: First and second elution from IL1RAPL1 Co-IP. Lane **6**: Flow-through following Mouse IgG control antibody coupling to column. Lane **7**: Mouse IgG Co-IP unbound fraction. Lanes **8** and **9**: First and second elution from Mouse IgG Co-IP.

5.10. Summary

IL1RAPL1 has been found to be significantly overexpressed in both CRC and oesophageal squamous cell carcinoma compared to corresponding normal tissues. The majority of normal colon tissues analysed were negative for IL1RAPL1 expression, with mainly weak and diffuse immunoreactivity observed if it was present. IL1RAPL1 expression is also absent or weak in all specimens from the benign colon disease spectrum analysed: chronic inflammation of mucosa, hyperplasia, polyps and adenoma. In contrast IL1RAPL1 is strongly expressed in the majority of adenocarcinoma and carcinoid tumours, a significant upregulation compared to normal colon. Whilst slightly less than 50% of mucinous adenocarcinoma and metastatic adenocarcinoma specimens were found to strongly express IL1RAPL1, this was still found to be a significant overexpression compared to normal colon. IL1RAPL1 immunoreactivity was also potentially observed in immune cells in both some normal colon specimens, and to a greater extent in the microenvironment of CRC specimens. In the small cohort of normal oesophagus and oesophageal cancer analysed, IL1RAPL1 was found to be significantly overexpressed in the squamous cell carcinoma subtype. IL1RAPL1 expression is absent or weak in normal oesophagus, carcinoma in situ, small cell undifferentiated carcinoma, carcinoma sarcomatodes, carcinosarcoma and adenocarcinoma specimens. In contrast IL1RAPL1 is strongly expressed in 100% of oesophageal squamous cell carcinoma specimens analysed.

IL1RAPL1 expression was found to be absent or minimally expressed in the majority of normal tissues analysed. However, some normal tissues did show some stronger immunoreactivity. One section of duodenum analysed (out of four) showed strong immunoreactivity within the goblet cells that line the crypts, showing IL1RAPL1 could be expressed in the proliferating cells of this tissue. Isolated cells in some other tissues, including gastric tissue and cerebral cortex, were also found to have some strong IL1RAPL1 immunoreactivity. The Immunohistochemical analysis revealed mainly cytoplasmic localisation of IL1RAPL1 in the tissues. The Immunocytochemical analysis of HCT116 and MIA PaCa-2 cells and the Immunofluorescent analysis of HCT116 and SW480 cells, also showed mainly cytoplasmic localisation for IL1RAPL1.

Despite showing no strong expression in the majority of PDAC and breast cancer tissues analysed, IL1RAPL1 was found to be expressed in all PDAC and breast cancer cell lines

analysed. Western blot analysis detected IL1RAPL1 at the expected MW of ~69kDa in both the whole cell lysate and membrane enriched fraction of all colon cancer and PDAC cell lines analysed. A lower MW band was also detected in three of the colon cancer lines and all of the PDAC cell lines, which correspond with the single band detected in the conditioned medium from MIA PaCa-2 and BXPC-3 cell lines. This indicates that a soluble form of IL1RAPL1 is produced by these cells.

Attempts at achieving transient siRNA mediated protein knockdown of IL1RAPL1, to assess the effect on the functional phenotype of colon cancer *in vitro*, were unfortunately unsuccessful. Despite carrying out a number of optimisations and confirming knockdown of IL1RAPL1 at the mRNA level by qRT-PCR analysis, no IL1RAPL1 protein knockdown was ever achieved. IL1RAPL1 protein may have a very long half-life, which didn't allow for the protein level to be reduced under the time-points assessed in our experimental set-up. SW480 cells were transfected with an IL1RAPL1 overexpression vector, to assess the functional effect of IL1RAPL1 protein overexpression in a colon cancer cell line that expresses IL1RAPL1 at a lower level to some of the other cell lines. However, to date, no apparent IL1RAPL1 protein overexpression was detected. The qRT-PCR analysis to confirm mRNA overexpression needs to be repeated, as this was only carried out once, and a big difference in the levels of endogenous control gene (B2M) was detected between cells only and IL1RAPL1 O.E. cells. The attempts at elucidating a possible function for IL1RAPL1 in the cancer cell phenotype by identifying interacting proteins by Co-IP were also unsuccessful. The antibodies used did not list IP as a proven application. Therefore, IL1RAPL1 has been shown to be significantly overexpressed in CRC and oesophageal squamous cell carcinoma, but a functional role in the cancer cell phenotype could not be determined to date.

Chapter 6. Discussion

6.1. Introduction

Gastrointestinal malignancies have a high incidence rate worldwide and are also a leading cause of cancer related deaths. CRC is the 3rd most commonly diagnosed cancer worldwide, and ranks 4th in mortality. (Karsa *et al.*, 2010) Oesophageal cancer is the 8th most commonly diagnosed and ranks 6th in mortality. (Zhang, 2013) Gastric cancer is the 5th most commonly diagnosed and ranks 3rd in mortality. (Harvey, 2017) Whilst pancreatic cancer is the 12th most commonly diagnosed and ranks 7th in mortality. Pancreatic cancer also has a dismal 5 year survival rate of just 5%. (Wood and Hruban, 2015) Chemotherapy remains the mainstay of treatment for most advanced GI cancers and despite significant advances in cancer management over the years, there has been little change in the overall survival of patients diagnosed with advanced stage GI cancers. The only targeted therapeutics approved for use in CRC, are unconjugated mAbs that target EGFR and VEGF. These therapies are used in combination with chemotherapy for the treatment of metastatic CRC, where they can prolong overall survival by ~5 months. (Dattatreya, 2013) Overall, currently approved therapeutics have limited efficacy. The identification of molecular targets overexpressed in these cancer types compared to normal tissues, could have the potential for the development of targeted therapeutics, such as ADCs, that could show greater therapeutic benefit than currently available therapies.

This study aimed to identify membrane-localised proteins overexpressed in CRC vs. normal colon, and also to determine whether any of the identified targets show relevance in other cancer types. Identified targets would also be assessed for their suitability as potential molecular targets for therapeutic antibody targeting, in particular ADCs, which are highly potent therapeutic agents. The identification of molecular targets for ADC targeting can be quite complex, with the basic criteria of 1) higher target expression in tumours vs. normal tissues, 2) target localisation to the plasma membrane, 3) internalisation of the target into the cell upon ADC binding. It can be difficult to identify targets that fit all of these criteria. Additionally, targets identified from mRNA expression data may not be expressed as assumed, there may be cases in which mRNA is not translated to protein, protein is produced but not presented on the cell surface, or protein is cell surface localised but does not internalise. Therefore, significant validations are required to determine if overexpressed proteins have the potential to be utilised as molecular targets for antibody-based therapeutic targeting.

6.2. Identification of Candidate Protein Targets Overexpressed in CRC

The first aim of this study was to identify novel membrane-localised proteins overexpressed in CRC vs. normal colon and to investigate their potential as molecular targets that could be amenable to therapeutic antibody targeting. Identified proteins would also be assessed for expression in other cancer types, e.g. PDAC, which is in desperate need of new treatment strategies. Potential cancer targets were identified by analysis of colon cancer gene expression microarray data available for download from the Gene Expression Omnibus (GEO) database, as described in Section 2.1. Searching for mRNA datasets that contained data from normal human colon and colon carcinoma tissue sections (not cell line data), a dataset by Skrzypczak *et al.*, (2010) was chosen for analysis. This dataset contains whole tissue section samples from 24 normal colon, 45 colon adenoma and 36 colon adenocarcinoma specimens. In-house bioinformatics analysis of this dataset, produced two lists of genes upregulated in (1) colon adenocarcinoma vs. normal colon and (2) colon adenoma vs. normal colon, with 1238 upregulated genes identified in colon adenocarcinoma and 1078 upregulated genes in adenoma. These genes were then annotated for membrane localisation, as we are in search of cell-surface proteins, with a fold change of ≥ 2 and an adjusted p-value of $\leq 1E^{-5}$ considered significant. This produced the final lists of predicted membrane localised genes, with 127 genes found to be upregulated in adenocarcinoma and 154 genes upregulated in adenoma compared to normal colon. In hindsight, it would have been beneficial to validate the expression of these genes in other independent colon cancer datasets, to increase confidence in the identified targets. However, as we are interested in protein overexpression, which mRNA overexpression does not always equate to, the protein validation steps are the most important aspect of this study. Potential candidate targets were selected for validation from these lists by manually identifying relatively novel targets by literature review and also depending on commercial antibody availability.

This resulted in the identification of 7 genes for validation: Lymphocyte antigen 6 complex, locus G6F (LY6G6F), Interleukin 1 receptor accessory protein-like 1 (IL1RAPL1), Neurotrimin (NTM), Leucine rich repeat containing 8 family, member E (LRRC8E), Epoxide hydrolase 4 (EPHX4), Beta-site APP-cleaving enzyme 2 (BACE2) and Interleukin 20 receptor, subunit Alpha (IL20RA). Validation of candidate target expression at the protein level was assessed in a panel of six colon cancer cell lines, that represent a range of the mutational subsets found in CRC, and also in CRC and normal colon tissue sections. This

would determine if the protein is expressed in CRC and if it is expressed at a higher level than normal colon, as mRNA overexpression does not always correlate to protein overexpression. The initial Western blot analysis of all targets in both the whole cell and membrane enriched fraction of the colon cancer cell lines revealed that all 7 targets are expressed in both fractions, indicating an association with the membrane. Two targets, EPHX4 and LRRC8E, could not be validated at the protein level in tissue sections, and it is uncertain if this is due to poor antibody quality or an example of the mRNA overexpression from the datasets not corresponding to protein expression in the tissues analysed. Therefore, EPHX4 and LRRC8E were not pursued further for the time being. It was also decided not to pursue NTM further as a candidate target, as similar protein expression levels were observed in normal colon and CRC tissue sections in the Immunohistochemical analysis. Despite showing a 5.4 fold increase in expression at the mRNA level vs. normal colon, this does not appear to correlate to protein overexpression of NTM in the CRC specimens analysed.

Two other targets, IL20RA and BACE2, were also ultimately decided not to pursue further, due to high expression in normal tissues. IL20RA initially showed promise due to its strong membrane localised expression in CRC tissues, including metastatic CRC, and it also showed higher expression in the SW620 metastatic cancer cell line vs. the SW480 primary tumour cell line. IL20RA was identified solely from the adenoma gene list, with a 4.2 fold increase in expression vs. normal colon, therefore we sought to validate whether this overexpression is maintained in CRC. However, despite further preliminary analysis showing strong IL20RA expression in both CRC and PDAC tissue specimens, a similar level of expression was observed in the corresponding normal tissues. IL20RA was reported in the literature to be expressed at the mRNA level in colon, colonic supepithelial myofibroblasts and colonic epithelial cell lines. (Blumberg *et al.*, 2001) This correlates with the strong immunoreactivity observed in the epithelium of normal colon and also duodenum tissue sections in this analysis. Therefore, it appears that IL20RA is expressed at a high level endogenously in normal colon and pancreas, with no overexpression observed in cancer tissues.

BACE2 was not as highly expressed in normal colon as IL20RA, however a similar level of immunoreactivity was observed in CRC tissue sections, indicating that BACE2 is not overexpressed at the protein level in CRC. BACE2 also showed stronger expression in the SW620 metastatic cancer cell line vs. the SW480 primary tumour cell line by Western blot analysis. BACE2 was identified from both the adenoma and adenocarcinoma gene lists, with

a higher fold change present in the adenoma dataset (6 fold increase) than the adenocarcinoma list (2.7 fold increase). No adenoma tissue sections were available for the preliminary analysis, therefore it could not be confirmed if this higher overexpression in adenoma validates at the protein level. BACE2 also showed some promise in PDAC, with strong cytoplasmic and membrane immunoreactivity observed in some specimens, but again the expression in normal pancreas was also high. Therefore, it appears that IL20RA and BACE2 would be unsuitable molecular targets for therapeutic targeting due to their high normal tissue expression and were not pursued further.

Out of the initial seven identified candidate targets, two were selected for wider validations and analysis – LY6G6F and IL1RAPL1. Both targets showed negative/minimal expression in normal colon and strong expression in the CRC tissue sections analysed, indicating protein overexpression in CRC. The protein expression of both targets was also confirmed in both the whole cell and membrane enriched fraction of all the colon cancer cell lines analysed, indicating an association with the membrane. Expression in cell lines will also allow for *in vitro* functional analysis to be carried out.

The fact that only two of the seven selected candidate targets showed tissue expression levels that warranted further investigation, shows some of the difficulties that can arise in using mRNA expression datasets to look for corresponding protein levels. The reliance on commercially available antibodies, which can sometimes be of poor quality (e.g. potentially the case for EPHX4 and LRRC8E) can also hinder successful protein validations. The mRNA dataset used also did not have a very large sample size. If this dataset had been combined with other suitable datasets for the bioinformatic analysis to identify genes upregulated in CRC vs. normal colon, this may have yielded more stringent results, and perhaps increased the likelihood that candidate gene targets would validate at the protein level. The method used however did successfully identify two targets upregulated in CRC vs normal colon. The subsequent investigation into the expression of LY6G6F and IL1RAPL1 in a larger cohort of CRC tissue specimens and other cancer types, as well as the investigation into their functional role will be discussed in the following two sections, 6.3 LY6G6F and 6.4 IL1RAPL1.

6.3. LY6G6F

LY6G6F was identified from the microarray data, as being significantly upregulated at the gene level in both adenoma (9.8 fold up) and adenocarcinoma (17.6 fold up) tissues compared to normal colon. The subsequent validation in this study, confirmed this upregulation at the protein level, with LY6G6F found to be significantly overexpressed in adenoma and adenocarcinoma tissues vs. normal colon. LY6G6F was also found to be significantly overexpressed in two other cancers of the digestive system, gastric cancer and PDAC. The expression of LY6G6F was first reported as a novel membrane protein in platelets and megakaryocytes (platelet producing cells in the bone marrow), with LY6G6F expression and function mainly being reported in blood cells to date. The mRNA expression of LY6G6F was investigated in purified populations of platelets, B-cells, T-cells, monocytes and granulocytes, with expression only detected in the megakaryocytes and platelets. LY6G6F was also detected in K562 cells (myelogenous leukemia cell line), with LY6G6F shown to recruit the proteins Grb2 and Grb7 upon phosphorylation of its cytoplasmic tail. The coupling of LY6G6F with the Ras-MAP kinase pathway is strongly suggested following its interaction with Grb2 and with FAK following its interaction with Grb7. (de Vet, Aguado and Campbell, 2003; Macaulay *et al.*, 2007) A ligand for LY6G6F has not been described to date.

The expression of LY6G6F in cancer has not been reported on widely in the literature. LY6G6F was reported as one of 29 proteins giving a Mucin 5AC hyposecretory phenotype in the human colonic adenocarcinoma cells HT29-18N2. (Mitrovic *et al.*, 2013) LY6G6F was also listed as a significantly downregulated gene in MSI vs. MSS CRC tumours. (Slattery *et al.,* 2015) However, a specific functional role for LY6G6F in GI cancers has not been reported in the literature.

During the course of this study, a report was published by Sewda *et al.*, (2016) that employed a similar method to ours, to identify cell-surface markers for colon adenocarcinoma by profiling the publicly available mRNA expression microarray datasets. Their objective was to identify cell-surface targets for molecular imaging agents for the non-invasive detection of CRC by molecular imaging-based colonoscopy using CT, MRI or fluorescence. They identified six markers for validation, including the candidate target which they designated LY6G6D/F, underpinning again the confusion surrounding LY6G6D and LY6G6F, as discussed in Section 4.1. They state that LY6G6D and LY6G6F proteins cannot be

distinguished from each other by the available antibodies, even though they have no exons in common. They have actually used an LY6G6F antibody for their analysis and a qRT-PCR primer targeting LY6G6D mRNA (NM_021246). They also incorrectly state that LY6G6D is a 133 residue truncated version of the 297 AA LY6G6F, when they are in fact completely separate transcripts with no amino acids in common (see Figure 4.1). Therefore, their study looking at LY6G6D/F incorporates mRNA and protein data from two different genes. However, their finding for LY6G6F protein expression does match ours, showing that LY6G6F is overexpressed in colon adenocarcinoma vs. normal colon. They also state that LY6G6F expression is significantly correlated with proximal tumour location (vs. distal) and with expression of mismatch repair genes PMS2 and MSH6, indicating MSS genotype, which correlates with previous reports of LY6G6F being expressed in MSS, but downregulated in MSI CRC tumours. (Slattery *et al.*, 2015)

6.3.1. LY6G6F Expression in Cell Lines

6.3.1.1. Protein Expression

LY6G6F expression was detected in the whole cell and membrane enriched fraction across the whole CRC, PDAC and breast cancer cell line panel analysed by Western blot analysis. This indicates an association between the membrane and LY6G6F in these cell lines. In the CRC panel, differential expression of LY6G6F was observed, with the T84 and HT29 cell lines displaying the strongest expression, with weaker expression observed in the other cell lines. This expression pattern doesn't appear to correlate with any of the mutational subsets listed (e.g. KRAS or BRAF mutational status) for the colon cancer cell line panel. There was also some differential expression observed in the PDAC cell lines, with higher expression observed in the BXPC-3, Capan-2, Capan-1 and AsPC-1 cell lines, with again no apparent correlation to a mutational subset or the classical and quasi-mesenchymal classifications.

Breast cancer is a complex, heterogeneous disease, with constant reclassification of the molecular subtypes associated with it. Recent studies divide breast cancer into four major molecular subtypes: Luminal A, Luminal B, Triple negative/Basal-like and HER2 type. The panel of breast cancer cell lines used in this study represent Luminal A, Luminal B and Basal (triple negative) subtypes. The majority of basal-like breast cancers lack or show low levels

of ER and PR, lack HER2 protein overexpression and HER2 gene amplification, whereas they express genes and proteins usually found in 'basal'/myoepithelial cells of the normal breast. Luminal tumours represent cancer cells that initiate in the inner (luminal) cell lining of mammary ducts. Luminal A is characterised as ER-positive and HER2-negative, whilst Luminal B tumours tend to be ER-positive and may be HER2-negative or HER2-positive. Luminal B tumours tend to have worse prognosis factors than Luminal A, including poorer tumour grade and lymph node metastasis. Basal/Triple negative subtype tumours are often aggressive and have a poorer prognosis compared to the Luminal subtype tumours. Western blot analysis (Figure 4.4) showed that LY6G6F expression is detected in all eight breast cancer cell lines analysed, but with lower expression observed in all of the Basal-like cancer cell lines (MDA-MB-468, BT20, MDA-MB-157 and MDA-MB-231) compared to the Luminal subtype cell lines. Therefore, low LY6G6F expression could possibly be a feature of the Basal cancer subtype. Using the online tools, MTCI BreastMark and KM plotter analysis (kmplot.com), low LY6G6F gene expression was found to be significantly associated with poorer survival vs. high LY6G6F gene expression in breast cancer patients. Both of these analyses grouped all breast cancer subtypes together, and possibly links in with our finding of lower LY6G6F expression in the Basal subtype, as this subtype has a poorer prognosis overall vs. the other subtypes.

6.3.1.2. mRNA Expression

As we were interested in whether candidate targets validated at the protein level, the mRNA expression levels of LY6G6F in cell lines were not examined until after siRNA mediated knockdown and subsequent functional analysis had been started. The qRT-PCR analysis of MIA PaCa-2 and HCT116 cells surprisingly revealed that LY6G6F mRNA transcript is present at very low abundance levels in these cell lines. The Ct values were >30, which is commonly taken as unreliable data. However, the fact that the Ct values decrease upon the addition of more cDNA template, and that the NTC samples gave no signal, indicates the signal observed is for LY6G6F transcript, and not due to non-specific signal. Additionally, the Ct values did increase in the siRNA treated samples, showing the siRNA is successfully targeting the mRNA, leading to the protein knockdown observed.

The mRNA expression levels were also analysed in the BXPC-3, SW480 and HT29 cell lines, and in the K562 cell line, which was used as a positive control, with LY6G6F mRNA detected at a Ct <30 in this cell line, showing that the Taqman assay is working correctly. A second LY6G6F Taqman assay was also obtained to ensure that the first one is working efficiently. There were differences in the Ct values between the two assays for two of the cell lines analysed (SW480 and BXPC-3), which is not fully explainable, but could be due to varying primer efficiency rates between the two assays in these cell lines. The qRT-PCR analysis of the MIA PaCa-2, BXPC-3, SW480 and HT29 cell lines showed that mRNA expression does not appear to correspond to protein expression in these cell lines. In the PDAC cell lines, BXPC-3 has higher protein expression than MIA PaCa-2 cells (as determined by Western blot analysis), but they both have similar mRNA levels, with in fact the BXPC-3s having a slightly higher Ct value of 36.9 vs. 34.4 in the MIA PaCa-2 cell line. Similarly, in the colon cancer cell lines, HT29 cells have a higher level of LY6G6F protein expression compared to SW480 cells, but the mRNA expression levels are similar, with a Ct value of 36 in HT29 cells and 34.2 in SW480 cells. This indicates that the level of LY6G6F protein expression is likely regulated after translation in these cell lines.

6.3.2. LY6G6F Expression in Normal and Cancer Tissues

LY6G6F was found to be significantly overexpressed in three GI cancers – Gastric cancer, CRC and PDAC vs. corresponding normal tissues by Immuohistochemical analysis. LY6G6F does not appear to be strongly expressed in oesophageal cancer, however a very small sample size was analysed (n=1). The subtype was not known in the breast cancer specimens analysed, with all cases showing a weak expression level similar to that observed in normal breast, therefore it could not be determined if the lower expression observed in the Basal cancer cell lines corresponds to tissues also. Wider analysis could be carried out in breast cancer to determine if LY6G6F does display differential expression between subtypes. However, for our purpose of identifying overexpressed molecular targets that could potentially be amenable to therapeutic antibody targeting, LY6G6F does not appear to be a candidate target in breast cancer.

The majority of normal colon and NAT colon specimens analysed were negative for LY6G6F or displayed weak and diffuse immunoreactivity, with a small number showing some strong

LY6G6F immunoreactivity. In the colon disease spectrum analysed, LY6G6F was found to be significantly overexpressed in colon adenocarcinoma (p-value <0.0001), as well as the benign spectrum representing: polyps (p-value <0.0001), hyperplasia (p-value <0.0001) and adenoma (p-value 0.0031) vs. normal colon. This validates the microarray data, that LY6G6F is overexpressed in both adenoma and adenocarcinoma tissues. LY6G6F is weakly expressed in the tissue samples representing chronically inflamed colon, where the colon epithelium itself has not transformed abnormally. This indicates that LY6G6F expression could be associated with the early stages of normal colon transformation, and the progression of CRC from polyp to adenoma to adenocarcinoma. LY6G6F was found to be strongly expressed in 70% of the adenocarcinoma specimens analysed, irrespective of tumour grade or mutational status. No differential expression was observed between the BRAF MT and WT subtypes, as all showed high expression. In the KRAS MT and WT groups, 100% of the KRAS MT showed high expression, with 88.9% of the KRAS WT highly expressing LY6G6F, which is not a significant difference. Therefore, LY6G6F expression appears to be associated with adenocarcinoma, regardless of the mutational subtype, which correlates with the expression pattern observed in the colon cancer cell lines.

Despite being strongly expressed in colon adenocarcinoma, low LY6G6F expression was observed in the majority (63.2%) of metastatic adenocarcinoma cases. These metastatic cancer specimens were derived from lymph node metastases. This could potentially indicate that LY6G6F is not highly expressed in the cancer cell populations that go on to metastasise or high expression is not maintained once the cancer cells have metastasised to a different microenvironment. However, an analysis of paired patient samples (tissue specimens from the primary tumour and metastatic site of the same patient) would be required to conclusively determine whether LY6G6F expression decreases in the metastatic vs. primary tumours. As a relatively small sample size (n=19) of metastatic adenocarcinoma specimens derived exclusively from lymph node metastases was used in this analysis, LY6G6F expression should be examined in a larger metastatic adenocarcinoma cohort, including other sites of metastases e.g. liver, the predominant site of CRC metastasis. If LY6G6F is found to consistently be lowly expressed in metastatic adenocarcinoma, then a potential LY6G6F targeting therapeutic agent would have no application in the metastatic disease setting.

LY6G6F was found to be weakly expressed in 100% of the carcinoid tumour specimens, a rare subtype of CRC arising from neuroendocrine cells in the colon. This indicates LY6G6F

overexpression is not associated with this subtype, however the very small sample size (n=2) analysed, means that a larger cohort would need to be examined to definitively conclude that. In the mucinous adenocarcinoma cohort, LY6G6F was found to be weakly expressed in the majority (73.3%) of cases, showing no significant overexpression vs. normal colon. Mucinous adenocarcinoma is a distinct form of CRC, characterised by abundant mucous secretion comprising at least 50% of the tumour volume and accounts for approximately 10-15% of CRC cases. (Hugen *et al.*, 2015) The observation of low LY6G6F expression in mucinous adenocarcinomas in this study, fits in with what has been reported about LY6G6F expression in CRC in the literature. LY6G6F expression was linked to the downregulation of Mucin 5AC in the colon cancer cell line HT29-18N2, therefore it makes sense that LY6G6F would be lowly expressed in CRC tumours with excessive mucin secretion. (Mitrovic *et al.,* 2013) LY6G6F was also listed as a significantly downregulated gene in MSI vs. MSS tumours, and mucinous adenocarcinomas have a higher propensity for MSI genotype. (Slattery *et al.,* 2015) Therefore, LY6G6F overexpression appears to be a specific feature of adenocarcinoma with MSS phenotype (the most commonly diagnosed form of CRC). MSS CRC tumours are associated with a higher rate of recurrence and poorer prognosis compared to MSI tumours. (Jung, Kim and Kim, 2016)

LY6G6F was shown to be highly expressed in PDAC vs. normal pancreas in the preliminary IHC screen. To investigate LY6G6F expression further, PDAC tissue specimens were obtained from a 57 patient cohort in collaboration with St.Vincent's University Hospital. Information on the pathological features and survival rates for this cohort was also provided. 89.4% of the tumours were at stage T3, representing the fact that PDAC is commonly not diagnosed until a late stage of tumour growth. LY6G6F was found to be significantly overexpressed in PDAC vs. normal pancreas (p-value <0.0001), with 78.9% of tumours highly expressing LY6G6F. In normal pancreas LY6G6F showed negative or weak and diffuse immunoreactivity. Whilst not deemed significant, higher LY6G6F expression was observed in T3 vs. T1-2 stage tumours, and in tumours where LVI, PNI, and PVI were present. Together with the Kaplan-Meier survival analysis in this patient cohort, which showed a distinct trend towards decreased survival in patients with high LY6G6F expression vs. low LY6G6F expression, this strongly suggests a potential role for LY6G6F in PDAC carcinogenesis.

LY6G6F was observed to be mainly localised in the cytoplasm of PDAC tumours, showing granular cytoplasmic immunoreactivity, localised to the apical membrane of ducts. Membrane localisation was only observed in a few specimens, with membrane–like immunoreactivity more likely to be observed in smaller tumour ducts or tumour buds. Tumour budding is a phenomenon encountered in various cancers, including PDAC and CRC, where individual malignant cells and/or small clusters of malignant cells, which have detached from the main tumour mass, are observed in the tumour stroma. Tumour budding is associated with poor outcomes in all of the cancers in which it has been described, and was found to be a highly unfavourable prognostic factor in PDAC. (Karamitopoulou *et al.*, 2013) Tumour buds have been suggested to undergo partial EMT, with the partial downregulation of epithelial markers and upregulation of mesenchymal markers described. Higher levels of stem-cell markers are also described in tumour buds, where they could be considered a form of the proposed migrating cancer stem cells theory. (Grigore *et al.*, 2016) The observation that LY6G6F is more likely to be membrane localised in tumour buds compared to the main tumour mass, could indicate a different function for LY6G6F in these cell populations, with LY6G6F perhaps only localised to the membrane in response to the activation of certain cellular pathways or tumour microenvironmental factors. However, this strong membrane localisation observed in tumour buds potentially conflicts with the observation that LY6G6F is more lowly expressed in metastatic CRC tumours, if tumour buds do represent the initial metastatic front of cancer cells. LY6G6F is potentially involved in the early spread/local invasion of tumours, but not distant metastases. It remains to be determined whether the membrane localisation observed in tumour buds, correlates to a different functional role for LY6G6F in these cells, compared to the cytoplasmic localisation observed in the main tumour mass.

Strong membrane localised LY6G6F immunoreactivity was also observed in the stroma of 40.4% of the PDAC specimens analysed. PDAC is characterised by an intense stromal desmoplastic reaction surrounding cancer cells, which includes α-SMA positive cancer-associated fibroblasts. (Nielsen, Mortensen and Detlefsen, 2016) PDAC tissue specimens could be stained for α-SMA to determine whether the LY6G6F immunoreactivity observed is consistent with this cell type. There is significant interest in stromal targeting in PDAC, to destroy the dense desmoplastic stroma and enable easier delivery of chemotherapeutic agents to the tumour. Therefore, LY6G6F could be relevant as a potential molecular target for both

PDAC tumour cells and the surrounding stroma. LY6G6F immunoreactivity was also observed in the stroma of some normal tissues. Some of the normal pancreas sections displayed strong stromal LY6G6F immunoreactivity in areas, but to a much smaller extent than that observed in PDAC. Strong LY6G6F immunoreactivity was also observed in the stroma surrounding the glandular tissue in bladder, kidney, larynx, and salivary gland. Therefore, LY6G6F may be expressed in some normal tissue fibroblasts, with stronger expression observed in the amplified cancer-associated fibroblast component of PDAC. Further investigation is required to determine the precise cellular component showing LY6G6F immunoreactivity in the stroma.

LY6G6F gene expression was investigated in gastric cancer using the online tool KM plotter. (Szász *et al.*, 2016) The resulting Kaplan-Meier survival analysis found that high LY6G6F mRNA levels are significantly associated with poorer survival in gastric cancer patients. Therefore, we decided to carry out preliminary analysis of LY6G6F expression at the protein level using a small gastric adenocarcinoma and normal gastric epithelium TMA. Gastric adenocarcinoma accounts for approximately 95% of gastric cancer cases. Gastric cancer has an extremely high mortality rate, with approximately 90% of the people diagnosed with gastric cancer, succumbing to the disease. (GE4GAC Group, 2017) LY6G6F was found to be weakly expressed in the majority (12/14) of normal gastric epithelium specimens, however in contrast 50% (8/16) of the gastric adenocarcinoma specimens strongly express LY6G6F. This was determined to be a significant overexpression (p-value 0.002). Again, a mixture of mainly cytoplasmic, with some membrane-like immunoreactivity was observed. LY6G6F expression should be examined in a larger cohort of gastric cancer patients, to determine if high LY6G6F expression correlates with any particular feature/subtype of gastric cancer, as half of the cancer specimens analysed showed weak LY6G6F immunoreactivity. The analysis of a gastric cancer patient cohort with survival information, would also enable us to determine if the high LY6G6F mRNA levels associated with poorer survival in the KM plotter analysis, corresponds to a similar association at the protein level.

An important feature of candidate therapeutic targets, is that they have minimal expression in normal tissues, particularly vital organs, with negative or minimal expression in the highly proliferating cells of normal tissues, to minimise off target toxicities. LY6G6F expression was investigated in the highly proliferating cells of normal proliferative tissues including colon, duodenum, gastric tissue and tonsil by staining serial tissue sections for Ki67, a marker

of cell proliferation. In general, LY6G6F did not appear to be present in the same cells as those stained for Ki67. Negative or minimal LY6G6F immunoreactivity was observed in most of the normal tissues analysed, apart from some stronger expression observed in a small number of normal colon specimens (8/42) and the strong stromal stain noted in some tissues, as discussed above. As already noted however, LY6G6F expression has been reported in megakaryocytes and platelets. The one bone marrow specimen analysed, did show some LY6G6F immunoreactivity in isolated cells (possibly megakaryocytes). ADC targeting of LY6G6F could potentially cause toxicity in these cells. Therefore, the expression of LY6G6F in blood cells and normal tissues, would have to be much more extensively examined for investigation of its potential as a molecular target for antibody-based therapeutics.

This study represents the first investigation of LY6G6F expression in PDAC and gastric cancer tissue specimens. Whilst LY6G6F overexpression in CRC tumours has already been reported (Sewda *et al.*, 2016), a functional role for LY6G6F in the colon cancer cell phenotype has not been described. This study showed that LY6G6F is highly expressed in these GI cancers, with 70% of colon adenocarcinoma, 78.9% of PDAC and 50% of gastric adenocarcinoma specimens highly expressing LY6G6F. These expression levels are comparable to other targets that are currently in clinical development as therapeutic targets for GI cancers. For example, the transmembrane cell surface receptor guanylyl cyclase C (GCC) is currently being evaluated as an ADC target for GI cancers in a Phase 1 trial. GCC is expressed in approximately 60-70% of pancreatic, gastric and oesophageal cancers and by 95% of CRCs. (Almhanna *et al.*, 2016)

Survival analysis of the PDAC patient cohort showed a trend towards decreased survival in the patients with high LY6G6F expressing tumours. If we had access to a larger patient cohort this may have reached significance. For the CRC analysis, we unfortunately did not have access to a patient cohort with survival information provided. We had access to 22 full-face CRC specimens, with information on their pathological grade diagnosis and KRAS/BRAF mutational status provided. Commercial TMAs made up the rest of the analysis. It would be beneficial to look at LY6G6F expression in a larger PDAC cohort, as well as CRC and gastric cancer patient cohorts that include survival information, to determine if there is a significant association between high LY6G6F expression and decreased survival in these GI cancers. However, the differential tumour/normal tissues expression of the target is on its own enough

to warrant investigation of LY6G6F as a therapeutic target in these cancers, an association with decreased survival is not a requirement.

6.3.3. LY6G6F Cellular Localisation

An association between LY6G6F and the membrane of CRC, PDAC and breast cancer cell lines was indicated from Western blot analysis of membrane enriched fractions of these cell lines. However, the Immunofluorescent and Immunocytochemical analysis of fixed MIA PaCa-2 cells showed mainly cytoplasmic and possibly inner plasma membrane LY6G6F localisation. No distinct membrane localisation was observed. However, this study was quite limited by the commercial antibodies available, with an antibody validated for Immunofluorescence only sourced towards the end of this study. Therefore, further optimisations and attempts at live cell immunofluorescence may have been able to show more distinct membrane localisation. Interestingly, in the study by Sewda *et al.*, (2016), that identified LY6G6D/F as a marker for CRC, they also failed to show LY6G6F expression on the surface of colon cancer cells by Immunofluorescence analysis. They tried to confirm LY6G6F expression on the cell surface of non-permabilised colon cancer cell lines, but LY6G6F was not observed on the surface of any of the cell lines surveyed. They state that this doesn't necessarily mean that surface expression will not be observed in CRC, since tumour microenvironmental factors can also affect gene expression and sub-cellular localisation. From our observations in the Immunohistochemical analysis of tissue sections, this could perhaps be true, with LY6G6F membrane-like expression more likely to be observed in smaller tumour ducts/ tumour buds at the invasive front of both PDAC and CRC, suggesting localisation to the membrane occurs only in particular circumstances. The prevalent type of LY6G6F immunoreactivity observed in the main tumour body of CRC, PDAC and gastric cancer was granular cytoplasmic, often localised to the apical membrane side of the tumour ducts.

Membrane localisation was observed in the stromal component of PDAC and some normal tissues, and it remains to be determined if these represent fibroblast cells or some other stromal cell component present in both normal and cancer tissues (and as previously mentioned, staining of PDAC for α-SMA, could confirm if LY6G6F is expressed on the cancer-associated fibroblasts). Studies in the literature did confirm cell surface localisation

of LY6G6F on the surface of platelets and K562 cells. (de Vet, Aguado and Campbell, 2003; Macaulay *et al.*, 2007) Again, perhaps indicating LY6G6F is only localised to the membrane in certain cell types or in response to certain intra/extracellular factors. Based on the cytoplasmic cellular localisation observed in the majority of cancer tissues analysed, it would previously have been assumed that LY6G6F would not be amenable to therapeutic antibody targeting, which requires cell-surface localisation of the target. However, recent studies have shown that mAbs generated against an intracellular antigen can show therapeutic efficacy, and there are also emerging strategies to target intracellular proteins via the presentation of peptides on the cell-surface in the context of HLA, such as TCRm mAbs mentioned in Section 1.3.4. (Dubrovsky *et al.*, 2016; Thura *et al.*, 2016)

6.3.4. Function of LY6G6F in the Cancer Cell Phenotype

Following on from the observation that LY6G6F is significantly overexpressed in CRC and PDAC tumours, the functional role for LY6G6F in these cancers was assessed *in vitro*. Transient protein knockdown of LY6G6F was carried out in the colon cancer cell line HCT116 and the PDAC cell line MIA PaCa-2, followed by analysis of the functional effect on the proliferation, 2D colony formation, migration and invasion of these cells. Three independent LY6G6F siRNAs were used, which gave varying amounts of protein knockdown in these cells, with complete protein knockdown never achieved. However, the effect of the partial protein knockdown was assessed, with the use of three siRNAs giving more confidence in the results found. LY6G6F protein knockdown was found to significantly decrease the proliferation of both cell lines, as determined by the acid phosphatase assay and the 2D colony formation assay. The acid phosphatase assay determines cell growth based on the quantification of cytosolic acid phosphatase activity, enabling comparison of proliferation rates between control and siRNA treated cells. Whereas, the 2D colony formation assay assesses the ability of single cells to survive and proliferate into colonies. LY6G6F KD was found to significantly decrease the proliferation of HCT116 cells, with a 21%, 36% and 38% decrease in proliferation vs. Negative siRNA control found for the three siRNAs. There was also a big decrease in the colony forming ability of these cells, with a reduction of 58.4%, 25.9% and 29.4% in the area covered vs. Negative control, but these results failed to reach significance due to high SDs. There was a more minimal reduction in

the proliferation of MIA PaCa-2 cells, with an 11%, 20% and 24% decrease observed, which was a significant decrease vs. Negative control. The effect on the colony forming ability of MIA PaCa-2 cells was even greater, with a significant decrease of 51.1% and 31.7% in the area covered vs. Negative control. The third siRNA also showed a decrease of 30.4%, but this failed to reach significance. Therefore, LY6G6F appears to have a role in the proliferation of both HCT116 and MIA PaCa-2 cells.

LY6G6F protein knockdown also decreased the migration and invasion of these cells. In the HCT116 cell line, LY6G6F KD led to a significant reduction in migration, with a decrease of 73%, 48% and 54% (this siRNA result is a trend, not significant) vs. Negative control. There was also a significant decrease in invasion, with a 70% and 59% reduction for two siRNAs, with the 3rd showing a 33% reduction in invasion, this siRNA result didn't reach significance however. In the MIA PaCa-2 cell line, no apparent effect was observed on migration, with just a 1%, 10% and 15% (this siRNA result was deemed significant) reduction observed. The effect on invasion was bigger, with a significant decrease of 26% and 34% found, and a trend to a 25% decrease with one of the siRNAs. Studies have shown that the processes of invasion and proliferation in cells are mutually exclusive, with cells required to stop dividing in order to invade. (Matus *et al.*, 2015) Therefore, it can be concluded that the decrease in migration and invasion following LY6G6F KD, is not simply due to the decrease in proliferation observed. In addition, there were only minimal effects on the migration of MIA PaCa-2 cells, but a significant decrease in invasion levels, increasing confidence that the decrease in proliferation is not the cause of the other functional assay results. This is the first study to show that knockdown of LY6G6F in a colon and pancreatic cancer cell line, decreases their proliferation, migration and invasion *in vitro*.

The association found between LY6G6F and proliferation, migration and invasion in the CRC and PDAC cell lines is substantiated by evidence found in the literature. A potential ligand for LY6G6F activation has still not been identified, but it has been shown to interact with the proteins Grb2 and Grb7 in the K562 cell line, upon phosphorylation of the single tyrosine residue present in the intracellular tail of LY6G6F. The tyrosine residue is present in a consensus-binding motif (YXN) for the Src homology 2 domains of Grb2 and Grb7. (de Vet, Aguado and Campbell, 2003) Grb2 and Grb7 have both been associated with cell proliferation and migration. Grb7 has been shown to interact with FAK, with the FAK-Grb7 complex involved in integrin signalling. Grb2 is a key molecule in intracellular signal

transduction, linking activated receptors to downstream targets and can activate the Ras MAPK pathway. (Giubellino, Burke and Bottaro, 2008) Antibody cross-linking of LY6G6F in the K562 cell line resulted in the phosphorylation of p42/44 MAPK. (de Vet, Aguado and Campbell, 2003) The MAPK cascade functions in cellular proliferation, differentiation and survival.

Therefore, to assess whether LY6G6F knockdown is affecting any of these pathways in the HCT116 and MIA PaCa-2 cells, potentially mediating the phenotypic effects observed, Western blot analysis was carried out to determine the activation levels of FAK and p42/44 MAPK. The results for p42/44 MAPK were inconclusive, with inconsistencies between triplicate experiments, perhaps due to the often variable amounts of protein knockdown achieved. However, there was a marked decrease in the levels of phosphorylated-FAK in both cell lines, following LY6G6F knockdown. FAK is an intracellular, highly conserved, non-receptor tyrosine kinase, which is overexpressed and activated in a wide variety of cancers including colon and pancreatic cancer. FAK activation results in the induction of multiple signalling molecules, involved in multiple cellular functions, including cell proliferation, survival, motility and invasion. (Hochwald *et al.*, 2009; Kanteti *et al.*, 2015) Constitutive phosphorylation of FAK has been associated with resistance to the chemotherapeutic gemcitabine in pancreatic cancer cell lines. (Huanwen *et al.*, 2009) High levels of FAK, in combination with Src, have been associated with tumour recurrence and metastasis in colorectal cancer. (de Heer *et al.*, 2008) LY6G6F could have a potential role in FAK activation in colon and pancreatic cancer cell lines, due to the decrease observed in FAK phosphorylation following LY6G6F knockdown. This decrease in FAK activation in the HCT116 and MIA PaCa-2 cell lines, following LY6G6F KD, could also be the mediator of the inhibitory effects observed on cell proliferation, migration and invasion, as FAK activation has previously been associated with these mechanisms in colon and pancreatic cancer.

To determine if the decrease in proliferation observed was due to cell cycle arrest or an increase in apoptotic cell death following LY6G6F knockdown, a small number of cell cycle and apoptosis markers were also assessed by Western blot analysis. The results for the cell cycle markers Cyclin A and p27 were inconsistent. However, the results did show that there is an increase in apoptosis following LY6G6F knockdown, confirmed by an increase in the levels of cleaved PARP, a marker of apoptosis. This increase in apoptosis could also be

mediated by the decrease in FAK activation, as studies have also linked FAK to an anti-apoptotic role in anchorage-dependent cells. (Sonoda et al., 2000) The pro-proliferative and anti-apoptotic functions of FAK have been shown to enhance tumour growth. (Sulzmaier, Jean and Schlaepfer, 2014) Inhibition of FAK phosphorylation has been shown to increase apoptosis of both colon and pancreatic cancer cell lines. (Hochwald *et al.*, 2009; Heffler *et al.*, 2013)

Therefore, these results link LY6G6F to a role in FAK activation, with the decrease in FAK activation following LY6G6F knockdown being the potential mediator of the observed increase in apoptosis and decrease in cell proliferation, colony formation, migration and invasion. These functional studies and the information from the literature also tie in with the fact that higher LY6G6F expression was associated with poorer prognosis vs. low LY6G6F expression in the PDAC patient cohort (n=57) analysed in the Immunohistochemical analysis and in gastric cancer patients in the KM plotter analysis, suggesting a role for LY6G6F in the growth and survival of these GI cancers.

Unfortunately, time did not allow for the investigation into other potential pathways affected by LY6G6F knockdown in these cell lines. Further investigation should be carried out to determine if any other pathways alongside FAK are affected by LY6G6F knockdown in colon and pancreatic cancer cell lines. The Co-Immunoprecipitation of LY6G6F from cancer cell lysates was also unfortunately unsuccessful, meaning that LY6G6F-protein interactions in the colon and pancreatic cancer cells lines could not be determined. Instead of the Western blot analysis for a small number of cell cycle and apoptosis markers, it would have been beneficial to carry out more in depth cell cycle and apoptosis assays to gather more information on the effects of LY6G6F knockdown. For example, the increase in apoptosis observed could be further verified by an Annexin-V Apoptosis assay (e.g. TUNEL assay), which enables the quantification of live, dead and early or late apoptotic cells in a sample. Analysis of cell cycle arrest by BrdU staining of cells for DNA content, would allow analysis of the cells through the full cycle (G0/G1, S and G2/M), as the two markers (Cyclin A and p27) assessed by Western blot analysis did not allow for this, and with the inconsistent result observed, no conclusion could be made on whether LY6G6F has any role in cell cycle arrest, as well as apoptosis.

The attempt at LY6G6F protein overexpression by vector transformation in MIA PaCa-2 and SW480 cells was also unsuccessful to date, therefore it could not be determined whether LY6G6F overexpression in cell lines with lower endogenous protein levels causes an increase in cell proliferation, migration or invasion. Despite achieving high LY6G6F overexpression at the mRNA level, this did not translate into any noticeable protein overexpression, as determined by Western blot analysis. It could not be determined whether the vector expressed version of LY6G6F protein was being translated at all, as the Western blot analysis for the FLAG-tag attached to the vector expressed LY6G6F did not work as anticipated. The expression of LY6G6F may be highly regulated at the translational level, meaning protein overexpression could not be achieved, despite the increase in LY6G6F mRNA observed in vector transformed cells. This could be happening by microRNA (miRNA) induced silencing of the overexpressed LY6G6F mRNA. Regulation of translation by miRNA can occur by mRNA degradation or the prevention of mRNA translation into protein. Or if the vector expressed version of LY6G6F is getting translated into protein, the process of ubiquitination may be maintaining protein levels at a similar level to non-vector transformed cells. The binding of the ubiquitin regulatory protein to another protein can amongst other things lead to the protein's degradation via the proteasome. Therefore, if overexpressed LY6G6F is being quickly degraded, it may not show up on Western blot analysis.

6.4. IL1RAPL1

IL1RAPL1 was not identified as a potential cancer target in a conventional way, as IL1RAP was the gene identified from the microarray dataset of genes upregulated in colon cancer vs. normal colon. However, the error in examining IL1RAPL1 rather than IL1RAP in the preliminary analysis, led to the discovery that IL1RAPL1 is in fact strongly expressed in colon cancer with minimal expression in normal colon. A link between IL1RAPL1 expression and colon cancer has not been previously reported in the literature. Indeed, IL1RAPL1 expression has mainly been associated with the brain and cognitive impairment. Therefore, it was decided to investigate the expression of this potentially novel colon cancer target further.

IL1RAPL1 belongs to a novel class of the IL-1/Toll receptor family, characterised by the presence of a 150 amino acid long C-terminal extension that has no significant homology with any protein of known function. IL1RAPL1 was hypothesised to play a similar role to that of IL-1R in the CNS, i.e. binding to IL-1 and initiating signalling events, including activation of JNK and NF-κB, which regulates the expression of many pro-inflammatory genes in the nucleus. However, IL1RAPL1 was initially found to not interact with IL-1 and signalling experiments showed IL1RAPL1 was unable to activate the transcription factor NF-κB, or the MAP kinases ERK and p38, but could activate JNK. Therefore, it was suggested that almost all physiological and biological features remain to be defined for this novel class, including their ligand(s) and downstream partners. (Chelly *et al.*, 1999; Born *et al.*, 2000)

IL1RAPL1 is abundantly expressed in the brain and high levels of expression are found in the CNS during development. IL1RAPL1 is a 696 AA protein consisting of an extracellular domain of three Ig-like domains and a cytoplasmic domain, containing a TIR (Toll/IL1R) domain and the specific 150 amino acids at the C-terminal end. This 150-amino acid extension was subsequently found to interact with the neuronal calcium sensor 1 (NCS-1) protein, taking part in downregulating the activity of voltage-dependent calcium channels, in calcium-dependent exocytosis and NGF induced neurite outgrowth. IL1RAPL1 has also been shown to interact in dendritic spine with PSD-95, a major scaffold protein of excitatory post-synaptic density. IL1RAPL1 is reported to regulate the synaptic localisation of PSD-95 by controlling JNK activity and PSD-95 phosphorylation. The activation of the JNK pathway in neurons by IL-1 was found to be mediated by IL1RAPL1, despite previous reports stating

that IL1RAPL1 was incapable of IL-1 interaction. Therefore, the function of IL1RAPL1 in neurons has been linked to synapse formation and stabilisation. (Pavlowsky *et al.*, 2010; Boraschi and Tagliabue, 2013) Reduced synapse formation has been proposed as a common pathogenic mechanism of cognitive impairment, which follows the finding that IL1RAPL1 gene deletions and non-sense mutations have been identified in patients suffering from X-linked intellectual disability. Mutations in IL1RAPL1 have also been associated with autism and schizophrenia. (Piton *et al.*, 2008)

IL1RAPL1 has been reported as being a common fragile site (CFS) gene contained within the FRAXC CFS region. Common fragile sites are large regions of profound genomic instability found in all individuals. They are biologically significant due to their role in a number of genomic alterations that are frequently found in many different types of cancer. IL1RAPL1 is abundantly expressed in normal brain but was found to be dramatically underexpressed in every brain tumour cell line and xenograft (derived from an intracranial model of GBM) examined. This suggests IL1RAPL1 may function as a tumour suppressor in this cancer type. (Smith *et al.*, 2006; McAvoy *et al.*, 2007) However another study that classified GBM into different subtypes, linked IL1RAPL1 expression to the proneural subtype. (Cruceru *et al.*, 2013) The expression of IL1RAPL1 in other cancer types has not been widely reported on and no functional studies in cancer have been carried out.

6.4.1. IL1RAPL1 Expression in Cell Lines

Western blot analysis detected IL1RAPL1 expression in all colon cancer, PDAC and breast cancer cell line panels analysed, at the predicted MW of ~69kDa. IL1RAPL1 was detected in both the whole cell lysate and the membrane enriched fraction of cells, indicating an association with the membrane in these cell lines. No notable differential expression between cell lines was observed. The Western blot analysis also revealed the presence of a lower MW isoform of IL1RAPL1 in all of the PDAC cell lines, and three of the colon cancer cell lines analysed. This band at ~58kDa, was also detected in conditioned medium from MIA PaCa-2 and BXPC-3 cell lines. Therefore, there appears to be a soluble form of IL1RAPL1 produced and secreted by these cell lines. The three colon cancer cell lines that express the lower MW isoform are SW480, SW620 and CaCo-2, which are distinguished from the other three cell lines (HCT116, T84 and HT29) by the expression of wildtype PIK3CA (refer to

Table 3.2). Therefore, perhaps the expression of this lower MW isoform is linked to a mutational subset of colon cancer. A smaller isoform produced by the IL1RAPL1 gene was originally reported in the discovery of the gene, which was suggested to not contain the transmembrane domain, a feature that was previously found in the mouse isoform. It was suggested to correspond to a soluble form of the putative extracellular domain of IL1RAPL1, with an unknown function. Cell-surface proteins can be proteolytically cleaved to release their biologically active extracellular domains into the extracellular milieu, in a process known as ectodomain shedding. Ectodomain shedding can rapidly downregulate the expression of cell surface proteins, and the released soluble extracellular ectodomains can then function in an autocrine or paracrine fashion. (Hayashida *et al.*, 2010) A function for the soluble form of IL1RAPL1 has not been reported yet. The potential secretion of soluble IL1RAPL1 by tumour cells could have implications for potential antibody targeting of tumour cells. Soluble antigen in the tumour microenvironment can bind ADCs, thus limiting the amount of ADC free to bind tumour cells and therefore decreasing efficacy. Therefore, further investigation into this soluble form of IL1RAPL1, and whether it is produced *in vivo* is required. If IL1RAPL1 was secreted highly *in vivo*, then it could have potential as a serum biomarker for CRC diagnosis or monitoring of recurrence.

6.4.2. IL1RAPL1 Expression in Normal and Cancer Tissues

The Immunohistochemical analysis of IL1RAPL1 expression in normal and cancer tissues, found that IL1RAPL1 is significantly upregulated in CRC and oesophageal squamous cell carcinoma vs. corresponding normal tissues. IL1RAPL1 was not found to be highly expressed in the small cohort of PDAC specimens analysed. And most of the breast cancer specimens showed weak immunoreactivity, with only one section displaying some stronger immunoreactivity compared to normal breast. Information on the subtype of the breast cancer specimens analysed was not available, therefore IL1RAPL1 could potentially be differentially expressed between different breast cancer subtypes, however it was decided to focus on cancers of the GI tract for this study and examine IL1RAPL1 expression further in CRC and oesophageal cancer.

IL1RAPL1 was found to have limited expression in normal colon, with the majority (28/42) of specimens negative for IL1RAPL1 expression, with the remainder (12/42) mainly showing

weak and diffuse immunoreactivity. Just 2/42 specimens showed some strong immunoreactivity. IL1RAPL1 is also lowly expressed in the benign spectrum of colon disease. All benign specimens analysed (chronic inflammation of mucosa, polyps, hyperplasia of glandular epithelium and adenoma) showed either negative or weak and diffuse IL1RAPL1 immunoreactivity, indicating that IL1RAPL1 is not upregulated in the initial stages of normal colon transformation.

In contrast IL1RAPL1 was found to be strongly expressed in all CRC specimens analysed (adenocarcinoma, mucinous adenocarcinoma, carcinoid cancer and metastatic adenocarcinoma), which was determined to be a significant overexpression vs. normal colon by Chi-square test. 100% of the carcinoid cancer subtype showed strong IL1RAPL1 immunoreactivity (p-value <0.0001). Carcinoid cancer arises from neuroendocrine cells and is a rare subtype of CRC, with an incidence of approximately 2.5-5 cases per 100,000 CRC cases annually. (Ni, Sheng and Du, 2010) The sample size was very small (n=2), however as IL1RAPL1 has been predominantly found to be expressed in neurons, it is perhaps not surprising that it is strongly expressed in cancer arising from neuroendocrine cells, which interact with the neuronal system. Investigation of a larger patient cohort of carcinoid tumours would need to be carried out to determine if this is a consistent overexpression in this subtype.

The majority (66.7%) of colon adenocarcinoma specimens analysed highly overexpress IL1RAPL1 vs. normal colon (p-value <0.0001). There is no apparent association between IL1RAPL1 expression and a particular mutational subset, with the majority of KRAS MT and WT, and BRAF MT and WT specimens showing strong IL1RAPL1 expression. Mucinous adenocarcinoma accounts for approx. 10-15% of CRC cases and is characterised by abundant mucous secretion comprising at least 50% of the tumour volume. (Hugen *et al.*, 2015) IL1RAPL1 was found to be strongly expressed in 46.7% of mucinous specimens analysed (p-value 0.0001). The metastatic cancer specimens were derived from lymph node metastases, with 47.2% of specimens showing strong IL1RAPL1 immunoreactivity (p-value <0.0001). IL1RAPL1 expression was not associated with the histopathological grade diagnosis of adenocarcinoma, mucinous or metastatic adenocarcinoma, but a higher percentage of the Grade 3 adenocarcinoma specimens showed strong IL1RAPL1 expression compared to Grade 1 and Grade 2 tumours. IL1RAPL1 expression is significantly associated with CRC, regardless of subtype. It appears to be specifically associated with malignant

transformation of colon cells, as low IL1RAPL1 expression was found in all specimens of the benign spectrum.

IL1RAPL1 expression was also assessed in oesophageal cancer, another cancer of the GI tract, as increased expression was found in oesophageal cancer vs. normal oesophagus in the preliminary IHC analysis. Oesophageal cancer is the eight most common form of cancer worldwide, and ranks sixth among all cancers in mortality. Despite advances in diagnostics and therapeutics, the prognosis for oesophageal cancer remains poor. There remains a need to elucidate further on the molecular mechanisms underlying this cancer type. The two main subtypes of oesophageal cancer are oesophageal squamous cell carcinoma (OSCC) and oesophageal adenocarcinoma (OAC). OSCC comprises approximately 90% of oesophageal cancer cases worldwide, however the incidence of OAC is increasing in Western countries. OAC arises from glandular cells in the distal oesophageal epithelium, with risk factors including exposure to tobacco smoke and the presence of gastroesophageal reflux disease, which triggers chronic inflammation and the development of intestinal metaplasia (Barrett's oesophagus), the precursor lesion to OAC. OSCC arises from the epithelial cell lining of the oesophagus and nearly 90% of the risk in developing OSCC can be attributed to tobacco and alcohol in Western countries. (Kato and Nakajima, 2013; Lin *et al.*, 2016)

A small oesophageal cancer test TMA was obtained to investigate the expression of IL1RAPL1, following the preliminary finding of increased IL1RAPL1 expression in a malignant oesophagus specimen vs. normal oesophagus (n=1). The test TMA had very small sample numbers, with 12 cases representing normal oesophagus and various oesophagus cancer subtypes. The majority of normal oesophagus specimens analysed did show some weak and diffuse IL1RAPL1 immunoreactivity, with negative expression observed in the remainder. The rarer cancer subtypes present on the TMA, including small cell undifferentiated carcinoma and carcinosarcoma, also showed negative or weak IL1RAPL1 immunoreactivity. Carcinoma in situ and OAC specimens both showed weak IL1RAPL1 expression. IL1RAPL1 was strongly expressed however in every OSCC specimen analysed, which was deemed a significant overexpression vs. normal oesophagus (p-value 0.0027). Therefore, IL1RAPL1 expression appears to be a specific feature of OSCC, and could perhaps have potential diagnostic application for this cancer type. However, as only a very small patient cohort was analysed for IL1RAPL1 expression, analysis in a larger patient cohort should be carried out to determine with more certainty if IL1RAPL1 overexpression

is specifically associated with OSCC, and found at low levels in the other oesophageal cancer types.

This study is the first investigation into IL1RAPL1 expression in CRC and oesophageal cancer, with IL1RAPL1 overexpression in CRC and OSCC a novel finding. As already discussed for LY6G6F, it would have been beneficial to have access to a larger CRC patient cohort, including larger numbers of the rarer subtypes (i.e. carcinoid tumours) to determine if IL1RAPL1 is consistently highly expressed across all CRC subtypes. Access to survival information also would have enabled us to determine if there is any association between IL1RAPL1 expression and survival in CRC patients. The investigation into IL1RAPL1 expression in oesophageal cancer was very preliminary, to determine if further investigation was warranted. It would have been beneficial to have access to a larger cohort of oesophageal cancer patient specimens, to follow up on the finding that IL1RAPL1 is specifically overexpressed in OSCC.

The expression of IL1RAPL1 in normal tissues was assessed by IHC analysis of a number of full-face tissue sections available to us from our collaboration with SVUH, and also commercial normal tissue TMAs. Most normal tissues showed negative or weak and diffuse IL1RAPL1 immunoreactivity. However stronger expression was noted in some normal tissues. Strong granular diffuse IL1RAPL1 immunoreactivity was observed in the pituitary gland, and isolated cells in the cerebral cortex were observed to have strong IL1RAPL1 immunoreactivity. This is not surprising, considering IL1RAPL1 is known to be localised in the brain. For the development of an antibody-based therapeutic against IL1RAPL1, the high expression of IL1RAPL1 in the brain should not be a cause for concern, as in general antibody therapeutics are too large to cross the blood brain barrier, which would limit the chances of off target toxicity. (Pardridge, 2005) Some strong IL1RAPL1 immunoreactivity was also observed in some of the normal tissues of the GI tract; 2/42 normal colon, 1/4 duodenum and 3/5 gastric specimens analysed showed some strong IL1RAPL1 immunoreactivity. In gastric epithelium, certain collections of individual cells were strongly positive for IL1RAPL1 expression with the remainder of the tissue showing negligible expression. This indicates that perhaps only a certain type of gastric cell is expressing IL1RAPL1, and the opinion of a pathologist will be sought, to determine if these IL1RAPL1 expressing cells represent a particular subset of gastric cells. In the colon and duodenum sections that displayed stronger staining, it was present in the luminal space of goblet cells

that line the crypts of these tissues, and it was difficult to determine in some cases if the immunoreactivity was in the cells or the extracellular space. This also resulted in difficulty in definitively determining if IL1RAPL1 is expressed in the highly proliferating cells of these tissues. The IHC analysis comparing serial normal tissue sections stained for IL1RAPL1 and Ki67, a marker of cellular proliferation, showed that IL1RAPL1 does not appear to be present in the proliferating cells of normal colon, but the results for duodenum and gastric epithelium were less clear cut. This analysis should be repeated on further tissue sections, to try and conclusively determine if IL1RAPL1 is present in highly proliferating normal cells. The reason for this analysis was to further assess if IL1RAPL1 could be a potential molecular target for therapeutic targeting, as minimal expression in the highly proliferating cells of normal tissues is a requirement to limit off-target toxicities. However, the limited expression of IL1RAPL1 overall in all normal tissues analysed, along with the strong expression in CRC and OSCC, indicates IL1RAPL1 could still have potential as a molecular target amenable to targeted therapeutics in these cancer types.

Strong IL1RAPL1 immunoreactivity was potentially observed in immune cells responding to the invasive front of a CRC tumour (see Figure 5.6), with IL1RAPL1 expression also observed in the "immune" cells of several other CRC tumours and also to a lesser extent in some normal colon specimens. Innate immune cells, such as macrophages, NK cells and dendritic cells can respond to inflammatory signals generated by damaged tissue and cancer cells. As discussed in Section 1.1.3, colon cancer is associated with the infiltration of a variety of different immune cells, which can play an important role in CRC pathogenesis, promoting angiogenesis, tumour proliferation and invasion. A study on cultured macrophages suggest that they respond to IL-38 through IL1RAPL1, as these cells were found to not express the IL-36 receptor but did express IL1RAPL1. (Mora *et al.*, 2016) Macrophages compose the largest immune population found in the tumour microenvironment and are also resident in normal colon, as part of the innate immune system. As discussed in Section 1.1.3.2, macrophages can polarise into two distinct subsets: pro-inflammatory M1 macrophages and anti-inflammatory M2 macrophages. M1 are anti-tumour and M2 are pro-tumour. Resident macrophages in normal colon are considered to be M2 macrophages as they are recruited from circulating monocytes which exhibit an inflammatory phenotype, but are subsequently polarised into anti-inflammatory macrophages in response to signals from the intestinal mucosa. IL1RAPL1 immunoreactivity was not observed in "immune" cells of any of the

chronic inflammation of colon mucosa tissue specimens. Chronic inflammation in colon (e.g. inflammatory bowel disease) is associated with massive infiltrate of pro-inflammatory/M1 macrophages. (Smith *et al.*, 2011; Kühl *et al.*, 2015) Therefore based on the observations in this study of IL1RAPL1 immunoreactivity in the colon specimens, and the fact that IL1RAPL1 has been reported as being expressed in cultured macrophages, IL1RAPL1 expression could be associated in particular with M2 macrophages.

However, it also must be said that IL1RAPL1 immunoreactivity in "immune" cells was more likely to be observed in the full-face tissue sections as opposed to TMA cores, as these provide much larger sections of tissue. All of the chronic inflammation tissues were from the TMA, therefore it could be possible that these didn't offer a big enough tissue section to observe any potential "immune" cells with IL1RAPL1 immunoreactivity. As there is no definite evidence that the IL1RAPL1 expression is on macrophages, IL1RAPL1 could be expressed on a number of other immune cells found in the colon microenvironment, such as dendritic cells, NK cells, mast cells or T-cells. Confirmation of the exact cell type observed to have IL1RAPL1 expression needs to be carried out. The CRC tissue sections could be stained for specific markers of immune cells to identify the type with IL1RAPL1 immunoreactivity. Barros *et al.*, (2013) described a double-staining IHC approach for the identification of M1 and M2 macrophages in tissues. They found that CD68 or CD163 in combination with pSTAT1 or RBP-J can be used to identify M1 macrophages, while in combination with CMAF they can identify M2 macrophages. Other immune cells can also be identified by a variety of markers, e.g. dendritic cells ($CD11c^+$, $HLA\text{-}DR^+$), NK cells ($CD3^-$, $CD56^+$, $CD94^+$, $NKp46^+$) and Treg cells ($CD8^+$, $CD4^+$, $Foxp3^+$). If IL1RAPL1 is expressed on tumour associated immune cells, then this could also have therapeutic potential, as there is increasing interest in targeting elements of the tumour microenvironment that contribute to tumour growth and invasiveness. For example, the high density of TAMs found in triple-negative breast cancer has been proposed as a potential target to control tumour growth. TAM targeted therapy in a mouse model of triple negative breast cancer was shown to decrease TAM population in tumours and inhibit tumour growth. (Niu *et al.*, 2016)

6.4.3. IL1RAPL1 Cellular Localisation

The predicted cellular localisation of IL1RAPL1 at the membrane, was confirmed by Bahi *et al.*, (2003) by Immuofluorescence staining of an IL1RAPL1 stably transfected CHO cell line. Our findings linked IL1RAPL1 to an association with the membrane of CRC, PDAC and breast cancer cell lines, with detection of IL1RAPL1 in the membrane enriched fraction of these cell lines by Western blot analysis. The Immunocytochemical analysis of fixed HCT116 and MIA PaCa-2 cells, showed only cytoplasmic localisation of IL1RAPL1 however. The Immunofluorescence analysis of fixed HCT116 and SW480 cells, also showed cytoplasmic localisation, with possibly some membrane localisation also. Overall the localisation of IL1RAPL1 on the surface of these cancer cell lines could not be confirmed. Attempts at optimisation of live cell Immunofluorescence to confirm if IL1RAPL1 is expressed on the cell surface are ongoing.

Similarly, the Immunohistochemical analysis of IL1RAPL1 expression in CRC and OSCC, showed mainly cytoplasmic immunoreactivity, with some membrane-like immunoreactivity observed in only a small number of cases. Therefore, despite being a predicted membrane localised protein, IL1RAPL1 does not appear to be localised to the membrane of the cancer tissues and cell lines analysed in this study. IL1RAPL1 may only be localised to the cell surface in response to certain stimuli/cellular signals.

6.4.4. Function of IL1RAPL1 in the Cancer Cell Phenotype

IL1RAPL1 has been shown to be significantly overexpressed in both CRC and OSCC compared to normal tissues in this study, which has not been previously reported in the literature. However, attempts to determine a possible function for IL1RAPL1 in the colon cancer cell phenotype *in vitro* were unsuccessful. Despite achieving transient siRNA mediated knockdown of IL1RAPL1 at the mRNA level, this was never translated into observable protein knockdown. Despite varying the time-points assayed post transfection (from 48-93hrs), no IL1RAPL1 protein knockdown was observed. Therefore, the effect of IL1RAPL1 knockdown on the cancer cell phenotype could not be assessed. IL1RAPL1 may have a long protein half-life in these cells, meaning the protein levels were not reduced even 93hrs post mRNA knockdown. The process of deubiquitination could have prevented the degradation of the protein already in the cell before mRNA knockdown. Ubiquitination is a

post-translational modification that generally directs proteins for degradation by the proteasome or by lysosomes, and deubiquitination can lead to protein stabilisation. (Stringer and Piper, 2011) Experiments were planned (but not yet carried out) to try and determine the protein half-life of IL1RAPL1 in these cells. Treating cells with a protein synthesis inhibitor, such as cycloheximide, in a time-course experiment, followed by Western blot analysis of the cell lysate for IL1RAPL1, could show at what time-point IL1RAPL1 protein degradation begins, with a comparison Western blot to a protein with a known short protein half-life.

In hindsight, a lot of time was spent optimising transfection conditions in the attempt to achieve siRNA mediated protein knockdown of IL1RAPL1, which could have been better spent on alternative methods to try and achieve this. Instead of transient knockdown with siRNA, stable knockdown of IL1RAPL1 could have been attempted by plasmid transfection of a short hairpin RNA (shRNA) sequence into the cells. The shRNA sequence would work in a similar way to the siRNA, targeting IL1RAPL1 mRNA to prevent protein translation, but as the shRNA sequence would be continuously expressed by the cells, unlike siRNA, it would allow for prolonged gene silencing. Therefore, if the issue was that IL1RAPL1 protein has a long half-life, this would allow time for the degradation of IL1RAPL1 already present in the cell at the time of vector transformation. The stable transfection of cells is quite time consuming initially, and it would be preferable to insert an shRNA sequence that is known to give high knockdown of IL1RAPL1 mRNA. However, if it worked, the effect of IL1RAPL1 protein knockdown on cellular function could have been assessed. Another method that could have been utilised is the CRISPR/Cas9 gene editing tool, to remove the IL1RAPL1 gene from the genome, and thus assess the impact on cellular function.

A different method that was considered to investigate the functional role of IL1RAPL1 *in vitro*, was antibody blocking, to inhibit the function of IL1RAPL1, rather than knocking it down. Treating cancer cells with an antibody directed against the extracellular domain of IL1RAPL1, could potentially block its function, allowing for subsequent functional analysis to assess the effect on cellular proliferation, migration and invasion. However, this was determined to not be a viable option in this study, as the costs of commercially available antibodies to IL1RAPL1 for such a large scale experiment would have been prohibitive. If we had generated our own mAb to IL1RAPL1, this could have been more easily achieved. Also, the analysis of the cellular localisation of IL1RAPL1 in the cancer cell lines examined in this study, casts some doubt on the suitability of the antibody blocking method, as no clear

membrane localisation of IL1RAPL1 was detected. If IL1RAPL1 is not expressed on the cell-surface, then the antibody would not be able to bind to inhibit its function.

The attempt to elucidate on a role for IL1RAPL1 in the colon cancer cell phenotype, by IL1RAPL1 overexpression in the SW480 cell line was also unsuccessful to date. IL1RAPL1 protein overexpression was not observed by Western blot analysis, however mRNA overexpression was also not conclusively confirmed, and the qRT-PCR and Western blot analysis was only carried out for one biological experiment to date. Time did not allow for further optimisation to try and successfully achieve protein overexpression for functional analysis. Similar to the LY6G6F overexpression experiment, if IL1RAPL1 mRNA was successfully overexpressed, then miRNA induced silencing of mRNA translation or post-translational modifications such as ubiquitination leading to excess protein degradation, could have prevented successful IL1RAPL1 overexpression. Co-Immunoprecipitation experiments to try and identify IL1RAPL1 interacting proteins, were also unsuccessful, which may have been due to the antibodies used not being suitable for IP. Therefore unfortunately, no function for IL1RAPL1 in the cancer cell phenotype could be determined.

IL1RAPL1 expression has mainly been reported in the brain to date, with a function in synapse formation and stabilisation reported. Compared to this expression in normal brain, IL1RAPL1 was reported to be underexpressed in brain tumour cell lines and xenograft models examined. (Smith *et al.*, 2006; McAvoy *et al.*, 2007) And its expression was also associated with the proneural subtype of glioblastoma multiforme. (Cruceru *et al.*, 2013) The overexpression of IL1RAPL1 in cancer has not been widely reported, with no known function for IL1RAPL1 in cancer pathogenesis. IL1RAPL1 has been shown to activate JNK in neuronal cells, therefore it potentially has a similar function in cancer cells. The JNK pathway represents one sub-group of MAP kinases that is activated primarily by cytokines and exposure to environmental stress, and has been implicated in oncogenic transformation. It's role in tumour development remains controversial however as various studies have linked JNK to both pro-oncogenic roles and tumour suppression. (Weston and Davis, 2007) High levels of JNK activity are found in several cancer cell lines however and a mouse model of intestinal cancer showed that ablation of the cJun gene or mutation of the JNK phosphorylation sites, reduced tumour number and size, and prolonged lifespan. (Nateri, Spencer-Dene and Behrens, 2005) Therefore if IL1RAPL1 is involved in JNK activation in CRC or OSCC, it could contribute to the cancer phenotype this way.

Additionally, miRNA involved in IL1RAPL1 gene silencing have been implicated in CRC pathogenesis. An analysis of the transcription factors (TF) and miRNA that regulate the expression of 158 IQ-related genes, found that IL1RAPL1 is a target for the TF MEF2 and the miRNAs hsa-miR-15b and hsa-miR-195. miRNA can regulate mRNA expression at the post-transcriptional level, by degradation or translational repression by binding the target gene with small complementary sequences. Both hsa-miR-15b and hsa-miR-195 belong to the miR-15 family, and can mediate wide gene silencing in the cell, with IL1RAPL1 a target for silencing for them both. (Zhao, Kong and Qu, 2014) Deregulated miRNAs and their role in cancer have attracted much attention in recent years. And miRNA hsa-miR-15b and hsa-miR-195 have both been reported to be downregulated in CRC. One study found that miR-195 was downregulated in CRC tissues and that restoration of miR-195 in the CRC cell lines HT29 and LoVo could reduce cell viability, promote cell apoptosis and suppress tumourigenicity. (Liu *et al.*, 2010) Another study showed that downregulation of miR-195 correlates with lymph node metastasis and poor prognosis in CRC and was an independent predictor of overall survival. (Wang *et al.*, 2012) In gastric cancer the downregulation of miR-15b was found to be concurrent with the upregulation of Bcl-2 protein, with a role suggested in the development of multi-drug resistance in gastric cancer. (Xia *et al.*, 2008) Another study found that miR-15b is significantly downregulated in the progression from non-neoplastic tissue to dysplasia and from dysplasia to cancer in CRC progression. (Kanaan *et al.*, 2012) Therefore the downregulation of these miRNAs in CRC suggests a potential mechanism for IL1RAPL1 overexpression in CRC.

6.5. Potential for LY6G6F and IL1RAPL1 as Molecular Targets for Therapeutic Antibody Targeting

LY6G6F and IL1RAPL1 have been investigated as potential molecular targets for antibody-based targeted therapeutics. They have both been found to show higher expression in tumours vs. normal tissues by Immunohistochemical analysis. LY6G6F has been shown to be overexpressed in colon adenocarcinoma, PDAC and gastric adenocarcinoma compared to normal tissues. IL1RAPL1 has been shown to be overexpressed in both OSCC and all subtypes of CRC. They also both show relatively limited expression in normal tissues and highly proliferating normal cells, which would enable selective targeting of cancer cells and limit off target toxicities. Target cell-surface localisation has been viewed as an important characteristic of potential molecular targets for therapeutic antibody targeting, with targets ideally expressed homogenously and at high density on the cancer cell surface. For potential ADC targets, it is also important that the antibody-antigen complex is internalised upon antibody binding. Despite predicted membrane localisation, to date we could not generate evidence by Immunofluorescence analysis (using commercial antibodies) that LY6G6F and IL1RAPL1 are presented on the cell surface of the CRC and PDAC cell lines analysed, even though membrane association was strongly suggested with observed expression of both targets in membrane enriched cell fractions. Intense LY6G6F membrane staining was observed in a number of tumours in the IHC analysis and was more likely to be associated with smaller groups of tumour cells e.g. tumour budding, an adverse prognostic factor in GI cancers. However, in the rest of the tumours, both LY6G6F and IL1RAPL1 showed mainly cytoplasmic staining. The failure to demonstrate cell-surface expression in PDAC and colon cancer cell lines, meant that target density on the cell surface and internalisation of the target upon antibody binding, could not be assessed.

The potential lack of cell-surface expression of LY6G6F and IL1RAPL1 in the cancers analysed, may not mean they are not amenable to therapeutic antibody targeting. Recent studies have shown that cell-surface localisation may not be necessary for antibodies to show therapeutic efficacy. Thura *et al.*, (2016) generated a mAb (PRL3-zumab) against an intracellular target, the tumour associated phosphatase PRL3, which is upregulated in multiple human cancers. Focusing on gastric cancer, they showed that despite being generated against an intracellular antigen, PRL3-zumab showed effective tumour suppression in a mouse model. Three possible mechanisms of anti-tumour activity by mAbs

against intracellular antigens were proposed: Antibody penetration into cells (anti-PRL3 antibodies were observed to be internalised by PRL3 expressing tumour cells *in vitro*; however this mode of action remains poorly defined), antibody binding to externalised antigen (supposed intracellular antigens have been reported to be externalised via secretion or cell surface re-localisation) and antibody recognition of MHC-bound antigen-derived peptides. The TCRm mAbs, mentioned in Section 1.3.4., also utilise intracellular antigen-derived peptides, presented on the cell-surface in the context of HLA, to target cancer cells. Therefore, intracellular antigens can be amenable to therapeutic antibody targeting in certain circumstances.

Both LY6G6F and IL1RAPL1 were observed as highly expressed in colon adenocarcinoma regardless of the presence of mutations in KRAS and BRAF genes (in the small number of tissues analysed with known KRAS/BRAF mutational status), suggesting their potential as targets in a large range of CRC tumours. The only currently approved antibody therapy that directly targets CRC tumour cells, is the unconjugated anti-EGFR mAb, Cetuximab (the other approved mAb, Bevacizumab, targets VEGF in the tumour microenvironment). EGFR and its associated downstream signalling pathways are involved in many malignant processes, including growth and invasion. Therefore, inhibition of EGFR activation, has been considered an important therapeutic target. EGFR is expressed in approximately 70-80% of CRC tumours, however only those that also express the KRAS wildtype gene are suitable for anti-EGFR therapy. Patients with activating KRAS mutations do not respond to Cetuximab. KRAS mutation testing is currently used as standard of care in metastatic CRC patients, to identify those that will benefit from anti-EGFR therapy. Recent studies suggest that patients with BRAF mutations are also associated with a lack of response to anti-EGFR therapy. (Watkins and Cunningham, 2007; Gonzalez-Pons and Cruz-Correa, 2015) As KRAS and BRAF mutations are present in approximately 40% and 5-10% of CRCs respectively, there is a significant patient population that cannot benefit from the only currently approved mAb targeting CRC tumour cells. (Fearon, 2011) Both mAbs currently approved (Cetuximab and Bevacizumab), are approved for metastatic CRC patients only, and overall have limited clinical efficacy. Therefore, there is a desperate need for the identification of other targets in CRC, that could be targeted by specific mAbs to improve survival of CRC patients. LY6G6F and IL1RAPL1 expression needs to be investigated in larger cohorts of CRC tumours with

wildtype and mutated KRAS and BRAF genes, to determine if they are consistently expressed regardless of mutational status.

This study has shown that knockdown of LY6G6F in a colon and pancreatic cancer cell line, led to a decrease in FAK activation, an increase in apoptosis and a significant reduction in the proliferation, migration and invasion of these cells *in vitro*, a finding which has not been previously reported in the literature. Higher LY6G6F expression was also associated with poorer prognosis vs. low LY6G6F expression in the PDAC patient cohort analysed in the Immunohistochemical analysis and in gastric cancer patients in the KM plotter analysis. Therefore, LY6G6F could potentially be utilised as an unconjugated mAb target, similar to EGFR, to inhibit LY6G6F activation and potentially inhibit tumour growth and invasion. Inhibitory mAbs are generally more effective however, when they also engage host defence mechanisms, resulting in CDC or ADCC of the tumour cells.

The potentially secreted form of IL1RAPL1 observed in this study (the lower molecular weight band detected in conditioned medium from cancer cells by Western blot analysis; see Figure 5.3) could have implications for its suitability as a potential molecular target for antibody based therapy. It has generally been assumed that the secretion of target antigen by cancer cells, is not an ideal characteristic, in particular for ADC targets, as soluble antigen in the tumour microenvironment can bind ADCs, thus limiting the amount of ADC free to bind tumour cells and therefore decreasing efficacy. However, recent studies have shown that ADCs that either do not internalise or that target elements in the tumour microenvironment, can still show potent anti-tumour activity, through the release of cytotoxic drug at the tumour site, exposing the tumour cells to drug indirectly or helping to dismantle the tumour microenvironment. (Gébleux *et al.*, 2017) Further investigation into this potentially secreted form of IL1RAPL1 is required, however if IL1RAPL1 is secreted highly *in vivo* then it could have potential as a serum biomarker for CRC diagnosis or monitoring of recurrence. There are currently only two blood-based biomarkers available to monitor CRC patients, carcinoembryonic antigen (CEA) and carbohydrate antigen 19-9 (CA19-9). CA19-9 is less sensitive and specific for CRC compared to CEA, which is the only acceptable tumour marker to monitor CRC recurrence to date. Elevated CEA serum levels are a poor prognostic factor for resectable CRC and correlate with cancer progression. CEA levels decrease after tumour resection, which are then monitored to check for disease recurrence. CEA is not suitable as a diagnostic marker for CRC screening as elevated levels are only detected in

advanced stages of a fraction of all CRC patients. The discovery of an effective blood-based screening method for CRC diagnosis would be ground breaking and likely increase patient adherence over current screening methods, such as the faecal occult blood testing and colonoscopy. (Gonzalez-Pons and Cruz-Correa, 2015) IL1RAPL1 was not expressed by 100% of all CRC specimens analysed, therefore if it is secreted *in vivo*, it is not likely to have potential as a single marker for CRC screening. A panel of serum biomarkers is likely to show more sensitivity and specificity for CRC diagnosis over a single biomarker.

There is increasing interest in targeting elements of the tumour microenvironment that contribute to tumour growth and progression, including tumour-infiltrating immune cells, and antigens in the tumour vasculature and stroma. Several target antigens in the tumour stroma are currently under research as potential therapeutic targets, including Collagen IV, Fibronectin extra-domain B and Tenascin C. (Diamantis and Banerji, 2016) Targeting of tumour-associated macrophages in a mouse model of triple negative breast cancer has been shown to inhibit tumour growth. (Niu *et al.*, 2016) Both LY6G6F and IL1RAPL1 expression has been observed in the stroma of tumour specimens; LY6G6F in possibly fibroblast-like cells in the stroma of PDAC and IL1RAPL1 in potentially immune cells of the CRC microenvironment. The precise cellular component displaying target immunoreactivity needs to be confirmed for both targets, but shows that LY6G6F and IL1RAPL1 could also have potential as targets for therapeutic targeting of the tumour microenvironment.

Overall this study has identified LY6G6F and IL1RAPL1 as novel targets overexpressed in GI cancers vs. normal tissues. LY6G6F was found to be overexpressed in 70% of colon adenocarcinoma, 78.9% of PDAC and 50% of gastric adenocarcinoma tumour specimens analysed. IL1RAPL1 was found to be overexpressed in 66.7% of colon adenocarcinoma, 100% of colon carcinoid and 100% of oesophageal squamous cell carcinoma specimens analysed. These expression levels are comparable to other targets that are currently in clinical development as ADC targets in GI cancers, e.g. GCC, which is expressed in approximately 60-70% of pancreatic, gastric and oesophageal cancers and by 95% of CRCs. (Almhanna *et al.*, 2016). Further investigation of LY6G6F and IL1RAPL1, and elucidation of their role in these cancers will be required to ascertain their full potential as targets for therapeutic antibody targeting.

6.6. Conclusions

Two lists were generated in-house by profiling of publicly available colon cancer gene expression microarray data from normal colon, adenoma and adenocarcinoma tissue sections. (1) A list of 1078 genes upregulated in adenoma vs. normal colon. (2) A list of 1238 genes upregulated in adenocarcinoma vs. normal colon. These gene lists were then annotated for membrane localisation and a fold change of ≥ 2 and an adjusted p-value of $\leq 1E^{-5}$ was considered significant. This produced the final lists of predicted membrane localised genes. (1) 154 genes upregulated in adenoma vs. normal colon. (2) 127 genes upregulated in adenocarcinoma vs normal colon. Candidate targets were selected for validation based on relative novelty in CRC by literature review and also based on commercial antibody availability. Seven candidate targets were identified for validation of expression at the protein level in CRC, and if promising, for subsequent investigation in further cancer types and investigation of their potential as molecular targets that may be amenable to therapeutic antibody targeting.

- The seven candidate targets selected for validation of expression at the protein level in colon cancer cell lines and normal colon and CRC tissue sections were: LY6G6F, IL1RAPL1, IL20RA, BACE2, NTM, EPHX4 and LRRC8E.
- The expression of all seven targets was detected in both the whole cell lysate and membrane enriched fraction of a panel of six colon cancer cell lines. This indicates an association with the membrane in these cell lines.
- Expression in normal colon and CRC tissues specimens could not be assessed for two of the targets, EPHX4 and LRRC8E. Therefore, they were not pursued further.
- NTM showed strong immunoreactivity in some of the CRC tissue specimens analysed. However, a similar level of expression was observed in normal colon. Therefore, NTM does not appear to be upregulated in CRC and was not chosen to pursue further.
- IL20RA showed strong membrane immunoreactivity in CRC tissues, and also in PDAC tissues. However strong expression was also detected in normal tissues including colon, pancreas and duodenum. Therefore, IL20RA does not appear to be upregulated in CRC or PDAC compared to corresponding normal tissues, and does

not fit the criteria for a molecular target to be amenable to therapeutic antibody targeting, and was not pursued further.

- BACE2 showed strong immunoreactivity in some CRC and PDAC tissues, with strong expression also detected in normal colon and pancreas however. Weak BACE2 immunoreactivity was observed in normal duodenum, gastric tissue and oesophagus. Therefore, BACE2 appears to be endogenously expressed at a higher level in normal colon and pancreas, with no overall overexpression detected in CRC or PDAC. Therefore, BACE2 was not pursued further as a candidate target.
- Two targets, LY6G6F and IL1RAPL1, successfully met the criteria in the initial validations to warrant further analysis of their expression in cancer and investigation of their potential as molecular targets amenable to therapeutic antibody targeting. Both LY6G6F and IL1RAPL1 showed minimal immunoreactivity in normal colon and strong immunoreactivity in CRC tissue sections. Their expression was also detected in both the whole cell and membrane enriched fraction across the colon cancer cell line panel analysed.

1) LY6G6F was found to be significantly overexpressed in colon adenocarcinoma, gastric adenocarcinoma and PDAC compared to corresponding normal tissues. Functional studies on LY6G6F in any of these cancer types have not previously been reported in the literature.

- LY6G6F is significantly overexpressed in both the benign spectrum of colon disease and colon adenocarcinoma tissue specimens. High LY6G6F expression was found in tissues representing hyperplasia of glandular epithelium, polyps, adenoma and adenocarcinoma. This suggests a role for LY6G6F in the initial abnormal transformation of normal colon cells, and potential to be utilised as an early diagnostic marker.
- High LY6G6F expression is not associated with the other CRC subtypes analysed. Low expression was detected in metastatic adenocarcinoma, mucinous adenocarcinoma and carcinoid tumours.

- LY6G6F is significantly overexpressed in PDAC vs. normal pancreas, with a trend towards decreased survival observed in patients with high LY6G6F expression vs. low LY6G6F expression.
- LY6G6F is significantly overexpressed in gastric adenocarcinoma vs. normal gastric epithelium in the small cohort analysed. This could be assessed further in a larger patient cohort.
- LY6G6F shows minimal expression in the majority of normal tissues and does not appear to be expressed in the highly proliferating cells of normal tissues. Strong LY6G6F expression was observed in the stroma of PDAC and some normal tissues. The identification of this cell type needs to be confirmed.
- LY6G6F expression was detected in the whole cell and membrane enriched fraction of every CRC and PDAC cell line analysed by Western blot analysis. Subsequent qRT-PCR analysis revealed that the LY6G6F mRNA transcript is expressed at low abundance levels in these cells and did not correspond to protein levels observed. This suggests LY6G6F protein expression levels are likely regulated after translation in these cell lines.
- Transient siRNA knockdown of LY6G6F in the colon cancer cell line HCT116 and the PDAC cell line MIA PaCa-2 was found to significantly decrease the proliferation of these cells, as determined by both the acid phosphastase assay and the 2D colony formation assay. A significant decrease in migration and invasion levels was also observed.
- The knockdown of LY6G6F in these cells was subsequently found to cause an increase in apoptosis (determined by an increase in PARP cleavage) and a decrease in FAK activation. The reduction of FAK activation could potentially be the mediator of the increase in apoptosis, and decrease in cell proliferation, migration and invasion observed following LY6G6F knockdown.
- Taken together with the Kaplan-Meier survival analysis of the PDAC patient cohort, which showed decreased survival in patients with high LY6G6F expression, these functional studies implicate LY6G6F in the growth and survival of these cancers.
- To date, the localisation of LY6G6F in cancer cell lines and tissues was mainly observed to be cytoplasmic. Localisation on the surface of cancer cells was not confirmed by Immunohistochemical or Immunofluorescence analysis.

2) IL1RAPL1 was identified as a novel overexpressed protein in CRC and OSCC. IL1RAPL1 overexpression in these cancers has not previously been reported in the literature and no functional studies on IL1RAPL1 in cancer have been carried out to date.

- IL1RAPL1 is lowly expressed in normal colon and the benign spectrum of colon disease (chronic inflammation, hyperplasia, polyps and adenoma).
- IL1RAPL1 is significantly overexpressed in all CRC subtypes analysed, with the highest degree of overexpression observed in carcinoid tumours, followed by adenocarcinoma, metastatic adenocarcinoma and mucinous adenocarcinoma specimens.
- IL1RAPL1 may have particular relevance in the carcinoid tumour subtype, which arises from neuroendocrine cells, as 100% of these specimens showed high IL1RAPL1 expression (although sample size was very small; n=2), and as IL1RAPL1 is known for its expression in neurons.
- High IL1RAPL1 expression is significantly associated with OSCC compared to normal oesophagus and other oesophageal cancer subtypes, including OAC. However, sample size was very small and these results should be confirmed in a larger patient cohort.
- The majority of normal tissues analysed showed weak IL1RAPL1 immunoreactivity. However, the strong expression observed in cells of some normal tissues (e.g. isolated cells in gastric epithelium, potentially immune cells in normal colon and CRC) needs to be investigated further. The presence of IL1RAPL1 expression in the highly proliferating cells of some normal tissues could also not be conclusively determined, with possible expression in the proliferating cells of normal duodenum and gastric tissue observed.
- IL1RAPL1 expression was detected in the whole cell lysate and membrane enriched fraction of all cell lines analysed in the CRC, PDAC and breast cancer cell line panels. Western blot analysis also revealed the presence of a potentially soluble/secreted isoform of IL1RAPL1 detected in cancer cell conditioned medium and expressed by all PDAC cell lines and three of the colon cancer cell lines.
- Transient siRNA knockdown of IL1RAPL1 successfully reduced mRNA levels, as determined by qRT-PCR analysis. However, protein knockdown could not be

observed by Western blot analysis, despite numerous optimisations, including time-course experiments. This suggests IL1RAPL1 may have a long protein half-life.

- Investigation of the functional role of IL1RAPL1 in the colon cancer cell phenotype *in vitro*, could not be determined due to the lack of protein knockdown observed.
- To date, the localisation of IL1RAPL1 in cancer cell lines and tissues was mainly observed to be cytoplasmic.

❖ Overall two novel candidate targets, LY6G6F and IL1RAPL1, successfully validated out of the seven selected from the microarray data and were found to be significantly overexpressed in a number of GI cancers.

❖ The overexpression of IL1RAPL1 in CRC and OSCC and the protein overexpression of LY6G6F in PDAC and gastric cancer is a novel finding.

❖ LY6G6F is potentially involved in the proliferation and survival of CRC, PDAC and gastric cancer.

❖ Both LY6G6F and IL1RAPL1 show preliminary potential as molecular targets that may be amenable to therapeutic antibody targeting, however further investigation is required.

6.7. Future Work

1) LY6G6F was found to be overexpressed in colon adenocarcinoma, PDAC and gastric adenocarcinoma compared to normal tissues, with a functional role in colon cancer and PDAC cell lines. There are a number of follow up experiments which could be carried out to further clarify the expression and functional role of LY6G6F.

- Generation of mAbs against either the whole LY6G6F protein or a peptide sequence of LY6G6F predicted to be highly immunogenic (peptide prediction studies have been carried out in collaboration with CRB, UK.) by hybridoma technology would facilitate further localisation and functional studies. A good antibody is crucial for further investigation of this target and a phenotypic hybridoma screen could isolate a functional blocking antibody and antibody suitable for localisation studies.
- Further investigation of the cellular localisation of LY6G6F could be carried out with a generated mAb using confocal microscopy and flow cytometry. If such studies can confirm membrane localisation then the density of LY6G6F on the cell surface can be determined by quantitative flow cytometry.
- If cell-surface localisation is confirmed, then internalisation of the antigen-antibody complex can be investigated by time-lapse microscopy using a fluorescently tagged mAb or using an assay such as the Fab-ZAP antibody internalisation kit.
- LY6G6F was found to be significantly overexpressed in gastric adenocarcinoma vs. normal gastric epithelium. However, the overexpression was observed in just 50% of the cancer specimens and in a small patient cohort. Therefore, LY6G6F expression could be investigated in a larger patient cohort to assess whether it is consistently overexpressed in gastric adenocarcinoma and whether LY6G6F overexpression is associated with a particular subtype, pathological feature or survival in gastric cancer.
- LY6G6F was found to be significantly overexpressed in colon adenocarcinoma regardless of KRAS or BRAF mutational status and also appears to be associated with MSS phenotype. However, this sample size was very small, therefore LY6G6F expression should be investigated in larger cohorts of CRC tumours to determine if LY6G6F is consistently expressed regardless of mutational status and if consistently associated with MSS over MSI phenotype. Any association between LY6G6F expression and survival in CRC should also be investigated.

- In the PDAC patient cohort analysed, high LY6G6F expression showed a trend towards decreased survival. Analysis of a larger PDAC patient cohort may lead to a significant association between high LY6G6F expression and decreased survival in PDAC.
- LY6G6F expression was observed in the stroma of PDAC and some normal tissues. The precise cell type should be determined; PDAC sections could be stained for various cell markers e.g. α-SMA on CAFS, and markers of various immune cells, such as TAMs (CD68, CD163) and Treg cells ($CD8^+$, $CD4^+$, $Foxp3^+$).
- Lower LY6G6F expression was observed in the metastatic CRC tumours derived from lymph node metastases. LY6G6F expression should be investigated in a larger metastatic CRC cohort and also in PDAC metastases, to determine if LY6G6F is consistently lowly expressed in metastatic tumours and thus whether a potential LY6G6F targeted therapeutic could have application in the metastatic disease setting.
- LY6G6F was more likely to be observed as membrane-localised in smaller tumour ducts and budding of CRC and PDAC. Tumour budding is associated with partial EMT. Therefore, serial tissue sections could be stained for markers of EMT (e.g. mesenchymal markers, vimentin and N-cadherin) to determine if LY6G6F expression is associated with tumour cells undergoing EMT.
- Transient siRNA knockdown of LY6G6F in HCT116 and MIA PaCa-2 cells decreased the proliferation, migration and invasion of these cells. Further functional assays could be carried out with both siRNA and a LY6G6F blocking antibody from the mAb generation. Anoikis assays and 3D soft agar colony formation assays could further elucidate on the function of LY6G6F in these cells.
- Preliminary Western blot analysis of signalling pathways affected by LY6G6F knockdown, showed a decrease in FAK phosphorylation in both the HCT116 and the MIA PaCa-2 cell line. Reverse phase protein array (RPPA) profiling could be carried out to look at a wider range of phosphorylated protein changes following both siRNA transfections and functional antibody blocking of cells (in collaboration with Prof. Bryan Hennessey's group in RCSI, Beaumont, Dublin).
- The ADCC activity of a mAb targeting LY6G6F could also be assessed using an *in vitro* ADCC assay. The activation of ADCC is important for the therapeutic efficacy of unconjugated mAbs.

- Transient siRNA knockdown of LY6G6F in HCT116 and MIA PaCa-2 cells caused an increase in apoptosis, as determined by increased PARP cleavage detected by Western blot analysis. More extensive apoptosis and cell cycle assays should be carried out. E.g Annexin-V Apoptosis assay (TUNEL assay), which enables the quantification of live, dead and early or late apoptotic cells in a sample. Cell cycle arrest could be analysed by BrdU staining of cells for DNA content, which would allow analysis of the cells through the full cycle (G0/G1, S and G2/M).
- *In vivo* studies could be carried out to further investigate the function of LY6G6F. LY6G6F gene knockout mice could be generated to observe any phenotypic changes, and thus elucidate further on the function of LY6G6F in normal tissues.
- Patient derived xenograft (PDX) models of PDAC have already been established in DCU. The biodistribution of LY6G6F in these tumour xenograft mouse models of PDAC could potentially be assessed using a radiolabelled mAb or antibody-targeted nanoparticles, in collaboration with Dr. Sandra Roche.
- PDX cell lines have also been established from these PDAC xenograft mouse models, which are low passage, and could be examined for LY6G6F expression and used for further functional studies.

2) IL1RAPL1 was found to be overexpressed in CRC and OSCC. A role for IL1RAPL1 in the cancer cell phenotype could not be determined. Follow up work that could be carried out includes:

- As already described for LY6G6F, generation of mAbs against IL1RAPL1 would facilitate further localisation and functional studies. The localisation of IL1RAPL1 could be further investigated using confocal microscopy and flow cytometry. If such studies can confirm membrane localisation then the density of IL1RAPL1 on the cell-surface and investigation of internalisation can be carried out as described for LY6G6F.
- A functional role for IL1RAPL1 in the colon cancer cell phenotype could not be assessed, as siRNA mediated knockdown of IL1RAPL1 protein could not be achieved. A generated mAb targeting IL1RAPL1 could potentially be used for functional blocking to assess the effect on the cancer cell phenotype, including *in vitro* proliferation, 2D and 3D colony formation, migration, invasion and anoikis assays.
- IL1RAPL1 was found to be strongly expressed in the rare carcinoid subtype of CRC, however sample size was very small, therefore a larger patient cohort should be analysed for IL1RAPL1 expression.
- IL1RAPL1 was found to be significantly overexpressed in a small sample size of colon adenocarcinoma regardless of KRAS or BRAF mutational status. IL1RAPL1 expression should be investigated in larger cohorts of CRC tumours to determine if IL1RAPL1 is consistently expressed regardless of mutational status and should also be investigated in MSS and MSI tumours. Any association between IL1RAPL1 expression and survival in CRC could also be investigated.
- IL1RAPL1 was found to be specifically overexpressed in OSCC, compared to other oesophageal cancer subtypes. However, this analysis was in a very small patient cohort. Investigation of IL1RAPL1 expression in a larger patient cohort of all oesophageal cancer subtypes, would show if IL1RAPL1 overexpression is consistently associated with the OSCC subtype.
- IL1RAPL1 expression was potentially observed in immune cells of normal colon and CRC. These tissue sections could be stained for markers associated with different types of immune cells e.g. TAMs (CD68, CD163), dendritic cells ($CD11c^+$, HLA-

DR^+), NK cells ($CD3^-$, $CD56^+$, $CD94^+$, $NKp46^+$) and Treg cells ($CD8^+$, $CD4^+$, $Foxp3^+$), to identify the cell type and further elucidate on the expression of IL1RAPL1 in normal and cancer tissues.

- IL1RAPL1 protein knockdown could not be achieved, possibly due to a long protein half-life. The protein half-life of IL1RAPL1 in the colon cancer cell lines could be determined by carrying out protein half-life experiments i.e. by treating cells with cycloheximide in a time-course experiment.
- The potential soluble isoform of IL1RAPL1 needs to be investigated further, and could be investigated in CRC patient serum samples.
- Further optimisation of the IL1RAPL1 overexpression work that was started could be carried out. The qRT-PCR needs to be repeated with a different endogenous control gene to determine if IL1RAPL1 mRNA was overexpressed. Then if protein overexpression is achieved, the effect on the cancer cell phenotype can be determined by a number of *in vitro* functional assays, including proliferation, migration and invasion assays.

Chapter 7. Bibliography:

Alley, S. C., Okeley, N. M. and Senter, P. D. (2010) 'Antibody–drug conjugates: targeted drug delivery for cancer', *Current Opinion in Chemical Biology*, 14(4), pp. 529–537. doi: 10.1016/j.cbpa.2010.06.170.

Almhanna, K., Kalebic, T., Cruz, C., Faris, J. E., Ryan, D. P., Jung, J., Wyant, T., Fasanmade, A. A., Messersmith, W. and Rodon, J. (2016) 'Phase I Study of the Investigational Anti-Guanylyl Cyclase Antibody-Drug Conjugate TAK-264 (MLN0264) in Adult Patients with Advanced Gastrointestinal Malignancies', *Clinical Cancer Research*, 22(20), pp. 5049–5057. doi: 10.1158/1078-0432.CCR-15-2474.

Amado, R. G., Wolf, M., Peeters, M., Van Cutsem, E., Siena, S., Freeman, D. J., Juan, T., Sikorski, R., Suggs, S., Radinsky, R., Patterson, S. D. and Chang, D. D. (2008) 'Wild-Type *KRAS* Is Required for Panitumumab Efficacy in Patients With Metastatic Colorectal Cancer', *Journal of Clinical Oncology*, 26(10), pp. 1626–1634. doi: 10.1200/JCO.2007.14.7116.

Aslam, M. I., Kelkar, A., Sharpe, D. and Jameson, J. S. (2010) 'Ten years experience of managing the primary tumours in patients with stage IV colorectal cancers', *International Journal of Surgery*, 8(4), pp. 305–313. doi: 10.1016/j.ijsu.2010.03.005.

Augsten, M. (2014) 'Cancer-associated fibroblasts as another polarized cell type of the tumor microenvironment', *Frontiers in oncology*, 4.

Ayyar, B. V., Arora, S. and O'Kennedy, R. (2016) 'Coming-of-Age of Antibodies in Cancer Therapeutics', *Trends in Pharmacological Sciences*, 37(12), pp. 1009–1028. doi: 10.1016/j.tips.2016.09.005.

Bachem, M. G., Schneider, E., Gross, H., Weidenbach, H., Schmid, R. M., Menke, A., Siech, M., Beger, H., Grünert, A. and Adler, G. (1998) 'Identification, culture, and characterization of pancreatic stellate cells in rats and humans.', *Gastroenterology*, 115(2), pp. 421–32.

Bahi, N., Friocourt, G., Carrié, A., Graham, M. E., Weiss, J. L., Chafey, P., Fauchereau, F., Burgoyne, R. D. and Chelly, J. (2003) 'IL1 receptor accessory protein like, a protein involved in X-linked mental retardation, interacts with Neuronal Calcium Sensor-1 and regulates exocytosis', *Human Molecular Genetics*, 12(>12), pp. 1415–1425. doi: 10.1093/hmg/ddg147.

Bailey, C., Negus, R., Morris, A., Ziprin, P. and Goldin, R. (2007) 'Chemokine expression is associated with the accumulation of tumour associated macrophages (TAMs) and progression in human colorectal cancer', *Clinical & experimental*, 24(2), pp.121-130.

Bailey, P., Chang, D. K., Nones, K., Johns, A. L., Patch, A.-M., Gingras, M.-C., Miller, D. K., Christ, A. N., Bruxner, T. J. C., Quinn, M. C., Nourse, C., Murtaugh, L. C., Harliwong, I., Idrisoglu, S., Manning, S., Nourbakhsh, E., Wani, S., Fink, L., Holmes, O., Chin, V., Anderson, M. J., Kazakoff, S., Leonard, C., Newell, F., Waddell, N., Wood, S., Xu, Q., Wilson, P. J., Cloonan, N., Kassahn, K. S., Taylor, D., Quek, K., Robertson, A., Pantano, L., Mincarelli, L., Sanchez, L. N., Evers, L., Wu, J., Pinese, M., Cowley, M. J., Jones, M. D., Colvin, E. K., Nagrial, A. M., Humphrey, E. S., Chantrill, L. A., Mawson, A., Humphris, J., Chou, A., Pajic, M., Scarlett, C. J., Pinho, A. V., Giry-Laterriere, M., Rooman, I., Samra, J.

S., Kench, J. G., Lovell, J. A., Merrett, N. D., Toon, C. W., Epari, K., Nguyen, N. Q., Barbour, A., Zeps, N., Moran-Jones, K., Jamieson, N. B., Graham, J. S., Duthie, F., Oien, K., Hair, J., Grützmann, R., Maitra, A., Iacobuzio-Donahue, C. A., Wolfgang, C. L., Morgan, R. A., Lawlor, R. T., Corbo, V., Bassi, C., Rusev, B., Capelli, P., Salvia, R., Tortora, G., Mukhopadhyay, D., Petersen, G. M., Munzy, D. M., Fisher, W. E., Karim, S. A., Eshleman, J. R., Hruban, R. H., Pilarsky, C., Morton, J. P., Sansom, O. J., Scarpa, A., Musgrove, E. A., Bailey, U.-M. H., Hofmann, O., Sutherland, R. L., Wheeler, D. A., Gill, A. J., Gibbs, R. A., Pearson, J. V., Waddell, N., Biankin, A. V. and Grimmond, S. M. (2016) 'Genomic analyses identify molecular subtypes of pancreatic cancer', *Nature*, 531(7592), pp. 47–52. doi: 10.1038/nature16965.

Baker, S. J., Fearon, E. R., Nigro, J. M., Hamilton, S. R., Preisinger, A. C., Jessup, J. M., vanTuinen, P., Ledbetter, D. H., Barker, D. F., Nakamura, Y., White, R. and Vogelstein, B. (1989) 'Chromosome 17 deletions and p53 gene mutations in colorectal carcinomas.', *Science*, 244(4901), pp. 217–21.

Baker, S. J., Preisinger, A. C., Jessup, J. M., Paraskeva, C., Markowitz, S., Willson, J. K., Hamilton, S. and Vogelstein, B. (1990) 'p53 gene mutations occur in combination with 17p allelic deletions as late events in colorectal tumorigenesis.', *Cancer research*, 50(23), pp. 7717–22.

Bardeesy, N. and DePinho, R. A. (2002) 'Pancreatic cancer biology and genetics', *Nature Reviews Cancer*, 2(12), pp. 897–909. doi: 10.1038/nrc949.

Barreyro, L., Will, B., Bartholdy, B., Zhou, L. and Todorova, T. (2012) 'Overexpression of IL-1 receptor accessory protein in stem and progenitor cells and outcome correlation in AML and MDS', *Blood*, 120(6), pp.1290-1298.

Barros, M. H. M., Hauck, F., Dreyer, J. H., Kempkes, B. and Niedobitek, G. (2013) 'Macrophage polarisation: an immunohistochemical approach for identifying M1 and M2 macrophages.', *PloS one*, 8(11), p. e80908. doi: 10.1371/journal.pone.0080908.

Beatty, G. L., Chiorean, E. G., Fishman, M. P., Saboury, B., Teitelbaum, U. R., Sun, W., Huhn, R. D., Song, W., Li, D., Sharp, L. L., Torigian, D. A., O'Dwyer, P. J. and Vonderheide, R. H. (2011) 'CD40 Agonists Alter Tumor Stroma and Show Efficacy Against Pancreatic Carcinoma in Mice and Humans', *Science*, 331(6024), pp. 1612–1616. doi: 10.1126/science.1198443.

Beatty, G. L., Torigian, D. A., Chiorean, E. G., Saboury, B., Brothers, A., Alavi, A., Troxel, A. B., Sun, W., Teitelbaum, U. R., Vonderheide, R. H. and O'Dwyer, P. J. (2013) 'A Phase I Study of an Agonist CD40 Monoclonal Antibody (CP-870,893) in Combination with Gemcitabine in Patients with Advanced Pancreatic Ductal Adenocarcinoma', *Clinical Cancer Research*, 19(22), pp. 6286–6295. doi: 10.1158/1078-0432.CCR-13-1320.

Beliakov, I. S., Karakasheva, T. A. and Mazurenko, N. N. (2009) 'Exon-intron structure of the LY6G6D gene', *Molecular Biology*, 43(4), pp. 543–551. doi: 10.1134/S0026893309040025.

Berman, B. P., Weisenberger, D. J., Aman, J. F., Hinoue, T., Ramjan, Z., Liu, Y., Noushmehr, H., Lange, C. P. E., van Dijk, C. M., Tollenaar, R. A. E. M., Berg, D. Van Den and Laird, P. W. (2012) 'Regions of focal DNA hypermethylation and long-range hypomethylation in

colorectal cancer coincide with nuclear lamina-associated domains', *Nature Genetics*, 44(1), pp. 40–46. doi: 10.1038/ng.969.

Berman, D. M., Karhadkar, S. S., Maitra, A., Montes de Oca, R., Gerstenblith, M. R., Briggs, K., Parker, A. R., Shimada, Y., Eshleman, J. R., Watkins, D. N. and Beachy, P. A. (2003) 'Widespread requirement for Hedgehog ligand stimulation in growth of digestive tract tumours', *Nature*, 425(6960), pp. 846–851. doi: 10.1038/nature01972.

Birnbaum, D. J., Finetti, P., Lopresti, A., Gilabert, M., Poizat, F., Turrini, O., Raoul, J.-L., Delpero, J.-R., Moutardier, V., Birnbaum, D., Mamessier, E. and Bertucci, F. (2016) 'Prognostic value of PDL1 expression in pancreatic cancer.', *Oncotarget*, 7(44), pp. 71198–71210. doi: 10.18632/oncotarget.11685.

Blumberg, H., Conklin, D., Xu, W., Grossmann, A., Brender, T., Carollo, S., Eagan, M., Foster, D., Haldeman, B. A., Hammond, A., Haugen, H., Jelinek, L., Kelly, J. D., Madden, K., Maurer, M. F., Parrish-Novak, J., Prunkard, D., Sexson, S., Sprecher, C., Waggie, K., West, J., Whitmore, T. E., Yao, L., Kuechle, M. K., Dale, B. A. and Chandrasekher, Y. A. (2001) 'Interleukin 20', *Cell*, 104(1), pp. 9–19. doi: 10.1016/S0092-8674(01)00187-8.

Boraschi, D. and Tagliabue, A. (2013) 'The interleukin-1 receptor family', *Seminars in Immunology*, 25(6), pp. 394–407. doi: 10.1016/j.smim.2013.10.023.

Borg, A., Sandberg, T., Nilsson, K., Johannsson, O., Klinker, M., Masback, A., Westerdahl, J., Olsson, H. and Ingvar, C. (2000) 'High Frequency of Multiple Melanomas and Breast and Pancreas Carcinomas in CDKN2A Mutation-Positive Melanoma Families', *JNCI Journal of the National Cancer Institute*. Oxford University Press, 92(15), pp. 1260–1266. doi: 10.1093/jnci/92.15.1260.

Born, T. L., Smith, D. E., Garka, K. E., Renshaw, B. R., Bertles, J. S. and Sims, J. E. (2000) 'Identification and characterization of two members of a novel class of the interleukin-1 receptor (IL-1R) family. Delineation of a new class of IL-1R-related proteins based on signaling.', *The Journal of biological chemistry*, 275(39), pp. 29946–54. doi: 10.1074/jbc.M004077200.

Bos, J., Fearon, E., Hamilton, S. and Vries, M. V. (1987) 'Prevalence of ras gene mutations in human colorectal cancers', *Nature*, 327(6120), pp.293-297.

Boyraz, B., Sendur, M. A. N., Aksoy, S., Babacan, T., Roach, E. C., Kizilarslanoglu, M. C., Petekkaya, I. and Altundag, K. (2013) 'Trastuzumab emtansine (T-DM1) for HER2-positive breast cancer', *Current Medical Research and Opinion*, 29(4), pp. 405–414. doi: 10.1185/03007995.2013.775113.

Brahmer, J. R., Tykodi, S. S., Chow, L. Q. M., Hwu, W.-J., Topalian, S. L., Hwu, P., Drake, C. G., Camacho, L. H., Kauh, J., Odunsi, K., Pitot, H. C., Hamid, O., Bhatia, S., Martins, R., Eaton, K., Chen, S., Salay, T. M., Alaparthy, S., Grosso, J. F., Korman, A. J., Parker, S. M., Agrawal, S., Goldberg, S. M., Pardoll, D. M., Gupta, A. and Wigginton, J. M. (2012) 'Safety and Activity of Anti–PD-L1 Antibody in Patients with Advanced Cancer', *New England Journal of Medicine*, 366(26), pp. 2455–2465. doi: 10.1056/NEJMoa1200694.

Bronner, C. E., Baker, S. M., Morrison, P. T., Warren, G., Smith, L. G., Lescoe, M. K., Kane, M., Earabino, C., Lipford, J., Lindblom, A., Tannergård, P., Bollag, R. J., Godwin, A. R.,

Ward, D. C., Nordenskj⊘ld, M., Fishel, R., Kolodner, R. and Liskay, R. M. (1994) 'Mutation in the DNA mismatch repair gene homologue hMLH 1 is associated with hereditary non-polyposis colon cancer', *Nature*, 368(6468), pp. 258–261. doi: 10.1038/368258a0.

Brosens, L. A. A., Hackeng, W. M., Offerhaus, J., Hruban, R. H. and Wood, L. D. (2015) 'Pancreatic adenocarcinoma pathology: Changing "landscape"', *Journal of Gastrointestinal Oncology*. AME Publications, pp. 358–374. doi: 10.3978/j.issn.2078-6891.2015.032.

Büchler, P., Reber, H. A., Büchler, M., Shrinkante, S., Büchler, M. W., Friess, H., Semenza, G. L. and Hines, O. J. (2003) 'Hypoxia-inducible factor 1 regulates vascular endothelial growth factor expression in human pancreatic cancer.', *Pancreas*, 26(1), pp. 56–64.

Burris, H., Gordon, M., Gerber, D., Spigel, D., Mendelson, D., Schiller, J., Wang, Y., Choi, Y., Kahn, R., Wood, K. and Maslyar, D., (2014) 'A phase I study of DNIB0600A, an antibody-drug conjugate (ADC) targeting NaPi2b, in patients (pts) with non-small cell lung cancer (NSCLC) or platinum-resistant ovarian cancer (OC).' *Journal of Clinical Oncology*, 32(15).

Calvanese, V., Mallya, M., Campbell, R. D. and Aguado, B. (2008) 'Regulation of expression of two LY-6 family genes by intron retention and transcription induced chimerism.', *BMC molecular biology*, 9, p. 81. doi: 10.1186/1471-2199-9-81.

Carson, J. D., Van Aller, G., Lehr, R., Sinnamon, R. H., Kirkpatrick, R. B., Auger, K. R., Dhanak, D., Copeland, R. A., Gontarek, R. R., Tummino, P. J. and Luo, L. (2008) 'Effects of oncogenic p110α subunit mutations on the lipid kinase activity of phosphoinositide 3-kinase', *Biochemical Journal*, 409(2), pp. 519–524. doi: 10.1042/BJ20070681.

Carvalho, S., Levi-Schaffer, F., Sela, M. and Yarden, Y. (2016) 'Immunotherapy of cancer: from monoclonal to oligoclonal cocktails of anti-cancer antibodies: IUPHAR Review 18', *British Journal of Pharmacology*, 173(9), pp. 1407–1424. doi: 10.1111/bph.13450.

Chalhoub, N. and Baker, S. J. (2009) 'PTEN and the PI3-kinase pathway in cancer.', *Annual review of pathology*, 4(1), pp. 127–50. doi: 10.1146/annurev.pathol.4.110807.092311.

Chang, A. Y., Gejman, R. S., Brea, E. J., Oh, C. Y., Mathias, M. D., Pankov, D., Casey, E., Dao, T. and Scheinberg, D. A. (2016) 'Opportunities and challenges for TCR mimic antibodies in cancer therapy', *Expert Opinion on Biological Therapy*, 16(8), pp. 979–987. doi: 10.1080/14712598.2016.1176138.

Chanmee, T., Ontong, P., Konno, K. and Itano, N., 2014. Tumor-associated macrophages as major players in the tumor microenvironment. *Cancers*, 6(3), pp.1670-1690.

Chelly, J., Carrié, A., Jun, L., Bienvenu, T., Vinet, M.-C., McDonell, N., Couvert, P., Zemni, R., Cardona, A., Van Buggenhout, G., Frints, S., Hamel, B., Moraine, C., Ropers, H. H., Strom, T., Howell, G. R., Whittaker, A., Ross, M. T., Kahn, A., Fryns, J.-P., Beldjord, C. and Marynen, P. (1999) 'A new member of the IL-1 receptor family highly expressed in hippocampusand involved in X-linked mental retardation', *Nature Genetics*. Nature Publishing Group, 23(1), pp. 25–31. doi: 10.1038/12623.

Chen, S. X., Xu, X. E., Wang, X. Q., Cui, S. J., Xu, L. L., Jiang, Y. H., Zhang, Y., Yan, H. B., Zhang, Q., Qiao, J., Yang, P. Y. and Liu, F. (2014) 'Identification of colonic fibroblast secretomes reveals secretory factors regulating colon cancer cell proliferation', *Journal of*

Proteomics, 110, pp. 155–171. doi: 10.1016/j.jprot.2014.07.031.

Choi, H. J., Hyun, M. S., Jung, G. J., Kim, S. S. and Hong, S. H. (1998) 'Tumor Angiogenesis as a Prognostic Predictor in Colorectal Carcinoma with Special Reference to Mode of Metastasis and Recurrence', *Oncology*, 55(6), pp. 575–581. doi: 10.1159/000011915.

Ciardiello, F. and Tortora, G. (2008) 'EGFR Antagonists in Cancer Treatment', *New England Journal of Medicine*, 358(11), pp. 1160–1174. doi: 10.1056/NEJMra0707704.

Cirri, P. and Chiarugi, P. (2011) 'Cancer associated fibroblasts: the dark side of the coin.', *American journal of cancer research*, 1(4), pp. 482–97.

Cohen, M. H., Chen, H., Shord, S., Fuchs, C., He, K., Zhao, H., Sickafuse, S., Keegan, P. and Pazdur, R. (2013) 'Approval Summary: Cetuximab in Combination With Cisplatin or Carboplatin and 5-Fluorouracil for the First-Line Treatment of Patients With Recurrent Locoregional or Metastatic Squamous Cell Head and Neck Cancer', *The Oncologist*, 18(4), pp. 460–466. doi: 10.1634/theoncologist.2012-0458.

Colangelo, T., Polcaro, G., Muccillo, L., D'Agostino, G., Rosato, V., Ziccardi, P., Lupo, A., Mazzoccoli, G., Sabatino, L. and Colantuoni, V. (2017) 'Friend or foe?: The tumour microenvironment dilemma in colorectal cancer', *Biochimica et Biophysica Acta - Reviews on Cancer*, pp. 1–18. doi: 10.1016/j.bbcan.2016.11.001.

Collisson, E. A., Sadanandam, A., Olson, P., Gibb, W. J., Truitt, M., Gu, S., Cooc, J., Weinkle, J., Kim, G. E., Jakkula, L., Feiler, H. S., Ko, A. H., Olshen, A. B., Danenberg, K. L., Tempero, M. A., Spellman, P. T., Hanahan, D. and Gray, J. W. (2011) 'Subtypes of pancreatic ductal adenocarcinoma and their differing responses to therapy', *Nature Medicine*, 17(4), pp. 500–503. doi: 10.1038/nm.2344.

Costa, L. da, Kern, S. E. and Hruban, R. H. (1994) 'p53 Mutations in Pancreatic Carcinoma and Evidence of Common Involvement of Homocopolymer Tracts in DNA Microdeletions', *Cancer Research*, 54(11), pp. 3025–3033.

Cowgill, S. M. and Muscarella, P. (2003) 'The genetics of pancreatic cancer', *The American Journal of Surgery*, 186(3), pp. 279–286. doi: 10.1016/S0002-9610(03)00226-5.

Cruceru, M. L., Neagu, M., Demoulin, J. B. and Constantinescu, S. N. (2013) 'Therapy targets in glioblastoma and cancer stem cells: Lessons from haematopoietic neoplasms', *Journal of Cellular and Molecular Medicine*, 17(10), pp. 1218–1235. doi: 10.1111/jcmm.12122.

Damelin, M., Zhong, W., Myers, J. and Sapra, P. (2015) 'Evolving Strategies for Target Selection for Antibody-Drug Conjugates', *Pharmaceutical Research*. Springer US, 32(11), pp. 3494–3507. doi: 10.1007/s11095-015-1624-3.

Danielsen, S., Lind, G., Bjørnslett, M. and Meling, G. (2008) 'Novel mutations of the suppressor gene PTEN in colorectal carcinomas stratified by microsatellite instability-and TP53 mutation-status', *Human*, 29(11).

Dattatreya, S. (2013) 'Metastatic colorectal cancer-prolonging overall survival with targeted therapies.', *South Asian journal of cancer*, 2(3), pp. 179–85. doi: 10.4103/2278-330X.114152.

Davies, H., Bignell, G.R., Cox, C. and Stephens, P., 2002. Mutations of the BRAF gene in human cancer. *Nature*, 417(6892), p.949.

Diamantis, N. and Banerji, U. (2016) 'Antibody-drug conjugates—an emerging class of cancer treatment', *British Journal of Cancer*. Nature Publishing Group, 114(4), pp. 362–367. doi: 10.1038/bjc.2015.435.

Dienstmann, R., Vermeulen, L., Guinney, J., Kopetz, S., Tejpar, S. and Tabernero, J. (2017) 'Consensus molecular subtypes and the evolution of precision medicine in colorectal cancer', *Nature Reviews Cancer*, 17(2), pp. 79–92. doi: 10.1038/nrc.2016.126.

Dietvorst, M. H. P. and Eskens, F. A. L. M. (2013) 'Current and Novel Treatment Options for Metastatic Colorectal Cancer: Emphasis on Aflibercept', *Biologics in Therapy*, 3(1), pp. 25–33. doi: 10.1007/s13554-013-0009-6.

Dong, H., Strome, S. E., Salomao, D. R., Tamura, H., Hirano, F., Flies, D. B., Roche, P. C., Lu, J., Zhu, G., Tamada, K., Lennon, V. A., Celis, E. and Chen, L. (2002) 'Tumor-associated B7-H1 promotes T-cell apoptosis: A potential mechanism of immune evasion', *Nature Medicine*, 8, pp. 793–800. doi: 10.1038/nm730.

Dubrovsky, L., Dao, T., Gejman, R. S., Brea, E. J., Chang, A. Y., Oh, C. Y., Casey, E., Pankov, D. and Scheinberg, D. A. (2016) 'T cell receptor mimic antibodies for cancer therapy', *OncoImmunology*, 5(1), p. e1049803. doi: 10.1080/2162402X.2015.1049803.

Eppert, K., Scherer, S. W., Ozcelik, H., Pirone, R., Hoodless, P., Kim, H., Tsui, L.-C., Bapat, B., Gallinger, S., Andrulis, I. L., Thomsen, G. H., Wrana, J. L. and Attisano, L. (1996) 'MADR2 Maps to 18q21 and Encodes a TGFβ–Regulated MAD–Related Protein That Is Functionally Mutated in Colorectal Carcinoma', *Cell*, 86(4), pp. 543–552. doi: 10.1016/S0092-8674(00)80128-2.

Erkan, M., Adler, G., Apte, M. V, Bachem, M. G., Buchholz, M., Detlefsen, S., Esposito, I., Friess, H., Gress, T. M., Habisch, H.-J., Hwang, R. F., Jaster, R., Kleeff, J., Klöppel, G., Kordes, C., Logsdon, C. D., Masamune, A., Michalski, C. W., Oh, J., Phillips, P. A., Pinzani, M., Reiser-Erkan, C., Tsukamoto, H. and Wilson, J. (2012) 'StellaTUM: current consensus and discussion on pancreatic stellate cell research', *Gut*, 61(2), pp. 172–178. doi: 10.1136/gutjnl-2011-301220.

Erreni, M., Mantovani, A. and Allavena, P. (2011) 'Tumor-associated Macrophages (TAM) and Inflammation in Colorectal Cancer.', *Cancer microenvironment : official journal of the International Cancer Microenvironment Society*. Springer, 4(2), pp. 141–54. doi: 10.1007/s12307-010-0052-5.

Esposito, I., Menicagli, M., Funel, N., Bergmann, F., Boggi, U., Mosca, F., Bevilacqua, G. and Campani, D. (2004) 'Inflammatory cells contribute to the generation of an angiogenic phenotype in pancreatic ductal adenocarcinoma.', *Journal of clinical pathology*, 57(6), pp. 630–6. doi: 10.1136/jcp.2003.014498.

Esteller, M. (2008) 'Epigenetics in Cancer', *n Engl j Med*, 358, pp. 1148–1159.

Facciabene, A., Motz, G. T. and Coukos, G. (2012) 'T Regulatory Cells: Key Players in Tumor Immune Escape and Angiogenesis', *Cancer Res.*, 72(9), pp. 2162–2171.

Fan, G., Wang, Z., Hao, M. and Li, J. (2015) 'Bispecific antibodies and their applications', *Journal of Hematology & Oncology*, 8(1), p. 130. doi: 10.1186/s13045-015-0227-0.

Fanoni, D., Tavecchio, S., Recalcati, S., Balice, Y., Venegoni, L., Fiorani, R., Crosti, C. and Berti, E. (2011) 'New monoclonal antibodies against B-cell antigens: Possible new strategies for diagnosis of primary cutaneous B-cell lymphomas', *Immunology Letters*, 134(2), pp. 157–160. doi: 10.1016/j.imlet.2010.09.022.

Farzan, M., Schnitzler, C. E., Vasilieva, N., Leung, D. and Choe, H. (2000) 'BACE2, a beta -secretase homolog, cleaves at the beta site and within the amyloid-beta region of the amyloid-beta precursor protein.', *Proceedings of the National Academy of Sciences of the United States of America*. National Academy of Sciences, 97(17), pp. 9712–7. doi: 10.1073/pnas.160115697.

Fearon, E. R. (2011) 'Molecular Genetics of Colorectal Cancer', *Annual Review of Pathology: Mechanisms of Disease*. Annual Reviews , 6(1), pp. 479–507. doi: 10.1146/annurev-pathol-011110-130235.

Fearon, E. R. and Volgelstein, B. (1990) 'A genetic model for colorectal cancer', *Cell*, 61(5), pp. 759–767.

Feldmann, G., Dhara, S., Fendrich, V., Bedja, D., Beaty, R., Mullendore, M., Karikari, C., Alvarez, H., Iacobuzio-Donahue, C., Jimeno, A., Gabrielson, K. L., Matsui, W. and Maitra, A. (2007) 'Blockade of Hedgehog Signaling Inhibits Pancreatic Cancer Invasion and Metastases: A New Paradigm for Combination Therapy in Solid Cancers', *Cancer Research*, 67(5), pp. 2187–2196. doi: 10.1158/0008-5472.CAN-06-3281.

Fokas, E., O'Neill, E., Gordon-Weeks, A., Mukherjee, S., McKenna, W. G. and Muschel, R. J. (2015) 'Pancreatic ductal adenocarcinoma: From genetics to biology to radiobiology to oncoimmunology and all the way back to the clinic', *Biochimica et Biophysica Acta - Reviews on Cancer*, pp. 61–82. doi: 10.1016/j.bbcan.2014.12.001.

Forssell, J., Öberg, Å., Henriksson, M. L., Stenling, R., Jung, A. and Palmqvist, R. (2007) 'High Macrophage Infiltration along the Tumor Front Correlates with Improved Survival in Colon Cancer', *Clinical Cancer Research*, 13(5).

Fricke, I. and Gabrilovich, D. I. (2006) 'Dendritic cells and tumor microenvironment: a dangerous liaison.', *Immunological investigations*, 35(3–4), pp. 459–83. doi: 10.1080/08820130600803429.

Froeling, F. E. M., Mirza, T. A., Feakins, R. M., Seedhar, A., Elia, G., Hart, I. R. and Kocher, H. M. (2009) 'Organotypic Culture Model of Pancreatic Cancer Demonstrates that Stromal Cells Modulate E-Cadherin, β-Catenin, and Ezrin Expression in Tumor Cells', *The American Journal of Pathology*, 175(2), pp. 636–648. doi: 10.2353/ajpath.2009.090131.

Funada, Y. and Moouchi, T. O. (2003) 'Prognostic significance of CDS + T cell and macrophage peritumoral infiltration in colorectal cancer', *Oncology*, 10(2), pp. 309–313.

Galon, J. (2006) 'Type, Density, and Location of Immune Cells Within Human Colorectal Tumors Predict Clinical Outcome', *Science*, 313(5795), pp. 1960–1964. doi: 10.1126/science.1129139.

Gascard, P. and Tlsty, T. D. (2016) 'Carcinoma-associated fibroblasts: Orchestrating the composition of malignancy', *Genes and Development*, pp. 1002–1019. doi: 10.1101/gad.279737.116.

Gébleux, R. and Casi, G. (2016) 'Antibody-drug conjugates: Current status and future perspectives', *Pharmacology & Therapeutics*, 167, pp. 48–59. doi: 10.1016/j.pharmthera.2016.07.012.

Gébleux, R., Stringhini, M., Casanova, R., Soltermann, A. and Neri, D. (2017) 'Non-internalizing antibody-drug conjugates display potent anti-cancer activity upon proteolytic release of monomethyl auristatin E in the subendothelial extracellular matrix', *International Journal of Cancer*, 140(7), pp. 1670–1679. doi: 10.1002/ijc.30569.

Giubellino, A., Burke, T. R. and Bottaro, D. P. (2008) 'Grb2 signaling in cell motility and cancer.', *Expert opinion on therapeutic targets*, 12(8), pp. 1021–33. doi: 10.1517/14728222.12.8.1021.

Goldmacher, V. S. and Kovtun, Y. V (2011) 'Antibody–drug conjugates: using monoclonal antibodies for delivery of cytotoxic payloads to cancer cells', *Therapeutic Delivery*, 2(3), pp. 397–416. doi: 10.4155/tde.10.98.

Gonçalves-Ribeiro, S., Guillen Díaz-Maroto, N., Berdiel-Acer, M., Soriano, A., Guardiola, J., Martínez-Villacampa, M., Salazar, R., Capellà, G., Villanueva, A., Martínez-Balibrea, E., Molleví, D. G., Gonçalves-Ribeiro, S., Guillen Díaz-Maroto, N., Berdiel-Acer, M., Soriano, A., Guardiola, J., Martínez-Villacampa, M., Salazar, R., Capellà, G., Villanueva, A., Martínez-Balibrea, E., Molleví, D. G., Gonçalves-Ribeiro, S., Díaz-Maroto, N. G., Berdiel, M., Soriano, A., Guardiola, J., Martínez-Villacampa, M., Salazar, R., Capellà, G., Villanueva, A., Martínez-Balibrea, E. and Molleví, D. G. (2016) 'Carcinoma-associated fibroblasts affect sensitivity to oxaliplatin and 5FU in colorectal cancer cells', *Oncotarget*, 7(37), pp. 59766–59780. doi: 10.18632/oncotarget.11121.

Gonzalez-Pons, M. and Cruz-Correa, M. (2015) 'Colorectal Cancer Biomarkers: Where Are We Now?', *BioMed research international*, p. 149014. doi: 10.1155/2015/149014.

Gorunova, L., Höglund, M., Andrén-Sandberg, Å., Dawiskiba, S., Jin, Y., Mitelman, F. and Johansson, B. (1998) 'Cytogenetic analysis of pancreatic carcinomas: Intratumor heterogeneity and nonrandom pattern of chromosome aberrations', *Genes, Chromosomes and Cancer*, 23(2), pp. 81–99. doi: 10.1002/(SICI)1098-2264(199810)23:2<81::AID-GCC1>3.0.CO;2-0.

Govindan, S. V and Goldenberg, D. M. (2012) 'Designing immunoconjugates for cancer therapy', *Expert Opinion on Biological Therapy*, 12(7), pp. 873–890. doi: 10.1517/14712598.2012.685153.

Grady, W. and Markowitz, S. (2002) 'Colorectal cancer: genetic alterations', *practice. Philadelphia: Lippincott Williams & Wilkins*, pp. 685–702.

Grigore, A., Jolly, M., Jia, D. and Farach-Carson, M. (2016) 'Tumor Budding: The Name is EMT. Partial EMT.', *Journal of clinical medicine,*, 5(5), p. 51.

Groden, J., Thliveris, A., Samowitz, W., Carlson, M., Gelbert, L., Albertsen, H., Joslyn, G., Stevens, J., Spirio, L. and Robertson, M. (1991) 'Identification and characterization of the

familial adenomatous polyposis coli gene.', *Cell*, 66(3), pp. 589–600.

Group, G. (2017) 'Genomics and epidemiology for gastric adenocarcinomas', *Applied Cancer Research*, 37(7). doi: 10.1186/s41241-017-0011-2.

Guzman, C., Bagga, M., Kaur, A., Westermarck, J. and Abankwa, D. (2014) 'ColonyArea: An ImageJ plugin to automatically quantify colony formation in clonogenic assays', *PLoS ONE*, 9(3). doi: 10.1371/journal.pone.0092444.

Hamid, O., Robert, C., Daud, A., Hodi, F. S., Hwu, W.-J., Kefford, R., Wolchok, J. D., Hersey, P., Joseph, R. W., Weber, J. S., Dronca, R., Gangadhar, T. C., Patnaik, A., Zarour, H., Joshua, A. M., Gergich, K., Elassaiss-Schaap, J., Algazi, A., Mateus, C., Boasberg, P., Tumeh, P. C., Chmielowski, B., Ebbinghaus, S. W., Li, X. N., Kang, S. P. and Ribas, A. (2013) 'Safety and Tumor Responses with Lambrolizumab (Anti–PD-1) in Melanoma', *New England Journal of Medicine*, 369(2), pp. 134–144. doi: 10.1056/NEJMoa1305133.

Harding, J. and Burtness, B. (2005) 'Cetuximab: An epidermal growth factor receptor chimeric human-murine monoclonal antibody', *Drugs of Today*, 41(2), p. 107. doi: 10.1358/dot.2005.41.2.882662.

Harvey, R. C. (2017) 'Second-line Treatments for Advanced Gastric Cancer: A Network Meta-Analysis of Overall Survival Using Parametric Modelling Methods', *Oncology and Therapy*, 5, pp. 53–67. doi: 10.1007/s40487-017-0048-0.

Hawinkels, L. J. A. C., Paauwe, M., Verspaget, H. W., Wiercinska, E., van der Zon, J. M., van der Ploeg, K., Koelink, P. J., Lindeman, J. H. N., Mesker, W., ten Dijke, P. and Sier, C. F. M. (2014) 'Interaction with colon cancer cells hyperactivates TGF-β signaling in cancer-associated fibroblasts', *Oncogene*, 33(1), pp. 97–107. doi: 10.1038/onc.2012.536.

Hayashida, K., Bartlett, A. H., Chen, Y. and Park, P. W. (2010) 'Molecular and Cellular Mechanisms of Ectodomain Shedding', *The Anatomical Record: Advances in Integrative Anatomy and Evolutionary Biology*, 293(6), pp. 925–937. doi: 10.1002/ar.20757.

de Heer, P., Koudijs, M. M., van de Velde, C. J. H., Aalbers, R. I. J. M., Tollenaar, R. A. E. M., Putter, H., Morreau, J., van de Water, B. and Kuppen, P. J. K. (2008) 'Combined expression of the non-receptor protein tyrosine kinases FAK and Src in primary colorectal cancer is associated with tumor recurrence and metastasis formation.', *European journal of surgical oncology,* 34(11), pp. 1253–61. doi: 10.1016/j.ejso.2008.05.003.

Heffler, M., Golubovskaya, V. M., Dunn, K. M. B. and Cance, W. (2013) 'Focal adhesion kinase autophosphorylation inhibition decreases colon cancer cell growth and enhances the efficacy of chemotherapy', *Cancer Biology & Therapy*, 14(8), pp. 761–772. doi: 10.4161/cbt.25185.

Herbeuval, J.-P., Lelievre, E., Lambert, C., Dy, M. and Genin, C. (2004) 'Recruitment of STAT3 for production of IL-10 by colon carcinoma cells induced by macrophage-derived IL-6', *Journal of immunology*, 172(7), pp. 4630–4636. doi: 10.4049/jimmunol.172.7.4630.

Hermann, P. C., Huber, S. L., Herrler, T., Aicher, A., Ellwart, J. W., Guba, M., Bruns, C. J. and Heeschen, C. (2007) 'Distinct Populations of Cancer Stem Cells Determine Tumor Growth and Metastatic Activity in Human Pancreatic Cancer', *Cell Stem Cell*, 1(3), pp. 313–323. doi: 10.1016/j.stem.2007.06.002.

Hochwald, S. N., Nyberg, C., Zheng, M., Zheng, D., Wood, C., Massoll, N. A., Magis, A., Ostrov, D., Cance, W. G. and Golubovskaya, V. M. (2009) 'A novel small molecule inhibitor of FAK decreases growth of human pancreatic cancer.', *Cell cycle*, 8(15), pp. 2435–43. doi: 10.4161/cc.8.15.9145.

Hodi, F., O'Day, S. J., McDermott, D., Weber, R., Sosman, J. A., Haanen, J. B., Gonzalez, R., Robert, C., Schadendorf, D., Hassel, J. C. and others (2010) 'Improved survival with ipilimumab in patients with metastatic melanoma', *N Engl J Med*, 363(8), pp. 711–723. doi: 10.1056/NEJMoa1109071.

Huanwen, W., Zhiyong, L., Xiaohua, S., Xinyu, R., Kai, W. and Tonghua, L. (2009) 'Intrinsic chemoresistance to gemcitabine is associated with constitutive and laminin-induced phosphorylation of FAK in pancreatic cancer cell lines', *Molecular Cancer*, 8(1), p. 125. doi: 10.1186/1476-4598-8-125.

Hugen, N., Brown, G., Glynne-Jones, R., de Wilt, J. H. W. and Nagtegaal, I. D. (2015) 'Advances in the care of patients with mucinous colorectal cancer', *Nature Reviews Clinical Oncology*, Advanced o(6), pp. 1–9. doi: 10.1038/nrclinonc.2015.140.

Hwang, R. F., Moore, T., Arumugam, T., Ramachandran, V., Amos, K. D., Rivera, A., Ji, B., Evans, D. B. and Logsdon, C. D. (2008) 'Cancer-Associated Stromal Fibroblasts Promote Pancreatic Tumor Progression', *Cancer Research*, 68(3), pp. 918–926. doi: 10.1158/0008-5472.CAN-07-5714.

Iacobuzio-Donahue, C. A., Fu, B., Yachida, S., Luo, M., Abe, H., Henderson, C. M., Vilardell, F., Wang, Z., Keller, J. W., Banerjee, P., Herman, J. M., Cameron, J. L., Yeo, C. J., Halushka, M. K., Eshleman, J. R., Raben, M., Klein, A. P., Hruban, R. H., Hidalgo, M. and Laheru, D. (2009) 'DPC4 gene status of the primary carcinoma correlates with patterns of failure in patients with pancreatic cancer.', *Journal of clinical oncology : official journal of the American Society of Clinical Oncology*, 27(11), pp. 1806–13. doi: 10.1200/JCO.2008.17.7188.

Inman, B. A., Longo, T. A., Ramalingam, S. and Harrison, M. R. (2016) 'Atezolizumab: a PD-L1 blocking antibody for bladder cancer', *Clinical Cancer Research*, 23(8), pp. 1886–1891. doi: 10.1158/1078-0432.CCR-16-1417.

Ino, Y., Yamazaki-Itoh, R., Shimada, K., Iwasaki, M., Kosuge, T., Kanai, Y. and Hiraoka, N. (2013) 'Immune cell infiltration as an indicator of the immune microenvironment of pancreatic cancer', *British Journal of Cancer*, 108(4), pp. 914–923. doi: 10.1038/bjc.2013.32.

Iovanna, J., Mallmann, M. C., Gonçalves, A., Turrini, O. and Dagorn, J.-C. (2012) 'Current knowledge on pancreatic cancer.', *Frontiers in oncology*, 2(6), pp. 1–24. doi: 10.3389/fonc.2012.00006.

Ishida, Y., Agata, Y., Shibahara, K. and Honjo, T. (1992) 'Induced expression of PD-1, a novel member of the immunoglobulin gene superfamily, upon programmed cell death.', *The EMBO journal*, 11(11), pp. 3887–95.

Issa, J.-P. (2008) 'Colon cancer: it's CIN or CIMP.', *Clinical cancer research : an official journal of the American Association for Cancer Research*, 14(19), pp. 5939–40. doi:

10.1158/1078-0432.CCR-08-1596.

Issa, J., Shen, L. and Toyota, M. (2005) 'CIMP, at last', *Gastroenterology*, 129(3), pp. 1121–1124.

Iwai, Y., Ishida, M., Tanaka, Y., Okazaki, T., Honjo, T. and Minato, N. (2002) 'Involvement of PD-L1 on tumor cells in the escape from host immune system and tumor immunotherapy by PD-L1 blockade.', *Proceedings of the National Academy of Sciences of the United States of America*, 99(19), pp. 12293–7. doi: 10.1073/pnas.192461099.

Jass, J. (2007) 'Classification of colorectal cancer based on correlation of clinical, morphological and molecular features.', *Histopathology*, 50(1), pp. 113–130.

Joesting, M., Perrin, S., Elenbaas, B. and Fawell, S. (2005) 'Identification of SFRP1 as a candidate mediator of stromal-to-epithelial signaling in prostate cancer', *Cancer research*, 65(22), pp.10423-10430.

Jung, S. H., Kim, S. H. and Kim, J. H. (2016) 'Prognostic Impact of Microsatellite Instability in Colorectal Cancer Presenting With Mucinous, Signet-Ring, and Poorly Differentiated Cells.', *Annals of coloproctology*, 32(2), pp. 58–65. doi: 10.3393/ac.2016.32.2.58.

Kakar, S., Aksoy, S., Burgart, L. J. and Smyrk, T. C. (2004) 'Mucinous carcinoma of the colon: correlation of loss of mismatch repair enzymes with clinicopathologic features and survival.', *Modern pathology : an official journal of the United States and Canadian Academy of Pathology, Inc*, 17(6), pp. 696–700. doi: 10.1038/modpathol.3800093.

Kaler, P., Godasi, B. N., Augenlicht, L. and Klampfer, L. (2009) 'The NF-kappaB/AKT-dependent Induction of Wnt Signaling in Colon Cancer Cells by Macrophages and IL-1beta.', *Cancer microenvironment : official journal of the International Cancer Microenvironment Society*, pp. 69–80. doi: 10.1007/s12307-009-0030-y.

Kanaan, Z., Rai, S. N., Eichenberger, M. R., Barnes, C., Dworkin, A. M., Weller, C., Cohen, E., Roberts, H., Keskey, B., Petras, R. E., Crawford, N. P. S. and Galandiuk, S. (2012) 'Differential MicroRNA expression tracks neoplastic progression in inflammatory bowel disease-associated colorectal cancer', *Human Mutation*, 33(3), pp. 551–560. doi: 10.1002/humu.22021.

Kanteti, R., Batra, S. K., Lennon, F. E. and Salgia, R. (2015) 'FAK and Paxillin, two potential targets in pancreatic cancer', *Oncotarget*, 7(21), pp. 31586–31601. doi: 10.18632/oncotarget.8040.

Karamitopoulou, E., Zlobec, I., Born, D., Kondi-Pafiti, A., Lykoudis, P., Mellou, A., Gennatas, K., Gloor, B. and Lugli, A. (2013) 'Tumour budding is a strong and independent prognostic factor in pancreatic cancer', *European Journal of Cancer*, 49(5), pp. 1032–1039. doi: 10.1016/j.ejca.2012.10.022.

Karsa, L. v., Lignini, T. A., Patnick, J., Lambert, R. and Sauvaget, C. (2010) 'The dimensions of the CRC problem', *Best Practice & Research Clinical Gastroenterology*, 24(4), pp. 381–396. doi: 10.1016/j.bpg.2010.06.004.

Kato, H. and Nakajima, M. (2013) 'Treatments for esophageal cancer: A review', *General Thoracic and Cardiovascular Surgery*, 61(6), pp. 330–335.

Khan, J. A., Brint, E. K., Neill, L. A. J. O. and Tong, L. (2004) 'Crystal Structure of the Toll / Interleukin-1 Receptor Domain of Human IL-1RAPL', *The Journal of biological chemistry*, 279(30), pp. 31664–31670. doi: 10.1074/jbc.M403434200.

Khoja, L., Butler, M. O., Kang, S. P., Ebbinghaus, S. and Joshua, A. M. (2015) 'Pembrolizumab', *Journal for ImmunoTherapy of Cancer*, 3(1), p. 36. doi: 10.1186/s40425-015-0078-9.

Kikuta, K., Masamune, A., Watanabe, T., Ariga, H., Itoh, H., Hamada, S., Satoh, K., Egawa, S., Unno, M. and Shimosegawa, T. (2010) 'Pancreatic stellate cells promote epithelial-mesenchymal transition in pancreatic cancer cells', *Biochemical and Biophysical Research Communications*, 403(3–4), pp. 380–384. doi: 10.1016/j.bbrc.2010.11.040.

Kindler, H. L., Ioka, T., Richel, D. J., Bennouna, J., Létourneau, R., Okusaka, T., Funakoshi, A., Furuse, J., Park, Y. S., Ohkawa, S., Springett, G. M., Wasan, H. S., Trask, P. C., Bycott, P., Ricart, A. D., Kim, S. and Van Cutsem, E. (2011) 'Axitinib plus gemcitabine versus placebo plus gemcitabine in patients with advanced pancreatic adenocarcinoma: a double-blind randomised phase 3 study', *The Lancet Oncology*, 12(3), pp. 256–262. doi: 10.1016/S1470-2045(11)70004-3.

Kindler, H. L., Niedzwiecki, D., Hollis, D., Sutherland, S., Schrag, D., Hurwitz, H., Innocenti, F., Mulcahy, M. F., O'Reilly, E., Wozniak, T. F., Picus, J., Bhargava, P., Mayer, R. J., Schilsky, R. L. and Goldberg, R. M. (2010) 'Gemcitabine plus bevacizumab compared with gemcitabine plus placebo in patients with advanced pancreatic cancer: phase III trial of the Cancer and Leukemia Group B (CALGB 80303).', *Journal of clinical oncology : official journal of the American Society of Clinical Oncology*, 28(22), pp. 3617–22. doi: 10.1200/JCO.2010.28.1386.

Kinzler, K. W. and Vogelstein, B. (1996) 'Lessons from hereditary colorectal cancer.', *Cell*, 87(2), pp. 159–70.

Kitadai, Y., Sasaki, T., Kuwai, T., Nakamura, T., Bucana, C. D. and Fidler, I. J. (2006) 'Targeting the expression of platelet-derived growth factor receptor by reactive stroma inhibits growth and metastasis of human colon carcinoma', *Am J Pathol*, 169(6), pp. 2054–2065. doi: 10.2353/ajpath.2006.060653.

Kleeff, J., Beckhove, P., Esposito, I., Herzig, S., Huber, P. E., Löhr, J. M. and Friess, H. (2007) 'Pancreatic cancer microenvironment', *International Journal of Cancer*, 121(4), pp. 699–705. doi: 10.1002/ijc.22871.

Ko, A. H., LoConte, N., Tempero, M. A., Walker, E. J., Kate Kelley, R., Lewis, S., Chang, W.-C., Kantoff, E., Vannier, M. W., Catenacci, D. V., Venook, A. P. and Kindler, H. L. (2016) 'A Phase I Study of FOLFIRINOX Plus IPI-926, a Hedgehog Pathway Inhibitor, for Advanced Pancreatic Adenocarcinoma', *Pancreas*, 45(3), pp. 370–375. doi: 10.1097/MPA.0000000000000458.

Kodama, R., Shiraga, H., Shigemori, K., Toyama, Y., Fujioka, S., Azechi, H., Fujita, H., Habara, H., Hall, T., Izawa, Y., Jitsuno, T., Kitagawa, Y., Krushelnick, K. M., Lancaster, K. L., Mima, K., Nagai, K., Nakai, M., Nishimura, H., Norimatsu, T., Norreys, P. A., Sakabe, S., Tanaka, K. A., Youssef, A., Zepf, M. and Yamanaka, T. (2002) 'Nuclear fusion: Fast heating scalable to laser fusion ignition', *Nature*, 418(6901), pp. 933–934. doi:

10.1038/418933a.

KÖHLER, G. and MILSTEIN, C. (1975) 'Continuous cultures of fused cells secreting antibody of predefined specificity', *Nature*, 256(5517), pp. 495–497. doi: 10.1038/256495a0.

Koong, A. C., Mehta, V. K., Le, Q. T., Fisher, G. A., Terris, D. J., Brown, J. M., Bastidas, A. J. and Vierra, M. (2000) 'Pancreatic tumors show high levels of hypoxia.', *International journal of radiation oncology, biology, physics*, 48(4), pp. 919–22.

van Kooten, C. and Banchereau, J. (2000) 'CD40-CD40 ligand.', *Journal of leukocyte biology*, 67(1), pp. 2–17.

Krall, N., Scheuermann, J. and Neri, D. (2013) 'Small Targeted Cytotoxics: Current State and Promises from DNA-Encoded Chemical Libraries', *Angewandte Chemie International Edition*, 52(5), pp. 1384–1402. doi: 10.1002/anie.201204631.

Kühl, A. A., Erben, U., Kredel, L. I. and Siegmund, B. (2015) 'Diversity of intestinal macrophages in inflammatory bowel diseases', *Frontiers in Immunology*, 6, p. 613. doi: 10.3389/fimmu.2015.00613.

Landmann, R. G. and Weiser, M. R. (2005) 'Surgical management of locally advanced and locally recurrent colon cancer.', *Clinics in colon and rectal surgery*, 18(3), pp. 182–9. doi: 10.1055/s-2005-916279.

Laurent-Puig, P., Cayre, A., Manceau, G., Buc, E., Bachet, J. B., Lecomte, T., Rougier, P., Lievre, A., Landi, B., Boige, V., Ducreux, M., Ychou, M., Bibeau, F., Bouché, O., Reid, J., Stone, S. and Penault-Llorca, F. (2009) 'Analysis of PTEN, BRAF, and EGFR status in determining benefit from cetuximab therapy in wild-type KRAS metastatic colon cancer', *Journal of Clinical Oncology*, 27(35), pp. 5924–5930. doi: 10.1200/JCO.2008.21.6796.

Leary, R. J., Lin, J. C., Cummins, J., Boca, S., Wood, L. D., Parsons, D. W., Jones, S., Sjöblom, T., Park, B.-H., Parsons, R., Willis, J., Dawson, D., Willson, J. K. V, Nikolskaya, T., Nikolsky, Y., Kopelovich, L., Papadopoulos, N., Pennacchio, L. A., Wang, T.-L., Markowitz, S. D., Parmigiani, G., Kinzler, K. W., Vogelstein, B. and Velculescu, V. E. (2008) 'Integrated analysis of homozygous deletions, focal amplifications, and sequence alterations in breast and colorectal cancers.', *Proceedings of the National Academy of Sciences of the United States of America*, 105(42), pp. 16224–9. doi: 10.1073/pnas.0808041105.

Lengauer, C., Kinzler, K. W. and Vogelstein, B. (1997) 'Genetic instability in colorectal cancers', *Nature*, 386(6625), pp. 623–627. doi: 10.1038/386623a0.

Levy, L. and Hill, C. S. (2005) 'Smad4 Dependency Defines Two Classes of Transforming Growth Factor (TGF-) Target Genes and Distinguishes TGF- -Induced Epithelial-Mesenchymal Transition from Its Antiproliferative and Migratory Responses', *Molecular and Cellular Biology*, 25(18), pp. 8108–8125. doi: 10.1128/MCB.25.18.8108-8125.2005.

Lewis, C. E. and Pollard, J. W. (2006) 'Distinct Role of Macrophages in Different Tumor Microenvironments Distinct Role of Macrophages in Different Tumor Microenvironments', *Cancer research*, 66(2), pp. 605–612. doi: 10.1158/0008-5472.CAN-05-4005.

Li, G., Wang, S., Xue, X., Qu, X. and Liu, H. (2013) 'Monoclonal antibody-related drugs for

cancer therapy', *Drug Discoveries & Therapeutics*, 7(5), pp. 178–184. doi: 10.5582/ddt.2013.v7.5.178.

Lin, E. W., Karakasheva, T. A., Hicks, P. D., Bass, A. J. and Rustgi, A. K. (2016) 'The tumor microenvironment in esophageal cancer', *Oncogene*, 35(41), pp. 5337–5349. http://doi.org/10.1038/onc.2016.34

Linke, R., Klein, A. and Seimetz, D. (2010) 'Catumaxomab: clinical development and future directions.', *mAbs*, 2(2), pp. 129–36.

Liu, L., Chen, L., Xu, Y., Li, R. and Du, X. (2010) 'Biochemical and Biophysical Research Communications microRNA-195 promotes apoptosis and suppresses tumorigenicity of human colorectal cancer cells', *Biochemical and biophysical research*, 400(2), pp. 236–240. doi: 10.1016/j.bbrc.2010.08.046.

Liyanage, U. K., Goedegebuure, P. S., Moore, T. T., Viehl, C. T., Moo-Young, T. A., Larson, J. W., Frey, D. M., Ehlers, J. P., Eberlein, T. J. and Linehan, D. C. (2006) 'Increased Prevalence of Regulatory T Cells (Treg) is Induced by Pancreas Adenocarcinoma', *Journal of Immunotherapy*, 29(4), pp. 416–424. doi: 10.1097/01.cji.0000205644.43735.4e.

Liyanage, U. K., Moore, T. T., Joo, H.-G., Tanaka, Y., Herrmann, V., Doherty, G., Drebin, J. A., Strasberg, S. M., Eberlein, T. J., Goedegebuure, P. S. and Linehan, D. C. (2002) 'Prevalence of regulatory T cells is increased in peripheral blood and tumor microenvironment of patients with pancreas or breast adenocarcinoma.', *Journal of immunology*, 169(5), pp. 2756–61.

Llosa, N. J., Cruise, M., Tam, A., Wicks, E. C., Hechenbleikner, E. M., Taube, J. M., Blosser, R. L., Fan, H., Wang, H., Luber, B. S., Zhang, M., Papadopoulos, N., Kinzler, K. W., Vogelstein, B., Sears, C. L., Anders, R. A., Pardoll, D. M. and Housseau, F. (2015) 'The vigorous immune microenvironment of microsatellite instable colon cancer is balanced by multiple counter-inhibitory checkpoints', *Cancer Discovery*, 5(1), pp. 43–51. doi: 10.1158/2159-8290.CD-14-0863.

Loughner, C. L., Bruford, E. A., McAndrews, M. S., Delp, E. E., Swamynathan, S. and Swamynathan, S. K. (2016) 'Organization, evolution and functions of the human and mouse Ly6/uPAR family genes', *Human Genomics*, 10(1), p. 10. doi: 10.1186/s40246-016-0074-2.

Luttenberger, T., Schmid-Kotsas, A., Menke, A., Siech, M., Beger, H., Adler, G., Grünert, A. and Bachem, M. G. (2000) 'Platelet-derived growth factors stimulate proliferation and extracellular matrix synthesis of pancreatic stellate cells: implications in pathogenesis of pancreas fibrosis.', *Laboratory investigation; a journal of technical methods and pathology*, 80(1), pp. 47–55.

Lynch, H. T., Lynch, J. F., Lynch, P. M. and Attard, T. (2008) 'Hereditary colorectal cancer syndromes: molecular genetics, genetic counseling, diagnosis and management', *Familial cancer*, 7(1), pp. 27–39.

Lyseng-Williamson, K. A. and Robinson, D. M. (2006) 'Spotlight on Bevacizumab in Advanced Colorectal Cancer, Breast Cancer, and Non-Small Cell Lung Cancer1', *BioDrugs*, 20(3), pp. 193–195. doi: 10.2165/00063030-200620030-00007.

Maby, P., Tougeron, D., Hamieh, M., Mlecnik, B., Kora, H., Bindea, G., Angell, H. K.,

Fredriksen, T., Elie, N., Fauquembergue, E., Drouet, A., Leprince, J., Benichou, J., Mauillon, J., Pessot, F. Le, Sesboüé, R., Tuech, J. J., Sabourin, J. C., Michel, P., Frébourg, T., Galon, J. and Latouche, J. B. (2015) 'Correlation between density of CD8+ T-cell infiltrate in microsatellite unstable colorectal cancers and frameshift mutations: A rationale for personalized immunotherapy', *Cancer Research*, 75(17), pp. 3446–3455. doi: 10.1158/0008-5472.CAN-14-3051.

Macaulay, I. C., Tijssen, M. R., Thijssen-Timmer, D. C., Gusnanto, A., Steward, M., Burns, P., Langford, C. F., Ellis, P. D., Dudbridge, F., Zwaginga, J. J., Watkins, N. A., Van Der Schoot, C. E. and Ouwehand, W. H. (2007) 'Comparative gene expression profiling of in vitro differentiated megakaryocytes and erythroblasts identifies novel activatory and inhibitory platelet membrane proteins', *Blood*, 109(8), pp. 3260–3269. doi: 10.1182/blood-2006-07-036269.

Malumbres, M. and Barbacid, M. (2003) 'Timeline: RAS oncogenes: the first 30 years', *Nature Reviews Cancer*, 3(6), pp. 459–465. doi: 10.1038/nrc1097.

Mantovani, A., Sica, A., Sozzani, S., Allavena, P., Vecchi, A. and Locati, M. (2004) 'The chemokine system in diverse forms of macrophage activation and polarization', *Trends in Immunology*, pp. 677–686. doi: 10.1016/j.it.2004.09.015.

Markowitz, S. D. and Bertagnolli, M. M. (2010) 'Molecular basis of colorectal cancer.', *N Engl J Med*, 362(13), pp. 1245–1247. doi: 362/13/1245 [pii] 10.1056/NEJMc1000949.

Markowitz, S., Wang, J., Myeroff, L., Parsons, R., Sun, L., Lutterbaugh, J., Fan, R. S., Zborowska, E., Kinzler, K. W. and Vogelstein, B. (1995) 'Inactivation of the type II TGF-beta receptor in colon cancer cells with microsatellite instability.', *Science (New York, N.Y.)*, 268(5215), pp. 1336–8.

Martinez, F. O. and Gordon, S. (2014) 'The M1 and M2 paradigm of macrophage activation: time for reassessment', *F1000Prime Reports*, 6. doi: 10.12703/P6-13.

Massagué, J., Blain, S. W. and Lo, R. S. (2000) 'TGFbeta signaling in growth control, cancer, and heritable disorders.', *Cell*, 103(2), pp. 295–309. doi: 10.1007/s00432-009-0691-4.

Matus, D. Q., Lohmer, L. L., Kelley, L. C., Schindler, A. J., Kohrman, A. Q., Barkoulas, M., Zhang, W., Chi, Q. and Sherwood, D. R. (2015) 'Invasive Cell Fate Requires G1 Cell-Cycle Arrest and Histone Deacetylase-Mediated Changes in Gene Expression', *Developmental Cell*, 35(2), pp. 162–174. doi: 10.1016/j.devcel.2015.10.002.

McAvoy, S., Ganapathiraju, S., Perez, D. S., James, C. D. and Smith, D. I. (2007) 'DMD and IL1RAPL1: Two large adjacent genes localized within a common fragile site (FRAXC) have reduced expression in cultured brain tumors', *Cytogenetic and Genome Research*, 119(3–4), pp. 196–203. doi: 10.1159/000112061.

Mews, P., Phillips, P., Fahmy, R., Korsten, M., Pirola, R., Wilson, J. and Apte, M. (2002) 'Pancreatic stellate cells respond to inflammatory cytokines: potential role in chronic pancreatitis.', *Gut*, 50(4), pp. 535–41.

Mitrovic, S., Nogueira, C., Cantero-Recasens, G., Kiefer, K., Fernández-Fernández, J. M., Popoff, J. F., Casano, L., Bard, F. A., Gomez, R., Valverde, M. A. and Malhotra, V. (2013) 'TRPM5-mediated calcium uptake regulates mucin secretion from human colon goblet cells',

eLife, (2). doi: 10.7554/eLife.00658.

Moore, G. L., Chen, H., Karki, S. and Lazar, G. A. (2010) 'Engineered Fc variant antibodies with enhanced ability to recruit complement and mediate effector functions', *mAbs*, 2(2), pp. 181–189. doi: 10.4161/mabs.2.2.11158.

Mora, J., Schlemmer, A., Wittig, I., Richter, F., Putyrski, M., Frank, A.-C., Han, Y., Jung, M., Ernst, A., Weigert, A. and Brüne, B. (2016) 'Interleukin-38 is released from apoptotic cells to limit inflammatory macrophage responses', *Journal of Molecular Cell Biology*, 8(5), pp. 426–438. doi: 10.1093/jmcb/mjw006.

Morin, P. J., Sparks, A. B., Korinek, V., Barker, N., Clevers, H., Vogelstein, B. and Kinzler, K. W. (1997) 'Activation of β-Catenin-Tcf Signaling in Colon Cancer by Mutations in β-Catenin or APC', *Science*, 275(5307).

Moskaluk, C. A., Hruban, R. H. and Kern, S. E. (1997) 'p16 and K-ras Gene Mutations in the Intraductal Precursors of Human Pancreatic Adenocarcinoma', *Cancer Research*, 57(11).

Muleris, M., Salmon, R. J. and Dutrillaux, B. (1990) 'Cytogenetics of colorectal adenocarcinomas', *Cancer Genetics and Cytogenetics*, 46(2), pp. 143–156. doi: 10.1016/0165-4608(90)90100-O.

Muleris, M., Salmon, R. J., Zafrani, B., Girodet, J. and Dutrillaux, B. (1985) 'Consistent deficiencies of chromosome 18 and of the short arm of chromosome 17 in eleven cases of human large bowel cancer: a possible recessive determinism.', *Annales de genetique*, 28(4), pp. 206–13.

Nateri, A. S., Spencer-Dene, B. and Behrens, A. (2005) 'Interaction of phosphorylated c-Jun with TCF4 regulates intestinal cancer development.', *Nature*, 437, pp. 281–285. doi: 10.1038/nature03914.

Neesse, A., Krug, S., Gress, T. M., Tuveson, D. A. and Michl, P. (2013) 'Emerging concepts in pancreatic cancer medicine: targeting the tumor stroma.', *OncoTargets and therapy*, 7, pp. 33–43. doi: 10.2147/OTT.S38111.

Ng, A. and Xavier, R. J. (2011) 'Leucine-rich repeat (LRR) proteins: integrators of pattern recognition and signaling in immunity.', *Autophagy*, 7(9), pp. 1082–4. doi: 10.4161/auto.7.9.16464.

Nguyen, D. X., Bos, P. D. and Massagué, J. (2009) 'Metastasis: from dissemination to organ-specific colonization', *Nature Reviews Cancer*, 9(4), pp. 274–284. doi: 10.1038/nrc2622.

Ni, S. J., Sheng, W. Q. and Du, X. (2010) 'Pathologic research update of colorectal neuroendocrine tumors', *World Journal of Gastroenterology*, 16(14), pp. 1713–1719. doi: 10.3748/wjg.v16.i14.1713.

Niedergethmann, M., Hildenbrand, R., Wostbrock, B., Hartel, M., Sturm, J. W., Richter, A. and Post, S. (2002) 'High expression of vascular endothelial growth factor predicts early recurrence and poor prognosis after curative resection for ductal adenocarcinoma of the pancreas.', *Pancreas*, 25(2), pp. 122–9.

Nielsen, M. F. B., Mortensen, M. B. and Detlefsen, S. (2016) 'Key players in pancreatic

cancer-stroma interaction: Cancer-associated fibroblasts, endothelial and inflammatory cells', *World Journal of Gastroenterology*, 22(9), pp. 2678–2700. doi: 10.3748/wjg.v22.i9.2678.

Nishisho, I., Nakamura, Y., Miyoshi, Y., Miki, Y., Ando, H., Horii, A., Koyama, K., Utsunomiya, J., Baba, S. and Hedge, P. (1991) 'Mutations of chromosome 5q21 genes in FAP and colorectal cancer patients.', *Science (New York, N.Y.)*, 253(5020), pp. 665–9.

Niu, M., Valdes, S., Naguib, Y. W., Hursting, S. D. and Cui, Z. (2016) 'Tumor-Associated Macrophage-Mediated Targeted Therapy of Triple-Negative Breast Cancer', *Molecular Pharmaceutics*, 13(6), pp. 1833–1842. doi: 10.1021/acs.molpharmaceut.5b00987.

Ntougkos, E., Rush, R., Scott, D., Frankenberg, T., Gabra, H., Smyth, J. F. and Sellar, G. C. (2005) 'The IgLON Family in Epithelial Ovarian Cancer: Expression Profiles and Clinicopathologic Correlates', *Clinical Cancer Research*, 11(16).

Ohno, S., Inagawa, H., Dhar, D. K., Fujii, T., Ueda, S., Tachibana, M., Suzuki, N., Inoue, M., Soma, G. and Nagasue, N. (2002) 'The degree of macrophage infiltration into the cancer cell nest is a significant predictor of survival in gastric cancer patients.', *Anticancer research*, 23(6D), pp. 5015–5022.

Olive, K. P., Jacobetz, M. A., Davidson, C. J., Gopinathan, A., McIntyre, D., Honess, D., Madhu, B., Goldgraben, M. A., Caldwell, M. E., Allard, D., Frese, K. K., DeNicola, G., Feig, C., Combs, C., Winter, S. P., Ireland-Zecchini, H., Reichelt, S., Howat, W. J., Chang, A., Dhara, M., Wang, L., Ruckert, F., Grutzmann, R., Pilarsky, C., Izeradjene, K., Hingorani, S. R., Huang, P., Davies, S. E., Plunkett, W., Egorin, M., Hruban, R. H., Whitebread, N., McGovern, K., Adams, J., Iacobuzio-Donahue, C., Griffiths, J. and Tuveson, D. A. (2009) 'Inhibition of Hedgehog Signaling Enhances Delivery of Chemotherapy in a Mouse Model of Pancreatic Cancer', *Science*, 324(5933), pp. 1457–1461. doi: 10.1126/science.1171362.

Omiecinski, C. J., Yang, X. and Laurenzana, E. M. (2012) 'Epoxide Hydrolases', in *Encyclopedia of drug metabolism and interactions*, II:1–30. pp. 393–422. doi: 10.1002/9780470921920.edm013.

Orimo, A., Gupta, P. B., Sgroi, D. C., Arenzana-seisdedos, F., Delaunay, T., Naeem, R., Carey, V. J., Richardson, A. L. and Weinberg, R. a (2005) 'Stromal Fibroblasts Present in Invasive Human Breast Carcinomas Promote Tumor Growth and Angiogenesis through Elevated SDF-1 / CXCL12 Secretion', *Cell*, 121, pp. 335–348. doi: 10.1016/j.cell.2005.02.034.

Östman, A. and Augsten, M. (2009) 'Cancer-associated fibroblasts and tumor growth–bystanders turning into key players', *Current opinion in genetics & development*, 19(1), pp.67-73.

Özdemir, B. C., Pentcheva-Hoang, T., Carstens, J. L., Zheng, X., Wu, C.-C., Simpson, T. R., Laklai, H., Sugimoto, H., Kahlert, C., Novitskiy, S. V., De Jesus-Acosta, A., Sharma, P., Heidari, P., Mahmood, U., Chin, L., Moses, H. L., Weaver, V. M., Maitra, A., Allison, J. P., LeBleu, V. S. and Kalluri, R. (2014) 'Depletion of Carcinoma-Associated Fibroblasts and Fibrosis Induces Immunosuppression and Accelerates Pancreas Cancer with Reduced Survival', *Cancer Cell*, 25(6), pp. 719–734. doi: 10.1016/j.ccr.2014.04.005.

Panowski, S., Bhakta, S., Raab, H., Polakis, P. and Junutula, J. R. (2014) 'Site-specific antibody drug conjugates for cancer therapy', *mAbs*, 6(1), pp. 34–45. doi: 10.4161/mabs.27022.

Pardoll, D. M. (2012) 'The blockade of immune checkpoints in cancer immunotherapy', *Nature reviews. Cancer*, 12(4), p. 252. doi: 10.1038/nrc3239.

Pardridge, W. M. (2005) 'The blood-brain barrier: bottleneck in brain drug development.', *NeuroRx : the journal of the American Society for Experimental NeuroTherapeutics*, 2(1), pp. 3–14. doi: 10.1602/neurorx.2.1.3.

Pastrello, C., Santarosa, M., Fornasarig, M., Sigon, R., Perin, T., Giannini, G., Boiocchi, M. and Viel, A. (2005) 'MUC gene abnormalities in sporadic and hereditary mucinous colon cancers with microsatellite instability.', *Disease markers*, 21(3), pp. 121–6. doi: 10.1155/2005/370908.

Paunescu, V., Bojin, F. M., Tatu, C. A., Gavriliuc, O. I., Rosca, A., Gruia, A. T., Tanasie, G., Bunu, C., Crisnic, D., Gherghiceanu, M., Tatu, F. R., Tatu, C. S. and Vermesan, S. (2011) 'Tumour-associated fibroblasts and mesenchymal stem cells: More similarities than differences', *Journal of Cellular and Molecular Medicine*, 15(3), pp. 635–646. doi: 10.1111/j.1582-4934.2010.01044.x.

Pavlowsky, A., Zanchi, A., Pallotto, M., Giustetto, M., Chelly, J., Sala, C. and Billuart, P. (2010) 'Neuronal JNK pathway activation by IL-1 is mediated through IL1RAPL1, a protein required for development of cognitive functions', *Commun Integr Biol*, 3(3), pp. 245–247.

Peddareddigari, V. G., Wang, D. and DuBois, R. N. (2010) 'The Tumor Microenvironment in Colorectal Carcinogenesis', *Cancer Microenvironment*, 3(1), pp. 149–166. doi: 10.1007/s12307-010-0038-3.

Perez, H. L., Cardarelli, P. M., Deshpande, S., Gangwar, S., Schroeder, G. M., Vite, G. D. and Borzilleri, R. M. (2014) 'Antibody–drug conjugates: current status and future directions', *Drug Discovery Today*, 19(7), pp. 869–881. doi: 10.1016/j.drudis.2013.11.004.

Perrino, E., Steiner, M., Krall, N., Bernardes, G. J. L., Pretto, F., Casi, G. and Neri, D. (2014) 'Curative Properties of Noninternalizing Antibody–Drug Conjugates Based on Maytansinoids', *Cancer Research*, 74(9).

Pierantoni, C., Pagliacci, A., Scartozzi, M., Berardi, R., Bianconi, M. and Cascinu, S. (2008) 'Pancreatic cancer: Progress in cancer therapy', *Critical Reviews in OncologyHematology*, 67, pp. 27–38. doi: 10.1016/j.critrevonc.2008.01.009.

Piton, A., Michaud, J. L., Peng, H., Aradhya, S., Gauthier, J., Mottron, L., Champagne, N., Lafrenière, R. G., Hamdan, F. F., Joober, R., Fombonne, E., Marineau, C., Cossette, P., Dubé, M. P., Haghighi, P., Drapeau, P., Barker, P. A., Carbonetto, S. and Rouleau, G. A. (2008) 'Mutations in the calcium-related gene IL1RAPL1 are associated with autism', *Human Molecular Genetics*, 17(24), pp. 3965–3974. doi: 10.1093/hmg/ddn300.

Provenzano, P. P., Cuevas, C., Chang, A. E., Goel, V. K., Von Hoff, D. D. and Hingorani, S. R. (2012) 'Enzymatic Targeting of the Stroma Ablates Physical Barriers to Treatment of Pancreatic Ductal Adenocarcinoma', *Cancer Cell*, 21(3), pp. 418–429. doi: 10.1016/j.ccr.2012.01.007.

Raedler, L. A. (2015) 'Opdivo (Nivolumab): Second PD-1 Inhibitor Receives FDA Approval for Unresectable or Metastatic Melanoma.', *American health & drug benefits*, 8(Spec Feature), pp. 180–3.

Redston, M. (2001) 'Carcinogenesis in the GI tract: from morphology to genetics and back again.', *Modern pathology : an official journal of the United States and Canadian Academy of Pathology, Inc*, 14(3), pp. 236–45. doi: 10.1038/modpathol.3880292.

Ribas, G., Neville, M. J. and Campbell, R. D. (2001) 'Single-nucleotide polymorphism detection by denaturing high-performance liquid chromatography and direct sequencing in genes in the MHC class III region encoding novel cell surface molecules', *Immunogenetics*, 53(5), pp. 369–381. doi: 10.1007/s002510100343.

Royal, R. E., Levy, C., Turner, K., Mathur, A., Hughes, M., Kammula, U. S., Sherry, R. M., Topalian, S. L., Yang, J. C., Lowy, I. and Rosenberg, S. A. (2010) 'Phase 2 Trial of Single Agent Ipilimumab (Anti-CTLA-4) for Locally Advanced or Metastatic Pancreatic Adenocarcinoma', *Journal of Immunotherapy*, 33(8), pp. 828–833. doi: 10.1097/CJI.0b013e3181eec14c.

Rudd, C. E., Taylor, A. and Schneider, H. (2009) 'CD28 and CTLA-4 coreceptor expression and signal transduction', *Immunological Reviews*, 229(1), pp. 12–26. doi: 10.1111/j.1600-065X.2009.00770.x.

Saito, T., Nishikawa, H., Wada, H., Nagano, Y., Sugiyama, D., Atarashi, K., Maeda, Y., Hamaguchi, M., Ohkura, N., Sato, E., Nagase, H., Nishimura, J., Yamamoto, H., Takiguchi, S., Tanoue, T., Suda, W., Morita, H., Hattori, M., Mori, M., Doki, Y. and Sakaguchi, S. (2016) 'Two FOXP3 + CD4 + T cell subpopulations distinctly control the prognosis of colorectal cancers', *Nature medicine*, 22(6), pp. 679–684. doi: 10.1038/pj.2016.37.

Samuels, Y., Wang, Z., Bardelli, A., Silliman, N., Ptak, J., Szabo, S., Yan, H., Gazdar, A., Powell, S. M., Riggins, G. J., Willson, J. K. V, Markowitz, S., Kinzler, K. W., Vogelstein, B. and Velculescu, V. E. (2004) 'High Frequency of Mutations of the PIK3CA Gene in Human Cancers', *Science*, 304(5670), pp. 554–554. doi: 10.1126/science.1096502.

Scarlett, C. J. (2013) 'Contribution of bone marrow derived cells to the pancreatic tumor microenvironment', *Frontiers in Physiology*, 4, p. 56. doi: 10.3389/fphys.2013.00056.

Schoppmann, S. F., Birner, P., Stöckl, J., Kalt, R., Ullrich, R., Caucig, C., Kriehuber, E., Nagy, K., Alitalo, K. and Kerjaschki, D. (2002) 'Tumor-Associated Macrophages Express Lymphatic Endothelial Growth Factors and Are Related to Peritumoral Lymphangiogenesis', *The American Journal of Pathology*, 161(3), pp. 947–956. doi: 10.1016/S0002-9440(10)64255-1.

Schutte, M., Hruban, R. H., Geradts, J., Maynard, R., Hilgers, W., Rabindran, S. K., Moskaluk, C. A., Hahn, S. A., Schwarte-Waldhoff, I., Schmiegel, W., Baylin, S. B., Kern, S. E. and Herman, J. G. (1997) 'Abrogation of the Rb/p16 tumor-suppressive pathway in virtually all pancreatic carcinomas', *Cancer Research*, 57(15), pp. 3126–3130. doi: 10.3349/YMJ.2005.46.4.519.

Scott, A. M., Wolchok, J. D. and Old, L. J. (2012) 'Antibody therapy of cancer', *Nature Reviews Cancer*. Nature Publishing Group, 12(4), pp. 278–287. doi: 10.1038/nrc3236.

Senter, P. D. and Sievers, E. L. (2012) 'The discovery and development of brentuximab vedotin for use in relapsed Hodgkin lymphoma and systemic anaplastic large cell lymphoma', *Nature Biotechnology*, 30(7), pp. 631–637. doi: 10.1038/nbt.2289.

Sewda, K., Coppola, D., Enkemann, S., Yue, B., Kim, J., Lopez, A. S., Wojtkowiak, J. W., Stark, V. E., Morse, B., Shibata, D., Vignesh, S. and Morse, D. L. (2016) 'Cell-surface markers for colon adenoma and adenocarcinoma.', *Oncotarget*, 7(14), pp. 17773–89. doi: 10.18632/oncotarget.7402.

Shakoori, A., Ougolkov, A., Yu, Z. W., Zhang, B., Modarressi, M. H., Billadeau, D. D., Mai, M., Takahashi, Y. and Minamoto, T. (2005) 'Deregulated GSK3β activity in colorectal cancer: Its association with tumor cell survival and proliferation', *Biochemical and Biophysical Research Communications*, 334(4), pp. 1365–1373. doi: 10.1016/j.bbrc.2005.07.041.

Sharma, P. and Allison, J. P. (2015) 'The future of immune checkpoint therapy', *Science*, 348(6230).

Sherman, M. H., Yu, R. T., Engle, D. D., Ding, N., Atkins, A. R., Tiriac, H., Collisson, E. A., Connor, F., Van Dyke, T., Kozlov, S., Martin, P., Tseng, T. W., Dawson, D. W., Donahue, T. R., Masamune, A., Shimosegawa, T., Apte, M. V., Wilson, J. S., Ng, B., Lau, S. L., Gunton, J. E., Wahl, G. M., Hunter, T., Drebin, J. A., O'Dwyer, P. J., Liddle, C., Tuveson, D. A., Downes, M. and Evans, R. M. (2014) 'Vitamin D Receptor-Mediated Stromal Reprogramming Suppresses Pancreatitis and Enhances Pancreatic Cancer Therapy', *Cell*, 159(1), pp. 80–93. doi: 10.1016/j.cell.2014.08.007.

Shields, J. M., Pruitt, K., McFall, A., Shaub, A. and Der, C. J. (2000) 'Understanding Ras: "it ain"t over 'til it's over'', *Trends in Cell Biology*, 10(4), pp. 147–154. doi: 10.1016/S0962-8924(00)01740-2.

Shirasawa, S., Furuse, M., Yokoyama, N. and Sasazuki, T., 1993. Altered growth of human colon cancer cell lines disrupted at activated Ki-ras. *Science*, 260, pp.85-85.

Sica, A., Allavena, P. and Mantovani, A. (2008) 'Cancer related inflammation: The macrophage connection', *Cancer Letters*, pp. 204–215. doi: 10.1016/j.canlet.2008.03.028.

Sica, A. and Bronte, V. (2007) 'Review series Altered macrophage differentiation and immune dysfunction in tumor development', *the Journal of Clinical Investigation*, 117(5), pp. 1155–1166. doi: 10.1172/JCI31422.to.

Skrzypczak, M., Goryca, K., Rubel, T., Paziewska, A., Mikula, M., Jarosz, D., Pachlewski, J., Oledzki, J. and Ostrowsk, J. (2010) Modeling oncogenic signaling in colon tumors by multidirectional analyses of microarray data directed for maximization of analytical reliability. *PloS one*, 5(10), p.e13091.

Slattery, M. L., Pellatt, D. F., Mullany, L. E., Wolff, R. K. and Herrick, J. S. (2015) 'Gene expression in colon cancer: A focus on tumor site and molecular phenotype', *Genes Chromosomes and Cancer*, 54(9), pp. 527–541. doi: 10.1002/gcc.22265.

Smith, D. I., Zhu, Y., McAvoy, S. and Kuhn, R. (2006) 'Common fragile sites, extremely large genes, neural development and cancer', *Cancer Letters*, pp. 48–57. doi: 10.1016/j.canlet.2005.06.049.

Smith, P. D., Smythies, L. E., Shen, R., Greenwell-Wild, T., Gliozzi, M. and Wahl, S. M. (2011) 'Intestinal macrophages and response to microbial encroachment', *Mucosal Immunology*, 4(1), pp. 31–42. doi: 10.1038/mi.2010.66.

Smyth, G. K. (2004) 'Linear Models and Empirical Bayes Methods for Assessing Differential Expression in Microarray Experiments', *Statistical Applications in Genetics and Molecular Biology*. De Gruyter, 3(1), pp. 1–25. doi: 10.2202/1544-6115.1027.

Stockmann, C., Schadendorf, D., Klose, R. and Helfrich, I. (2014) 'The Impact of the Immune System on Tumor: Angiogenesis and Vascular Remodeling', *Frontiers in Oncology*, 4. doi: 10.3389/fonc.2014.00069.

Stringer, D. K. and Piper, R. C. (2011) 'Terminating protein ubiquitination: Hasta la vista, ubiquitin.', *Cell cycle*, 10(18), pp. 3067–71. doi: 10.4161/cc.10.18.17191.

Sugimoto, H., Mundel, T. M., Kieran, M. W. and Kalluri, R. (2006) 'Identification of fibroblast heterogeneity in the tumor microenvironment', *Cancer Biology and Therapy*, 5(12), pp. 1640–1646. doi: 10.4161/cbt.5.12.3354.

Sugita, J., Ohtani, H., Mizoi, T., Saito, K. and Shiiba, K. (2002) 'Close Association between Fas Ligand (FasL; CD95L)-positive Tumor-associated Macrophages and Apoptotic Cancer Cells along Invasive Margin of Colorectal', *Cancer Science*, 93(3), pp.320-328.

Sulzmaier, F. J., Jean, C. and Schlaepfer, D. D. (2014) 'FAK in cancer: mechanistic findings and clinical applications', *Nature Reviews Cancer*, 14(9), pp. 598–610. doi: 10.1038/nrc3792.

Suzuki, M., Kato, C. and Kato, A. (2015) 'Therapeutic antibodies: their mechanisms of action and the pathological findings they induce in toxicity studies', *Journal of Toxicologic Pathology*, 28(3), pp. 133–139. doi: 10.1293/tox.2015-0031.

Szász, A. M., Lánczky, A., Nagy, Á., Förster, S., Hark, K., Green, J. E., Boussioutas, A., Busuttil, R., Szabó, A. and Győrffy, B. (2016) 'Cross-validation of survival associated biomarkers in gastric cancer using transcriptomic data of 1,065 patients', *Oncotarget*, 7(31), pp. 49322–49333. doi: 10.18632/oncotarget.10337.

Taniwaki, K., Fukamachi, H., Komori, K., Ohtake, Y., Nonaka, T., Sakamoto, T., Shiomi, T., Okada, Y., Itoh, T., Itohara, S., Seiki, M. and Yana, I. (2007) 'Stroma-derived matrix metalloproteinase (MMP)-2 promotes membrane type 1-MMP-dependent tumor growth in mice', *Cancer Research*, 67(9), pp. 4311–4319. doi: 10.1158/0008-5472.CAN-06-4761.

Teague, A., Lim, K.-H. and Wang-Gillam, A. (2015) 'Advanced pancreatic adenocarcinoma: a review of current treatment strategies and developing therapies.', *Therapeutic advances in medical oncology*, 7(2), pp. 68–84. doi: 10.1177/1758834014564775.

Terme, M., Ullrich, E., Aymeric, L., Meinhardt, K., Desbois, M., Delahaye, N., Viaud, S., Ryffel, B., Yagita, H., Kaplanski, G., Prévost-Blondel, A., Kato, M., Schultze, J. L., Tartour, E., Kroemer, G., Chaput, N. and Zitvogel, L. (2011) 'IL-18 Induces PD-1–Dependent Immunosuppression in Cancer', *Cancer Research*, 71(16).

Thibodeau, S. N., Bren, G. and Schaid, D. (1993) 'Microsatellite instability in cancer of the proximal colon.', *Science*, 260(May), pp. 816–819. doi: 10.1126/science.8484122.

Thomas, A., Teicher, B. A. and Hassan, R. (2016) 'Antibody–drug conjugates for cancer therapy', *The Lancet Oncology*, 17(6), pp. e254–e262. doi: 10.1016/S1470-2045(16)30030-4.

Thura, M., Al-Aidaroos, A. Q. O., Yong, W. P., Kono, K., Gupta, A., Lin, Y. Bin, Mimura, K., Thiery, J. P., Goh, B. C., Tan, P., Soo, R., Hong, C. W., Wang, L., Lin, S. J., Chen, E., Rha, S. Y., Chung, H. C., Li, J., Nandi, S., Yuen, H. F., Zhang, S.-D., Guan, Y. K., So, J. and Zeng, Q. (2016) 'PRL3-zumab, a first-in-class humanized antibody for cancer therapy', *JCI Insight*, 1(9). doi: 10.1172/jci.insight.87607.

Tijink, B. M., Buter, J., De Bree, R., Giaccone, G., Lang, M. S., Staab, A., Leemans, C. R. and Van Dongen, G. A. M. S. (2006) 'A phase I dose escalation study with anti-CD44v6 bivatuzumab mertansine in patients with incurable squamous cell carcinoma of the head and neck or esophagus', *Clinical Cancer Research*, 12(20 PART 1), pp. 6064–6072. doi: 10.1158/1078-0432.CCR-06-0910.

Toda, D., Ota, T., Tsukuda, K., Watanabe, K., Fujiyama, T., Murakami, M., Naito, M. and Shimizu, N. (2006) 'Gefitinib decreases the synthesis of matrix metalloproteinase and the adhesion to extracellular matrix proteins of colon cancer cells', *Anticancer Research*, 26(1 A), pp. 129–134.

Topalian, S. L., Sznol, M., McDermott, D. F., Kluger, H. M., Carvajal, R. D., Sharfman, W. H., Brahmer, J. R., Lawrence, D. P., Atkins, M. B., Powderly, J. D., Leming, P. D., Lipson, E. J., Puzanov, I., Smith, D. C., Taube, J. M., Wigginton, J. M., Kollia, G. D., Gupta, A., Pardoll, D. M., Sosman, J. A. and Hodi, F. S. (2014) 'Survival, durable tumor remission, and long-term safety in patients with advanced melanoma receiving nivolumab', *Journal of Clinical Oncology*, 32(10), pp. 1020–1030. doi: 10.1200/JCO.2013.53.0105.

Tosolini, M., Kirilovsky, A., Mlecnik, B., Fredriksen, T., Mauger, S., Bindea, G., Berger, A., Bruneval, P., Fridman, W. H., Pagès, F. and Galon, J. (2011) 'Clinical impact of different classes of infiltrating T cytotoxic and helper cells (Th1, Th2, Treg, Th17) in patients with colorectal cancer', *Cancer Research*, 71(4), pp. 1263–1271. doi: 10.1158/0008-5472.CAN-10-2907.

Veigl, M. L., Kasturi, L., Olechnowicz, J., Ma, A. H., Lutterbaugh, J. D., Periyasamy, S., Li, G. M., Drummond, J., Modrich, P. L., Sedwick, W. D. and Markowitz, S. D. (1998) 'Biallelic inactivation of hMLH1 by epigenetic gene silencing, a novel mechanism causing human MSI cancers.', *Proceedings of the National Academy of Sciences of the United States of America*, 95(15), pp. 8698–702. doi: 10.1073/pnas.95.15.8698.

de VET, E. C. J. M., AGUADO, B. and CAMPBELL, R. D. (2003) 'Adaptor signalling proteins Grb2 and Grb7 are recruited by human G6f, a novel member of the immunoglobulin superfamily encoded in the MHC', *Biochemical Journal*, 375(1).

Vilar, E. and Gruber, S. B. (2010) 'Microsatellite instability in colorectal cancer—the stable evidence', *Nature Reviews Clinical Oncology*. Nature Publishing Group, 7(3), pp. 153–162. doi: 10.1038/nrclinonc.2009.237.

Vogel, C. L., Cobleigh, M. A., Tripathy, D., Gutheil, J. C., Harris, L. N., Fehrenbacher, L., Slamon, D. J., Murphy, M., Novotny, W. F., Burchmore, M., Shak, S., Stewart, S. J. and Press, M. (2002) 'Efficacy and safety of trastuzumab as a single agent in first-line treatment

of HER2-overexpressing metastatic breast cancer.', *Journal of clinical oncology : official journal of the American Society of Clinical Oncology*, 20(3), pp. 719–26. doi: 10.1200/JCO.2002.20.3.719.

Vogelstein, B., Lane, D. and Levine, A. J. (2000) 'Surfing the p53 network.', *Nature*, 408(6810), pp. 307–310. doi: 10.1038/35042675.

Wang, X., Wang, J., Ma, H., Zhang, J. and Zhou, X. (2012) 'Downregulation of miR-195 correlates with lymph node metastasis and poor prognosis in colorectal cancer', *Medical Oncology*, 29(2), pp. 919–927. doi: 10.1007/s12032-011-9880-5.

Watkins, D. and Cunningham, D. (2007) 'The role of epidermal growth factor receptor-targeted antibody therapy in previously treated colorectal cancer.', *Clinical colorectal cancer*. Elsevier, 6 Suppl 2, pp. S47-52. doi: 10.3816/CCC.2007.s.002.

Wegenka, U. M. (2010) 'IL-20: Biological functions mediated through two types of receptor complexes', *Cytokine & Growth Factor Reviews*, 21(5), pp. 353–363. doi: 10.1016/j.cytogfr.2010.08.001.

Wei, C. C., Hsu, Y. H., Li, H. H., Wang, Y. C., Hsieh, M. Y., Chen, W. Y., Hsing, C. H. and Chang, M. S. (2006) 'IL-20: Biological functions and clinical implications', *Journal of Biomedical Science*, pp. 601–612. doi: 10.1007/s11373-006-9087-5.

Weston, C. R. and Davis, R. J. (2007) 'The JNK signal transduction pathway', *Current Opinion in Cell Biology*, 19(2), pp. 142–149. doi: 10.1016/j.ceb.2007.02.001.

Winter, G. and Milstein, C. (1991) 'Man-made antibodies', *Nature*, 349(6307), pp. 293–299. doi: 10.1038/349293a0.

Wood, L. D. and Hruban, R. H. (2015) 'Genomic landscapes of pancreatic neoplasia.', *Journal of pathology and translational medicine*, 49(1), pp. 13–22. doi: 10.4132/jptm.2014.12.26.

Wood, L., Parsons, D., Jones, S. J., Lin, J., Sjoblom, T., Leary, R., Shen, D., Boca, S., Barber, T. D., Ptak, J., Silliman, N., Szabo, S., Dezso, Z., Ustyanksky, V., Nikolskaya, T., Nikolsky, Y., Karchin, R., Wilson, P., Kaminker, J., Zhang, Z., Croshaw, R., Willis, J. H., Dawson, D., Shipitsin, M., Willson, J., Sukumar, S., Polyak, K., Park, B., Pethiyagoda, C., Pant, P., Ballinger, D., Sparks, A., Hartigan, J., Smith, D., Suh, E., Papadopoulos, N., Buckhaults, P., Markowitz, S., Parmigiani, G., Kinzler, K., Velculescu, V. and Vogelstein, B. (2007) 'The Genomic Landscapes of Human Breast and Colorectal Cancers', *Science*, 318, pp. 1108–1113. doi: 10.1126/science.1145720.

Xia, L., Zhang, D., Du, R., Pan, Y., Zhao, L., Sun, S., Hong, L., Liu, J. and Fan, D. (2008) 'miR-15b and miR-16 modulate multidrug resistance by targeting BCL2 in human gastric cancer cells', *International Journal of Cancer*, 123(2), pp. 372–379. doi: 10.1002/ijc.23501.

Xu, Z., Vonlaufen, A., Phillips, P. A., Fiala-Beer, E., Zhang, X., Yang, L., Biankin, A. V., Goldstein, D., Pirola, R. C., Wilson, J. S. and Apte, M. V. (2010) 'Role of Pancreatic Stellate Cells in Pancreatic Cancer Metastasis', *The American Journal of Pathology*, 177(5), pp. 2585–2596. doi: 10.2353/ajpath.2010.090899.

Yachida, S. and Iacobuzio-Donahue, C. A. (2013) 'Evolution and dynamics of pancreatic

cancer progression', *Oncogene*, 32(45), pp. 5253–5260. doi: 10.1038/onc.2013.29.

Yaeger, R., Cowell, E., Chou, J. F., Gewirtz, A. N., Borsu, L., Vakiani, E., Solit, D. B., Rosen, N., Capanu, M., Ladanyi, M. and Kemeny, N. (2015) 'RAS mutations affect pattern of metastatic spread and increase propensity for brain metastasis in colorectal cancer', *Cancer*, 121(8), pp. 1195–1203. doi: 10.1002/cncr.29196.

Yang, L., Lin, C. and Liu, Z. R. (2006) 'P68 RNA Helicase Mediates PDGF-Induced Epithelial Mesenchymal Transition by Displacing Axin from ??-Catenin', *Cell*, 127(1), pp. 139–155. doi: 10.1016/j.cell.2006.08.036.

Zhang, X., Kelaria, S., Kerstetter, J. and Wang, J. (2015) 'The functional and prognostic implications of regulatory T cells in colorectal carcinoma', *The journal of Gastrointestinal Oncology*, 10(8), pp. 307–313. doi: 10.3978/j.issn.2078-6891.2015.017.

Zhang, Y. (2013) 'Epidemiology of esophageal cancer.', *World journal of gastroenterology*, 19(34), pp. 5598–606. doi: 10.3748/wjg.v19.i34.5598.

Zhao, K., Yin, L.-L., Zhao, D.-M., Pan, B., Chen, W., Cao, J., Cheng, H., Li, Z.-Y., Li, D.-P., Sang, W., Zeng, L.-Y. and Xu, K.-L. (2014) 'IL1RAP as a surface marker for leukemia stem cells is related to clinical phase of chronic myeloid leukemia patients', *International Journal of Clinical and Experimental Medicine*, 7(12), pp. 4787–4798.

Zhao, L. and Vogt, P. K. (2008) 'Class I PI3K in oncogenic cellular transformation', *Oncogene*, 27(41), pp. 5486–5496. doi: 10.1038/onc.2008.244.

Zhao, M., Kong, L. and Qu, H. (2014) 'A systems biology approach to identify intelligence quotient score-related genomic regions, and pathways relevant to potential therapeutic treatments.', *Scientific reports*, 4, p. 4176. doi: 10.1038/srep04176.

Zhou, Q., Peng, R.-Q., Wu, X.-J., Xia, Q., Hou, J.-H., Ding, Y., Zhou, Q.-M., Zhang, X., Pang, Z.-Z., Wan, D.-S., Zeng, Y.-X. and Zhang, X.-S. (2010) 'The density of macrophages in the invasive front is inversely correlated to liver metastasis in colon cancer', *Journal of Translational Medicine*, 8(1), p. 13. doi: 10.1186/1479-5876-8-13.

Zhu, C.-Q., Popova, S. N., Brown, E. R. S., Barsyte-Lovejoy, D., Navab, R., Shih, W., Li, M., Lu, M., Jurisica, I., Penn, L. Z., Gullberg, D. and Tsao, M.-S. (2007) 'Integrin alpha 11 regulates IGF2 expression in fibroblasts to enhance tumorigenicity of human non-small-cell lung cancer cells.', *Proceedings of the National Academy of Sciences of the United States of America*, 104(28), pp. 11754–9. doi: 10.1073/pnas.0703040104.

Zhu, J., Yamane, H. and Paul, W. E. (2010) 'Differentiation of Effector CD4 T Cell Populations', *Annual Review of Immunology*, 28(1), pp. 445–489. doi: 10.1146/annurev-immunol-030409-101212.